MULTI-OBJECTIVE OPTIMAL DESIGN OF HYBRID RENEWABLE ENERGY SYSTEMS USING SIMULATION-BASED OPTIMIZATION

By
MASOUD SHARAFI

A Thesis submitted to the Faculty of Graduate Studies of
The University of Manitoba
in partial fulfillment of the requirements of the degree of

DOCTOR OF PHILOSOPHY

Department of Mechanical Engineering
University of Manitoba
Winnipeg

Abstract

Renewable energy (RE) resources are relatively unpredictable and dependent on climatic conditions. The negative effects of existing randomness in RE resources can be reduced by the integration of RE resources into what is called Hybrid Renewable Energy Systems (HRES). The design of HRES remains as a complicated problem since there is uncertainty in energy prices, demand, and RE sources. In addition, it is a multi-objective design since several conflicting objectives must be considered. In this thesis, an optimal sizing approach has been proposed to aid decision makers in sizing and performance analysis of this kind of energy supply systems.

First, a straightforward methodology based on ε-constraint method is proposed for optimal sizing of HRESs containing RE power generators and two storage devices. The ε-constraint method has been applied to minimize simultaneously the total net present cost of the system, unmet load, and fuel emission. A simulation-based particle swarm optimization approach has been used to tackle the multi-objective optimization problem.

In the next step, a Pareto-based search technique, named dynamic multi-objective particle swarm optimization, has been performed to improve the quality of the Pareto front (PF) approximated by the ε-constraint method. The proposed method is examined for a case study including wind turbines, photovoltaic panels, diesel generators, batteries, fuel cells, electrolyzers, and hydrogen tanks. Well-known metrics from the literature are used to evaluate the generated PF.

Afterward, a multi-objective approach is presented to consider the economic, reliability and environmental issues at various renewable energy ratio values when optimizing the design of building energy supply systems. An existing commercial apartment building operating in a cold Canadian climate has been described to apply the proposed model. In this test application, the model investigates the potential use of RE resources for the building. Furthermore, the

application of plug-in electric vehicles instead of gasoline car for transportation is studied. Comparing model results against two well-known reported multi-objective algorithms has also been examined.

Finally, the existing uncertainties in RE and load are explicitly incorporated into the model to give more accurate and realistic results. An innovative and easy to implement stochastic multi-objective approach is introduced for optimal sizing of an HRES.

Acknowledgements

First, I have to thank my research supervisor Dr. Tarek ElMekkawy who offered his continuous advice and encouragement throughout the course of this thesis. Without his assistance and dedicated involvement in every step throughout the process, this thesis would have never been accomplished. I really would like to appreciate him for his support and understanding over these past three years.

I also would like to show gratitude to my committee members, Dr. Ali Elkamel, Dr. Qingjin Peng, and Dr. Shaahin Filizadeh for their efforts put into reviewing the thesis, and their excellent comments and suggestion. Besides, I would like to thank Dr. Eric Bibeau for enlightening me with various great ideas.

I would like to express my very sincere gratitude to University of Manitoba for providing me the circumstance to perform my doctoral research and for their financial support. I acknowledge the funding received from the NSERC discovery grants and CancerCare Manitoba (CCMB) to support this research. Heartfelt thanks goes to Ms.Sue Bates who was an utmost director at CancerCare Manitoba for her various supports.

Carrying out my thesis demanded more than academic aids, and I have many friends to express my appreciation for their friendship. I also would also like to thank both Sirous Ghelichkhani and his wife (Ayda) who kindly opened their house and heart to my wife and me when we arrived in Winnipeg.

Most importantly, none of this was possible without the encouragement and supports that I got from my family who have sacrificed their lives for me and provided unconditional love and care.

Finally, I undoubtedly would like to be grateful from the most important person in my life i.e. my wife Monireh who has constantly inspired me and honestly made it possible for me to see this project as finished.

Table of Contents

List of Figures

List of Tables

List of Abbreviations

ANOVA	Analysis of Variance
DMOPSO	Dynamic Multi-Objective Particle Swarm Optimization
DM	Decision Makers
DiM	Diversification Metric
DOE	Design of Experiment
GHG	Greenhouse Gas
GA	Genetic Algorithm
FC	Fuel Cell
HWD	Hot Water Demand
HRES	Hybrid Renewable Energy System
LLP	Loss of Load Probability
MS	Maximum Spread
MOP	Multi-objective Optimization Problem
MOGA	Multi-Objective Genetic Algorithm
MLMOPSO	Multi-Leaders Multi-Objective Particle Swarm Optimization
MOPSO	Multi-Objective Particle Swarm Optimizers
NPC	Net Present Cost
PF	Pareto Front
PSO	Particle Swarm Optimization
PEV	Plug-in Electric Vehicle
PV	Photovoltaic
RE	Renewable Energy

RER	Renewable Energy Ratio
SAM	Sampling Average Method
SO	Single Objective
SPEA	Strength Pareto Evolutionary Algorithm
SM	Spacing Metric
SC	Set Coverage Metrics
ZEB	Zero Energy Building

Declaration the academic achievement

The outline of this thesis follows “sandwich format” whose guidelines are appointed by the Faculty of Graduate Studies, University of Manitoba. It merges four individual papers prepared for publication in peer-reviewed journals. Chapter 1 contains an introduction about the problem statement and the thesis contributions; Chapters 2 to 5 are manuscripts containing an abstract, introduction, methods, results and discussion; Chapter 6 provides the conclusions of the work and recommendations for future research direction.

Chapters 2 to 5 have been published as four journal papers. The contributions of M. Sharafi in all the papers are listed as following: developing the research idea, developing the mathematical model, implementing the simulation and optimization algorithms in C++, data analysis, drawing the figures, writing all the manuscripts; submitting the manuscripts and responding to reviewers’ comments. My co-authors contributed in developing the research idea, analysing data, preparing the manuscripts, or submitting the manuscripts for publication.

Copyright Notices

1. With kind permission from Elsevier Publishers:

- **Sharafi M**, ELMekkawy T. Stochastic Optimization of Hybrid Renewable Energy System Using Sampling Average Method. Renewable & Sustainable Energy Reviews 2015; 52: 1668–1679.

- **Sharafi M**, ELMekkawy T, Bibeau EL. Optimal Design of Hybrid Renewable Energy Systems in Buildings with Low to High Renewable Energy Ratio. Renewable Energy 2015; 83: 1026–1042.

- **Sharafi M**, ELMekkawy T. Multi-Objective Optimal Design of Hybrid Renewable Energy Systems using PSO-Simulation Based Approach. Renewable Energy 2014; 68: 67-79.

2. With kind permission from John Wiley&Sons Publishers:

- **Sharafi M,** ELMekkawy T. A Dynamic MOPSO Algorithm for Multi-Objective Optimal Design of Hybrid Renewable Energy Systems. International Journal of Energy Research 2014; 38(15): 1949-1963.

Chapter 1

Introduction

1.1. Background

1.1.1. Renewable Energy Sources

Energy is assumed as a production factors same as labor, capital, and land. Hence, the efficient use of energy can reduce total cost of a system and minimize negative environmental impacts. Presently, the major share of total energy use (more than 80%) is related to traditional fuels such as oil, coal, and natural gas [1]. The increasing demand for energy leads to dramatic consumption of fossil fuels and fast rising energy prices. Moreover, conventional energy resources are bounded, scarce and quickly diminishing, which make an unbalanced condition for the future energy supply and demand sectors. Besides, the growing consumption of fossil fuels has significant impact on the level of greenhouse gas (GHG) emissions and global warming [2].

Fluctuation of energy prices endangers the energy security of fuel-importing countries. Additionally, the Kyoto protocol adopted in 1997 has obligated countries to reduce greenhouse gas emissions [3]. Therefore, developing a sustainable energy system, which is defined as an eco-friendly system, is mandatory to tackle the mentioned challenges [2]. Renewable energy

(RE) sources including solar, hydro, wind, biomass, and geothermal are appropriate options for such systems. The common characteristic of RE resources is that they are replaced in a very short time contrary to fossil fuels that take years to be replenished [4]. In addition, REs can decrease GHG, reduce transmission losses, and increase energy security. These can be interpreted as sensible reasons that has accelerated the advancement of RE technologies in recent years.

1.1.2. Hybrid Renewable Energy Systems

Renewable energy resources are relatively unpredictable and dependent on climatic conditions [5]. For example, solar energy is available in the daytime but when it comes to nights, other energy alternatives or stored energy is requested. Therefore, renewable energy resources individually may not meet the energy demand of a given area independently. In this context, a combination of renewable energy sources can reduce the impact of uncertainties existing in Res and makes them more reliable. The integration of renewable energy sources, which is named hybrid renewable energy system (HRES), can be categorized into two main types: stand-alone or grid-connected type [6], [7]. In a grid-connected or parallel application, HRESs can be connected to electricity grids to buy or sell electricity at a predefined price whenever there is excess energy or energy deficiency. The stand-alone or off-grid application is appropriate to provide the energy needs of remote areas where an electrical network is not available or it is costly to install an electricity grid. Hence, HRESs are becoming popular for remote area power generation applications as they are often the most cost-effective and reliable way to produce energy for this application.

1.1.3. Optimal Design of HRESs

It can be a challenge to decide where renewable energy systems should be established, and what combination or corresponding capacities of RE technologies are required to be installed [1]. These challenges have motivated researchers to develop models for optimal design of HRESs. That design problem means identifying the best combination of RE technologies as well as recognizing their optimal capacities that is needed to provide required energy. It can make using RE more cost effective and reliable. In recent years, numerous researches have been conducted for optimal design of an HRES but it still remains a complex problem due to precarious energy prices, fluctuations in energy demand, and uncertainties existing in RE resources. Moreover, environmental issues are becoming increasingly important in the design phase of energy systems [2]. Hence, in the design step of these facilities, many aspects must be taken into account such as the total cost of the system, environmental concerns, reliability, and power quality. In order to handle such a complex problem, multi-objective optimization methods are needed to tackle the issue of conflicting objective functions. Due to the complexity of optimal design of an HRES, classical optimization techniques are not able to effectively and efficiently find a solution [3]. In these cases, meta-heuristic techniques are proposed to deal with these complicated optimization models where the classical approaches are not able to obtain good results. A meta-heuristic is formally defined as an "*iterative generation process which guides a subordinate heuristic by combining intelligently different concepts for exploring and exploiting the search space, learning strategies are used to structure information in order to find efficiently near-optimal solutions*" [8].

1.2. Research Aims

The main goal of this study is to establish a general methodology for stochastic multi-objective optimal design of a hybrid renewable energy system including various generators and storage devices. That is, the final aim would be developing an efficient and effective engineering tool to handle the multi-objective problem incorporating uncertainties existing in RE resources and energy demand. Thus, this study deals with optimal sizing of HRESs to meet a specified reliability, minimize total net present cost (NPC) and pollution emission, and maximize renewable energy ratio (RER).

1.2.1. Problem Definition

Hybrid renewable energy systems have been identified as the empirical options for power generating in remote areas where extending the electricity network is too expensive to supply required electricity. Their application in grid-connected situations can be justified when the objectives of reduction in CO_2 emission and increasing RER would be integrated with economic goals. The typical drawback distinguishing RE resources is that these sources are dependent on climatic conditions and therefore naturally uncertain [9]. Furthermore, it is difficult to predict the energy load as it fluctuates through seasons, even it changes hourly. Thus, these energy supply systems generally have to be designed with high reliability and small loss of power supply probability as they usually run in off-grid condition. Additionally, the design of such systems must be cost-effective with highest efficiency as they should produce electricity with minimum cost and maximum efficiency.

Optimal design of an HRES requires correct selection and sizing of different options based on an appropriate optimization strategy. Figure 1-1 demonstrates a sample HRES including *n*

generators to provide required energy. Without considering the design optimization, there is a possibility that the selected size of these energy generators be above the required capacities and consequently resulting in a higher cost. Hence, in the design phase of these generators, it is desired to evaluate any possible configuration of $\{G_1, G_2, \ldots, G_n\}$ to get the optimal alternative and the corresponding optimal capacity of selected generators based on a set of predefined criteria.

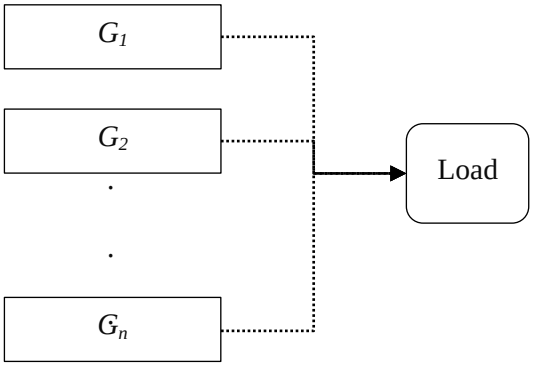

Figure 1-1: Example of an HRES

Although the optimal design of an HRES can make it cost effective, reliable and environment friendly, it still remains a complex problem due to precarious energy prices, fluctuations in energy demand, and uncertainties in RE resources. Moreover, non-linear characteristics of RE technologies makes the HRES difficult to be designed and their performance be evaluated [10]. In order to handle such a complicated problem, complex optimization methods have been employed to find optimum solution in a reasonable time.

In line with the mentioned concepts, this study attempts to emphasize multi-objective optimization of sizing an HRES. The main aim of the model is to investigate the interaction between the environment, reliability, and economy to design an HRES within different values of renewable energy ratio (RER) as shown in Figure 1-2. RER is defined as the amount of used renewable energy divided by used total primary energy. The objective function of the

optimization model can be the maximization of reliability, the minimization of net present cost, CO_2 emission, and the maximization of RER of the employed HRES. The results of the approach are optimal size of components and optimal energy flow between these components.

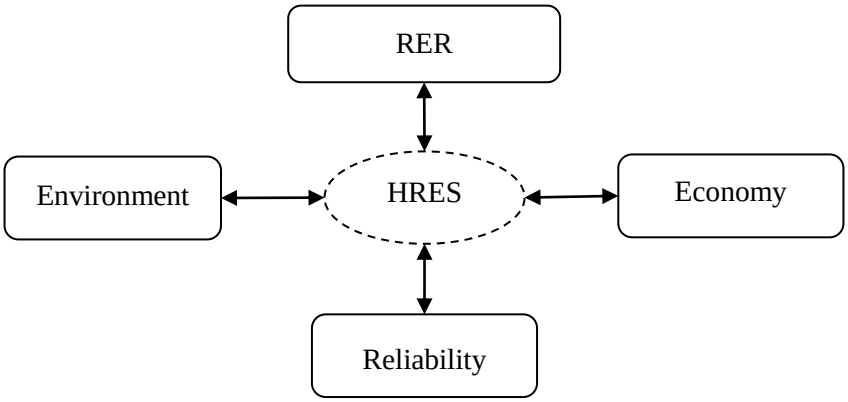

Figure 1-2: Interaction between HRES and employed objective functions

Therefore, this research deals with the problem of multi-objective optimal sizing of an HRES. Different multi-objective optimization methods incorporating uncertainties or deterministic approaches are developed to return the optimal or near optimal design of an off-grid and grid-connected application of HRES. The employed multi-objective optimization methods are implemented using meta-heuristic approaches.

1.2.2. Research Motivation

In the last decade, many authors developed optimization methods for optimal design of an HRES considering several objectives such as minimization of fuel emission, maximization of reliability, or minimization of cost. In general, the optimization methodologies which were performed in the related literature can be divided into two main groups named single objective and multi-objective optimization framework. Mostly, previous studies have been carried out based on the single objective optimization framework [11]. They essentially considered the economic performance

as the design criterion. Although those studies delivered promising results, they did not address the emission affect and reliability analysis of HRES. In addition, their studies lack the capabilities of providing a set of alternative solutions that compare different objectives against each other.

Multi-objective optimization framework is another approach that has been used to design an HRES. By considering conflicting objectives, a set of solutions can be generated which are recognized as non-dominated, non-inferior, or Pareto front (PF) [12]. In general, there are two types of search techniques to tackle multi-objective optimization (MOP) formulations called Pareto-based techniques and non Pareto-based techniques [13]. The basic idea of Pareto-based techniques is that Pareto front is directly generated by using ranking and selection over populations [12]. It requires a ranking procedure and a technique to maintain diversity in the population [12]. Non Pareto- based techniques are approaches that do not directly incorporate the concept of Pareto optimum [12].

Presently, few articles applied MOP to design an HRES usually using Pareto-based techniques which require ranking and pairwise comparison operations. Most of them used well-known MOP algorithms without modifications while an efficient meta-heuristic algorithm requires modifications to be adapted for a specific problem. In addition, there is a drawback of generating a high performance PF. That is, in previous study, the quality of PF is neglected while an important issue in MOP is the quantitative evaluation of the quality of the approximate set. On the other hand, literature review shows that the number of researches on MOP framework is not comparable to studies followed the single objective methodology. Moreover, in the related literature, there is a lack of studies that consider the trade-off between system emission, system reliability, system cost, and renewable energy ratio (RER). Furthermore, there are not enough

algorithms developed to cope with stochastic analysis of the design process of HRES. Moreover, available tools do not deal with providing energy simultaneously for appliance, heating, cooling, and transportation sectors.

However, persisted research and development are still required to improve these systems sizing process. This research has advanced to incorporate a number of these current research gaps.

1.2.3. Research Objectives

The chief aim of this thesis is to develop an optimal sizing approach to efficiently and economically employ RE resources. This optimization tool can be applied in the feasibility study of an HRES to identify the optimal capacity of different RE suppliers and assist decision makers in their performance analysis. For this purpose, the developed tool would get the hourly climate data of a given location, its fluctuating energy demand, and the economic characteristic of HRES to identify the size and the type of examined components based on the most fitted options. Therefore, the tool would integrate an optimization algorithm and a simulation approach to attain the most favorable composition of the examined HRES. In this thesis, the economic model containing total net present cost, the reliability model of loss of load probability (LLP), total fuel emission, and renewable energy ratio are presented for system configurations evaluations rather than the system components models. Different search techniques have been proposed to optimize simultaneously the mentioned objectives when the goal is computation time or it would be generating a higher performance PF than well-known MOP approaches. Finally, the proposed approach is aimed to address the uncertainties existing in RE resources and energy load. Briefly, the general objective of this thesis is summarized into addressing the following research questions.

- For a given load characteristic**,** what is the optimal combination and component size of an HRES by which the HRES will be cost-effective, reliable and environmentally friendly? That is, what is the competition between renewable energy resources to meet energy demand of a given area?
- What is the economic and environment impact of an HRES with different renewable energy ratio?
- How much GHG emission decline can be achieved by the application of HRESs?
- How the quality of generated PFs for the mentioned multi-objective problem can be quantified and measured?
- How much considering required energy for transportations rather than heating, cooling, and electricity load does affect the configuration of HRESs?
- What is the impact of uncertainties (randomness in wind speed, solar irradiation and energy load) on the design of an HRES?

1.2.4. Significance of the Research

As mentioned in Section 1.2.2, in spite of the huge number of articles in the literature regarding optimal design of HRES, there is still plentiful room for advancing the design procedure of these energy supply systems. In this thesis, to fill the gap of the existing related literature, various multi-objective optimization approaches enhanced simulation-based optimization methods are developed. The advantages of these developed methodologies are summarized as the following.

- Creating an optimization tool for optimal design of an HRES in order to find the optimal capacity and type of its components.

- Proposing a novel approach based on ε-constraint method for optimal design of HRES including various generators and storage devices. The attractive features of this proposed approach are its simplicity and the relatively less computational effort. Moreover, the proposed model is flexible to consider simultaneously more renewable sources and storage devices.
- Establishing an innovative approach named Dynamic Multi-Objective Particle Swarm Optimization algorithm to generate a higher performance PF than well-known MOP approaches.
- Performing a multi-objective optimization methodology to examine renewable energy ratio as an objective function rather than the economic and environmental issues when optimizing the design of buildings energy supply system.
- Studying a comprehensive energy supply system in which required energy for transportation load is considered rather than electricity, heating, and cooling load.
- Developing a new stochastic multi-objective methodology to incorporate the existing uncertainties in RE resource and energy load when sizing a buildings energy supply system. A MOP incorporating a comprehensive stochastic analysis is implemented to size the renewable energy suppliers of a building. In other words, the randomness in wind speed, solar radiation, ambient temperature, electricity load, heating and cooling load, hot water demand (HWD), and transportation load are simultaneously considered in the sizing process of HRESs.

1.3. Outline of the Thesis

In this thesis, in order to introduce an appropriate tool for optimal design of an HRES, a methodology is followed that is described in Figure 1-3. First, the optimization problem is considered in a mathematical form. The energy analysis, reliability, and fuel emission of the HRES must be mapped mathematically. The mathematical model for HRES components are implemented in a simulation module. Meta-heuristic multi-objective optimization algorithms based on particle swarm optimization (PSO) are developed to search the optimal solution of the optimization problem. The simulation and optimization part are executed in C++ programming environment. The required input data for a case study such as meteorological data, economic data, and load profile are entered to the developed model to get a proper PF. Finally, a sensitivity analysis is run to study the impact of used parameters' values on the obtained results. This general process that is shown in the right side of the depicted methodology (Figure 1-3) is repeated in the rest of the thesis (Chapter 2 to 5). This thesis is provided in a sandwich format merging four papers that are separated into different chapters beginning with Chapter 2 as described in Figure 1-3 as well.

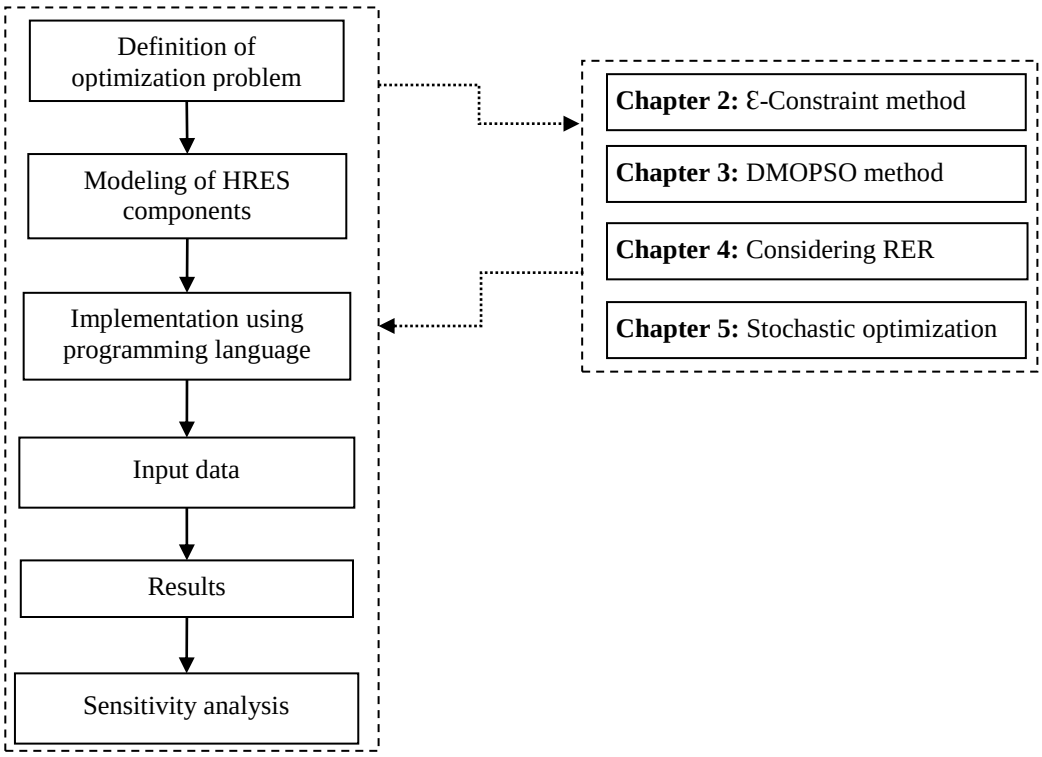

Figure 1-3: The research methodology integrated with the organization of the thesis

Chapter two proposes a novel approach with emphasis on simplicity or computational effort to find the optimal sizing of an HRES. The chapter introduces an ε-constraint method, which is a non Pareto-based search technique for the purpose of HRES design. First, the recent related literature in the area of optimal design of HRES is reviewed according to using single objective or multi-objective approaches. Then, the developed multi-objective problem is described by covering its objective functions, constraints, decision variables and the mathematical models used in the simulation. Moreover, the proposed simulation-PSO based approach is presented to solve the developed MOP. Chapter 2 also exhibits the results of the developed tool in the application of a case study taken from the literature along with its sensitivity analysis result.

In Chapter three, a Pareto-based search technique named dynamic multi-objective particle swarm optimization (DMOPSO) has been performed to improve the quality of approximated PF in Chapter two. First, the literature on optimal design of HRES is updated to include recent studies

containing multi-objective design of an HRES. Furthermore, it discusses the idea of how well-known metrics are used to evaluate the generated Pareto front. The chapter shows the result of proposed DMOPSO by applying it into the same case study used in Chapter two and with comparison against three popular multi-objective algorithms.

Chapter four presents a multi-objective approach to consider the economic, reliability and environmental issues at various renewable energy ratio values when optimizing the design of buildings energy supply system. An existing apartment building operating in cold Canadian climate is described to apply the proposed model. In this test application, the model investigates the potential of using a heat pump, biomass boiler, wind turbines, solar heat collector, photovoltaic panels, and heat storage tank to produce renewable energy for the building. Furthermore, the application of plug-in electric vehicles instead of gasoline car for transportation is studied in this chapter. That is, this chapter studies a comprehensive energy supply system, which is considering required energy for transportation rather than electricity, heating, and cooling load. The detail mathematical model of components and optimization problem is presented in the chapter. Comparing model results against two well-known reported multi-objective algorithms is also examined in this chapter. Furthermore, it represents the sensitivity analysis of the studied multi-objective optimization problem with respect to the entered data of inspected case study. It also covers the simulation result of components over one sample year.

The developed model in Chapter four would be more accurate and the decision is more realistic, if the characteristic of uncertainties are explicitly incorporated. In Chapter five, the developed model in the previous chapters is extended and introduces an innovative and easy to implement stochastic multi-objective approach. It incorporates the existing uncertainties in RE resource and energy load when sizing a buildings energy supply system. In other words, this chapter is the

extension of the developed model in Chapter 4 with difference in involving the stochastic evaluation instead of using a deterministic design methodology. Additionally, simple methods for synthetic generation of daily load profile and weather data has been employed to handle the existing uncertainties in the model. The chapter also explains the sampling average approximation which is integrated with DMOPSO to help in solving the complex optimization problem. The generated solutions by the implemented approach are evaluated by comparing with the solutions obtained by deterministic analysis. Then, a sensitivity analysis is carried out to identify the economic parameters that have significant impact on the design objectives.

Lastly, in Chapter six, the key findings, limitations and the implications of the thesis are summarized. Then, the chapter covers some recommended directions for future work.

1.4. References

[1] Anon. Annual energy outlook 2013. Energy Information Administration, Washington (DC); 2012.

[2] Ekren O, Ekren BY. Size optimization of a PV/wind hybrid energy conversion system with battery storage using simulated annealing. Applied Energy 2010; 87: 592–598.

[3] Cormio C, Dicorato M, Minoia A, Trovato M. A regional energy planning methodology including renewable energy sources and environmental constraints. Renewable and Sustainable Energy Reviews 2003; 7: 99–130.

[4] Masters GM. Renewable and efficient electric power systems. Hoboken, New Jersey: John Wiley & Sons, Inc.; 2004.

[5] Yang H, Zhou W, Lu L, Fang Z. Optimal sizing method for stand-alone hybrid solar–wind system with LPSP technology by using genetic algorithm. Solar Energy 2008;82:354–67.

[6] Nema P, Nema RK, Rangnekar S. A current and future state of art development of hybrid energy system using wind and PV-solar: A review. Renewable and Sustainable Energy Reviews 2009; 13: 2096–2103.

[7] Wang L, Singh C. PSO-based multi-criteria optimum design of a grid-connected hybrid power system with multiple renewable sources of energy. In: Swarm intelligence symposium (SIS) IEEE 2007; 250-257.

[8] Osman IH, Laporte G. Metaheuristics: A bibliography. Annual Operation Research 1996:511–623.

[9] Deshmukh MK, Deshmukh SS. Modeling of hybrid renewable energy systems. Renewable and Sustainable Energy Reviews 2008;12: 235–249.

[10] Fazlollahi S, Mandel P, Becker G, Maréchal F. Methods for multi-objective investment and operating optimization of complex energy systems. Energy 2012; 45:12–22.

[11] Sharafi M, ELMekkawy TY. Multi-objective optimal design of hybrid renewable energy systems using PSO-simulation based approach. Renewable Energy 2014; 68: 67–79.

[12] Coello CAC, Lamont GB, Veldhuizen DA Van, Goldberg DE, Koza JR. Evolutionary algorithms for solving multi-objective problems. 2nd Edition, New York, USA, Springer; 2007.

[13] Sharafi M, Elmekkawy TY. A dynamic MOPSO algorithm for multiobjective optimal design of hybrid renewable energy systems. International Journal of Energy Research 2014; 35(15): 1949-1963

[14] Dufo-López R, Bernal-Agustín JL, Contreras J. Optimization of control strategies for stand-alone renewable energy systems with hydrogen storage. Renewable Energy 2007; 32:1102–1126.

Chapter 2

Multi-Objective Optimal Design of Hybrid Renewable Energy Systems Using PSO-Simulation Based Approach

2.1. Abstract

Recently, increasing energy demand has caused dramatic consumption of fossil fuels and unavoidable rising energy prices. Moreover, environmental effects of fossil fuels led to the need of using renewable energy (RE) to meet the rising energy demand. Unpredictability and cost are the main challenges of renewable energy usage. In this direction, the integration of RE technologies to meet the energy demand of a given area can overcome the RE challenges. In this study, a novel approach is proposed for optimal design of hybrid renewable energy systems consisting of various energy suppliers and storage devices. ε-constraint method has been applied to minimize simultaneously total cost of the system, unmet load, and fuel emission. A particle swarm optimization- based simulation approach has been used to tackle the multi-objective optimization problem. The proposed approach has been tested on a case study of an HRES system that includes wind turbines, photovoltaic (PV) panels, a diesel generator, batteries, a fuel cell (FC), an electrolyzer and a hydrogen tank. Finally, a sensitivity analysis study is carried out to investigate the sensitivity of different parameters to the developed model.

2.2. Introduction

Sustainable energy systems have a pivotal role to overcome concerns about global warming and the depletion of conventional energy resources. RE systems as sustainable energy suppliers can decrease greenhouse gas emission, transmission and transformation losses, and increase energy security. Stand-alone RE sources may not meet the hourly energy demand either due to the lack of the energy source level or its time variability. Hence, HRES can reduce the impact of uncertainties of RE resources. In addition, the optimal design of HRESs makes them cost effective, reliable and environment friendly.

Optimizing the design of an HRES is essential especially with the high present cost of an HRES and consequently adopting a suboptimal design can significantly affect the economic performance of the HRES on the long run. Furthermore, the Kyoto protocol, adopted in 1997, obligates industrialized countries to reduce GHG emissions. Hence, more research is required to minimize total cost and fuel emission.

Due to the complexity of optimal design of an HRES, classical optimization techniques are not able to tackle the complicated optimization problems where the effectiveness or efficiency of meta-heuristics techniques is proved [1]. Particle swarm optimization approach is one of the meta-heuristic approaches that can be used for solving many complex problems. PSO is based on swarm intelligence. Compared with other meta-heuristics algorithms, PSO is simple and easy to implement, and it needs fewer parameters [2].

Optimization techniques need explicit mathematical representation of systems. With complex optimization problems, it is difficult to use mathematical models since the system has a high dimensional space or non-linear nature. On the other hand, simulation can be used as a tool for evaluating the performance of complex systems with almost no simplifying assumptions.

However, using a simulation model alone does not obtain the optimal solution of the optimization problems. Hence, the simulation models have to be combined with an optimization search technique to deliver optimal (or near optimal) solutions. That is, developing a hybrid approach would be able to model the complex system and search for optimal solutions. This combination resulted in the development of simulation-based optimization methods, which is employed in this paper.

In the last decade, many authors developed optimization methods to achieve several objectives for HRES design, e.g. minimize emission, maximize reliability, minimize cost, etc. The relevant articles are divided into two main categories, single objective (SO) and multi-objective optimization problem (MOP). Few articles used MOP for optimal design of HRESs. The existing literature can further be categorized based on the considered energy resources, type of models, and solution approaches. The cited articles are summarized according to these features and presented in Table 2-1.

Table 2-1: Summary of the literature review

Authors	System components								MOP	Pareto based	Objective function	Optimization approach	Model period
	Wind turbine	PV panel	FC	Biomass	Hydro power	Geothermal	Storage	Diesel& other					
Eke et al. [3]	●	●							NO	---	Minimizes total cost	LP	1 year
Ludwig et al. [4]	●						●	●	NO	---	Minimizes total cost	SMIP	1 year
Garyfallos et al. [5]	●	●	●				●	●	NO	---	Minimizes total cost	SA	10 years
Akella et al. [6]	●	●		●	●				NO	---	Minimizes total operation cost	LP	1 year
Dagdougui et al. [7]	●	●	●				●		NO	---	Minimizes difference between hydrogen demand and supplied	MINLP	30 days
Cai et al. [8]	●	●			●			●	NO	---	Minimizes total cost	ISITSP	15 years
Lagorsea et al. [9]		●	●				●		NO	---	Minimizes total cost	Simulation	1 year
Orhan et. [10]	●	●					●		NO	---	Minimizes total cost	SA	20 years
Kashefi et al. [11]	●	●	●				●		NO	---	Minimize annualized cost	PSO	20 years
Raquel et al. [12]	●		●				●	●	NO	---	Minimizes the LEC	LP + heuristic	1 year
Iniyan et al. [13]	●	●		●				●	NO	---	Minimize cost/efficiency ratio	LP	11 years
Juhari et al. [14]	●	●			●		●		NO	---	Minimizes cost of energy	Simulation	1 year
Katsigiannis et al.[15]	●	●					●	●	NO	---	Minimizes cost of energy	Tabu search	20 years
Budischak et al.[16]	●	●	●				●	●	NO	---	Minimizes cost of energy	Enumerative method	20 years
Elliston et al. [17]	●	●		●	●		●		NO	--	Minimize annualized cost	GA	1 year
Katsigiannis et al. [19]	●	●	●				●	●	Yes	Yes	Minimizes cost of energy Minimizes total GHG emissions	NSGA	1 year
Trivedi et al. [20]	●							●	Yes	Yes	Minimizes fuel cost Minimizes SO_2 and NO_x emission	MOGA	1 day
Dufo et al. [21]	●	●	●				●	●	Yes	Yes	Minimizes total cost Minimizes unmet load Minimizes fuel emission	SPEA	25 year
Abedi et al. [22]	●	●	●				●	●	Yes	Yes	Minimizes total cost Minimizes unmet load Minimizes fuel emission	DEA/Fuzzy technique	1 year
Bernal et al. [23]	●	●	●		●		●	●	NO	---	Minimizes total cost	GA	1 year
Ahmarinezhad et al. [29]	●	●	●		●		●	●	NO	---	Minimizes total cost	PSO	20 years

Many articles used single-objective optimization. Although single objective models can provide decision makers (DM) with insights into the nature of the problem, they usually cannot provide a set of alternative solutions that trade different objectives against each other. Eke et al. [3] developed a linear mathematical model to minimize total cost of an HRES. They only considered solar panels with wind turbines and used a graphical method to find a solution for the optimization problem. Ludwig et al. [4] proposed a stochastic mixed integer programming model to identify the optimal size of a hybrid power system containing wind turbines, storage device, transmission network, and thermal generators. They used Benders' decomposition algorithm with Pareto-optimal cuts to solve the design problem. Garyfallos et al. [5] developed an optimization model to design a power supply system including RE generators and hydrogen storage. The model was executed in a case study that involves wind turbines, PV panels, accumulators, an electrolyzer, storage tanks, a compressor, a fuel cell and a diesel generator. They considered uncertainties to examine the effect of weather fluctuations. A stochastic simulated annealing algorithm was used to find minimum net present value of cost for ten years. Akella et al. [6] projected a linear programming model for the optimal design of an HRES which consists of micro hydro power, PV panels, wind turbines, and biomass. Hanane et al. [7] developed a mathematical programming model for a wind/PV/fuel cell/electrolyzer system to supply electricity and hydrogen to a green hydrogen refueling station network. The proposed system was designed to meet required hydrogen and minimize the difference between hydrogen demands and supply. In [8] an interval-parameter superiority–inferiority-based two-stage programming (ISITSP) was proposed for planning renewable energy management systems. The ISITSP is the combination of interval linear programming (ILP), two-stage programming (TSP) and superiority–inferiority-based fuzzy-stochastic programming (SI-FSP). The final goal of their

model was to identify the optimal capacity of facilities in order to minimize the sum of the relevant cost. By using Matlab/Simulink, Jeremy [9] has evaluated three different HRESs based on fuel cells, PV panels and batteries to simulate different configurations and investigate the operation of the system over one year. The considered criterion was minimizing total cost. In [10-12] meta-heuristic algorithms were developed to optimize the sizing of an HRES to return the minimum total cost of the system. While by using simulation approach and Tabu search algorithm in [13-15], the optimal configuration of a power generating system was presented with considering the cost of energy. Budischak et al. [16] evaluated various compounds of renewable electricity generators including inland wind, offshore wind turbines, PV panels, and electrochemical storages. They used enumerative method to find the least combination with minimum net present cost over 20 years. In another similar study, Ellison et al. [17] proposed a cost optimization model to find least cost options to supply the Australian National Electricity Market (NEM) using renewable power generation. They considered wind, PV panels, concentrating solar thermal with storage, hydro power and a biofuelled gas turbine. In their study, genetic algorithms with integration of a simulation tool were applied to return the least cost combination of renewable energy technology subjected to meet NEM reliability standard. They concluded that the dominated generation mix including wind turbine, PV, CST is cheaper than a replacement fleet between 2029 and 2043 as it is projected that the carbon price will be in range of $50-100.

In summary, although SO has been used in several HRES studies and delivered promising results, most SO methods do not address emission affect and reliability analysis of HRESs. In addition, SO lacks the capabilities providing a set of alternative solutions that compare different objectives against each other.

Multi-objective optimization problem is another approach that has been used to design an HRES. By considering conflicting objectives a group of solutions noted as non-dominated, non-inferior or Pareto-optimal solutions can be generated [26]. The following classification of search approaches is used, which handle MOP: Pareto-based techniques and non Pareto-based techniques. The basic idea of Pareto-based techniques is that a Pareto front is directly generated by using ranking and selection in the population. It requires a ranking procedure and a technique to maintain diversity in a population. Non Pareto-based techniques are approaches that do not directly incorporate the concept of Pareto optimum [26]. Katsigiannis et al. [19] developed a multi-objective optimization model to generate Pareto front to minimize total cost of energy and total greenhouse gas emissions of an HRES during its lifetime by using non-dominated sorting genetic algorithm (NSGA). In [20] multi-objective genetic algorithm (MOGA) was applied to solve a nonlinear multi objective optimization problem for scheduling a wind/diesel system, which aims to minimize fuel cost as well as SO_2 and NO_x emission. Dufo et al. [21] applied a strength Pareto evolutionary algorithm (SPEA) to determine the optimal size and optimal power management strategy parameters for an HRES with aim of minimizing total cost, unmet load, and fuel emission simultaneously. Abedi et al. [22] presented a MOP to minimize simultaneously total cost, pollutant emissions and unmet load. For this task, differential evolution algorithm (DEA) and fuzzy techniques have been used to find the best combination of components and control strategies for the HRES.

In brief, although few articles have applied MOP to design an HRES, they are usually using MOEA Pareto-based techniques, which require expensive ranking and pairwise comparison operations [30].

In this paper, a novel approach is proposed for optimal design of an HRES including various generators and storage devices. ε-constraint method, which is a non Pareto-based search technique, has been applied to minimize simultaneously total cost of the system, unmet load, and fuel emission. The idea of this approach is to minimize total cost while CO_2 emission and unmet load are considered as constraint bound by permissible levels. By varying these levels, non-inferior solutions can be obtained. PSO-based simulation technique has been used to handle the developed multi-objective optimization problem. The attractive features of this proposed approach are its simplicity [26], [30] or less computational effort since excessive operations of ranking and pairwise comparison that are required by Pareto-based techniques are eliminated [30]. Moreover, the model is flexible to consider simultaneously more renewable sources and storage devices.

The rest of this Chapter is formed as following. First the problem description and the proposed approach are given in Section 2.4, and 2.5 respectively. The simulation module of the proposed approach and the mathematical models of system's components are described in Section 2.6. Section 2.7 is devoted to explaining the optimization module and the proposed PSO algorithm. The results of optimizing a case study along with sensitivity analysis result are exhibited in Section 2.8. Finally, conclusion and future research are given in Section 2.9.

2.3. Nomenclature

A_{PV}	PV panel area [m^2]	P_{PV}	PV panel capacity [kW]
A_{WG}	Wind turbine rotor swept area [m^2]	P_{WG}	Wind turbine capacity [kW]
C_I	Investment cost [€/KW]	$P_{WG,r}$	Wind turbine rated power [kW]
$C_{O\&M}$	O& M cost [€/year]	P_{bat}	Battery capacity [kWh]
C_{rep}	Replacement cost [€/year]	P_{El}	Electrolyzer capacity [kW]
C_p	Power coefficient	P_{tank}	H_2-tank capacity [kW]
CRF	Capital recovery factor	P_{FC}	Fuel cell capacity [kW]
C_{fuel}	Fuel cost [€/year]	P_{Dis}	Diesel generator capacity [kW]
C	Constant weighting parameter	P_{n-FC}	FC nominal output power [kW]
$CO2_{emi}$	System CO_2 emission [kg/year]	P_{a-FC}	FC actual output power [kW]
D	Hourly energy demand [kWh]	P_{id}	Best experience for particles
E_{PV}	Energy produced by PV panels [kWh]	PSO	Particle Swarm Optimization
E_{WG}	Energy produced by wind turbines [kWh]	P_{a-DG}	Diesel generator actual output power [kW]
E_{Ex}	Excess energy [kWh]	Q_{n-H_2}	Electrolyzer nominal hydrogen mass flow [kg/hr]
E_{Ex-bat}	Excess energy put into batteries [kWh]	Q_{H_2}	Electrolyzer actual hydrogen mass flow [kg/hr]
E_{Ex-El}	Excess energy put into the electrolyzer [kWh]	SOC	Battery state of charge [%]
$E_{El-tank}$	Energy put into the H_2-tank by the electrolyzer [kWh]	SOC_{min}	SOC lower limit [%]
$E_{tank-FC}$	Energy put into the fuel cell by the H_2-tank [kWh]	SOC_{max}	SOC upper limit [%]
$E_{FC-load}$	Energy put into load by the fuel cell [kWh]	$shortage$	Unmet load during time step *t* [kWh]
$E_{bat-loa}$	Energy put into load by batteries [kWh]	$SPEA$	Strength Pareto evolutionary algorithm
E_{bat}	Power charged or discharged from batteries [kWh]	T	Project life time [year]
EF	Emission factor [kg/lit]	t_{zone}	Time zone difference compared to GMT [hr]
EOT	Equation of time [min]	V	wind speed [m/s]
f_{FC}	FC hydrogen consumption constant	V_c	Cut-in wind speed [m/s]
$fuel_{con}$	Diesel generator fuel consumption [lit/hr]	V_r	Rated wind speed [m/s]
g_{id}	Global best particle	V_f	Cut-off wind speed [m/s]
$H_{2_{level}}$	H_2-tank inventory level [kg]	v	Particles speed vector
$H_{2_{level-}}$	H_2-tank inventory level upper limit [%]	x	Particles position vector
$H_{2_{level-}}$	H_2-tank inventory level lower limit [%]	η_{FC}	Fuel cell energy efficiency [%]
$H2_{cons-}$	H_2 consumption of the fuel cell [kg/hr]	η_{El}	Electrolyzer energy efficiency [%]
HHV_{H_2}	H_2 higher heating value [kWh/kg]	η_{DG}	Diesel generator energy efficiency [%]

HRES	Hybrid renewable energy systems	η_{H_2-tank}	H_2-tank storage efficiency
I_T	Total solar radiation on tilted surface [kWh/m^2]	η_{bat}	Battery round trip efficiency [%]
$I_{b,tilt}$	Beam radiation [kWh/m^2]	η_{pv}	PV panel efficiency [%]
$I_{d,tilt}$	Sky diffuse radiation [kWh/m^2]	ρ	Air density [kg/m^{-3}]
$I_{r,tilt}$	Ground reflected solar radiation [kWh/m^2]	ε_{LLP}	LLP desirable level [%]
$I_{b,n}$	Direct normal irradiance [kWh/m^2]	ε_{CO2}	CO_2 emission desirable level [kg/year]
i	interest rate [%]	φ	Uniform random number
K	Single payment worth	ω	Inertia coefficient
LHV_{H_2}	H_2 lower heating value [kWh/kg]	ϕ	Tilt angle from the horizontal surface [Degree]
LHV_{gas}	Gas oil lower heating value [kWh/kg]	ξ	Azimuth angle [Degree]
LLP	Loss of load probability [%]	ρ	Reflection index
L	Components life time [year]	χ	Sun zenith angle [Degree]
LST	local standard time	ζ	Plate azimuth angle [Degree]
L_{local}	local longitude [Degree]	δ	Solar declination angle [Degree]
MOP	Multi objective optimization	λ	Latitude [Degree]
n_{max-FC}	Fuel cell optimal operation power divide by nominal capacity [%]	α	Solar angle [Degree]
P_{n-DG}	Diesel generator nominal output power [kW]		

2.4. Problem Description

In this study, the considered hybrid renewable energy system is adopted from [21, 23]. The system includes PV panels, a wind turbine, a diesel generator, and two storage systems. Batteries and electrolyzer/hydrogen tank/FC are the storage devices. The energy flow of the employed system is shown in Figure 2-1. The PV panels and wind turbine produce electricity from solar and wind energy to meet the energy requirement of a specific load. When produced energy is more than the needed load, the excess energy is stored in the storage systems. A share of excess energy is put into batteries and the remaining energy is put into the electrolyzer and converted to hydrogen. The hydrogen tank is used to store the produced hydrogen by the electrolyzer. When the produced energy by the PV panels and wind turbines cannot meet the load, the batteries and

fuel cell can provide power to fulfill electricity load based on the charge level of batteries and H_2 level of the tank. When the batteries and H_2-tank are not able to meet the deficit energy, the diesel generator is used as an emergency power-supply.

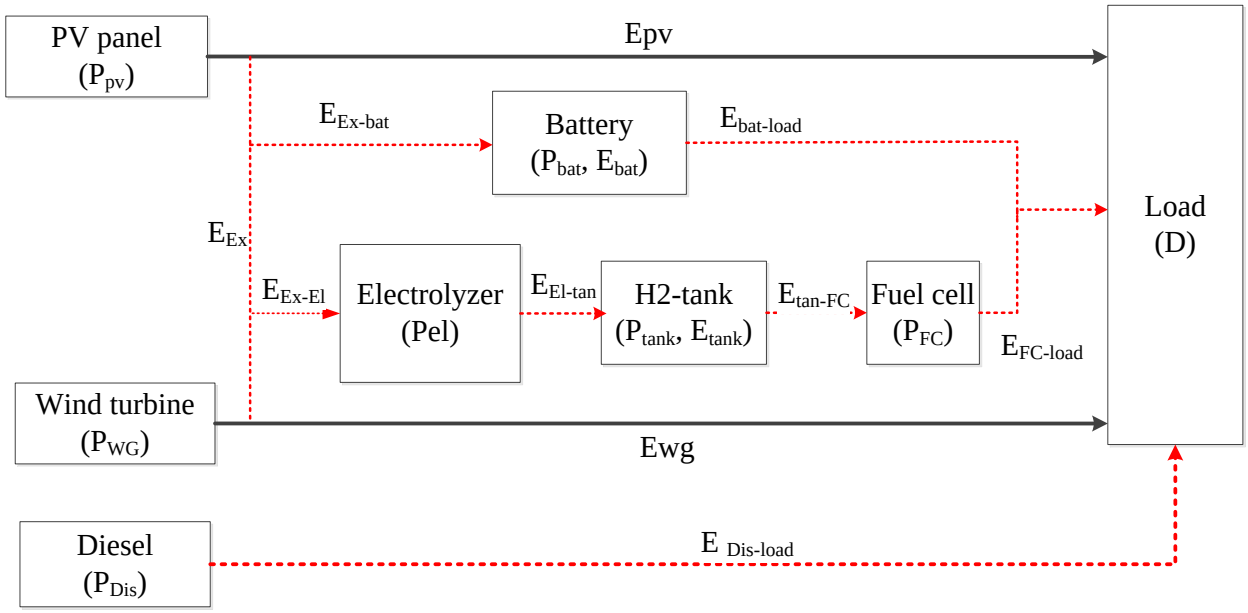

Figure 2-1: The energy flow of the employed system

2.5. Proposed Approach

This study attempts to emphasize optimization of an HRES design by using a PSO-simulation based approach. Simulation can be used as an effective evaluation tool whenever mathematical models are not applicable due to system complexity or existing uncertainties. The main advantage of using simulation is the fact that all system's details and uncertainties can be accommodated accurately compared to other modeling methodologies. However, simulation inherently cannot be used as a stand-alone tool to deliver an optimal design of the system. On the other hand, optimization techniques need explicit mathematical representation of the system. In complex systems, it is a complex task to formulate a mathematical model since there is this possibility that the studied system has a high dimensional space or non-linear nature. Therefore,

combining a simulation module with an optimization method allows overcoming their shortcomings. That is, the hybrid approach is able to model the complex features of the system as well as obtaining the optimal solution in reasonable time. In this paper, to find the optimal (or near optimal) design of an HRES, PSO-based simulation approach has been proposed as outlined in Figure 2-2 and Figure 2-4. There is this feature that the proposed approach can be modified to associate additional components of the HRES.

The decision variables, fitness and constraints are defined in the PSO algorithm. Design variables that are the capacity of the components are defined in a vector named particle. In other words, each particle represents a certain configuration of the HRES. Total net present cost that is specified by the design variables is considered as the fitness of particles for evaluation. Moreover, each particle generated randomly should meet the constraints of the model, which will be presented in Section 2.7.2. After initializing a population of particles, each particle is sent to the simulation module to check its feasibility. The simulation model is run for one year to evaluate the performance of each particle. The simulation module calculates the yearly unmet load and CO_2 emission for the HRES using the equations which are presented in Section 2.6. In the next step, the values of unmet load and CO_2 emission are sent to the optimization algorithm to check if the particle meets the desirable level of unmet load and CO_2 emission. If the particle did not meet the constraints, it is modified and sent back to simulation. After initializing feasible particles, they are evaluated in the PSO algorithms based on their fitness. A stopping criterion is checked, if it is not met, each particle is updated for the next generation in the framework of the PSO algorithm, Section 2.7.3 and Figure 2-4. After updating, the particles are sent back to the simulation module to review their feasibility again and the simulation result is sent to the

optimization algorithm for evaluation. This cycle is terminated if the stopping criterion is met. After terminating the cycle, the best of all considered solutions will be returned.

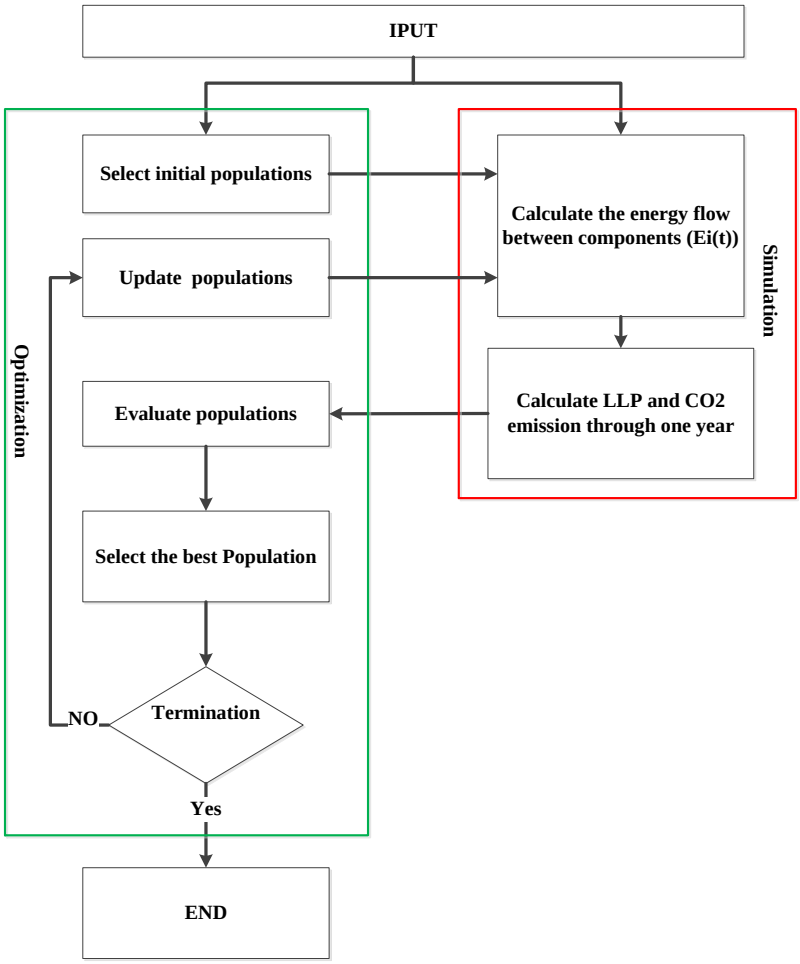

Figure 2-2: PSO-simulation based approach flowchart

2.6. Simulation Module

As mentioned in the previous section, the simulation is run for checking the feasibility of a particle that represents a certain configuration of the HRES for one year. The simulation output is the yearly unmet load and CO_2 emission for that HRES configuration. The considered HRES in this paper is depicted in Figure 2-1. The HRES includes seven main components comprising PV/wind turbine/diesel/batteries/FC/electrolyzer/H_2-tank. The simulation module is based on the

hourly time interval analysis of electricity demand, wind speed, and solar irradiation. The wind model converts the hourly wind velocity to energy output. Similarly, the PV panels convert total radiation on the horizontal surface to energy output. The diesel model uses the fuel consumption curve data, for a given choice of diesel generator, to calculate its output. The electrolyzer model calculates the hydrogen production by using coefficients of its electrical consumption curve. The FC model uses the hydrogen consumption curve to calculate the hydrogen consumed from the hydrogen tank. The battery and hydrogen tank models use the excess energy and deficit energy to update the battery state of charge and hydrogen level, respectively. The components mathematical models which are used in the simulation are summarized below.

- Wind turbine: Essentially in wind turbines, wind power generation is produced from conversion of wind kinetic energy into electrical energy. Energy resulted from a wind turbine is calculated by Equation (2-1) [10, 31].

$$\mathrm{E_{WG}(t)} = \begin{cases} 0 & V < V_c \\ \frac{1}{2} C_p \, \rho A_{WG} V^3(t) \;\; \Delta \mathrm{t} & V_c < V < V_r \\ P_{WG,r} & V_r < V < V_f \\ 0 & V > V_f \end{cases} \tag{2-1}$$

Wind speed for each time period *V(t)* is as an input of the model. C_p is the coefficient of performance and it is defined as the ratio of the power output of a wind generator divide by maximum power. It is a characteristic of wind turbines obtained from the manufacture firm. The rotor swept area is named A_{WG} and the air density is equal to ρ. V_c is cut-in wind velocity which is considered 4 (m/s). V_r is rated wind velocity is set as 14 (m/s) and V_f is cut-off wind speed considered 20 (m/s) [21]. $P_{WG,r}$ is the wind turbine rated power [21].

- PV panel: Solar or photovoltaic cells are electronic devices that convert solar energy of sun light into electricity. Produced energy by PV panels is calculated by Equation (2-2) [10].

$$E_{PV}(t) = \left(\eta_{pv} A_{PV}\right) I_T(t) \quad (2\text{-}2)$$

where, *I(t)* is the hourly total solar radiation on tilted surface, η_{pv} is PV modules efficiency and A_{PV} stands for the PV panels area(m^2). In this study, η_{pv} is assumed to be constant and is equal to 7%. This value covers power losses in PV panels due to temperature change, shadows, dirt, and losses in inverter. Solar radiation on a tilted surface having a tilt angle of ϕ from the horizontal surface and an azimuth angle of ξ is the sum of components consisting of beam ($I_{b,tilt}$), sky diffuse ($I_{d,tilt}$) and ground reflected solar radiation ($I_{r,tilt}$) [32]:

$$I_T = I_{b,tilt} + I_{d,tilt} + I_{r,tilt} \quad (2\text{-}3)$$

$$I_T = I_{tilt} = I_{b,n}[cos(\theta) + C\, cos^2\left(\frac{\phi}{2}\right) + \rho(cos\chi + C)sin^2\left(\frac{\phi}{2}\right)] \quad (2\text{-}4)$$

where, $I_{b,n}$ is direct normal irradiance on a surface perpendicular to the sun's rays, θ is the angle between the tilted surface and the solar rays which is calculated by Equation (2-5), *C* is diffuse portion constant for calculation of diffuse radiation, ρ is the reflection index, and χ is the zenith angle.

$$\cos(\theta) = [\cos\phi\ \cos\chi + \sin\phi \sin\chi \cos(\xi - \zeta)] \quad (2\text{-}5)$$

ξ and ζ are stand for sun azimuth and plate azimuth angle, respectively. The Equation (2-6) and Equation (2-7) are used to calculate the sun zenith and azimuth angle [32]:

$$cos\,\chi = sin\,\delta\, sin\,\lambda + cos\,\delta\, cos\,\lambda\, cos\,\alpha \quad (2\text{-}6)$$

$$tan\,\xi = \frac{sin\,\alpha}{sin\,\lambda\, cos\,\alpha - cos\,\lambda\, tan\,\delta} \quad (2\text{-}7)$$

Where, δ is solar declination angle and is calculated by Equation (2-8), λ is latitude per degree and α is solar angle which is determined by using Equations (2-9) to (2-12) [32].

$$\delta = 23.44\ sin[360(\frac{d-80}{365.25})] \quad (2\text{-}8)$$

$$\alpha = \frac{360}{24}(t-12) \quad (2\text{-}9)$$

$$t = LST + EOT - 4L_{local} + 60t_{zone} \quad (2\text{-}10)$$

$$B\ =\ 360(n\ -\ 81)/364 \quad (2\text{-}11)$$

$$EOT\ (minutes) = -(9.87\ sin\ 2B - 7.53\ cos\ B - 1.5\ sin\ B) \quad (2\text{-}12)$$

where, *d* is the number of day when January 1st is equal to one. *t* is solar time and identified by Equation (2-10) [32]. *LST* is local standard time or real time; *EOT* is equation of time to account for irregularity of the earth speed around the sun (minutes); L_{local} is local longitude (degrees East> 0 and West < 0) and t_{zone} is the time zone difference compared to GMT (East > 0 and West < 0) [32].

- Electrolyzer: In electrolyzer, hydrogen and oxygen gases are generated from water by using electrical energy. In this study, the electrolyzer electrical consumption ($Elec_{EL}$) is modeled as a function of nominal hydrogen mass flow (Q_{n-H2}) and actual hydrogen mass flow (Q_{H2}) as given in Equation (2-13) [21]:

$$Elec_{EL} = \alpha_E Q_{n-H2} + \beta_E Q_{H2} \quad (2\text{-}13)$$

where, α_E and β_E are the coefficients of electrical consumption curve per hydrogen mass flow. The electrolyzer efficiency is defined as the heating value of produced hydrogen divide by electrical consumption, Equation (2-14) [21].

$$\eta_{El} = \frac{Q_{H2} \times HHV_{H_2}}{\mathrm{Elec_{EL}}} \quad (2\text{-}14)$$

In this study, HHV_{H_2} is set at 39.4 kWh/kg, $\alpha_E = 20$ kWh/kg , and $\beta_E = 40$ kWh/kg [21].

- Fuel cell: Fuel cells which convert the chemical energy of hydrogen and oxidant to electrical energy are selected as a backup generator. The output power of a fuel cell can be expressed as a function of the hydrogen consumption of fuel cell ($H2_{cons-FC}$), Equation (2-15) [21].

$$\begin{cases} H2_{cons-FC} = \alpha_{FC} P_{n-FC} + \beta_{FC} P_{a-FC} & if \ \dfrac{P_{a-FC}}{P_{n-FC}} \leq n_{\max-FC} \\ H2_{cons-FC} = \alpha_{FC} P_{n-FC} + \beta_{FC} P_{a-FC}\left(1 + f_{FC}\left(\dfrac{P_{a-FC}}{P_{n-FC}} - n_{max-FC}\right)\right) & if \ \dfrac{P_{a-FC}}{P_{n-FC}} \geq n_{\max-FC} \end{cases} \quad (2\text{-}15)$$

Where, α_{FC} and β_{FC} are the coefficients of hydrogen consumption curve, which are defined by users. $P_{n-FC}(kw)$, $P_{a-FC}(kw)$ are the nominal output power and actual power of fuel cell. $n_{\max-FC}$ in % of P_{n-FC} is the power that FC has maximum efficiency and f_{FC} is a constant. In this study, $\alpha_{FC} = 0.004 kg/kwh$, $\beta_{FC} = 0.05 kg/kwh$, $f_{FC} = 1$. η_{FC} is the energy efficiency of FC and it is defined by Equation (2-16) [21, 22, 24].

$$\eta_{FC} = \frac{P_{a-FC}}{H2_{cons-FC} \times LHV_{H_2}} \quad (2\text{-}16)$$

Diesel generator: Diesel generator sets are used as emergency power-supply. In this study, the fuel consumption of a diesel generator depends on the generator size and the load at which the generator is operating. The fuel consumption of a diesel generator is approximated by Equation (2-17) [21].

$$fuel_{cons} = \alpha_{DG} P_{n-DG} + \beta_{DG} P_{a-DG} \quad (2\text{-}17)$$

where ,α_{DG} and β_{DG} are the coefficients of fuel consumption curve, P_{n-DG} and P_{a-DG} are nominal capacity and power output of the diesel generator, respectively. In this study, $\alpha_{DG} = 0.081451\ l/kwh$ and $\beta_{DG} = 0.2461\ l/kwh$. The diesel generator efficiency, η_{DG}, is defined as power output divide by heating value of fuel consumption [21].:

$$\eta_{DG} = \frac{P_{a-DG}}{fuel_{cons} \times LHV_{Gas\ oil}} \quad (2\text{-}18)$$

where, $LHV_{Gas\ oil}$ is the lower heating value of gas oil and it is equal to 10-11.6 kWh/lit [21].

- Battery: The state of charge of battery at any time step is calculated by using following equation [22]:

$$SOC(t) = SOC(t-1) \pm \frac{E_{bat}(t)\eta_{bat}}{P_{bat}}.100 \quad (2\text{-}19)$$

Positive sign is for charging modes and negative one is for discharging. $SOC(t)$ and $SOC(t-1)$ are the state of charge of batteries in time step *t* and *t*-1, $\eta_{bat}$is the batteries round trip efficiency, $E_{bat}(t)$ is power charged or discharged from the batteries during time step *t* and P_{bat} (kWh) is nominal capacity of the batteries. The batteries can supply energy to demand until the lower limit of SOC_{min}. Moreover, the batteries can be charged until SOC_{max} is reached. In this study, η_{bat} is considered 80% in charging state and 100% in discharging state, $SOC_{min} = 30\%$ and $SOC_{max} = 100\%$ [22].

- Hydrogen tank: Hydrogen level of the H_2-tank at time step *t* depends on hydrogen level at time *t*-1 ($H_{2_{level}}(t-1)$), output hydrogen mass flow of the electrolyzer at time step *t* (Q_{H2}), and hydrogen consumption of the FC at time *t*, ($H2_{cons-FC}(t)$), i.e. [11]:

$$H_{2_{level}}(t) = H_{2_{level}}(t-1) + Q_{H2}(t) - \frac{H2_{cons-FC}(t)}{\eta_{H2\_tank}} \quad (2\text{-}20)$$

where, η_{H2_tank} represents the storage efficiency which is indicated losses associated with leakage and pumping. In this study, η_{H2_tank} is assumed 95%. Furthermore, there is upper and lower limit for hydrogen level. The upper limit is the nominal capacity of tank and lower limit is considered 5% of the rated capacity

- Dispatch strategy: When produced energy by the wind turbine and PV panels is more than the electricity demand, excess energy is sent to the storage systems. First, the excess energy put into batteries until the SOC_{max} is reached, if there is excess energy yet, the excess energy is converted to H_2 in the electrolyzer and then sent to the H_2-tank for storage purpose. In other words, the batteries have the highest priority for charging. If the produced renewable energy is less than the required energy, the batteries and fuel cell are respectively used to provide the difference in power. If the power shortage exceeds the stored power in both storage devices, the diesel generator is used to keep the load as fulfilled. If this shortage goes beyond the generator rated capacity, the shortage is considered as unmet load. After discharging the storage level of the batteries and H_2-tank are updated, Equation (2-19) and Equation (2-20).

- LLP and CO_2 emission: As the most of the exhaust gases of the diesel generator is CO_2, in this study the number of kg produced CO_2 by the diesel generator is considered to represent the pollutant emission. For each time period during one year the shortage of energy, loss of load probability (LLP) and CO_2 emission are calculated by using Equations (2-21) and (2-22) [21, 22].

$$\text{LLP} = \frac{\sum_{t=1}^{8760} shortage\ (t)}{\sum_{t=1}^{8760} D\ (t)} \tag{2-21}$$

$$CO2_{emission} = \sum_{t=1}^{8760} fuel_{cons}(t) \times EF \tag{2-22}$$

where, *D(t)* is electricity demand, and *shortage(t)* is unmet load during time period *t*, EF is the emission factor for the diesel generator, which depends on the type of the fuel and diesel engine characteristics. Here, that is considered as 2.4-2.8 kg/lit rang [21].

2.7. Optimization Module

2.7.1. ε-Constraint Method

ε-constraint method is a simple MOP technique that can be used where one objective is chosen to be optimized and the resting objectives are considered as constraint bounds by given target levels (ε_i) [25]. By varying these levels, the non-inferior solutions of the introduced problem can be obtained. Consider the following MOP:

Min $\{f_1(x), f_2(x), \dots, f_k(x)\}$

where, x is the decision vector, f_i (i=1, 2, . . ., k) are the objective functions. A solution x^* is noted as non-dominated or non-inferior if there is not another feasible solution x such that $f_i(x) \leq f_i(x^*)$ for all i=1, 2, . . ., k, and at least one inequality is strict.

In ε-constraint method, if $f_j(x),\ j \in \{1,..,k\}$ is the objective function that is examined to be minimized, and $f_i(x)$ is the objective considered as the constraint, we have the following problem [25, 26]:

Min $f_j(x) \quad j \in \{1,..,k\}$

Subject to

$f_i(x) \leq \varepsilon_i \ \ \forall\, i \in \{1,..,k\}, i \neq j\ , x \in S$

where, S is the feasible solution space, k represents the number of objective functions, and ε_i is assumed the value of the objective function that must not be exceeded.

In this paper, three objective functions are considered. These three objective functions are minimizing total net present cost of the system, total CO_2 emissions produced by the diesel generators, and LLP. The overall cost of the system includes the investment costs, operation and

maintenance costs, replacement costs, and fuel costs of diesel generators during the lifespan of the system. LLP represents the energy deficit, which is the ratio of unmet load to total load. In the proposed ε-constraint approach, total cost is chosen as the objective function to optimize and total CO_2 emission and LLP incorporate as inequality constraints in the forms: $CO2_{emission} \leq \varepsilon_{CO2}$ and $LLP \leq \varepsilon_{LLP}$. Hence, in this study, k=3, ε_{CO2} and ε_{LLP} are chosen by DMs as the desirable values.

2.7.2. Objective Functions and Constraints

As it was mentioned earlier, total cost over the life time of the HRES is considered as objective function and CO_2 emission and LLP during one year are considered as the constraint bounds. The life time of the system is considered 25 years the same as life time of the PV panels since this element has the longest lifespan [21]. Decision variables of the model are summarized in the following vector:

$$P = [P_{PV}, P_{WG}, P_{bat}, P_{El}, P_{tank}, P_{FC,} P_{Dis}]$$

where, P_{WG} is the capacity of the wind turbine (kW), P_{PV} is the capacity of PV panels (kW), P_{bat} is the capacity of batteries (kWh), P_{FC} is the capacity of the fuel cell (kW), P_{EL} is the capacity of the electrolyzer (kW), P_{tank} is the capacity of the H_2-tank (kWh), and P_{Dis} is the capacity of the diesel generator (kW). The system costs consist of investment costs, operation and maintenance costs, fuel costs, and replacement costs over the project life time, Equation (2-23).

$$Min\ cost = \sum_{j} [C_{I,j} + C_{O\&M,j} \times \frac{1}{CRF(i,T)} + C_{rep,j} \times K_j] \times P_j + C_{fuel} \times fuel_{cons,yr} \times \frac{1}{CRF(i,T)} \quad (2\text{-}23)$$

where, j is components indicator, $C_{I,j}$ is the capital cost per unit for the component j (€/unit), $C_{O\&M,j}$ is the operation and maintenance cost per unit for the component j (€/unit), C_{fuel} is the fuel cost (€/lit), $C_{rep,j}$ is the cost of each replacement per unit for the component j (€/unit), and $P_j \in \{P_{PV}, P_{WG}, P_{bat}, P_{El}, P_{tank}, P_{FC,} P_{Dis}\}$, $fuel_{cons,yr}$ is the annual fuel consumption (lit/year). K_j and CRF are single payment present worth and capital recovery factor, respectively, which are calculated using the following equations, Equations (2-24) to (2-26) [11, 21, 22].

$$K_j = \sum_{n=1}^{Y} \frac{1}{(1+i)^{L \times n}} \quad (2\text{-}24)$$

$$\begin{cases} Y = \left[\frac{T}{L}\right] - 1 & T\%L = 0 \\ Y = \left[\frac{T}{L}\right] & T\%L \neq 0 \end{cases} \quad (2\text{-}25)$$

$$CRF = \frac{i(1+i)^T}{(1+i)^T - 1} \quad (2\text{-}26)$$

where, i is the real interest rate, L and Y are life time and number of replacement of the component j, respectively, and T is the project life time which is considered 25 years in this study.

The problem constraints that should be met are: LLP of the system should be less than allowable LLP reliability index Equation (2-27). CO_2 emission should be less than allowable emission level, Equation (2-28). In addition, energy and storage level of components are subjected to some

other feasible operation constraints. The energy flow (energy produced by or entered to each component) in every time, $E_j(t)$, should be less than the capacity of the component, Equation (2-29). Δt is time interval that is one hour. As mentioned in Section 2.6, the batteries can supply energy to load until the lower limit of SOC_{min}, and can be charged until SOC_{max} is reached, Equation (2-30). Furthermore, there is upper and lower limit for hydrogen level which is presented in Section 2.6, Equation (2-31). Finally, there are non-negativity constraints for decision variables and energy flow as well as upper limit for decision variables, Equations (2-32) and (2-33).

$$LLP \leq \varepsilon_{LLP} \tag{2-27}$$

$$CO2_{emission} \leq \varepsilon_{CO2} \tag{2-28}$$

$$E_j(t) \leq P_j \times \Delta t \tag{2-29}$$

$$SOC_{min} \leq SOC(t) \leq SOC_{max} \tag{2-30}$$

$$H2_{level-min} \leq H2_{level}(t) \leq H2_{level-max} \tag{2-31}$$

$$0 \leq P_j \leq P_{max,j} \tag{2-32}$$

$$E_j(t) \geq 0 \tag{2-33}$$

2.7.3. Particle Swarm Optimization Algorithm

PSO, a meta-heuristic optimization technique, was firstly developed by Kennedy and Eberhart in 1995. PSO algorithm is able to solve continuous problems as well as binary or discrete problems. It is a "*multi-agent parallel search technique*" that is inspired by the social behavior of "*birds flocking*" or "*fish schooling*" [27]. In PSO, a set of particles or swarms which are described by their positions and velocity vectors fly through the search space following the current optimum

particle. Particles motions are defined by a vector, which defines the velocity of the swarm in each direction. The best solution for each particle obtained so far is stored in a particle memory and named particle experience. In addition, the best obtained solution among all particles so far is named the best global particle. The velocity and position of each swarm is updated according to its experience and the best global particle. The experience sharing of each particle with other swarms is the most important reason behind PSO success, and it leads the particle move to better region [27].

First a random population of swarms is generated with random position vectors ($\vec{x}$) and velocity vectors ($\vec{v}$). The fitness value of each particle is calculated to evaluate the current position of particles and compare it with its best experience and other swarms fitness value. If the current position of a swarm is indicated an improvement compared to best historically obtained one, the experience of the particle is adjusted. Moreover, the velocity of the particle is adjusted according to global best particle and its bests own experience. In fact, particles move toward the best global particle in the each iteration. Finally, the best global particle is updated, Figure 2-3.

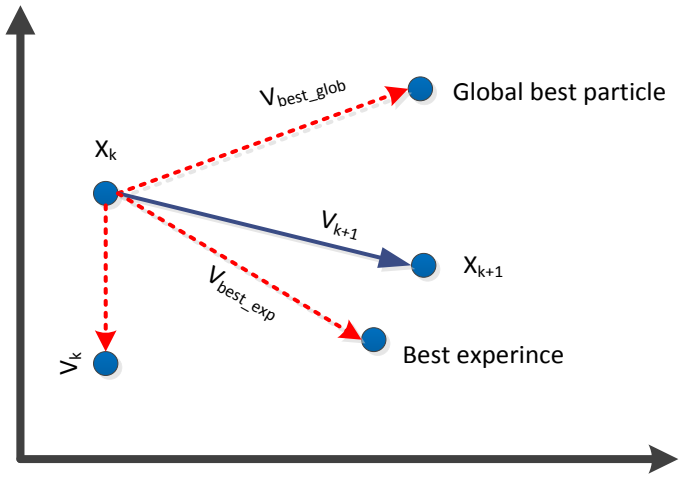

Figure 2-3: Dynamic of swarms in PSO

As mentioned earlier, two state variables are defined for the particles that are named current position $\overrightarrow{x_i}(t)$ and velocity $\overrightarrow{v_i}(t)$. The best experience for each particle is stored in the particle memory $\overrightarrow{p_i}(t)$ while $\vec{g}(t)$ denotes the best global particle among the population. In each iteration, the d[th] dimension of the position and velocity of the particles are updated toward the best experience and the best global particle by applying recursive Equations (2-34) and (2-35) [28].

$$v_{id}(t+1) = \omega . v_{id}(t) + C_1 . \varphi_1 . \left(P_{id}(t) - x_{id}(t)\right) + C_2 . \varphi_2 . \left(g_{id}(t) - x_{id}(t)\right) \quad (2\text{-}34)$$

$$x_{id}(t+1) = x_{id}(t) + v_{id}(t+1) \quad (2\text{-}35)$$

As seen from Equation (2-34), there are three terms to update the velocity; The first term, $v_{id}(t)$, stands for the inertia velocity and ω is called the inertia coefficient. This term is used to incorporate the previous velocity and consequently prevent the unexpectedly change of the particle velocity. That is the reason that particles broadly are biased to keep the direction that they have been moving on it. The parameters C_1 and C_2 are positive weighting constants, and denoted as the "*self-confidence*" and "*swarm confidence*", respectively. They control the movement of each particle towards its individual versus global best position. The parameters φ_1 and φ_2 are two uniform random numbers within interval (0 1) [28]. The first iteration is terminated after adjusting the velocities and positions for the next time step $t + 1$. Consistently, this process is executed till a determined stopping criterion is achieved. The stopping criterion can be the maximum number of time steps, improvement of the best obtained value for the objective function, or the average value that is calculated using the values of all population. Figure 2-4 shows PSO algorithm that is explained above.

Through the PSO algorithm, the critical parameters are ω, C_1, C_2 and the swarm size. These parameters are exogenous which are initialized by users before an execution. An optimal setting of the parameters depends on the problem at hand. According to literatures a suitable interval for setting PSO parameters are suggested as following:

- **Inertia weight ω:** the high settings in the range [0.5, 1] and near 1 facilitates global search [28].
- **Swarm size:** depending on problem search space, the number of particles can be in the range (20–60) [28].
- **Acceleration coefficients**: Usually an equal value of C_1 and C_2 is used within the range [0, 4] [28].

The above mentioned intervals are used in an exhaustive study to obtain the best values of these parameters. That is, the PSO parameters were changed in the intervals and the performance of PSO was monitored. The result of the study shows that the appropriate value for the parameters are at population size = 60, C_1 = 0.25, C_2 = 1.75, and ω=1. The maximum number of iteration is set to 1000.

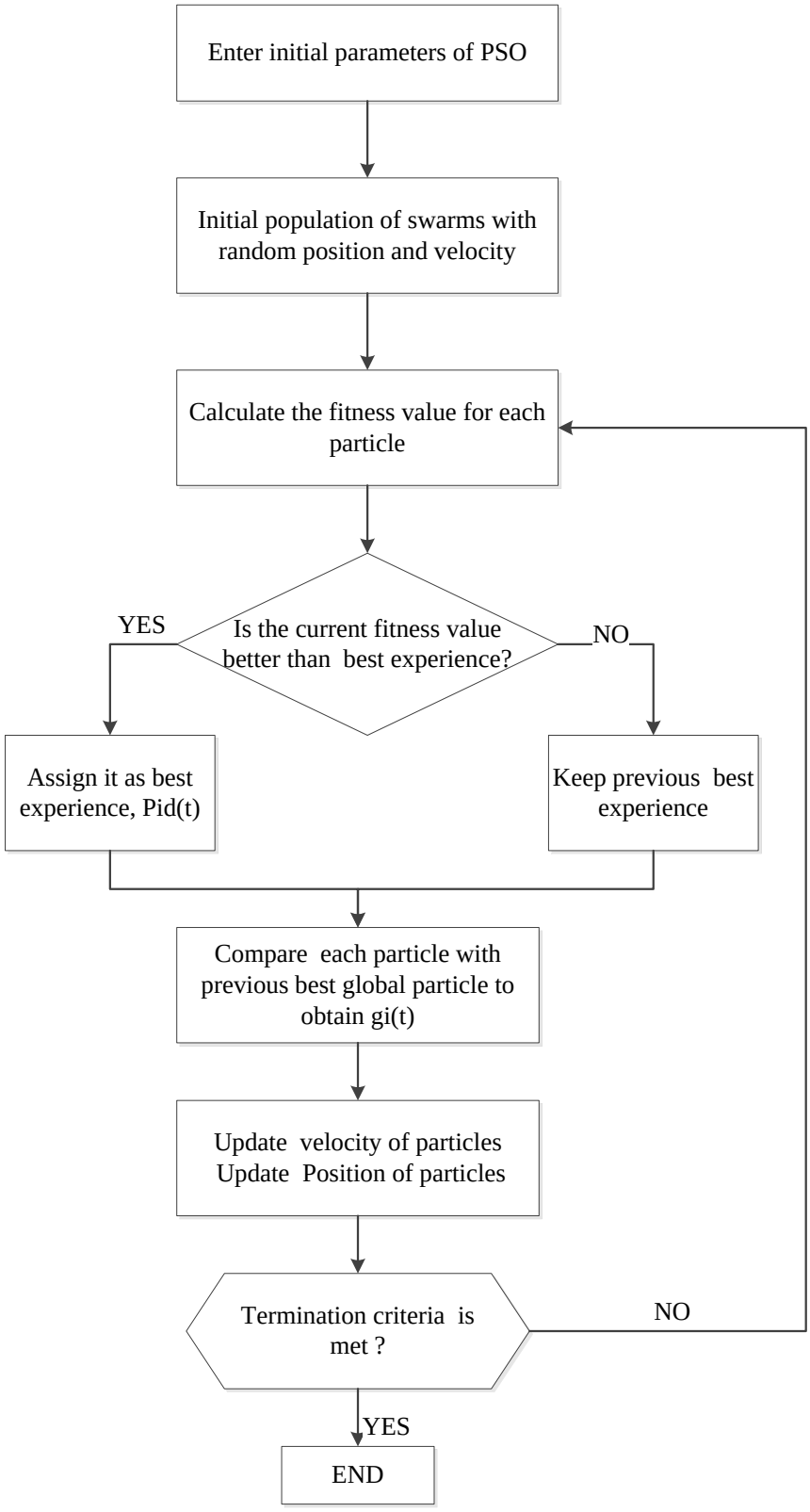

Figure 2-4: PSO algorithm flowchart

2.8. Results

The proposed approach was coded in C++ programming environment in a 2.4 GHz core 2 processor. By implementing the approach, a stand-alone hybrid system including PV panels/wind turbine/batteries/fuel cell/H_2 tank/ electrolyzer/diesel generator system has been designed to supply power for a small building located in a remote area at Zaragoza (latitude 41.65^0), Spain. Daily load variation during various seasons is shown in Figure 2-5. The time step is considered 1 hour and during this time step the wind energy, solar energy and load are assumed to be constant [21].

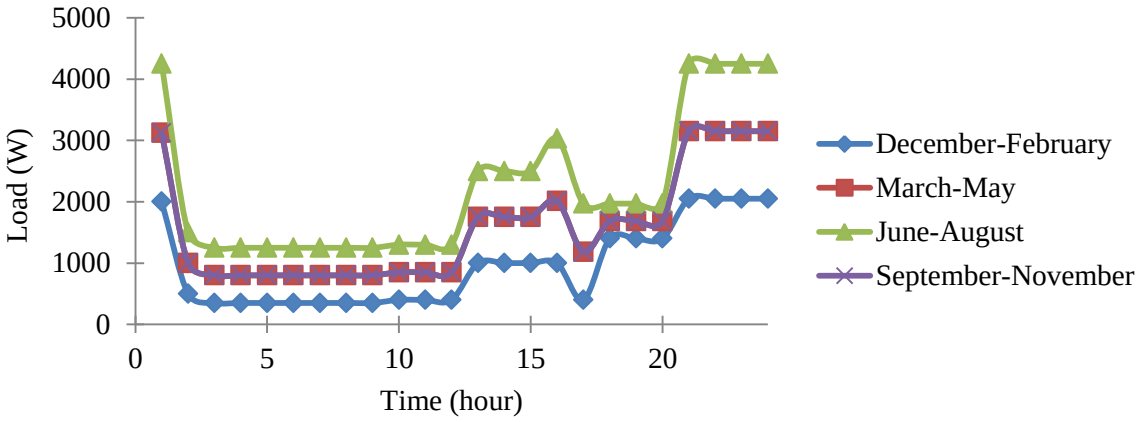

Figure 2-5: Daily load profile in the various seasons

The daily solar irradiation on the horizontal surface and wind speed data at 10 m height are plotted in Figure 2-6 and Figure 2-7 which are obtained by the average of last 10 years data.

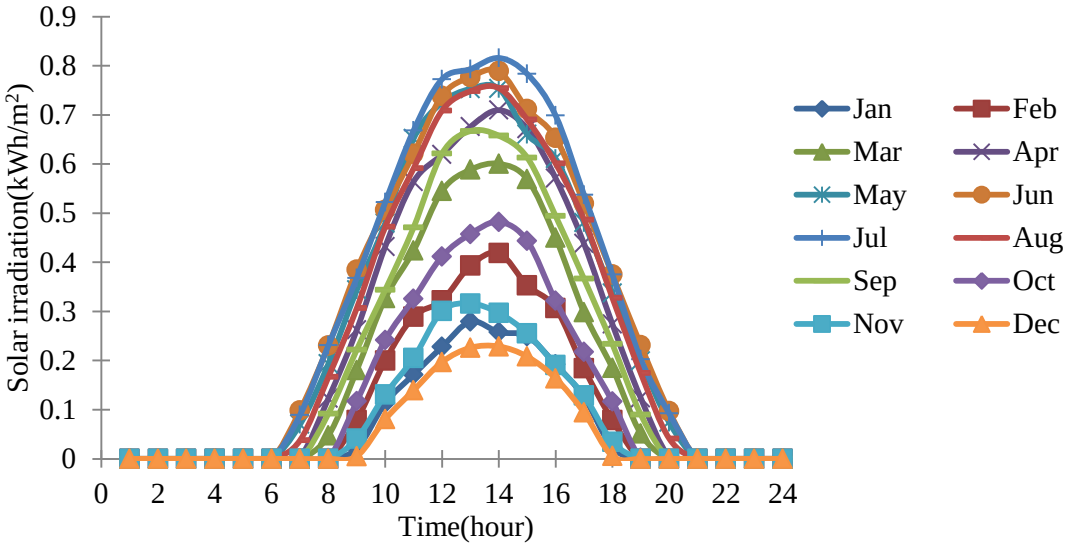

Figure 2-6: Hourly solar irradiation during one year

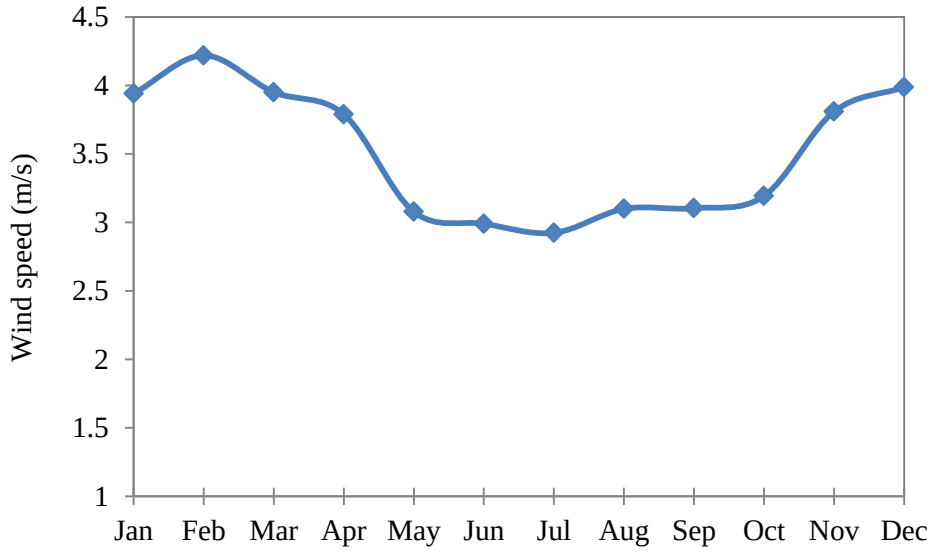

Figure 2-7: Average monthly wind speed at 10 m height during one year

The initial costs, operation costs, and the characteristics of components vary with their size and model. In this study, the initial costs, maintenance costs, and the characteristics of the components are presented in Table 2-2 and Figure 2-8 [11, 21, 22, 29].

Table 2-2: The characteristics of components

Components	PV panel	Wind turbine	Fuel cell	Electrolyzer	H_2 tank	Battery	Diesel generator
Life time	25yr	20yr	15000hr	10yr	20yr	5yr	7000hr

The initial cost of H_2-tank is assumed 1000€/kg, its operation and maintenance cost is 50€/year. The considered fuel is gas oil and its unit price is assumed as 1.2€/lit and the inflation rate is considered 10% [21].

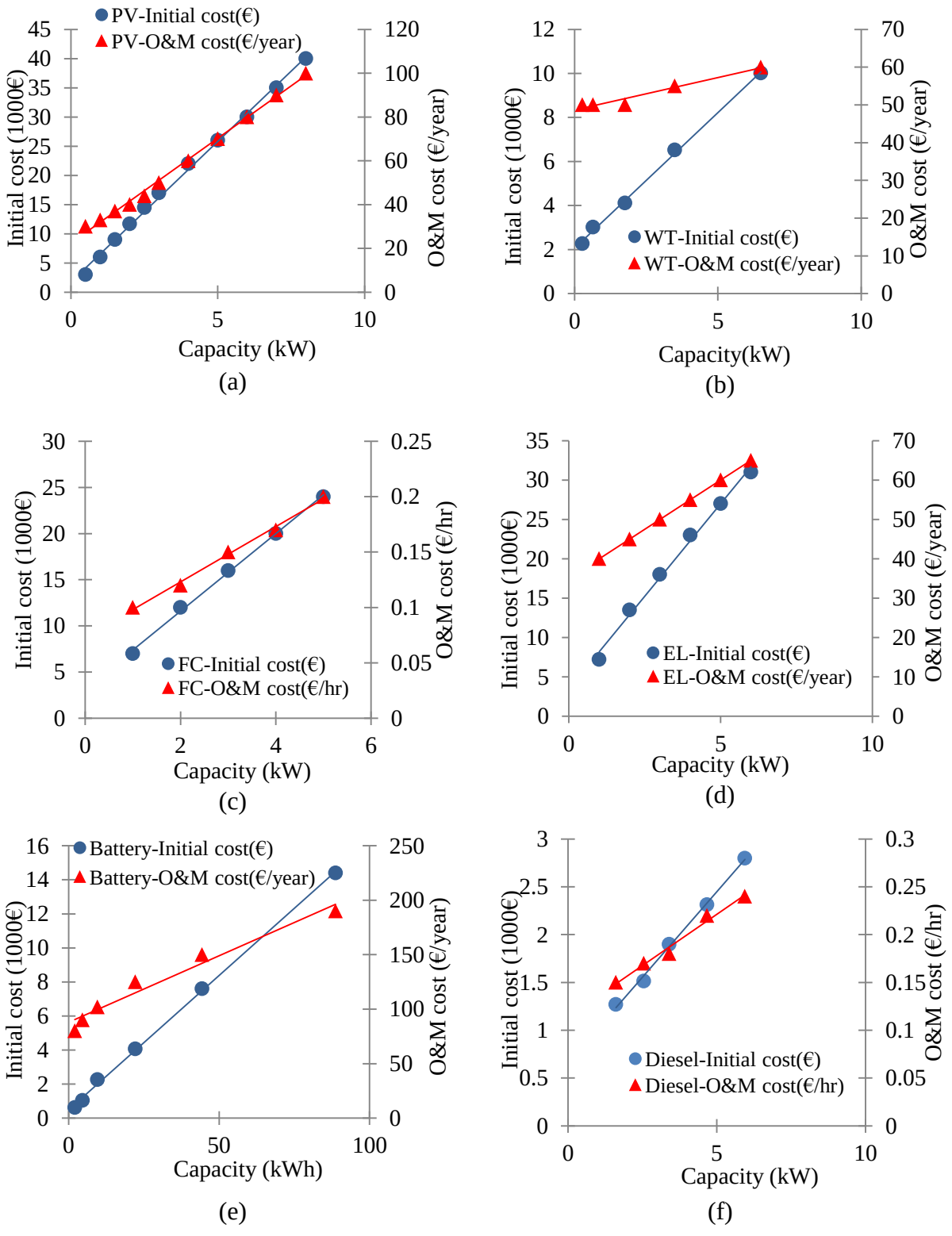

Figure 2-8: Components initial costs and operation and maintenance (O&M) costs: (a) PV panel costs, (b) Wind turbine costs, (c) fuel cell costs, (d) Electrolyzer costs, (e) Battery costs, (f) Diesel generator costs

The set of non-inferior solutions obtained by ε-constraint method is shown in Figure 2-9 to Figure 2-12. In these figures, there are 50 solutions in the non-inferior set which demonstrate the minimum total cost of the system for different LLP and CO_2 emission. The range of the objective space is obtained by varying ε_{LLP} and ε_{CO2}. It can be seen in these figures that CO_2 emission of the system decrease significantly as the LLP increase to about 0.15%. Increasing LLP of the system from 0.15% to 4.5% decreases the CO_2 emission moderately.

The Pareto front contains a large number of non-dominated points. Selecting a solution from such a large set is potentially difficult for a decision maker. In this study, the post-Pareto analysis is done for these 50 solutions, to provide the decision maker a workable sub-set of the solutions. The Post-Pareto analysis aids decision makers in choosing a single solution from a potentially large set of Pareto front. To find a representative subset of the solution set, first the objective values are normalized based on their maximum value among all non-dominated solutions. Six clusters are considered and the non-dominated solutions are distributed in these clusters such that objectives within the same cluster have a high degree of similarity. For distributing the solutions in the clusters, three cases are considered, first, the non-dominated solutions are ranked based on normalized cost, and then a cluster is assigned to each solution regarding its normalized cost. The best ranked solution in each cluster is selected and shown in Figure 2-13. Similarly, in the second case and the last one the solutions are ranked based on normalized LLP and normalized CO_2 emission, respectively. In these cases the best solution of each cluster is also depicted in Figure 2-14 and Figure 2-15, respectively. In Figure 2-13 to Figure 2-15 each line describes an objective function, and each index is devoted to a solution. The index 1 stands for the solution with the best rank based on the normalized objective function, while index 6 stands for the worst one.

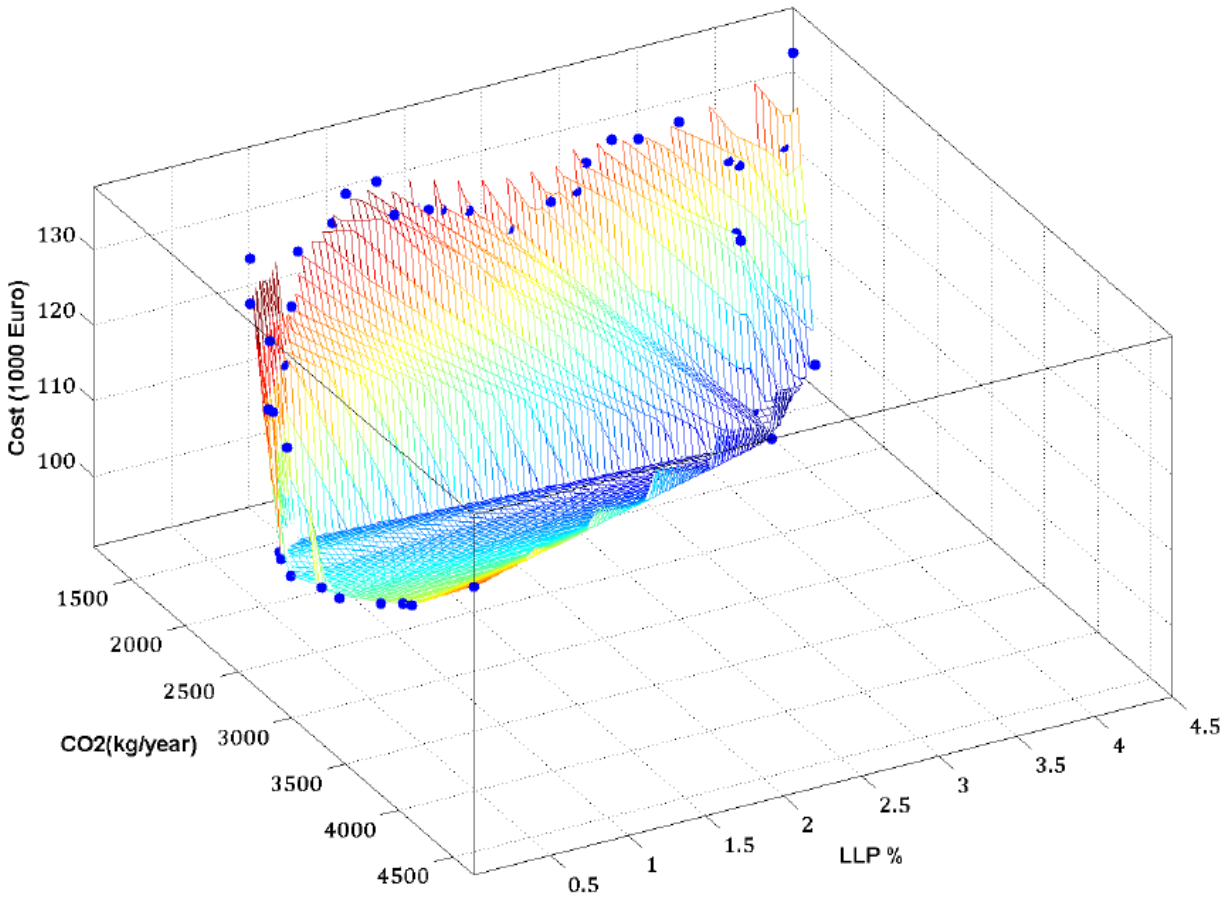

Figure 2-9: The 3D set of non-inferior solutions obtained by the ε-constraint method

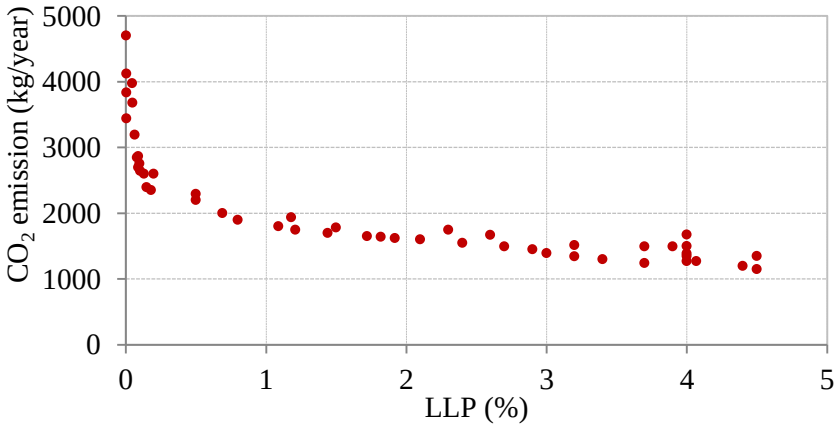

Figure 2-10: The 2D set of non-inferior solutions. CO_2 emission vs. LLP

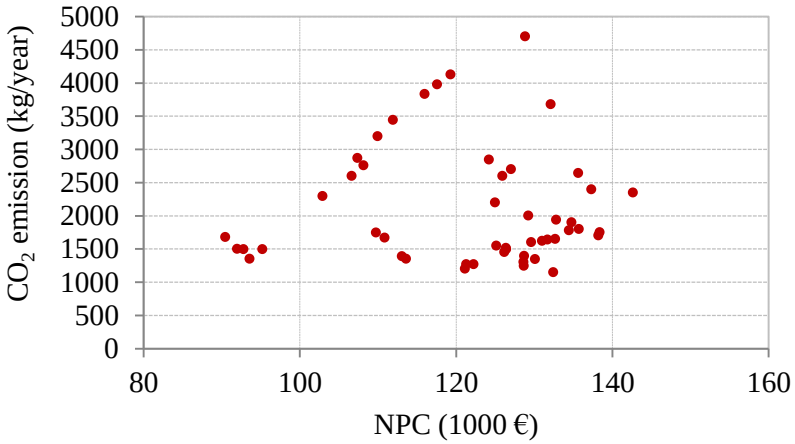

Figure 2-11: The 2D set of non-inferior solutions. CO_2 emission vs. NPC

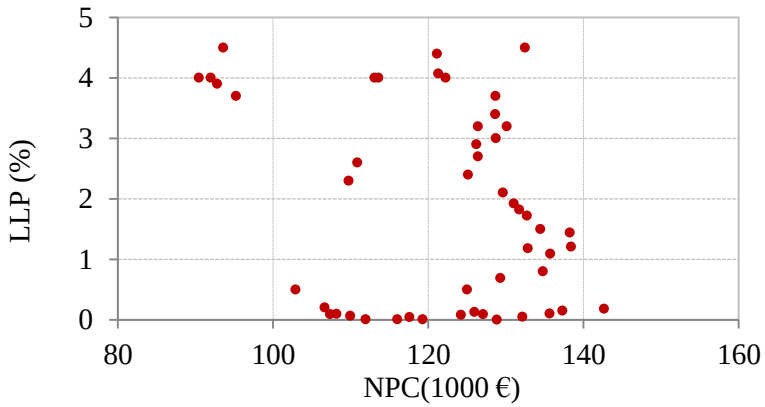

Figure 2-12: The 2D set of non-inferior solutions. LLP emission vs. cost

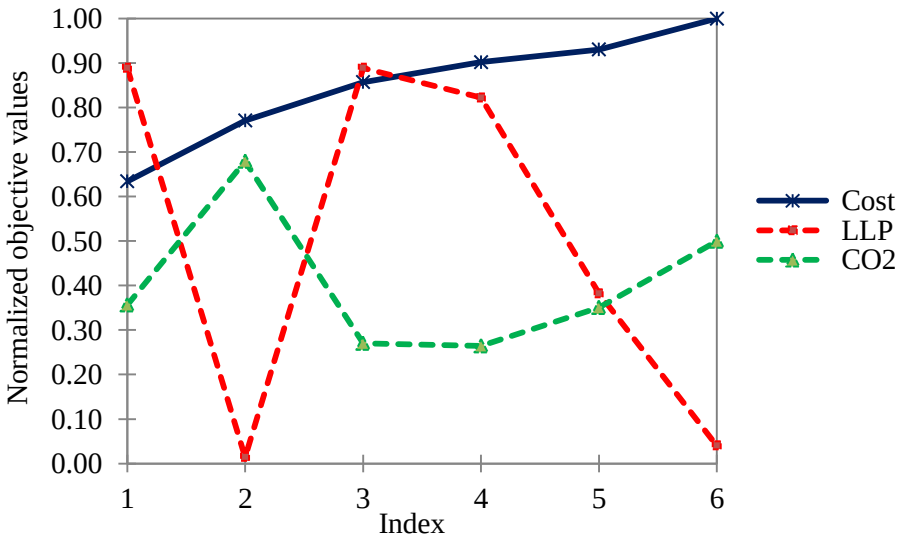

Figure 2-13: Pruned solutions when NPC objective function is preferred

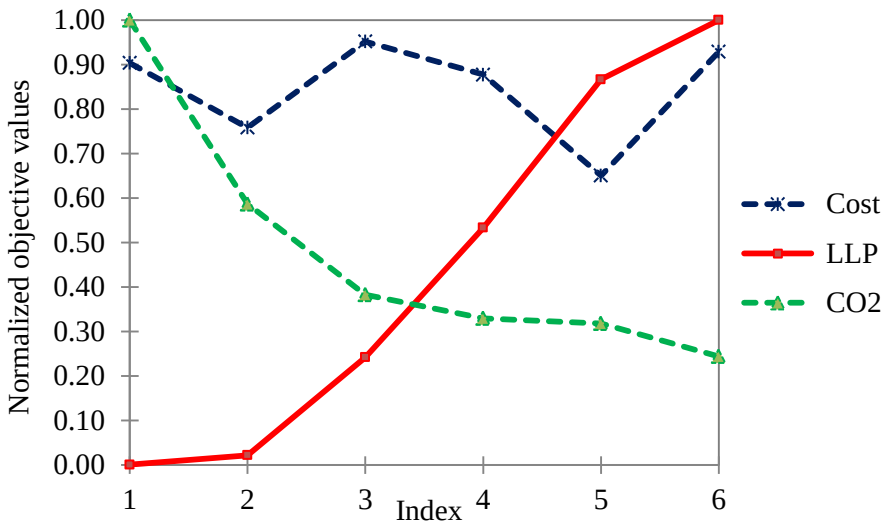

Figure 2-14: Pruned solutions when LLP objective function is preferred

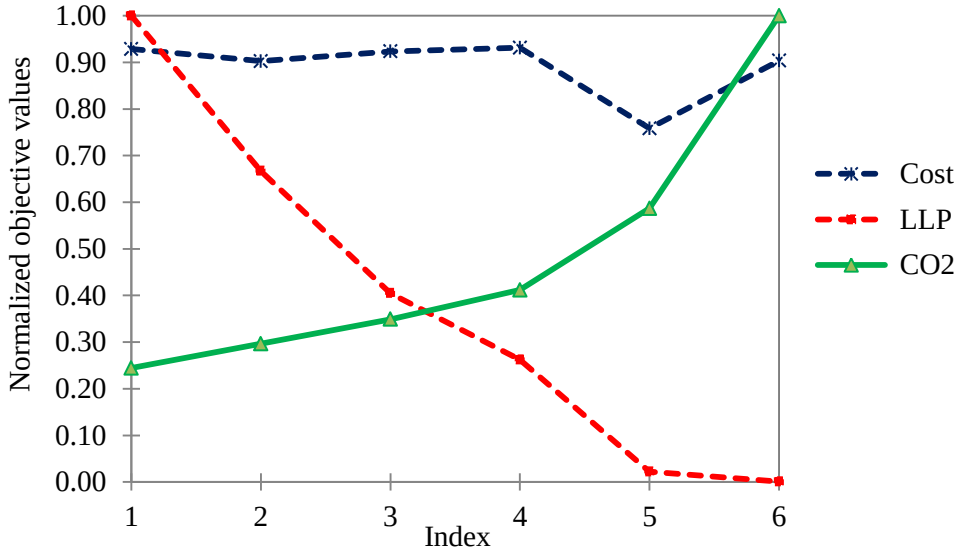

Figure 2-15: Pruned solutions when CO_2 objective function is preferred

For comparing the results of SPEA approach developed by [21] with the proposed approach, three cases which are mentioned in details by [21] are used. In these cases the desirable level for CO_2 emission and LLP are defined. In case 1: $\varepsilon_{LLP} = 4.5\%$, $\varepsilon_{CO2} = 1351$ kg/yr, in case 2: $\varepsilon_{LLP} = 0.5\%$, $\varepsilon_{CO2} = 2421$ kg/yr, finally in case 3: ε_{LLP} and ε_{CO2} are set as 1.8% and 1778 kg/year, respectively. For these cases, the proposed approach is employed to minimize total NPC of the system. The optimal size of the components and the corresponding total cost are presented

in Table 2-3 and Figure 2-16. It is noteworthy to mention that in this study the rectifiers cost, inverters and batteries charge regulator costs are neglected since the optimal sizing of these components are not considered. The result shows little contribution of hydrogen storage. One reason for this fact can be that hydrogen storage device is more expensive. In addition, the maximum overall energy efficiency of a hydrogen storage device is 28.9% which is less than batteries overall energy efficiency (80%).

Table 2-3: Optimal size of components in three illustrated solutions

		PV (kW)	Wind (kW)	Diesel (kW)	Fuel Cell (kW)	Battery (kWh)	Electrolyzer (kW)	H2-tank(kg)
Case 1	Proposed approach	8	6.5	1.8	0	66.4	0	0
	SPEA [21]	8	6.5	1.9	0	88.7	0	0
Case 2	Proposed approach	8	6.5	3.9	0	45.9	0	0
	SPEA [21]	8	6.5	4	0	44.3	0	0
Case 3	Proposed approach	8	6.5	3	0.11	88.7	1.1	4.2
	SPEA [21]	8	6.5	3	3	88.7	4	10

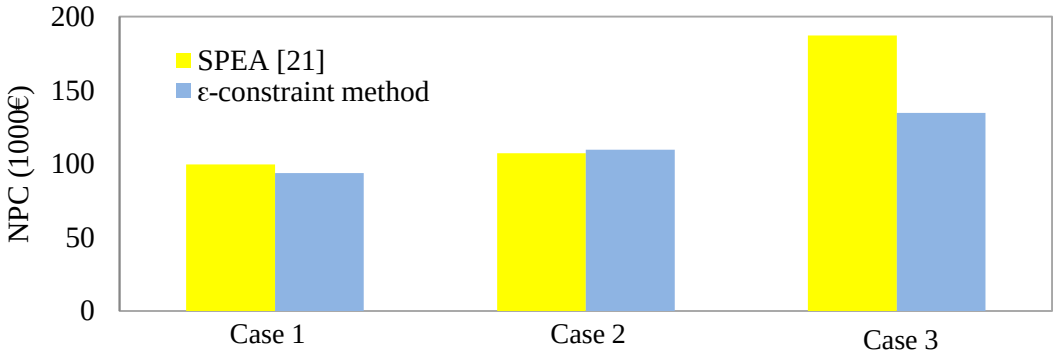

Figure 2-16: Optimal costs using ε-constraint method and SPEA [21]

Dufo et al. [21] utilized discrete values for decision variables while the proposed approach deals with continuous optimization problem; Hence, this fact can explain a slight difference between

the proposed model results and Dufo et al.[19] results in cases 1 and 2. As shown in Figure 2-16, it is observed that in the case 3, ε -constraint method yields a better cost (27% less) than SPEA.

Sensitivity analysis is the investigation of how the possible variation of the input parameters may impact the optimal solutions provided by the optimization algorithm under a given set of assumptions [33]. In a sensitivity analysis, the values of parameters or inputs are changed and resulted changes in performance indices are measured. Therefore, a main goal of a sensitivity analysis is to identify which parameters are the most sensitive and most likely to affect system behavior [33]. In this study, a sensitivity analysis is performed to investigate the effect of the input parameters on the optimal solution provided by the proposed approach in the case 1, if the parameters take other possible values. The considered parameters are the interest rate, PV panels capital cost, fuel cell capital cost, wind turbine capital cost, electrolyzer capital cost, battery capital cost, fuel price, battery life time, CO_2 emission and LLP allowable levels. The sensitivity analysis results of the case 1 are shown in Figure 2-17. The optimal solution for the case resulted in total cost of 93587€ for 25 years. The annual energy delivered to the load is 13407 kWh and the gas oil consumption is 562 lit/year. By creating 20 additional scenarios:

- 50% Increase scenarios for following parameters: interest rate, PV panel capital cost, fuel cell capital cost, wind turbine capital cost, electrolyzer capital cost, battery capital cost, fuel price, battery life time, CO_2 emission and LLP allowable level.
- 50% decrease on following parameters: interest rate, PV panel capital cost, fuel cell capital cost, wind turbine capital cost, electrolyzer capital cost, battery capital cost, fuel price, battery life time, 15% decrease on CO_2 emission allowable level, and 30% decrease on LLP allowable level.

The optimal configuration is remained unchanged in the 16 scenarios, which are 50% increase and 50% decrease scenarios for interest rate, PV panel capital cost, fuel cell capital cost, wind turbines capital cost, electrolyzer capital cost, battery capital cost, fuel price, and battery life time. A PV/wind turbine/battery/diesel system is resulted as the optimal configuration in these scenarios. The total cost approximately increases or decreases with the changes in these parameters while the components configurations are the same, Figure 2-17(a).

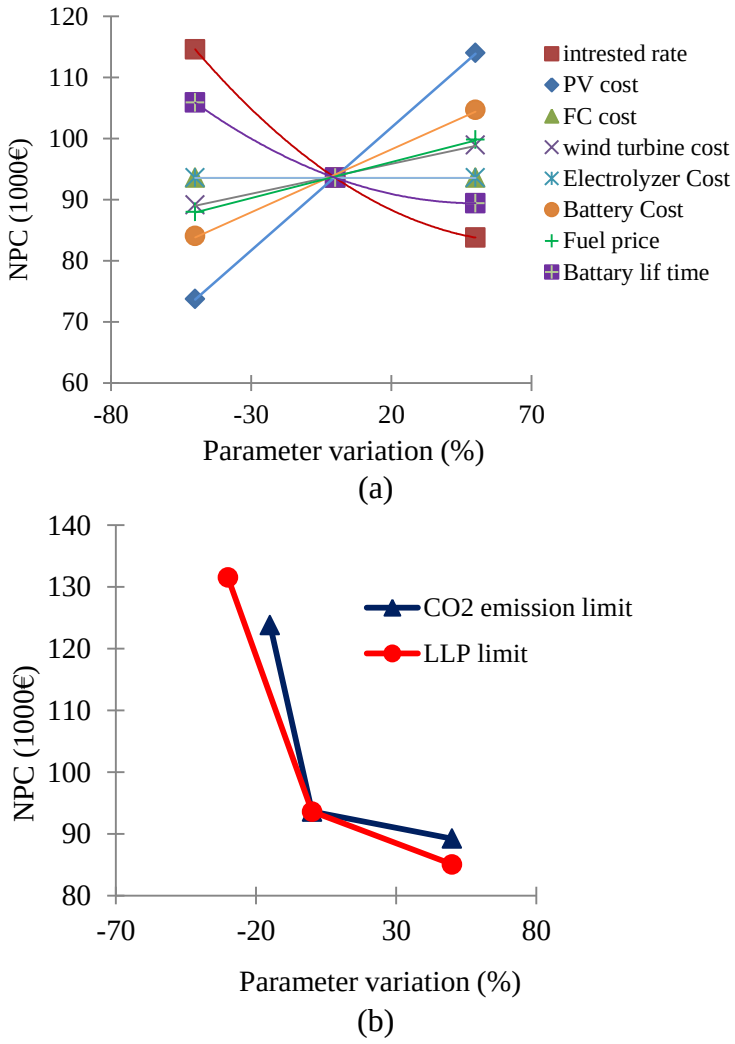

Figure 2-17: Sensitivity analysis result

With 50% increase in allowable level of LLP and CO_2 emission, the optimal configuration do not change. As it is obvious from the result, there is a reduction in total cost of the HRES since the

optimal value of decision variables is decreased. As these allowable levels decrease 50%, the current solution becomes infeasible. Figure 2-17 (b) shows that total cost significantly is increased when LLP and CO_2 emission allowable levels are decreased 30% and 15%, respectively. The result indicates that in these two scenarios, the optimal configuration is changed because satisfying the model constraints needs storing energy in hydrogen tank as well as using a fuel cell and electrolyzer that are inefficient than storing energy in batteries.

2.9. Conclusion

In this study, a novel and simple approach is presented to optimize the size of a hybrid renewable energy system. ε-constraint method has been applied to minimize three objectives: loss of load probability, CO_2 emission, and total net present cost of the system. The proposed tool used a PSO-based simulation method to solve the multi-objective optimization problem. The chief benefit of the proposed approach is its simplicity which leads to computational efficiency.

In a case study including a wind turbine, PV panels, a diesel generator, a fuel cell, an electrolyzer, batteries and a hydrogen tank the proposed approach is evaluated. By comparing the proposed approach results with the previous methods results, it has been concluded that an improvement in total cost is obtained while achieving same fuel emission and LLP. A sensitivity analysis study is performed to study the sensibility of the input parameters to the developed model. The sensitivity analysis indicates that if the life time of the batteries and interest rate are reduced, total cost is increased. Furthermore, total net present cost of the system is more sensitive to the allowable level of CO_2 emission compared to the other variables. The proposed model can be used in feasibility studies and the design of an HRES.

For future research, a detailed load analysis that takes into consideration the heat and electricity loads separately and load shifting would be performed to recommend an optimum system configuration that matches loads. In addition, uncertainties of the renewable energy sources availability and energy load will also be taken into account.

2.10. References

[1] Dufo-Lopez R, Bernal-Augstin JL, Contreras J. Optimization of control strategies for stand-alone renewable energy systems with hydrogen storage. Renewable Energy 2007; 32(7):1102–1126.

[2] Qinghai B. Analysis of particle swarm optimization algorithm. Computer and Information Science 2010; 3(1):180-184.

[3] Eke R, Kara O, Ulgen, K. Optimization of a Wind/PV hybrid power generation gystem. International Journal of Green Energy 2005; 2(1):57-63.

[4] Ludwig K, Bo Z, Grisselle C, Zhixin M. Stochastic optimization for power system configuration with renewable energy in remote areas. Annuals of operations Research 2012; 195:1-22.

[5] Garyfallos G, Athanasios IP, Panos S, Spyros V. Optimum design and operation under uncertainty of power systems using renewable energy sources and hydrogen storage. Hydrogen Energy 2010; 35(3):872-889.

[6] Akella AK, Sharma MP, Saini RP. Optimum utilization of renewable energy sources in a remote area. Renewable and Sustainable Energy Reviews 2007; 11(5):894–908.

[7] Hanane D, Ahmed O, Roberto S. Modeling and control of hydrogen and energy flows in a network of green hydrogen refueling stations powered by mixed renewable energy systems. Hydrogen Energy 2012; 37(6): 5360-5371.

[8] Cai YP, Huang GH, Tana Q, Yang ZF. Planning of community-scale renewable energy management systems in a mixed stochastic and fuzzy environment. Renewable Energy 2009; 34(7):1833–1847.

[9] Jeremy L, Marcelo GS, Abdellatif M, Philippe C. Energy cost analysis of a solar-hydrogen hybrid energy system for stand-alone applications. Hydrogen Energy 2008; 33(12):2871–2879.

[10] Orhan E, Banu YE. Size optimization of a PV/wind hybrid energy conversion system with battery storage using simulated annealing. Applied Energy 2010; 87(2):592–598.

[11] Kashefi A, Riahy GH, Kouhsari SM. Optimal design of a reliable hydrogen-based stand-alone wind/PV generating system, considering component outages. Renewable Energy 2009; 34(11):2380–2390.

[12] Raquel SG, Daniel W. A wind–diesel system with hydrogen storage: Joint optimization of design and dispatch. Renewable Energy 2006; 31(14):2296–2320.

[13] Iniyan S, Suganthi L, Anand AS. Energy models for commercial energy prediction and substitution of renewable energy sources. Energy Policy 2006; 34(17):2640–2653.

[14] Juhari AR, Kamaruzzaman S, Yusoff A. Optimization of renewable energy hybrid system by minimizing excess capacity. International Journal of Energy 2007; 3(1):77-81.

[15] Katsigiannis YA, Georgilakis PS. Optimal sizing of small isolated hybrid power systems using Tabu search. Optoelectronics and advanced materials 2008; 10(5):1241-1245.

[16] Budischak C, Sewell DA, Thomson H, Mach L, Veron DE, Kempton W. Cost-minimized combinations of wind power, solar power and electrochemical storage, powering the grid up to 99.9% of the time. Journal of Power Sources 2013; 225: 60-74.

[17] Elliston B, MacGill I, Diesendorf M. Least cost 100% renewable electricity scenarios in the Australian National Electricity Market. Energy Policy 2013. 59: 270–282.

[18] Banos R, Manzano F, Montoya FG. Optimization methods applied to renewable and sustainable energy: A review. Renewable and Sustainable Energy Reviews 2011; 15(4):1753–1766.

[19] Katsigiannis YA, Georgilakis PS, Karapidakis ES. Multi objective genetic algorithm solution to the optimum economic and environmental performance problem of small autonomous hybrid power systems with renewable. IET Renewable Power Generation 2010; 4(5):404–419.

[20] Trivedi M. Multi-objective generation scheduling with hybrid energy. PhD Dissertation, Department of Electrical Engineering, Clemson University, USA; 2007.

[21] Rodolfo DL, Jose LBA. Multi-objective design of PV–wind–diesel–hydrogen–battery systems. Renewable Energy 2008; 33(12):2559–2572.

[22] Abedi S, Alimardani A, Gharehpetian GB, Riahy GH, Hosseinian SH. A comprehensive method for optimal power management and design of hybrid RES-based autonomous energy systems. Renewable and Sustainable Energy Reviews 2012; 16(3):1577–1587.

[23] Jose LBA, Rodolfo DL. Efficient design of hybrid renewable energy systems using evolutionary algorithms. Energy Conversion and Management 2009; 50(3):479–489.

[24] Ganguly A, Misra D, Ghosh S. Modeling and analysis of solar photovoltaic-electrolyzer-fuel cell hybrid power system integrated with a floriculture greenhouse. Energy and Buildings 2010; 42(11):2036–2043.

[25] Kaveh KD, Amir-Reza A, Madjid T. A new multi-objective particle swarm optimization method for solving reliability redundancy allocation problems. Reliability Engineering and System Safety 2013; 111:58–75.

[26] Coello CC, Lamont GB, Van-Veldhuizen DA. Evolutionary algorithms for solving multi-objective problems. 2nd ed. New York: Springer; 2007.

[27] Hazem, A, Janice G. Swarm Intelligence: concepts, models and applications. Technical Report. School of Computing. Queen's University, Canada; 2012.

[28] Swagatam D, Ajith A, Amit K. Particle swarm optimization and differential evolution algorithms: Technical Analysis, Applications and Hybridization Perspectives. Studies in Computational Intelligence (SCI) 2008; 116:1–38.

[29] Ahmarinezhad A, Abbaspour-Tehranifard A, Ehsan M, Fotuhi-Firuzabad M. Optimal sizing of a stand alone hybrid system for Ardabil area of Iran. IJTPE 2012; 4(12):118-125

[30] Ranjithan SR, Chetan SK, Dakshima HK. Constraint method-based evolutionary algorithm (CMEA) for multi-objective optimization. Lecture Notes in Computer Science (LNCS) 2001; 1993:299–313.

[31] Francisco G. Design optimization of stand-alone hybrid energy systems. Msc thesis. Univesity of Porto, Portugal; 2010.

[32] Da-Rosa AV. Fundamentals of renewable energy processes. 2nd ed. Elsevier Academic Press ; 2009.

[33] Frederick S H, Gerald J L. Introduction to operations research. 9th ed. New York: Mc Graw Hill; 2010.

Chapter 3

A Dynamic MOPSO Algorithm for Multi-Objective Optimal Design of Hybrid Renewable Energy Systems

3.1. Abstract

In this paper, a dynamic multi-objective particle swarm optimization (DMOPSO) method is presented for optimal design of hybrid renewable energy systems. The main goal of the design is to minimize simultaneously total net present cost of the system, unmet load, and fuel emission. A simulation-based DMOPSO approach has been used to approximate a Pareto front to help decision makers in selecting an optimal configuration for an HRES. The proposed method is examined for a case study including wind turbines, photovoltaic panels, diesel generators, batteries, fuel cells, electrolyzers and hydrogen tanks. Well known metrics are used to evaluate the generated Pareto front. The average spacing and diversification metrics obtained by the proposed approach are 1386 and 4656, respectively. Additionally, the set coverage metric value shows that at least 67% of Pareto solutions obtained by DMOPSO dominate the solutions resulted by the other reported algorithms. By using a sensitivity analysis for the case study, it is found that if the PV panel and wind turbine capital costs are decreased by 50%, the total net present cost of the system would be decreased by 18.8% and 3.7%, respectively.

3.2. Introduction

Renewable energy resources are alternatives to replace fossil fuels considering they are inexhaustible and environmentally friendly. Utilization of RE resources has significantly increased since the oil crisis in the early 1970s. The common drawback identified with RE resources is that these sources are dependent on climatic conditions and naturally unpredictable [1]; Hence, stand-alone RE sources may not meet the hourly energy demand. Hybrid renewable energy systems are becoming popular for remote area power generation applications, which can reduce the impact of uncertainties in RE resources. The term HRES is used to describe any energy system with more than one type of generator [1]. For remote areas, HRES are often the most cost-effective and reliable way to produce power.

Most engineering problems need simultaneous optimization of many conflicting objectives. These require using a multi-objective optimization formulation to approximate a set of compromised solutions in the search space. The set of optimal solutions provides decision makers worthwhile information about all possible designs and help them to make a trade-off between different objectives and choose the best option [2]. In general, multi-objective optimization problems are difficult to implement and need expensive computation to find the set of optimal solutions [3]. Hence, recently the design of efficient and effective optimization algorithms for handling MOP has undergone important development.

Governments and companies face challenges regarding whether a given place is proper for establishing renewable energy systems or not, and which combination of renewable energy sources and what capacity is the optimal decision [4]. These challenges have motivated researchers to develop models for optimal design of HRESs. The optimal design of HRESs can make them cost-effective, reliable and environment friendly. The optimal design of an HRES

remains a complex problem due to precarious energy price, fluctuations in energy demand, and uncertainty in RE resources. Moreover, environmental issues are becoming increasingly important in designing an energy system [5]. In designing an energy system many aspects must be taken into account such as economic, environmental concern, reliability, and power quality. In order to handle such a complex problem, multi-objective optimization methods are employed, which tackle the issue of conflicting objective functions.

Although many authors used a single objective optimization for optimal design of an HRES and delivers promising results [6-15], most of the single objective methods do not address the emission effect and reliability analysis of HRESs. The application of multi-objective optimization methods in optimal design of an HRES is still in primary step of development as only few articles have been published in this area recently [4]. The relevant articles are reviewed in which MOP methods were used and divided them into two main categories: Pareto-based techniques and non Pareto-based techniques. The basic idea of Pareto-based techniques is that Pareto front (PF) is directly generated by using ranking and selection in population. It requires a ranking procedure and a technique to maintain diversity in the population. Non Pareto-based techniques are approaches that do not directly incorporate the concept of Pareto optimum [16]. Hongxing et al. [17] developed an optimal sizing method based on Genetic Algorithm (GA) to identify the optimum configurations of a hybrid solar–wind and battery system. The GA determined minimum annualized cost of system (ACS) with different customers required loss of power supply probability (LPSP). In other words, they performed a non-Pareto based approach to calculate total cost of system with a certain desired LPSP. Galvez et al. [18] used an enumerative optimization approach implemented in Hybrid Optimization Model for Electric Renewable (HOMER) program to carry out a multi-objective optimization of autonomous

systems with hydrogen storage. The enumerative search was used to generate a set of solutions to optimize the two objective functions, namely; net present cost and net avoided emissions in the system life cycle. They used a method called compromise programming to select the best alternative based on multiple criteria. In another similar study [19], they extended their work and compared two HRES in a rural university and in a rural community using multi-criteria analysis tool. They used compromise programming and take into account the technical, economic, environmental and social criteria. A heuristic methodology is presented by Protogeropoulos et al. [20] for sizing a renewable power supply systems including PV panels and wind turbines. The least expensive system configurations were found by their optimization approach, which achieves the required autonomy levels. Despite its simplicity, their approach like other non-Pareto approaches suffer from several drawbacks; this approach needs huge efforts to generate a PF as it only returns a single solution at the end of their search process.

Katsigiannis et al. [21] developed a multi-objective optimization model to generate a PF to minimize total cost of energy and total greenhouse gas emissions of an HRES during its lifetime by using non-dominated sorting genetic algorithm (NSGA). In [22] multi-objective genetic algorithm (MOGA) was applied to deal with a nonlinear multi-objective optimization problem for scheduling a wind/diesel system, which aims to minimize fuel cost as well as SO_2 and NO_x emission. Rodolfo et al. [23] applied a strength Pareto evolutionary algorithm (SPEA) to determine the optimal size and optimal power management strategy parameters for an HRES with the aim of minimizing total cost, unmet load, and fuel emission simultaneously. Abedi et al. [24] presented a MOP to minimize simultaneously total cost, pollutant emissions, and unmet load of an HRES. For this task, differential evolution algorithm (DEA)/fuzzy techniques have been used to find the best combination of the components and control strategies for the HRES. In

another research, Ould Bilal et al. [25] carried out an optimal sizing of an HRES including solar–wind–battery system for the Potou site in the North Coast of Senegal. They used multi-objective genetic algorithm with two objectives: minimization of the annualized cost of the system and minimization of loss of power supply probability. Shi et al. [26] used a multi-objective genetic algorithm (non-dominated sorting genetic algorithm, NSGA-II) to find a set of Pareto-optimal solutions in a single run for optimization of isolated hybrid systems. They tested the proposed method on a hybrid PV-wind-battery power system using total system cost, autonomy level and wasted energy as the objective functions.

In brief, few articles applied MOP to design an HRES usually using Pareto-based techniques which require ranking and pairwise comparison operations. Most of them used the well-known MOP algorithms without modifications while an efficient meta-heuristic algorithm requires modifications to be adapted for a specific problem. In addition, there is a lack of generating a high performance PF. That is, the quality of PFs is not discussed in the previous studies. The quality of a PF reflects its characteristics such as diversity of points and uniformity of points over the non-dominated set [16]. However, there is a need for using quantitative measures to evaluate the quality of approximate PF sets.

In this paper, a novel approach is established for optimal design of an HRES including various generators and storage devices. A dynamic multi-objective particle swarm optimization algorithm which is a Pareto-based search technique has been proposed to minimize simultaneously total net present cost of the system, unmet load, and fuel emission. The attractive features of this approach are generating a higher performance PF than well-known MOP approaches. It means the outcome PF is assigned a vector of real numbers that reflect different aspects of the quality for comparing the obtained result by different algorithms. Furthermore, the

generated PF is exhibited by an innovative way, which significantly helps DMs in interpreting its attributes. The flexibility in considering more renewable sources and storage devices as well as more precise models for the components is another advantage of the model.

This paper is adopted from the previous work developed by the authors [27] in which ε-constraint method was proposed for optimal design of an HRES. In the previous work, the used mathematical models in the simulation module and the optimization problem are demonstrated. In this study, the chief aim is to design an efficient and effective Pareto-based MOP algorithm to generate a Pareto front with high quality.

The basic concepts for the multi-objective optimization problems are introduced in Section 3.4. Section 3.5 is devoted to the problem description. The solution approach and the proposed multi-objective PSO algorithm are described in Sections 3.6 and 3.7. The used performance metrics to assess the PF quality are introduced in Section 3.8. The results of optimizing a case study along with sensitivity analysis result are exhibited in Section 3.9. Finally, conclusion and future research are given in Section 3.10.

3.3. Nomenclature

C_I	Investment cost [€/unit]	$H2_{level-m}$	Hydrogen upper limit level in the H_2-tank [m^3]
$C_{O\&M}$	O& M cost [€/unit]	i	Interest rate [%]
C_{rep}	Replacement cost [€/unit]	K	Single payment worth
CRF	Capital recovery factor	K_i	Number of cells designed for i^{th} dimension
C_{fuel}	Fuel cost [€/lit]	N	Number of solutions
C	Constant weighting parameter	LLP	Loss of load probability [%]
$CO2_{emission}$	System CO_2 emission [kg/year]	P_{PV}	PV panels capacity [kW]
C_s	Sigmoid function	P_{WG}	Wind turbines capacity [kW]
D	Hourly energy demand [kWh]	$P_{WG,r}$	Wind turbine rated power [kW]
d_i^g	Cell width of the i^{th} objective Dimension of g^{th} generation	P_{bat}	Battery capacity [kWh]
DiM	Diversification metric	P_{El}	Electrolyzer capacity [kW]
$E_j(t)$	Energy produced by or entered in the component j [kWh]	P_{tank}	H_2-tank capacity [kW]
E_{PV}	Energy produced by PV panels [kWh]	P_{FC}	Fuel cell capacity [kW]
E_{WG}	Energy produced by wind turbines [kWh]	P_{Dis}	Diesel generator capacity [kW]
E_{Ex}	Excess energy [kWh]	P_{id}	Best experience for particles
E_{Ex-bat}	Excess energy put into batteries [kWh]	PF_{true}	True Pareto front
E_{Ex-El}	Excess energy put into the electrolyzer [kWh]	$P_{max,j}$	Maximum capacity of the component j
$E_{El-tank}$	Energy put into the H_2-tank by electrolyzer [kWh]	$r(x,g)$	Rank of the solution x in generation g
$E_{tank-FC}$	Energy put into the fuel cell by the H_2-tank [kWh]	SM	Spacing metric
$E_{FC-load}$	Energy put into load by the fuel cell [kWh]	SC	Set coverage metric
$E_{bat-load}$	Energy put into load by batteries [kWh]	SOC	Battery state of charge [%]
E_{bat}	Power charged or discharged from batteries [kWh]	SOC_{min}	SOC lower limit [%]
EF	Emission factor [kg/lit]	SOC_{max}	SOC upper limit [%]
f_i^g	i^{th} objective function in g^{th} generation	$Shortage$	Unmet load during time step t [kWh]
$Fuel_{cons,yr}$	Annual fuel consumption (lit/year).	T	Project life time [year]
Fit	Fitness value	x_{id}	The d^{th} dimension of particles position vector
g_{id}	Global best particle	v_{id}	The d^{th} dimension of particles velocity
$H2_{level}$	Hydrogen level in the H_2-tank [m^3]	ω	Inertia coefficient
$H2_{level-min}$	Hydrogen lower limit level in the H_2-tank [m^3]	α	Crowding distance value

3.4. Multi-Objective Optimization Problem

In multi objective problems, the goal is to optimize *k* objective functions simultaneously that have a possibility of conflict to one other [16]. The basic concepts are introduced for the multi-objective optimization problems.

Definition 1 (Multi-objective optimization problem): A general MOP is characterized as [16, 28, 29]:

Minimize (or Maximize) $F(x) = (f_1(x), \ldots, f_k(x))$ (3-1)

Subject to:

$g_i(x) \leq 0,\ i = \{1, \ldots, m\}$ (3-2)

$h_j(x) = 0, j = \{1, \ldots, p\}$ (3-3)

$x \in \Omega$

where, Ω contains all possible x that can be used to evaluate *F(x)*.

Definition 2 (Pareto dominance): A vector $u = (u_1, \ldots, u_k)$ is said to dominate another vector $v = (v_1, \ldots, v_k)$ (noted by $u \preccurlyeq v$) if and only if *u* is partially less than *v*, [16]:

$\forall i \in \{1, \ldots, k\}, \quad u_i \leq v_i \wedge \exists i \in \{1, \ldots, k\}: u_i < v_i$ (3-4)

Definition 3 (Pareto optimality): A solution $x \in \Omega$ is said to be Pareto optimal with respect to Ω if and only if there is no $x' \in \Omega$ for which $v = F(x') = \{f_1(x'), \ldots, f_k(x')\}$ dominates $u = F(x) = \{f_1(x), \ldots, f_k(x)\}$ [16]. This definition says that x^* is Pareto optimal, if there is no feasible vector x which would decrease some criterion without causing a simultaneous increase in at least one other criterion (assuming minimization).

Definition 4 (Pareto optimal set): For a given MOP the Pareto optimal set (P^*) is defined as [16]:

$$P^* := \{x \in \Omega \mid \neg\exists\, x' \in \Omega\, F(x') \prec F(x)\} \tag{3-5}$$

Definition 5 (Pareto Front): The definition of the Pareto front (PF^*) is described as Equation (3-6) for a given Pareto optimal set of a specific MOP [16]:

$$PF^* := \{u = F(x) | x \in P^*\} \tag{3-6}$$

In this paper, the true PF for the problem is not known. Accordingly, it is distinguished as the true Pareto optimal front, termed PF_{true}, and the final set of non-dominated solutions obtained by a multi-objective optimization algorithm, termed as PF_{known}. The aim of the multi-objective optimization algorithms is to find a PF_{known} and approximates PF_{True} as close as possible [2].

3.5. Problem Description

To perform and evaluate the proposed methodology described in this study, a stand-alone PV/wind/diesel/battery/FC/electrolyzer/H_2-tank system which originates from [23, 24, 27] has been used. It involves PV panels, a wind generator, a diesel generator, and two storage devices which are batteries and hydrogen tanks. The configuration of the employed system is depicted in Figure 3-1. The PV panels and wind turbine as the main generators produce electricity while the diesel generator is used in emergency situations. When the load is less than produced energy by the PV panels and wind turbine, the excess energy is put into batteries to charge them. If there is still excess energy, it is put into the electrolyzer to convert to hydrogen and stored in the H_2-tank. The batteries and fuel cell help in supplying energy, when the load is more than that generated power.

The design problem of the HRES is formulated as a multi-objective optimization problem to improve simultaneously the environmental, technical, and economic performances. Three objective functions (minimizing NPC of the system, total CO_2 emissions produced by diesel generators, and loss of load probability) are considered with the following decision variables:

$$P = [P_{PV}, P_{WG}, P_{bat}, P_{El}, P_{tank}, P_{FC,} P_{Dis}]$$

where, P_{PV} is the capacity of PV panels (kW), P_{WG} is the capacity of the wind turbine (kW), P_{bat} is the capacity of batteries (kWh), P_{FC} is the capacity of the fuel cell (kW), P_{EL} is the capacity of the electrolyzer (kW), P_{tank} is the capacity of the H_2-tank (kWh), and P_{Dis} is the capacity of the diesel generator (kW). Our goal is to seek the optimal system configuration with low total system NPC, low LLP, and low CO_2 emission. The following three subsections express the optimization problem in more details.

3.5.1. Objective Functions

-**Total net present cost (NPC) of the system**: The overall NPC of the system includes the investment costs, operation and maintenance costs, replacement costs, and fuel costs of diesel generators during the lifespan of the system (Equation (3-7)) [27].

$$NPC = \sum_{j} [C_{I,j} + C_{O\&M,j} \frac{1}{CRF(i,T)} + C_{rep,j} K_j] P_j + C_{fuel} fuel_{cons,yr} \frac{1}{CRF(i,T)} \quad (3\text{-}7)$$

where, j is components indicator, $C_{I,j}$ is the capital cost per unit for the component j, $C_{O\&M,j}$ is the operation and maintenance cost per unit for the component j, C_{fuel} is the fuel cost, $C_{rep,j}$ is the cost of each replacement per unit for the component j, and $P_j \in \{P_{PV}, P_{WG}, P_{bat}, P_{El}, P_{tank}, P_{FC,} P_{Dis}\}$, $fuel_{cons,yr}$ is the annual fuel consumption

(lit/year). K_j and CRF are single payment present worth and capital recovery factor, respectively [11, 23, 24]. i is the real interest rate, and T is the project life time which is considered 25 years in this study.

-Loss of load probability (LLP): The system LLP represents the energy deficit, which is the ratio of the unmet load to the total load. The system loss of load probability is calculated from the ratio of annual energy shortage to electricity demand (Equation (3-8)) [23, 24, 27].

$$LLP = \frac{\sum_{t=1}^{8760} shortage\ (t)}{\sum_{t=1}^{8760} D\ (t)} \tag{3-8}$$

where, *D(t)* is electricity demand, and *shortage(t)* is unmet load during time period *t*.

-CO_2 emission: For simplification as well as since CO_2 is the most common exhaust gas of the diesel generator, only CO_2 produced by the diesel generator is considered as pollutant emission. In this study, the number of kg of CO_2 produced by the diesel generator is calculated using Equation (3-9) [23, 24, 27].

$$CO2_{emission} = \sum_{t} fuel_{cons}(t) \times EF \tag{3-9}$$

where, EF is the emission factor for diesel generator which is considered as 2.4-2.8 kg/lit range [23]. It depends on the type of fuel and diesel engine characteristics.

3.5.2. Constraints

The MOP is subject to technical constraints that are essential to meet for generating feasible solutions by solving the problem. Energy balance between supply section and load in each time period is the first constraint, Equation (3-10). The next three constraints deal with energy and

storage level of components. The energy produced by or entered to each component in every time, $E_j(t)$, should be equal or less than its capacity, Equation (3-11); where, Δt is the time interval that is considered as one hour. There is upper and lower limit for the state of charge of batteries, in which they are allowed to be charged or discharged, Equation (3-12). Furthermore, the hydrogen tank can supply energy till an allowable lower level and can receive hydrogen until an upper limit, Equation (3-13). Finally, Equation (3-14) and Equation (3-15) represent non-negativity constraints for decision variables and energy flow as well as upper limit for decision variables.

$$E_{PV}(t) + E_{WG}(t) + E_{Dis-load}(t) + E_{bat-load}(t) + E_{FC-load}(t) + shortage\ (t) = D(t) \quad (3\text{-}10)$$

$$E_j(t) \leq P_j \times \Delta t \quad (3\text{-}11)$$

$$\mathrm{SOC}_{min} \leq \mathrm{SOC(t)} \leq \mathrm{SOC}_{\max} \quad (3\text{-}12)$$

$$\mathrm{H2}_{level-min} \leq \mathrm{H2}_{level}(\mathrm{t}) \leq \mathrm{H2}_{level-max} \quad (3\text{-}13)$$

$$0 \leq P_j \leq P_{max,j} \quad (3\text{-}14)$$

$$E_j(t) \geq 0 \quad (3\text{-}15)$$

The produced energy by the wind turbine, PV panels, electrolyzer, FC, and diesel generator are calculated by the models which are used in [23, 24, 27]. These models are implemented in a simulation module. The proposed methodology searches for the configuration of PV/wind/diesel/battery/FC/electrolyzer/H_2-tank that minimizes three mentioned objectives. It is suggested that readers refer to the previous works [23, 27] for a detailed explanation of the mathematical models and the optimization problem.

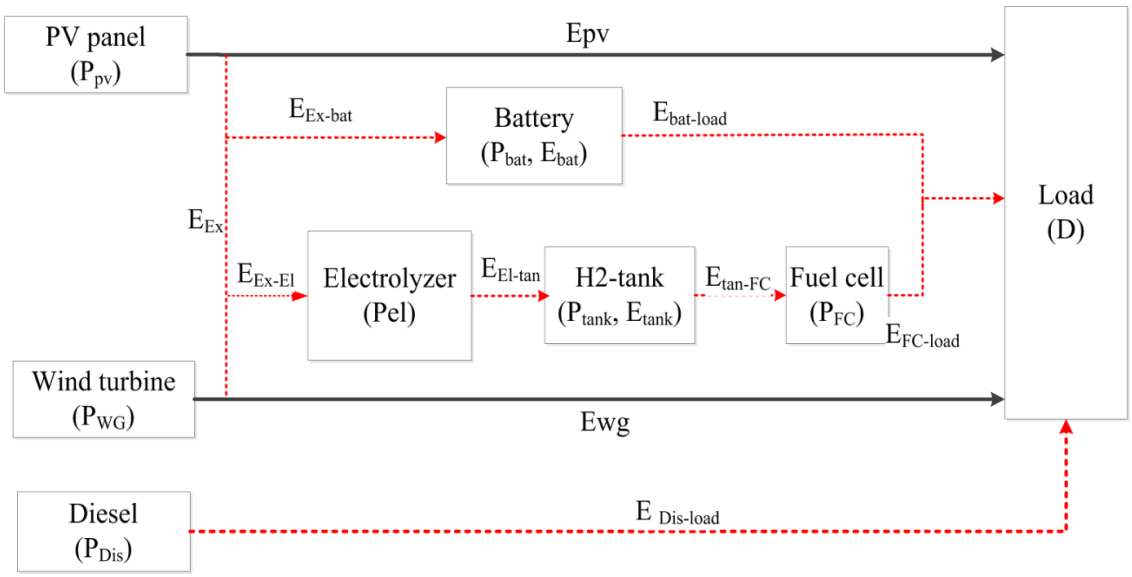

Figure 3-1: The energy flow of the employed system [27]

3.6. Solution Approach

Due to the complexity of the optimal design of an HRES, in this study a simulation-based dynamic multi-objective particle swarm optimization approach is used to tackle the complex optimization problem. In complex systems, the optimization techniques alone are not effective because of the high dimensional space or nonlinear nature of the problem. It is difficult to represent the exact mathematical model of the system while the exact mathematical representation of the system has pivotal role in optimization techniques. Additionally, the main advantage of using simulation is that all system's details and uncertainties can be accommodated accurately with almost no simplifying assumptions [27]. However, a simulation inherently cannot return the optimal design of the system. Consequently, the integration of simulation with an optimization search technique can be a legitimate way to represent the complexity of the system as well as deliver optimal (or near optimal) solutions in reasonable time. This combination is named simulation-based optimization method. In this paper, simulation-based

DMOPSO approach has been used to find the optimal (or near optimal) design of the HRES (Figure 3-2).

The decision variables, fitness and constraints are defined in the DMOPSO algorithm. Design variables assigned to the capacity of the components are defined in a vector named particle. In other words, each particle represents a certain configuration of the HRES. After initializing a random population of particles, each particle is sent to a simulation module for checking its feasibility. In the simulation, the mathematical model of the components is used to predict their output in each time period. The verification must be performed to ensure the accuracy of the simulation, its specifications and algorithms, and also its implementation. In this study, a divide-and-conquer approach is applied to verify the simulated module [28]. First, the simulation model is built in a small size and checked whether it is rightly and logically coded or not. After verifying the small model, it is expanded gradually by adding more components to the final model. The simulation is run for 25 years to evaluate the performance of each particle. The simulation model calculates the yearly unmet load and CO_2 emission produced by the HRES. After initializing feasible particles, they are evaluated in the DMOPSO algorithm based on their fitness. Stopping criterion is checked, if it is not met, each particle is updated for next generations in the framework of the DMOPSO algorithm which will be explained in Section 3.7 (Figure 3-4). After updating, the particles are sent back to simulation to review their feasibility again, and then the simulation result is sent to optimization algorithm for evaluation. This cycle is terminated if a stopping criterion is met. After terminating the cycle, the best solutions will be returned.

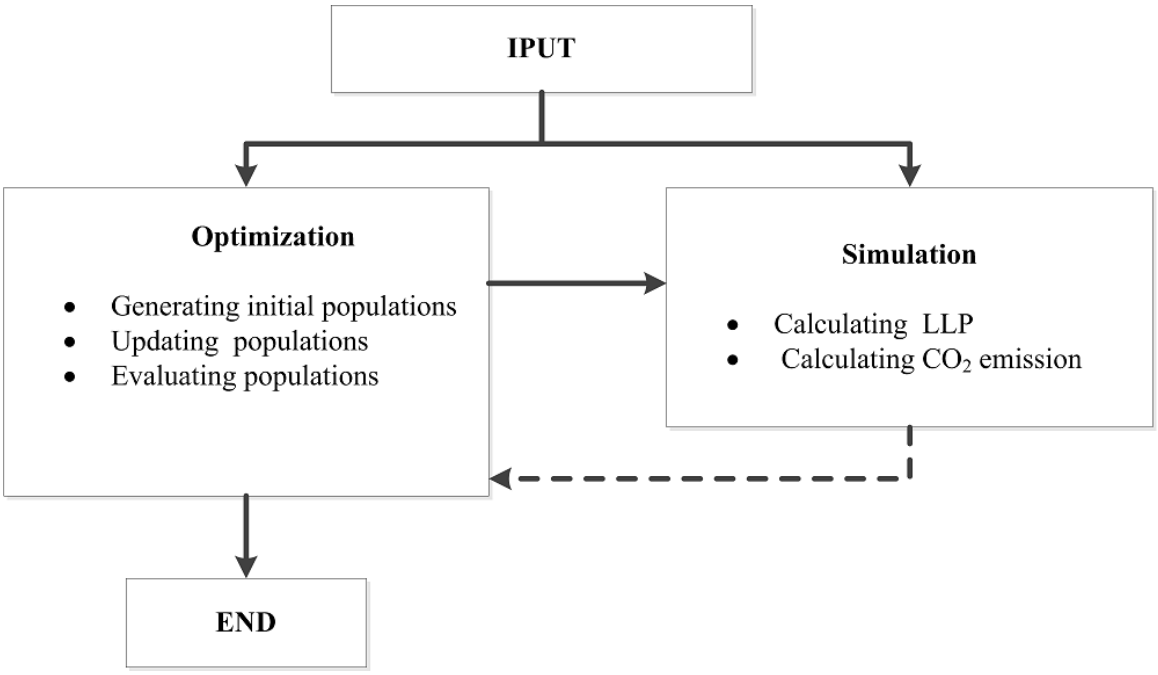

Figure 3-2: Flow chart of the DMOPSO-simulation

3.7. Proposed Multi-Objective PSO Algorithm

Particle swarm optimization, a meta-heuristic optimization technique, was firstly developed by Kennedy and Eberhart in 1995. PSO algorithm is able to solve continuous problems as well as binary or discrete problems. It is inspired by the social behavior of birds flocking [29]. PSO algorithm is very simple to implement and can obtain optimal solutions fast [3]. In PSO, a set of particles or swarms, which are described by their position and velocity vectors, fly through search space by following the current optimum particle. Particles' motions are defined by a vector which defines the velocity of a swarm in the each direction. The best solution for each particle obtained so far is stored in a particle memory and named particle experience. In addition, the best global particle or social leader denotes as the best solution obtained so far among all particles. The velocity and position of each swarm is updated according to its experience and the social leader. The achievement of PSO in single objective optimization problems has motivated

researchers to modify it for solving MOP which is named multi-objective particle swarm optimizers (MOPSO) [3].

This paper presents a dynamic MOPSO algorithm for optimal design of an HRES. The idea of proposed algorithm is taken from MOPSO and multi-leader multi-objective optimization algorithm (MLMOPSO) developed by Carmelo et al. [3] and Kian et al. [30], respectively. Carmelo et al. [3] applied an external list with limited size to keep all non-dominated solutions during generations. Besides, in order to maintain diversity in a swarm, they divided objectives space to hyper cubes and considered their fitness. The fitness is equal to the number of non-dominated solutions inside a hyper cube. Then, a hyper-cube is chosen based on roulette-wheel, and a particle inside the hyper cube is randomly selected as the social leader [3]. Kian et al. introduced MLMOPSO which is the implementation of multiple leaders in guiding particle flights [30]. In this paper, MOPSO concept is used with a different leader selection scheme, maintaining diversity approach, and Pareto ranking operator. Generally, there are two methods for selecting leaders: selecting one of the best solutions or using multiple leaders to guide the particles' flight [31]. MOPSO selects randomly one leader among all non-dominated solutions to use as a guide for the particles in updating their velocities. An improved leader guidance introduced by Kian et al. [30] is used in addition to dynamic cell-based density calculation strategy which is used to maintain a diverse population [32].

In dynamic cell-based density calculation strategy, density information for cells and solutions is used to achieve diversity in swarms. The objective space is divided into $K_1 \times K_2 \times \dots K_m$ cells [32] (see Figure 3-3). Consequently, the cell width in the i^{th} objective dimension and g^{th} generation, d_i^g, can be calculated as Equation (3-16) [32]:

$$d_i^g = \frac{\max_{x \in X} f_i^g(x) - \min_{x \in X} f_i^g(x)}{K_i} \quad (3\text{-}16)$$

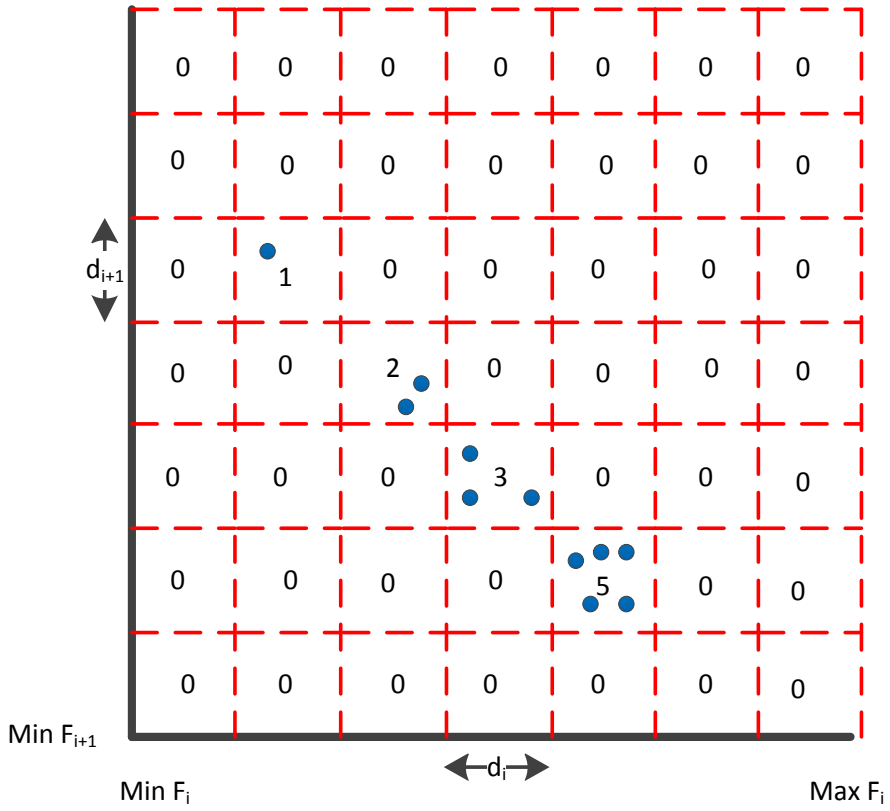

Figure 3-3: Example of diversity methods used in DMOPSO

where, K_i refers to the number of cells designed for ith dimension, f_i^g is the ith objective function in gth generation, and x is a feasible solution. This method named dynamic since the cells width is changed dynamically based on the maximum and minimum of the objectives during generations. The density of a cell is defined with the number of solutions inside the cell (Figure 3-3). Thus, the density of the cell is saved as the density value of solutions which are dwelled in it. Between two non-dominated solutions, the one with a lower density is preferable. The density information can encourage the search toward sparsely inhabited regions of the objective function space [33]. The advantage of this approach is its computational efficiency

compared to niching or neighborhood-based density techniques [33]. The steps of the proposed DMOPSO algorithm are as following (Figure 3-4):

Step 1: A pool of candidate solutions is randomly generated.

Step 2: Divide the objective space into K^m hyper cubes, where K is the number of cells designed for an objective axis and m is the number of objectives. A density is estimated for each hyper cube, which is equal to number of non-dominated solutions inside the hyper cube.

Step 3: The accumulated ranking density strategy is applied to rank the population. In this ranking method, the rank of a solution (x) is dependent on the rank of the solutions dominating this solution (Equation (3-17)) [33].

$$r(x,g) = 1 + \sum_{y \in P, y > x} r(y,g) \tag{3-17}$$

Where, $r(x,g)$ is the rank of a solution in generation g, and $r(y,g)$ is the rank of the solution y which is dominating the solution x.

Step 4: Each solution is assigned a fitness value based on its rank in the population. The best solutions or first rank are assigned one and the worst swarms are identified by zero. The rest of populations are assigned a linear fitness as following, in which N is the number of solutions.

$$Fit = \frac{N - r(x,g)}{N - 1} \tag{3-18}$$

Step 5: After assigning fitness to population, the best solutions are stored in an external list. In the next step, the best leaders among all non-dominated solutions stored in the external list are selected for guiding the particles to update their velocity. In this paper, multi-leader method is utilized to guide the particles flight. First, a set of solutions is defined as leaders for each particle

since they dominate the particle. Each particle has two state variables, its current position $\overrightarrow{x_i}(t)$ and its velocity $\overrightarrow{v_i}(t)$. The best experience for each particle is stored in a particle memory $\overrightarrow{p_i}(t)$ while $\vec{g}(t)$ denotes the best global particle among the population. In each iteration, the dth dimension of the position and the velocity of the particles are updated toward the best experience and the leaders by applying recursive Equation (3-19) and Equation (3-20) [30].

$$v_{id}(t+1) = \omega . v_{id}(t) + C_1 . \varphi_1 . \left(P_{id}(t) - x_{id}(t)\right) + C_2 . \varphi_2 \sum_{S=1}^{|PF_i|} C_s \left(PF_{id,s} - x_{id}(t)\right) \quad (3\text{-}19)$$

$$x_{id}(t+1) = x_{id}(t) + v_{id}(t+1) \quad (3\text{-}20)$$

where, the term $v_{id}(t)$ stands for the inertia velocity and ω is called inertia coefficient. This term ensures that not only the velocity of each particle is not changed abruptly but also the previous velocity of the particle is taken into consideration. The parameters C_1 and C_2 are positive weighting constants, and denoted as the "*self-confidence*" and "*swarm confidence*", respectively. They control the movement of each particle towards its individual versus the global best position. The parameters φ_1 and φ_2 are two uniform random numbers within interval (0 1) [34]. PF_{id} refers to a set that stores non-dominated solutions dominating the ith particle; C_s is a sigmoid function that is given by Equation (3-21):

$$C_S = \frac{1}{1 + |PF_i| e^{-|PF_i|\alpha}} \quad (3\text{-}21)$$

where, α is the crowding distance value for each non-dominated solution [29].

Step 6: The mutation is performed in the swarms.

Step 7: The grid is updated by incorporating the updated population.

Step 8: The external list is updated according the dominance rule and by using new solutions resulted from the new population [31]. A new solution is entered to the external list, if it dominates one or more solutions or it is not dominated by any solution in the external list. When it is compared to solutions in the external list regarding dominance rule, the following cases could happen;

Case 1: If there is one solution in the external list that dominates the new solution, the new solution is ignored.

Case 2: If some solutions in the external list are dominated by the new solution, those dominated solutions are discarded from the external list and the new solution is added to the external list. The density of the hyper cubes is updated.

Case 3: If the new solution does not dominate any solution in external list and also there is not any solution in the external list that dominates it, this solution is added to the external list. If the external list size reaches its maximum size, one solution randomly is selected from the most crowded hyper cube to discard. Then, the density of the hyper cube is updated.

Step 9: If the stopping criterion is satisfied, the algorithm is terminated and it returns the external list. If not, it goes to step 3.

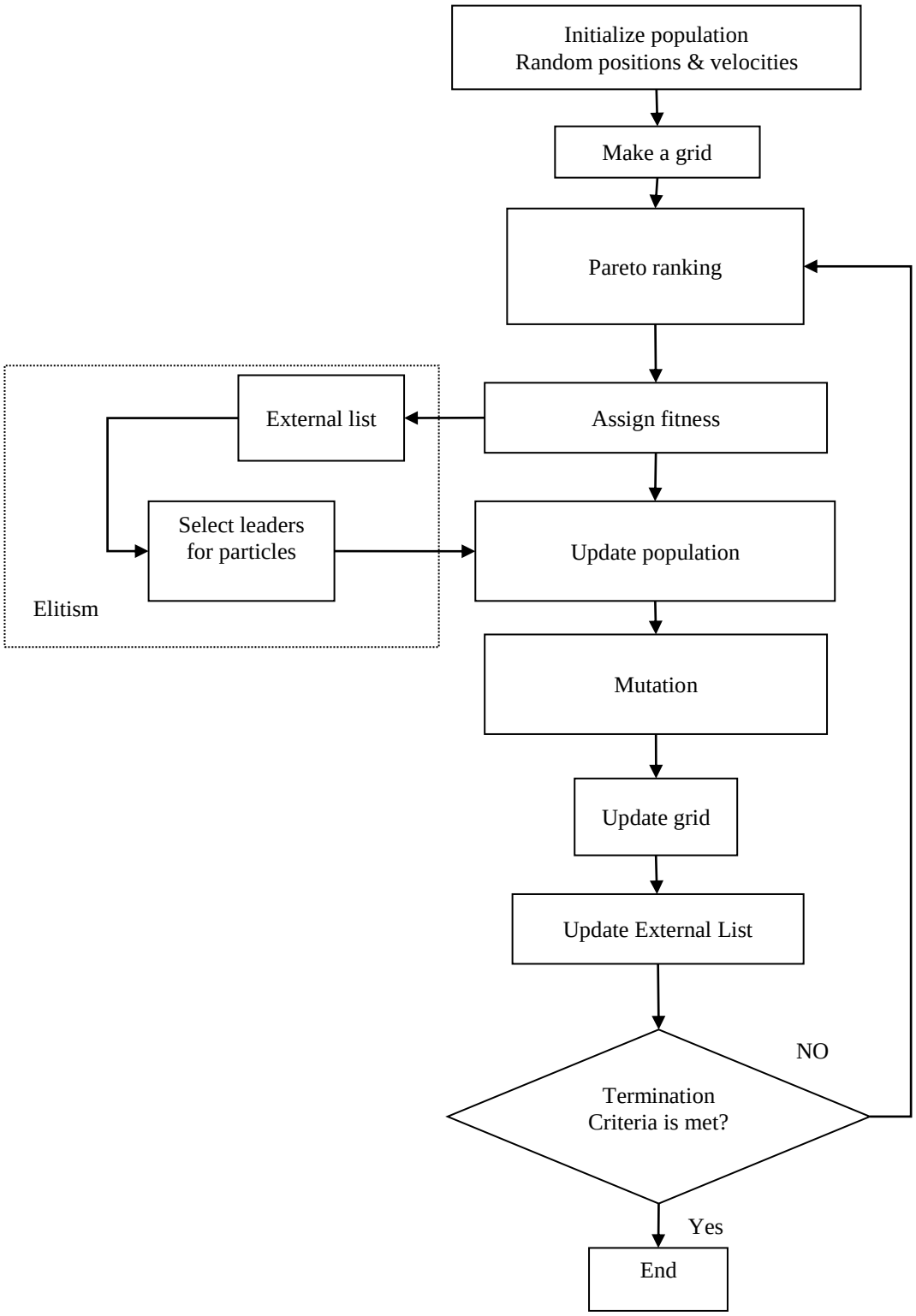

Figure 3-4: The flow chart of the proposed DMOPSO algorithm

3.8. Performance Metrics

Although, generating a PF can be done easily by a multi-objective algorithm, the quality of the generated PF has to be evaluated [30]. Thus, it is essential to use quantitative performance metrics to evaluate the quality of an approximated set of solutions. In this paper, three popular performance measures are used, which are spacing metric, diversification metric, and set coverage [35]. These three metrics do not need the true PF for assessment.

-Spacing metric (SM): It numerically measures the distribution of individuals over a PF. This metric is calculated by measuring distance variance of neighboring solutions in PF_{known}, Equation (3-22) and Equation (3-23) [16, 35].

$$SM = \sqrt{\frac{1}{n-1} \times \sum_{i=1}^{n} (d_i - \bar{d})^2} \tag{3-22}$$

$$d_i = min_j \sum_{k=1}^{m} \left| (f_k^i - f_k^j) \right| \quad i, j = 1, 2, 3, \ldots, n \tag{3-23}$$

where, n is the number of non-dominated solutions in the PF_{known}, m is the number of objectives and $\bar{d}$ is the mean value of all d_i. When *SM* is zero, it means all the points spread uniformly [16]. That is a PF with less *SM* is preferred.

-Diversification metric (DiM): It measures the maximum extension covered by a non-dominated solution set. Mathematically, this is evaluated by using Equation (3-24) [35]:

$$DiM = \sqrt{\sum_{i=1}^{n} max(\left\| x_i^t - y_i^t \right\|)} \tag{3-24}$$

where, $\|x_i^t - y_i^t\|$ states the Euclidean distance between two non-dominated solutions of x_i and y_i. The distance of each non-dominated solution to all other solutions should be calculated. The maximum distance is used in Equation (3-24). In this equation, *n* indicates the number of non-dominated solution stored in the external list.

-Set coverage metrics (SC): It is used to compare two sets of non-dominated solution, Equation (3-25) [16, 35].

$$SC(X', X^{"}) = \frac{\left|\{a^{"} \in X^{"} | \exists a' \in X' : a' \leq a^{"}\}\right|}{|X^{"}|} \tag{3-25}$$

where, $X'$and $X^{"}$ are two sets of non-dominated solutions. If *SC* = 1, all points in X' dominate or are equal to all points in $X^{"}$ while the *SC* = 0 implies the opposite [16]. Generally, as there are intersections between sets, it is more common to consider both $SC(X', X^{"})$ and $SC(X^{"}, X')$. We can say that $X^{"}$ is better than X' if and only if $SC(X', X^{"}) = 0$ and $SC(X^{"}, X') = 1$ [16].

3.9. Analysis of Results

The proposed methodology is applied for the optimal design of a hybrid PV panels/wind turbine/batteries/fuel cell/H_2 tank/ electrolyzer/diesel system in a case study located at Zaragoza (latitude 41.65^0), Spain. The proposed approach is coded in C++ programming environment in a 2.4 GHz core 2 processor. In this study, three different electricity load profiles are assumed for seasons [23, 27]. The average hourly load in the various seasons is shown in Figure 3-5. The load in winter time (December-February) is the lowest one and in summer (June-August) is the highest. The time step is considered 1 hour and during this period, wind energy, solar energy and load are assumed to be constant [23, 27].

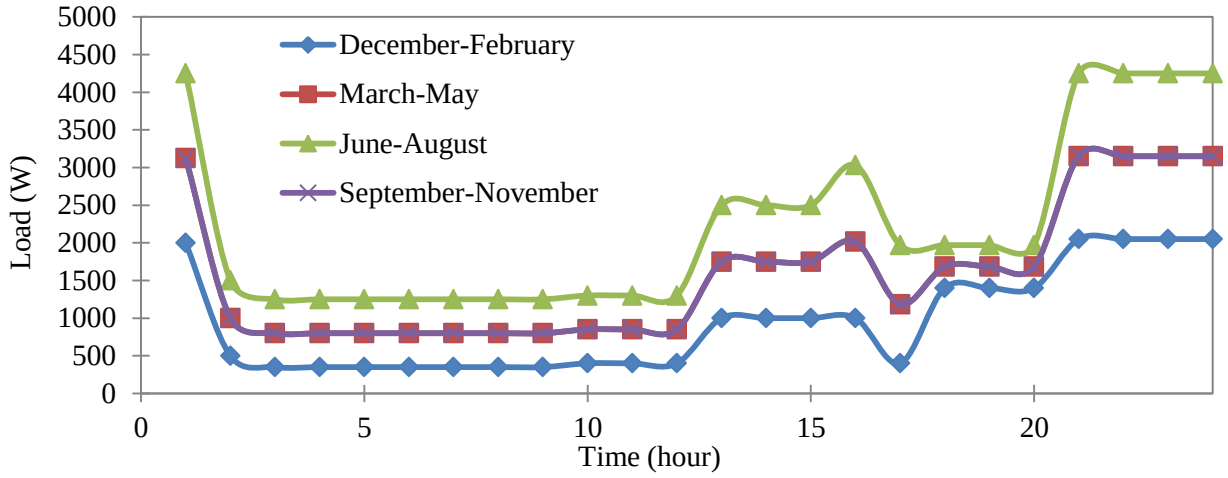

Figure 3-5: Daily load profile in the various seasons [27]

The solar irradiation on the horizontal surface and wind speed profile of the area are shown in Figure 3-6 and Figure 3-7. These data are assumed deterministic and the average of last 10 years climate data is used for the case study [23, 27]. In Figure 3-6, typical daily horizontal solar radiation over different months is shown.

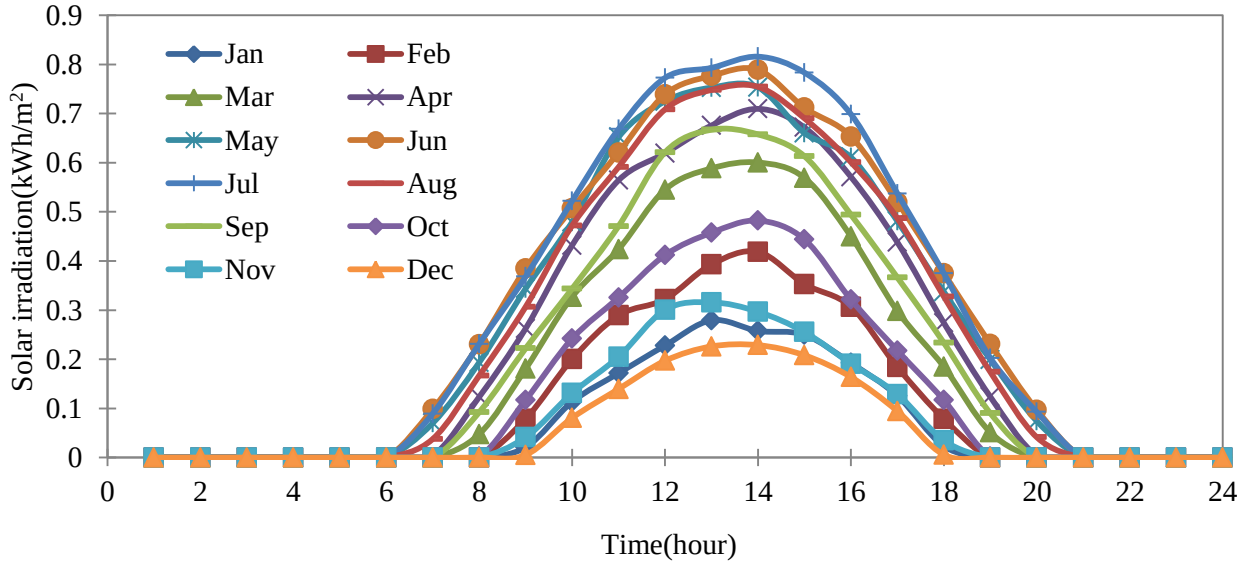

Figure 3-6: Hourly solar irradiation during one year [27]

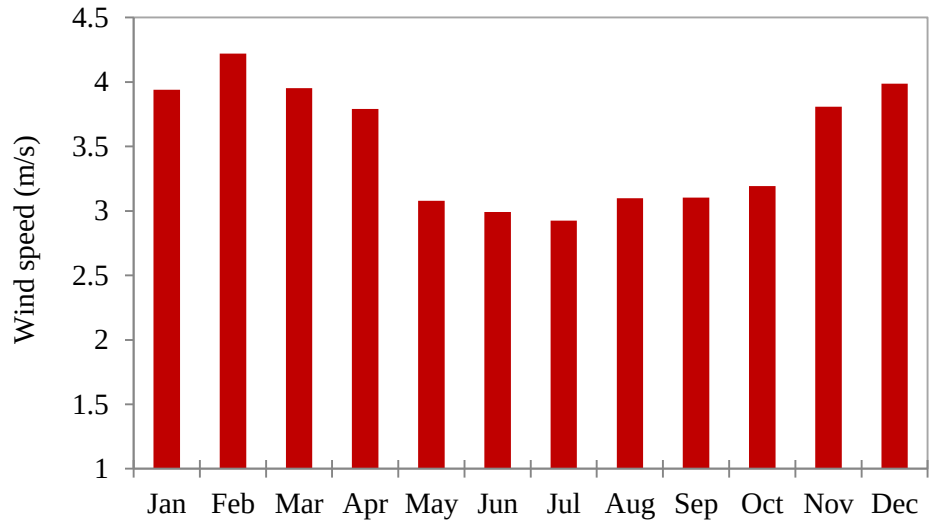

Figure 3-7: Average monthly wind speed at 10m height (measurement height) during one year [27]

The initial cost, operation cost, and characteristics of components vary with their size and type. In this study, initial costs, maintenance costs, and the characteristics of components are considered the same as what have been used in the references [23, 27].

The application of simulation-based DMOPSO approach in the case study resulted in two hundred non-dominated solutions, which are described in Figure 3-8 to Figure 3-11. For further analysis, four candidate solutions are chosen and labeled with a boxed design number in Table 3-1. These 200 solutions demonstrate minimum NPC of the system for different LLP and CO_2 emission. It can be seen in these figures that CO_2 emission of the system is decreased significantly as LLP is increased to 0.8%. Increasing LLP of the system from 0.8% to 12% decreases the CO_2 emission moderately. When LLP is larger than 15%, CO_2 emission cannot be changed significantly.

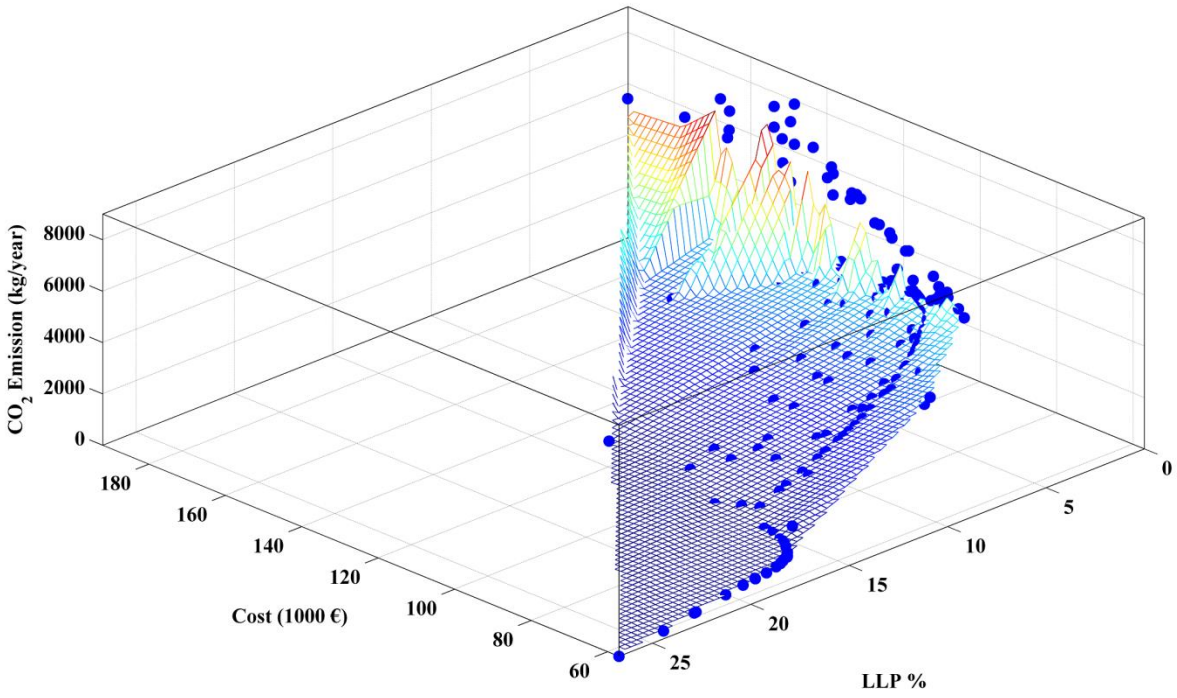

Figure 3-8: The 3D set of non-dominated solutions obtained by DMOPSO

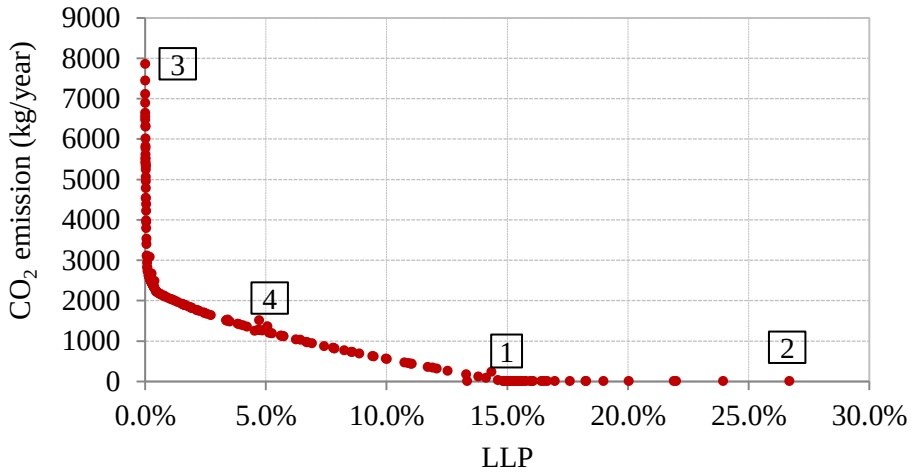

Figure 3-9: The 2D set of non-dominated solutions. CO_2 emission vs. LLP

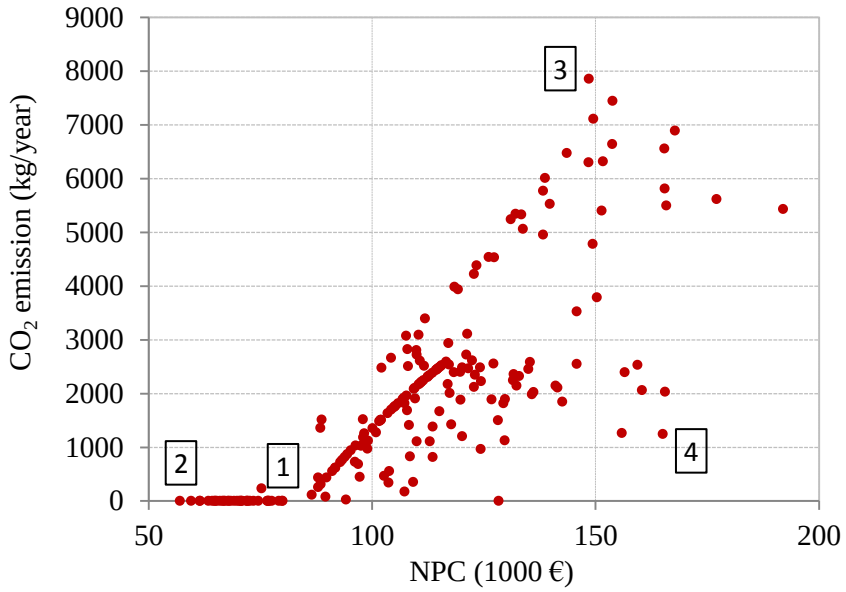

Figure 3-10: The 2D set of non-dominated solutions. CO_2 emission vs. NPC

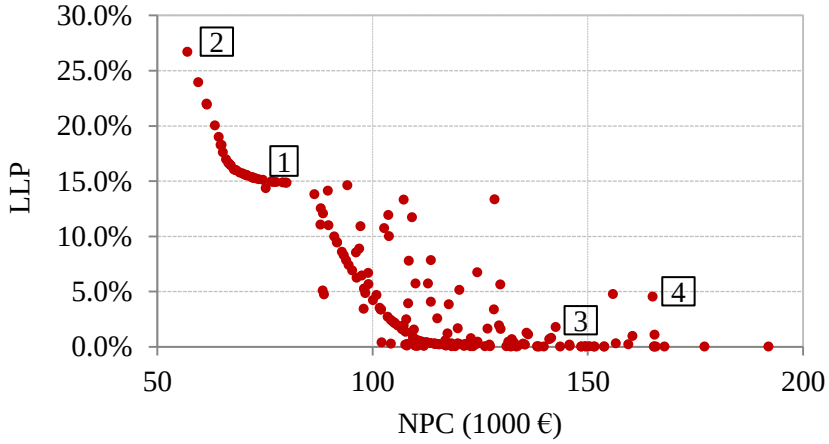

Figure 3-11: The 2D set of non-dominated solutions. LLP vs. NPC

For further analysis, four Pareto solutions are chosen from two hundred non-dominated solutions based on their distribution in the objective space and listed in detail in Table 3-1. Four Pareto solutions are distinguished with their design number in Figure 3-9 to Figure 3-11. For each design, Table 3-1 demonstrates the objective functions values (NPC, LLP, and CO_2 emission), and decision variables values. It can be observed from the table that the installation capacity of the wind generator is preferred over PV panels since the capital cost of a PV array is larger than

a wind turbine. In addition, the result shows a little contribution of hydrogen storage. One reason for this result can be that hydrogen storage device is more expensive than batteries. Additionally, the maximum overall energy efficiency of hydrogen storage device has resulted in 28.9% which is less than battery overall energy efficiency (80%).

Table 3-1: Four candidate designs for the hybrid renewable energy system

No. of design	1	2	3	4
PV (kW)	8	6.7	6	8
Wind (kW)	6.5	6.5	6.5	6.5
Diesel (kW)	0	0	4.5	1.3
Fuel Cell (kW)	0	0	0	5
Battery (kWh)	88.7	31.4	6.1	88.7
Electrolyzer (kW)	0	0	0	1.6
H_2-tank(m^3)	0	0	0	1.6
NPC(€)	80065.3	57065.4	148577	165134
LLP (%)	15	26.7	0	4.5
CO_2 Emission(kg/yr)	0	0	7853.02	1243.9

The performance of the algorithm is tested against three reported multi-objective algorithms in the optimal design of the HRES problem. These algorithms are multi-objective particle swarm optimization (MOPSO) [36], multi-objective genetic algorithm (MOGA) [16], and ε-constraint method [27]. They are implemented in C++ source code.

For fair comparison, all algorithms are run with 1000 generations. ε-constraint method, a non-Pareto based approach, is run 50 times to generate a PF including 50 non-dominated solutions, and the other experiments are conducted for 50 runs to obtain the average value of SM and DiM metrics for comparison. In other words, by conducting 50 runs for all algorithms, 50 different PF are obtained except ε-constraint method resulting only one PF.

Figure 3-12, Figure 3-13, Table 3-2, and Table 3-3 are the comparative results of 50 independent runs of all mentioned algorithms. Table 3-2 presents the average value of the metrics: spacing, diversification, PF size and time. It shows that DMOPSO has the largest PF size. It has greater PF size than MOPSO since using multi-leader in DMOPSO helps the search procedure to discover more non-dominated solutions. This results in keeping the search in diverse regions in the search space. The least average of computational time is for ε-constraint method because it exclusively returns one solution, and it does not need ranking and pairwise comparison operations to identify non-dominated solutions.

Table 3-2: The performance metric values obtained by the algorithms

	DMOPSO	MOGA	MOPSO	ε-constraint
Spacing	1386.44	2790.3	2270.35	960
Diversification	4656.52	2357.47	6266.82	1391.04
PF size	200	49.38	193.24	50
Time (s)	288.28	281.3	361.1	256

Figure 3-12 shows box-plot for the spacing metric of the generated PF by the Pareto-based algorithms for optimizing the HRES design. It shows that DMOPSO has the lowest spacing metric for the problem, thus it generates more uniformity PF than the others. The reason for this fact can be that in DMOPSO, using multiple-leaders strategy is much more efficient than using roulette-wheel scheme in MOPSO.

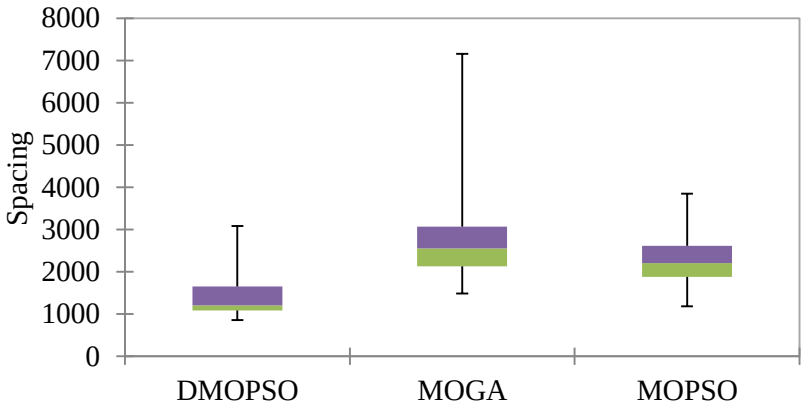

Figure 3-12: The Spacing metric value obtained by the algorithms (50 Runs)

Figure 3-13 represents the result obtained for the D metric. It is observed that D is a positive metric; hence, MOPSO is in the first rank because it has maximum average among the other algorithms. The next algorithm in terms of D metric is DMOPSO and MOGA, respectively.

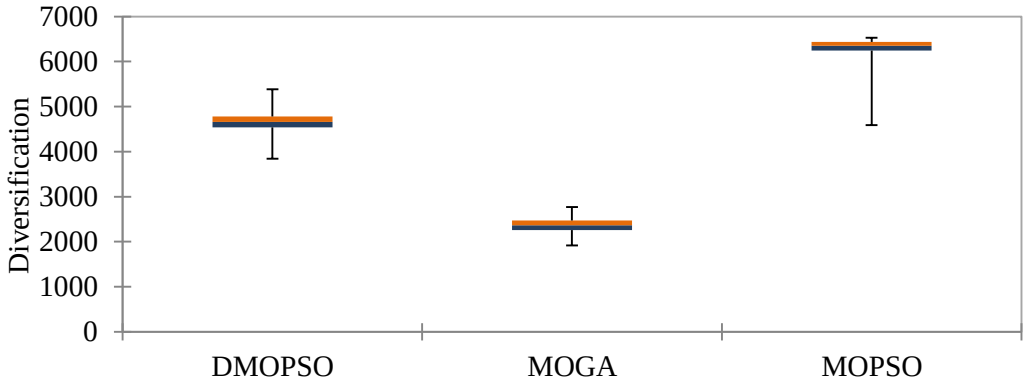

Figure 3-13: The diversification metric value obtained by the algorithms (50 Runs)

Table 3-3 compares the SC metric for DMOPSO and the other algorithms. It shows that most of non-dominated solutions generated by DMOPSO dominate those generated by MOPSO and MOGA. It can easily be checked by observing the row 1 to 6 in Table 3-3. For example, from row 1 and 2 it can be observed that all non-dominated solutions obtained by DMOPSO dominate the solutions achieved by MOGA. In addition, 81% of non-dominated solutions generated by DMOPSO are dominating the solutions provided by ε-constraint method which was developed by the authors in the previous work [27]. The main reason for this fact can be using different

leader selection in the PSO algorithm. The result shows that using multi-leader scheme makes the PSO more effective in the multi-objective problem. Additionally, using an external list to store non-dominated solutions and updating PF in each generation can be another reason for improvement in generated solutions by DMOPSO compared to ε-constraint method results.

In general, by achieving good values for SM, DiM, and SC in DMOPSO result, It can be realized that using cell-base density and multi-leaders in MOPSO have significant influences on spacing, convergence and diversity of non-dominated solutions. Thus, it can be claimed that the generated PF by DMOPSO is closer to true PF, and DMOPSO is efficient and stable for using in the optimal design of an HRES.

Table 3-3: The set coverage metric value obtained by the algorithms

1	SC(DMOPSO, MOGA)	1
2	SC(MOGA, DMOPSO)	0
3	SC(DMOPSO, MOPSO)	0.67
4	SC(MOPSO, DMOPSO)	0.028
5	SC(DMOPSO, ε-constraint)	0.81
6	SC(ε-constraint, DMOPSO)	0

Sensitivity analysis is the investigation of how possible variation of input parameters may impact optimal solutions provided by an optimization algorithm under a given set of assumptions [37]. In a sensitivity analysis, the value of parameters is changed and the resulted changes in performance indices are measured. Therefore, a main goal of a sensitivity analysis is to identify which parameters are the most sensitive and most likely to affect system behavior [37].

In this optimization problem, there are several parameters that are predicated before optimization and entered to the model as fixed parameters. In this regard, economic parameters including interest rate, PV panel capital cost, fuel cell capital cost, wind turbine capital cost, electrolyzer capital cost, battery capital cost, fuel price, and battery life time can be denoted as the fixed parameters. In this section, a sensitivity analysis is performed to investigate how the variations

of these parameters from their predicted values affect the values of the optimal objective functions provided by the DMOPSO algorithm. For this purpose, an upper limit and a lower limit for the parameters is considered. By setting the parameters at their lower and upper limits the DMOPSO is performed. In our optimization problem, the optimal solutions for the origin result in average total cost of 106255.7€ for 25 years, LLP of 7.4%, and CO_2 emission of 1889.6 (kg/year).

Table 3-4 presents the sensitivity analysis results for eight input parameters used in our analysis. Eight parameters that are interested to know the sensitivity of the result respect to their changes and the predicted lower and upper limits for them are indicated in column one and two of Table 3-4. By running DMOPSO for 50 times, it is resulted that NPC, LLP, and environmental objectives have respectively 3.8%, 11.6% and 11.7% standard deviation. Regarding this fact, a differences between an objective function and its original value can be ignored when it is equal or less than the standard deviation of that objective function. In Table 3-4, those columns designated with the symbols "L" and "U" referrer to variety of objective functions in percent from its original value while parameters are set at their lower and upper bounds, respectively. For instance, when the interest rate is 50% lower than its predicted value (7%), total NPC, LLP and CO_2 emission objectives are respectively 22.4% higher, 2.6% lower, and 3% higher than the original values of these three objectives. As it is obvious from the result, the interest rate and PV panel capital cost have more effect on NPC than the others. It is clear that changing the parameters does not have significant effect on LLP and CO_2 emission as in Table 3-4 all corresponding values to these parameters are less than their standard deviation.

Table 3-4: The results of sensitivity analysis of objective functions to the variation of the design parameters

Parameters	Percentage of variations for each parameter from its original value used in this study		Cost objective		Reliability objective		Environmental objective	
	L	U	L	U	L	U	L	U
Interest rate	-50%	50%	22.4	-11.8	-2.6	-2.2	3.0	4.1
PV panel capital cost	-50%	50%	-18.8	20.3	-0.1	-5.1	0.4	4.7
Fuel cell capital cost	-50%	50%	0.8	3.8	-7.6	-10.5	2.2	8.4
Wind turbine capital cost	-50%	50%	-3.0	7.4	-5.4	-8.0	5.5	6.2
Electrolyzer capital cost	-50%	50%	-0.2	2.2	0.0	-8.0	1.1	3.7
Battery capital cost	-50%	50%	-6.7	7.5	-3.6	5.4	3.1	-3.4
Fuel price	-50%	50%	-6.3	8.3	-10.8	1.4	9.9	0.6
Battery life time	-50%	50%	10.6	-1.6	1.4	-9.5	1.3	7.7

3.10. Conclusion

In this paper, a dynamic multi-objective particle swarm optimization method is proposed to optimize the design of a hybrid renewable energy system. The solutions define the type and size of the included equipment in the HRES. The main criteria of design are to minimize loss of load probability, CO_2 emission, and total NPC of the system. The main advantage of the proposed approach is that it is able to generate a PF with higher quality than the other reported methods.

The proposed approach is evaluated using a case study that includes a wind turbine, PV panels, a diesel generator, a fuel cell, an electrolyzer, batteries and a hydrogen tank. The case study result indicates that wind generators is preferred over PV panels as well as it shows that there is little contribution of hydrogen storage. Three well-known metrics are used to evaluate the generated PF. By comparing the results of the proposed method with the other reported MOP algorithm, it has been concluded that the average spacing metric obtained by the proposed approach is

1386.44 which is less than the others. The diversification index is calculated as 4656 which is less than MOPSO and greater than the others. The set coverage metric shows that 67% of Pareto solutions obtained by DMOPSO dominate the solutions obtained by MOPSO. In conclusion, the proposed optimization method can find better solutions and provide a larger range and more uniform PF including the system configurations.

A sensitivity analysis has been performed to test the effect of changing the input parameters on the obtained optimal solutions. It is found that by decreasing PV panel capital cost, total NPC would be decreased by 18.8% while changing wind turbine capital cost by -50% leads to 3.7% change in total NPC. Moreover, changing the investigated parameters does not have significant effect on LLP and CO_2 emission.

The proposed model can be used in feasibility studies to design an HRES. For future research, stochastic optimization of the hybrid system will be considered since there is uncertainty in the availability of renewable energy sources and electricity load.

3.11. References

[1] Deshmukh MK, Deshmukh SS. Modeling of hybrid renewable energy systems. Renewable and Sustainable Energy Reviews 2008; 12(1): 235–249.

[2] Kaveh A, Laknejadi K. A new multi-swarm multi-objective optimization method for structural design. Advances in Engineering Software 2013; 58: 54–69.

[3] Carmelo JA, Bastos-Filho, P´ericles-Miranda BC. Multi-objective particle swarm optimization using speciation. IEEE Symposium on Swarm Intelligence (SIS) 2011.

[4] Fadaee M, Radzi MAM. Multi-objective optimization of a stand-alone hybrid renewable energy system by using evolutionary algorithms: A review. Renewable and Sustainable Energy Reviews 2012; 16(5):3364– 3369.

[5] Fazlollahi S, Mandel P, Becker G, Maréchal F. Methods for multi-objective investment and operating optimization of complex energy systems. Energy 2012; 45(1): 12-22.

[6] Eke R, Kara O, Ulgen, K. Optimization of a wind/PV hybrid power generation system. International Journal of Green Energy 2005; 2(1):57-63.

[7] Garyfallos G, Athanasios IP, Panos S, Spyros V. Optimum design and operation under uncertainty of power systems using renewable energy sources and hydrogen storage. Hydrogen Energy 2010; 35(3):872-889.

[8] Akella AK, Sharma MP, Saini RP. Optimum utilization of renewable energy sources in a remote area. Renewable and Sustainable Energy Reviews 2007; 11(5):894–908.

[9] Hanane D, Ahmed O, Roberto S. Modeling and control of hydrogen and energy flows in a network of green hydrogen refueling stations powered by mixed renewable energy systems. Hydrogen Energy 2012; 37(6): 5360-5371.

[10] Jeremy L, Marcelo GS, Abdellatif M, Philippe C. Energy cost analysis of a solar-hydrogen hybrid energy system for stand-alone applications. Hydrogen Energy 2008; 33(12):2871–2879.

[11] Raquel SG, Daniel W. A wind–diesel system with hydrogen storage: Joint optimization of design and dispatch. Renewable Energy 2006; 31(14):2296–2320.

[12] Iniyana S, Suganthi L, Anand AS. Energy models for commercial energy prediction and substitution of renewable energy sources. Energy Policy 2006; 34(17):2640–2653.

[13] Juhari AR, Kamaruzzaman S, Yusoff A. Optimization of renewable energy hybrid system by minimizing excess capacity. International Journal of Energy 2007; 3(1):77-81.

[14] Katsigiannis YA, Georgilakis PS. Optimal sizing of small isolated hybrid power systems using Tabu search. Optoelectronics and advanced materials 2008; 10(5):1241-1245.

[15] Ahmarinezhad A, Abbaspour-Tehranifard A, Ehsan M, Fotuhi-Firuzabad M. Optimal sizing of a stand alone hybrid system for Ardabil area of Iran. IJTPE 2012; 4(12):118-125

[16] Coello CC, Lamont GB, Van-Veldhuizen DA. Evolutionary algorithms for solving multi-objective problems. 2nd ed. New York: Springer; 2007.

[17] Hongxing Y, Wei Z, Lin L, Zhaohong F. Optimal sizing method for stand-alone hybrid solar–wind system with LPSP technology by using genetic algorithm. Solar Energy 2008; 82(4): 354–367.

[18] Galvez GH, Probst O, Lastres O, Rodríguez AN, Ugás AJ, Durán EA, Sebastian PJ. Optimization of autonomous hybrid systems with hydrogen storage: life cycle assessment. International Journal of Energy Research 2012; 36 (6):749–763.

[19] Galvez GH, Portela JDR, Rodríguez AN, Danguillecourt OL, Cortés LI, Ugás AJ, Martínez OS, Sebastian PJ. Selection of hybrid systems with hydrogen storage based on multiple criteria: application to autonomous systems and connected to the electrical grid. International Journal of Energy Research 2014; 38 (6): 702–713.

[20] Protogeropoulos C, BrinkWorth BJ, Marshall RH. Sizing and techno-economical optimization for hybrid solar photovoltaic/wind power systems with battery storage. International Journal of Energy Research 1997; 21(6): 465–479.

[21] Katsigiannis YA, Georgilakis PS, Karapidakis ES. Multi objective genetic algorithm solution to the optimum economic and environmental performance problem of small autonomous hybrid power systems with renewable. IET Renewable Power Generation 2010; 4(5):404–419.

[22] Trivedi M. Multi-objective generation scheduling with hybrid energy. PhD Dissertation, Department of Electrical Engineering, Clemson University, USA; 2007.

[23] Rodolfo DL, Jose LBA. Multi-objective design of PV–wind–diesel–hydrogen–battery systems. Renewable Energy 2008; 33(12):2559–2572.

[24] Abedi S, Alimardani A, Gharehpetian GB, Riahy GH, Hosseinian SH. A comprehensive method for optimal power management and design of hybrid RES-based autonomous energy systems. Renewable and Sustainable Energy Reviews 2012; 16(3):1577–1587.

[25] Ould-Bilal B, Sambou V, Ndiaye PA, Kébé CMF, Ndongo M. Optimal design of a hybrid solar-wind–battery system using the minimization of the annualized cost system and the minimization of the loss of power supply probability (LPSP). Renewable Energy 2010; 35 (10): 2388-2390.

[26] Shi JH, Zhu XJ, Cao GY. Design and techno-economical optimization for stand-alone hybrid power systems with multi-objective evolutionary algorithms. International Journal of Energy Research 2007; 31(3): 315–328.

[27] Sharafi M, ELMekkawy T Y. Multi-objective optimal design of hybrid renewable energy systems using PSO-simulation based approach. Renewable Energy 2014; 68: 67-79.

[28] Simulation modeling handbook: a practical approach, by Christopher A. Chung. ISBN 0-8493-1241-8, CRC Press LLC, 2004.

[29] Hazem, A, Janice G. Swarm Intelligence: concepts, models and applications. Technical Report. School of Computing. Queen's University, Canada; 2012.

[30] Kian SL,Salinda B,Anita A, Zuwairie I, An improved leader guidance in multi-objective particle swarm optimization. in IEEE Sixth Asia Symposium on Modelling, 2012.

[31] Yong Z, Dun-wei G, Zhong-hai D. Handling multi-objective optimization problems with a multi-swarm cooperative particle swarm optimizer. Expert Systems with Applications 2011; 38 (11): 13933–13941.

[32] Gary G. Y. Dynamic multiobjective evolutionary algorithm: adaptive cell-based rank and density estimation. IEEE Transactions on Evolutionary Computation.2003; 7(3): 253-274.

[33] Abdullah K, David W. C, Alice ES. Multi-objective optimization using genetic algorithms: A tutorial. Reliability Engineering and System Safety 2006; 91(9) 992–1007.

[34] Swagatam D, Ajith A, Amit K. Particle swarm optimization and differential evolution algorithms: technical analysis, applications and hybridization perspectives. Studies in Computational Intelligence (SCI) 2008; 116:1–38.

[35] Moslemi H, Zandieh M. Comparisons of some improving strategies on MOPSO for multi-objective (r, Q) inventory system. Expert Systems with Applications 2011; 38(10): 12051–12057.

[36] Coello-Coello CA, Pulido GT, Lechuga MS. Handling multiple objectives with particle swarm optimization. IEEE Transaction on Evolutionary Computation 2004; 8(3): 256-279.

[37] Frederick S H, Gerald JL. Introduction to operations research. 9th ed. New Tork: Mc Graw Hill; 2010.

Chapter 4

Optimal Design of Hybrid Renewable Energy Systems in Buildings with Low to High Renewable Energy Ratio

4.1. Abstract

We develop a simulation-based meta-heuristic approach that determines the optimal size of a hybrid renewable energy system for residential buildings. This multi-objective optimization problem requires the advancement of a dynamic multi-objective particle swarm optimization algorithm that maximizes the renewable energy ratio of buildings and minimizes total net present cost and CO_2 emission for required system changes. Of interest is to select the renewable energy ratio rather than CO_2 emissions and total net present cost as an optimization criterion in support of developing more sustainable approach for designing building energy systems. Three proven performance metrics then evaluate the quality of the Pareto front generated by the proposed approach. To evaluate the result of the algorithm, its result is compared against two reported multi-objective optimization algorithms in the related literature. Finally, an existing residential apartment located in a cold Canadian climate provides a test case to apply the proposed model and optimally size a hybrid renewable energy system to achieve various renewable energy ratios with minimizes total net present cost. In this test application, the model investigates the potential

use of a heat pump, a biomass boiler, wind turbines, solar heat collectors, photovoltaic panels, and a heat storage tank to produce renewable energy for the building. Furthermore, the utilization of plug-in electric vehicles for transportation reduces gasoline use where all power is generated by the building, and the utility provides the means to match intermittent renewable generation from solar and wind to building electrical loads. Model results show that under the chosen meteorological conditions and building parameters, a wind turbine and plug-in electric vehicle technologies are consistently the optimal option to achieve a target renewable energy ratio. In particular, the optimization result shows that the renewable energy ratio can achieve near 100% by installing a 73 kW wind turbine, a 200 kW biomass boiler, and using plug-in electric vehicles. This option has a net present cost of C$705180 and results in total CO_2 emission of 2.4 ton/year. Finally, a sensitivity analysis is performed to investigate the impact of economic constants on net present cost of the obtained non-dominated solutions.

4.2. Introduction

In the last decades, fossil fuel consumption and consequently its environmental impact has become a substantial universal concern. The building sector amounts to 40% of total energy demand. Currently, residential buildings are responsible for the major share (70%) of energy consumption in the building sector [1]. Thus, demand and supply side planning is required to decrease the energy demand of buildings and to provide the rest of the energy load with potential renewable resources. In addition, political limitations and state subsidies encourage users to search for environmental friendly solutions [1, 2]. The concept of Zero Energy Building (ZEB), which is expected to be the future perspective of buildings design has become a worldwide issue over the last decade [2]. ZEB are defined as buildings whose annual energy requirement is

supplied purely by renewable energy sources (RES) [1]. Therefore, ZEB can be stated as master plan for increasing the renewable energy ratio (RER). RER is defined as the amount of renewable energy generated divided by the total primary energy used.

The cost of renewable energy technologies can be attractive in the case of wind and solar energy. Their intermittent nature makes them more difficult to integrate to the grid. Hence, optimal sizing of a building renewable energy supply system can significantly impact its economic performance and consequently its reliability. In the design stage of a building energy supply system, many aspects have to be considered including economic performance, environmental impact, and reliability issues. In other words, decision makers, who are in charge of building energy system design, must make a trade-off between different options providing a wide range of cost, renewable energy ratio, need for energy storage, environmental impact, and reliability. It means this engineering problem needs simultaneous optimization of these conflicting objectives. Multi-objective optimization methods can be applied as a worthwhile alternative to address conflicting objective functions of complex optimization problems. The outcome of multi-objective optimization approaches is a set of solutions named the Pareto front. It provides information for decision makers to do a comparison between solutions and select a solution according to preferred objectives [3]. Many studies have proved that implementation of a multi-objective optimization problem (MOP) is not only difficult, but requires a large number of calculations to return a set of non-dominated solutions [4]. Similarly, multi-objective design of a hybrid renewable energy system (HRES) is a complex problem because of fluctuating energy prices, variable energy demand, and randomness of weather conditions.

Many models are developed to assess and design energy supply of buildings. Designers of ZEB often use trial and error approaches to find the optimal energy supply system design for a

specific building. The summary of studied recent literature in optimal design of hybrid renewable energy system for the buildings sector is summarized in Table 4-1 with most researchers using a single objective approach to design energy supply systems. Milan et al. [1] performed a linear programming model for optimal sizing of 100% renewable supply systems for a ZEB. The chief aim of their model was to find the minimum of the overall system costs. They applied their methodology for a building located in Denmark with three technologies including PV panels, solar collector, and heat pump. Dagdougui et al. [5] implemented a dynamic model using an integrated HRES to supply a building thermal and electrical energy loads. The model was applied to optimize a complex hybrid system including PV panels, a wind turbine, solar collectors, biomass heating, electrical network, and storage devices. In their study, a model predictive control (MPC) was employed to search the optimal solution. Lee et al. [6] explained a methodology for determining the optimal size of RE technologies which can be applied in the conceptual design of the energy supply systems of buildings. The method was described based on using RETScreen software developed by Natural Resource Canada. The proposed approach was tested in two case studies: a solar water-heating system merged to a district heating network and an integrated energy system for an office building. The second case comprised a solar water-heating, a heat pump, PV panels, an electric chiller, and a NG boiler. They considered four design criteria to optimize separately; initial cost, annual reduction of CO_2 emissions, cost effectiveness, and net present value. Their method is simple to implement but it suffers from simultaneously considering all objective functions as well as looking for optimal solutions in the whole search space. Prasad et al. [7] used HOMER simulation software to design an energy system consisting of PV panels, a wind turbine, and a standby generator for ZEB. The net present cost was considered as the performance metric of the system to evaluate different

configurations. Rezaei et al. [8] stated an analysis to compare various renewable energy options for four different buildings in Canada. A heat pump for heating and cooling purpose, solar collectors for space heating or hot water, and PV panels to generate electricity was dedicated to the case studies. Their results indicated that if the target would be obtaining minimum budget, the solar water heaters are the best choice while the hybrid systems are the best choice in terms of CO_2 emissions. Jiang et al. [9] designed and tested a green building energy system including renewable energy, energy storage, and energy management. They described the architecture of the proposed green building energy system and a computer simulation model to study the control strategies for the energy system. Although, they used plug-in electric vehicle (PEV) to meet the transportation load, the optimal sizing of the energy system was not investigated as well as they did not study the impact of using renewable energy on the total net present cost (NPC) and CO_2 emission. Fabrizio et al. in [10] and [11] presented a methodology based on the energy hub concept to model and optimize the energy system of buildings. The model was customized to be applied at the step of conceptual design of buildings when cost, energy consumption, and CO_2 emission are examined as the design criteria. Although their approach seems effortless in implementation, ignoring storage devices may be one of its drawbacks. Ooka et al. [12] used genetic algorithm (GA) for optimal sizing of building energy supply systems. The main goal of the their method was to return the best combination of components, capacity and operational planning for providing cooling, heating, and power load regarding minimum CO_2 emission. Thompson et al. [13] used RETScreen software to analyze and compare three renewable energy technologies (PV panels, wind turbine and a biomass CHP) for a small off-grid research facility. On the other hand, they applied demand side management (DSM) and supply side management

(SSM) simultaneously to improve the energy situation in lower energy cost and cleaner energy production.

More contributions are required in the area of multi-objective optimization methodology for building energy supply systems as recommended by many researchers [10]. Few studies can be found that applied a multi-objective optimization methodology in designing building energy supply systems. Hassoun et al. [14] performed a simulations to identify best possible power design options for a ZEB located in Lebanon. They compared different power configurations to provide all electrical load with least NPC, maximum renewable energy fraction, and least greenhouse gases emissions. Their results proposed a combination of PV, a wind turbine, batteries, a converter and diesel generator as the optimum renewable energy system for the total load of 90 kWh/day. Furthermore, an exergy analysis was carried out to explore the impact of using a PV/thermal system to heat the water instead of using a PV stand alone system. Fux et al. [15] developed a simulation tool to compare different configurations of a stand-alone building energy system for determining the best sizes of the employed components. In the employed HRES, both thermal and electric RE resources were integrated and mentioned as the contribution of the tool. By performing the simulation for different configurations, they generated a PF including 13 non-dominated solutions regarding both NPC and global warming potential. Rosiek et al. [16] compared three different solar-assisted hybrid building cooling, heating and power systems which are reported as alternatives to the conventional system for the existent office building located in Almería (Spain). They calculated a set of performance indexes that consists of primary energy and CO_2 savings, initial cost, operating cost, maintenance cost, avoided costs and payback period. Chua et al. [17] developed an evaluation tool based on a simulation approach to study the potential of hybridizing renewable technologies in aiding tri-

generation systems to fulfill required cooling, heating and power load of a commercial building. Their hybrid system consists of four key components: PV/thermal, solar/thermal, fuel cell, micro turbine and absorption chiller-water system. They analyzed 8 different cases based on the operation cost reduction, energy saving, and minimum environmental impact. Besides, they defined performance factor indicator (PFI) to combine three main criteria for the evaluation process.

In summary, there is a lack of using an efficient multi-objective optimization algorithm to search for optimal solutions instead of using simulation approach that evaluates the performance of a limited number of configurations. Additionally, the integration of transportation into a building energy supply system is seldom considered so that PEV are not part of an optimal HRES design. Hence, it can be represented as a future research direction to study how new transportation technologies may affect total NPC and CO_2 emission of HRESs. In other words, the design of HRESs should consider not only electricity, cooling and heating load but also the required energy for transportation.

In this paper, a multi-objective approach is proposed to take into account the renewable energy ratio as performance indicators rather than economic and environmental criteria when optimizing the design of buildings energy supply systems. The contribution of the present work is that a comprehensive energy supply system is studied by addressing the optimal component sizing of a building energy system integrating electric, thermal, cooling, and transportation demand. Moreover, previous work tried to design a 100% renewable energy supply system while in this study renewable energy ratio is examined as an objective function to provide solutions that consider the trade-off between the economic aspect and the RER level. The renewable energy system is simulated on an hourly basis within a C++ programming environment. Then a dynamic

multi-objective particle swarm optimization algorithm (DMOPSO) is implemented and linked to the simulation to handle the optimization. The generated PF is evaluated by three well-known performance metrics that will be explained in Section 4.7. This paper is the extension of the previous work [18] in which DMOPSO algorithm was demonstrated for optimal sizing of HRESs. In this study, the main aim is to utilize the designed Pareto-based MOP algorithm in a new design problem. A MOP algorithm is implemented to obtain the optimal design of a RE supply system of a building.

Section 4.4 describes an overview of the design problem. Section 4.5 presents the mathematical models employed in the optimization problem as well as in the simulation module. The basic concepts of DMOPSO are discussed in Section 4.6. Section 4.7 is devoted to the definitions of used performance metrics to evaluate the generated Pareto fronts. Section 4.8 represents a case study including the evaluation of its results and usability testing. Finally, Section 4.9 summarizes the research findings, proposed approach strengths, limitations, and suggested future research.

Table 4-1: The summary of the literature review

Authors	System components								MOP	Objective functions	End-use section					Optimization approach
	Wind turbine	PV panel	Solar Collector	Biomass	Heat Pump	PEV	Storage	Diesel& other			Heating	Cooling	Electricity	Hot water	Transportation	
Milan et al. [1]		●	●		●		●		NO	Minimize total NPC	●	●	●	●		LP
Dagdougui et al. [5]	●	●	●	●			●		NO	Minimize deviation from energy demands	●	●	●	●		MPC
Lee et al. [6]		●	●		●			●	NO	Minimize initial system cost Minimize CO_2 emissions Minimize cost effectiveness Minimize net present value	●	●	●	●		GRG nonlinear
Prasad et al. [7]	●	●					●	●	NO	Minimize total NPC			●			Simulation
Rezaei et al. [8]		●	●		●				NO	Minimize total NPC Minimize CO_2 emission	●	●	●	●		Calculation-based
Jiang et al. [9]	●	●	●			●	●	●	NO	Energy management	●	●	●	●	●	Simulation
Fabrizio et al. [10], [11]		●	●	●	●			●	NO	Minimize total NPC Minimize CO_2 emission Minimize energy consumption	●	●	●	●		Calculation-based
Ooka et al.[12]					●			●	NO	Minimize CO_2 emission	●	●	●	●		GA
Thompson et al. [13]	●	●	●					●	NO	Minimize energy cost Minimize CO_2 emission	●	●	●	●		Simulation
Hassoun et al. [14]	●	●					●	●	Yes	Minimize total NPC Maximize RER Minimize CO_2 emission			●			Simulation
Fux et al. [15]		●	●				●	●	Yes	Minimize total NPC Minimize CO_2 emission	●	●	●	●		Simulation
Rosiek et al. [16]		●	●		●			●	Yes	Minimize total NPC Minimize CO_2 emission Maximize energy saving	●	●	●	●		Calculation-based
Chua et al. [17]		●	●					●	Yes	Minimize operation cost Maximize energy saving Minimize CO_2 emission	●	●	●	●		Simulation

4.3. Nomenclature

$A_{Land,b}$	Required land for biomass production [m^2]	E_{HP}	Electricity consumption by heat pump [kWh]
A_{Max}	Upper limit for building roof area [m^2]	E_{EV}	Electricity consumption by PEV [kWh]
A_{PV}	Area of PV panels installed on the building roof [m^2]	E_{Sold}	Sold electricity to the grid [kWh]
A_{SC}	Area of solar collectors installed on the building roof [m^2]	E_{PV}	Net power generated by PV panel [kWh]
A_r	Wind turbine rotor swept area [m^2]	E_{PV-Re}	PV panel power output [kWh]
$Biomass_{Max}$	Annual available biomass [ton/year]	E_{PVR-Re}	Rural PV panel power output [kWh]
C	Coverage metric	E_{WT}	Net power generated by Wind turbine [kWh]
$C_{b,Col}$	Biomass collection cost [C$/ton]	E_{WT-Re}	Wind turbine power output [kWh]
$C_{b,St}$	Biomass storage cost [C$/ton]	EF_E	Emission factor of grid electricity [kg CO_2/KWh]
$C_{b,Tr}$	Biomass transportation cost [C$/ton.km]	EF_{Gas}	Emission factor of gasoline [kg/lit]
$C_{elec,s}$	Sold electricity price [C$/kWh]	EF_{NG}	Emission factor of NG [kg CO_2/m^3]
$C_{elec,b}$	Purchasing electricity price [C$/kWh]	$El_{b,y}$	Annual electricity bought from the grid [kWh/year]
C_{Gas}	Gasoline price [C$/litre]	$El_{s,y}$	Annual sold electricity [kWh/year]
$C_{I,j}$	Capital cost of component *j* [C$/unit]	EOT	Equation of time [min]
C_{NG}	Natural gas price [C$/$m^3$]	GAS	Hourly gasoline consumption [kWh]
C_P	Wind turbine power coefficient	Gas_y	Annual gasoline consumption [lit/year]
$C_{O\&M,j}$	Operation& maintenance of component *j* [C$/unit]	HE_{Bio}	Heating load provided by biomass boiler [kWh]
$C_{rep,j}$	Replacement cost of component j [C$/unit]	HE_{HP}	Heating load provided by heat pump [kWh]
CO_{AR}	Cooling load provided by air refrigerator [kWh]	HE_{NG}	Heating energy generated by NG boiler [kWh]
CO_{HP}	Cooling load provided by heat pump [kWh]	HHV_b	Higher heating value of biomass [Mj/kg]
COP_{AR}	Coefficient of performance for air refrigerator	HHV_{Gas}	Higher heating value of gasoline [Mj/kg]
COP_{HP-CO}	Coefficient of performance of heat pump in cooling mode	HHV_{NG}	Higher heating value of NG [Mj/kg]
COP_{HP-HE}	Coefficient of performance for heat pump in heating mode	$HP(t)$	Hourly heat pump energy output [kWh]
CRF	Capital recovery factor	$HST(t)$	Level of hot water in storage tank in time step *t* [kWh]
E_{EX}	Excess electricity [kWh]	$HW_{Bio-tank}$	Hot water load provided by biomass boiler [kWh]
E_{bought}	Bought electricity [kWh]	$HW_{HP-tank}$	Hot water load provided by heat pump [kWh]
E_{AR}	Electricity consumption by air refrigerator [kWh]	$HW_{NG-tank}$	Hot water generated by NG boiler [kWh]
$HW_{SC-tank}$	Hot water generated by SC [kWh]	Un_E	Hourly unmet electricity [kWh]
HW_{T-load}	Total hot water sent to load [kWh]	Un_{HE}	Hourly unmet heating [kWh]

i	Interest rate [%]	$T_{SC,in}$	Solar collector water input temperature [^{0}C]
$I_{b,n}$	Direct normal irradiance [kWh/m^2]	t_{zone}	Time zone difference
$I_{b,tilt}$	Beam radiation [kWh/m^2]	U_{loss}	Solar collector heat loss coefficient [W/m^{2}K]
$I_{d,tilt}$	Sky diffuse radiation [kWh/m^2]	$Un_{Cooling}$	Hourly unmet cooling energy [kWh]
$I_{r,tilt}$	Ground reflected solar radiation [kWh/m^2]		
I_T	Total solar radiation on tilted surface [kWh/m^2]	Un_{HW}	Hourly unmet hot water[kWh]
K	Single payment present worth	V_C	Wind turbine cut-in wind speed [m/s]
$L_{Cooling}$	Cooling demand [kWh]	V_f	Wind turbine cut-off wind speed [m/s]
L_{HE}	Heating demand [kWh]	V_r	Wind turbine rated wind speed [m/s]
L_{HW}	Hot water demand [kWh]	$W_{com,max}$	Compressor capacity [kW]
L_{local}	Local longitude [Degree]	Z	Wind turbine hub height [m]
LLP_{max}	Loss of load probability upper limit[%]	η_{pv}	PV panel efficiency[%]
m_b	Biomass flow rate [kg/hr]	η_{SC}	Solar collector efficiency[%]
MS	Maximum spread metric	η_{bb}	Biomass boiler efficiency[%]
NG_y	Annual NG consumption [m^3/year]	η_{In}	Inverter efficiency[%]
P_{Bio}	Biomass boiler capacity [kW]	η_{NGb}	Natural gas boiler efficiency [%]
$P_{j,max}$	Upper limit of the capacity of components	η_{Re}	Rectifier efficiency[%]
$P_{j,min}$	Lower limit of the capacity of components	$\varepsilon_{Tr,gas}$	Transportation allocation coefficient of gasoline car
P_{HP}	Heat pump capacity [kW]	$\varepsilon_{Tr,PEV}$	Transportation allocation coefficient of PEV
P_{HST}	Heat storage tank capacity [m^3]	$\varepsilon_{CO,AR}$	Cooling allocation coefficient of air refrigerator
P_{SC}	Solar collector capacity [kW]	$\varepsilon_{CO,HP}$	Cooling allocation coefficient of heat pump
P_r	Wind turbine rated output power [kW]	$\varepsilon_{HE,bb}$	Heating and hot water allocation coefficient of biomass boiler
P_{WT}	Wind turbine capacity [kW]	$\varepsilon_{HE,HP}$	Heating and hot water allocation coefficient of heat pump
S	Spacing metric	ξ	Sun azimuth angle [Degree]
T	Project life time[year]	ε	Tilt angle [Degree]
RER	Renewable energy ratio[%]	λ	Latitude[Degree]
$T_{ambeint,hr}$	Hourly ambient temperature [^{0}C]	δ	Solar declination angle [Degree]
$T_{d,cool}$	Summer design temperature [^{0}C]	χ	Zenith angle [Degree]
$T_{d,heat}$	Heating design temperature [^{0}C]	ζ	Plate azimuth angle [Degree]
T_{ewt}	Entering fluid temperature in HP [^{0}C]	ρ	Air density [kg/m^3]
T_g	Ground temperature [^{0}C]		

4.4. Problem Statement

The main goal of this study is to increase the renewable energy ratio of a building located in cold climate by using different renewable energy conversion technologies. To supply the energy need of a building, a grid-connected hybrid renewable energy system has been designed. This energy system may include wind turbine, PV panels, solar thermal collectors, heat pump, biomass boiler and heat storage tanks. Figure 4-1 demonstrates the arrangement of the employed energy supply system. A natural gas boiler, air refrigerators, and grid are utilized as backup systems when the RE sources are not able to provide the energy demand. It is supposed that PV panels and wind turbines are the main electricity generators, where the grid is utilized as a backup source. In other words, the grid helps in supplying electricity when the produce electricity by RE resources is less than electricity load.

There is a constraint on the available installation area of PV panels in the building as well as it is not permitted to install wind turbine within the city boundaries. In this study, in order to overcome these limitations a heuristic approach is proposed. The wind turbines would be installed outside the city boundaries in a rural area. PV panels can be installed on both building rooftops and in rural areas. The produced electricity by PV panels and wind turbines installed in rural areas can be sold to the electric utility using net metering so that each building can gain the benefit of using wind turbines and PV panels in more optimal locations, reduces urban sprawl, and prevents ZEB to contribute to GHG's by allocating limited financial resources less optimally.

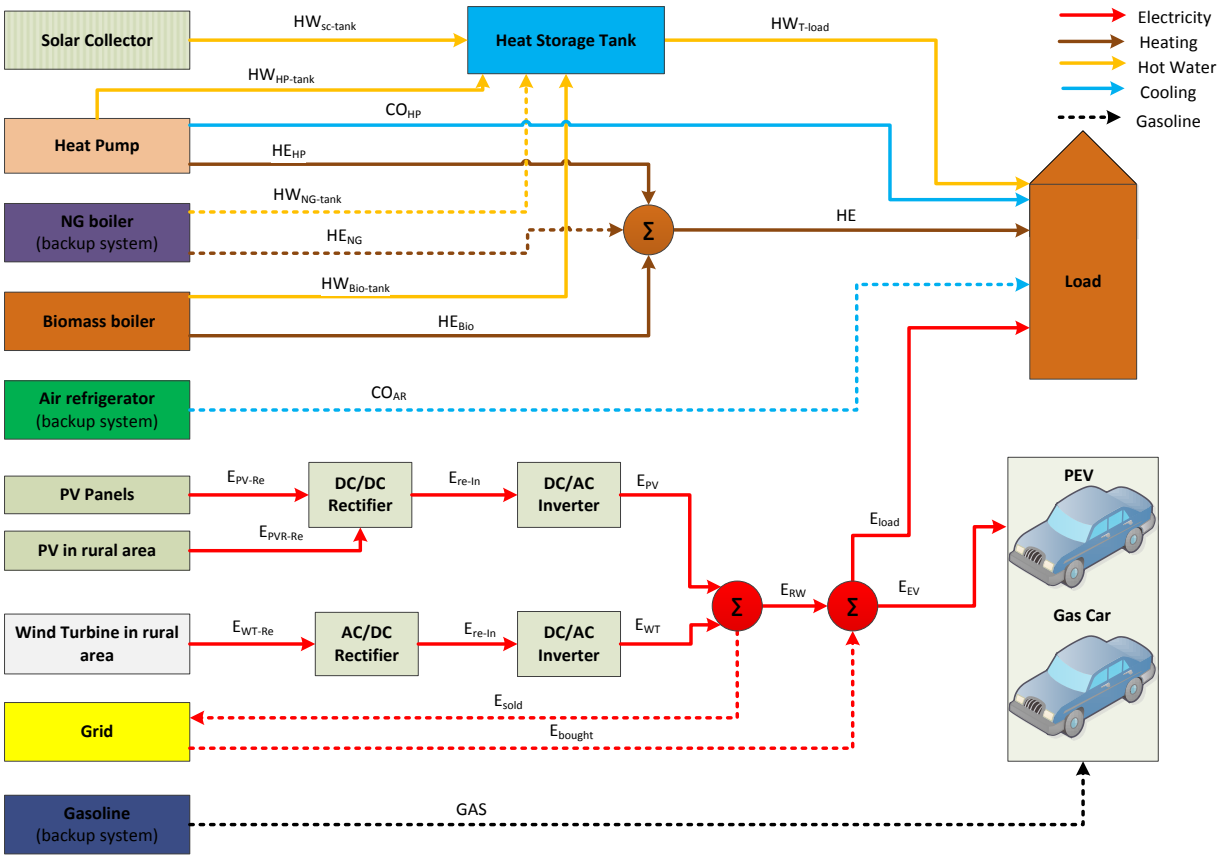

Figure 4-1: Energy flow of the proposed hybrid renewable energy system

The heat pump extracts heat from the ground to meet the heating load in winters and cooling load in summer time. A heat pump transfers heat by circulating a fluid refrigerant. In winter, the refrigerant is evaporated at low pressure and absorbs heat from the ground. A compressor increases the pressure of refrigerant to be condensed at high pressure in a condenser and releases the heat that it absorbed in the cycle into the building. In summer time, the process is reversed, and the heat pump extracts heat from the indoor air and releases it to the ground. The biomass boiler combusts solid biomass fuel to provide required heating for space heating and hot water. In this study, it is assumed that the biomass can be cultivated, collected and stored elsewhere and then transported to the building place on demand. The biomass is considered to be 40 km from the building location, as shown in Figure 4-2. We assume there is no limitation to grid connect

the wind turbine and PV panels and using net metering if the facilities meet technical requirements [19]. Solar collectors provide hot water for the building. A heat pump and biomass boiler also supply hot water when the solar collectors are not able to meet load. Heat storage tanks are used to store hot water. Furthermore, when the heat pump, biomass boiler and solar collectors are not able to provide the heating and hot water demand, the existing natural gas boiler supplies the required energy.

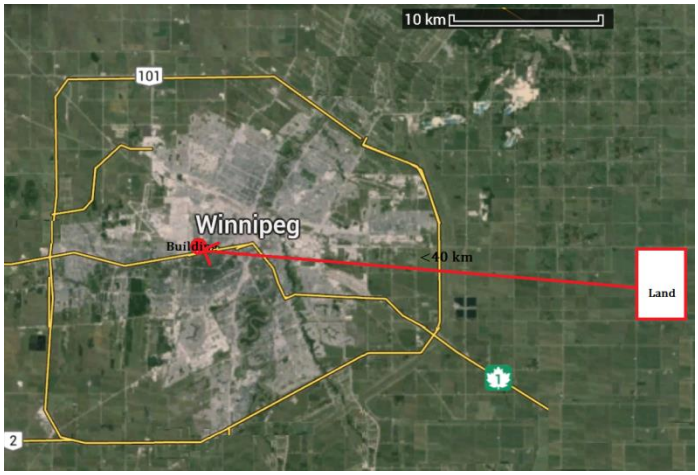

Figure 4-2: Distance between solar and wind generation and the building

There are two options to meet required transportation of the building, using PEV and gasoline cars. It is assumed that the energy required for PEV is met by electricity, if there is no enough electricity, gasoline will be used to guarantee the load. A heat pump or backup air refrigerators will cover the cooling load during summers.

There are two options to meet the transportation requirements of building occupants: PEV and gasoline cars. Hydrogen vehicles are not considered as round trip efficiencies for hydrogen made from renewable electricity are to low compared to PEV which requires accounting for GHG's due to large conversion losses. It is assumed that the energy required for PEV is met by building

electricity when possible. A heat pump or air conditioners will cover the cooling load during summers.

The main goal of this study is to provide the most suitable energy supply system configuration for a building. In other words, the developed approach returns the best combination of proposed technologies and corresponding optimal size of its components. It is intended to simultaneously minimize the total net present cost of the system for its entire life time, minimize annual CO_2 emission and maximize RER while satisfying a certain level of reliability. For this purpose, a practical optimization tool has been developed, which is constructed based on hybridizing simulation with an optimization algorithm. In this regards, the heating, cooling, and electricity load profile on hourly basis is defined for the building in a reference year. Further, relevant hourly weather data of the year is entered to the model as input data. To specify employed technologies, the actual cost data is considered as well mathematical models and the technical structures are stated for the components. Based on these data, three objective functions are optimized with respect to the energy balance equations and other technical constraints. The expected results of the model are the optimal combinations of the examined renewable energy conversion technologies and their corresponding optimal capacities. Besides, the model returns system performance throughout a reference year. It is notable that in this study, the main focus is on the energy supply system whereas the life cycle cost analysis of the whole building is not carried out. Additionally, the optimization of building envelope is not considered, and it is assumed as its current situation.

4.5. Multi-Objective Optimization Problem Formulation

This study attempts to emphasize optimization of the proposed design problem by using a simulation-based optimization approach, Figure 4-3. The main feature of using simulation module is that we can incorporate all details and randomness of the system with an acceptable accuracy level. In this case, the optimization algorithm is responsible to search for optimal design [20].

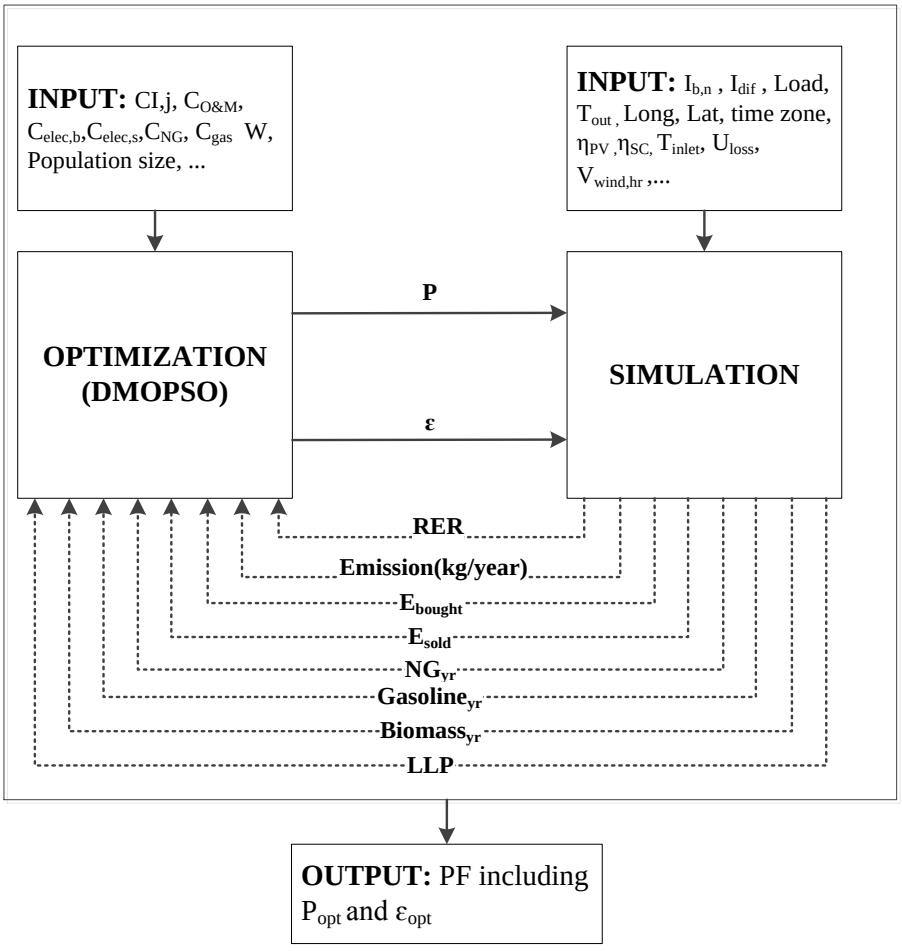

Figure 4-3: The simulation-based optimization approach flow diagram

The formulation of the optimization problem including decision variables, objectives and constraints exactly has been implemented through the employed optimization algorithm. The simulation module is responsible for accommodation of mathematical models of the energy

suppliers. First, a set of random solutions is generated to initialize the population of particles, and then the simulation module receives the candidate solutions to test their practicability. Indeed, the role of simulation module is to compute the performance of each proposed configuration such as RER, CO_2 emission, and LLP. The next step is related to checking the stopping criterion, if that will not be satisfied, the set of solutions are updated according to operators applied in the optimization algorithm. The updated population again has to send back to the simulation module to check its feasibility. The finishing point of this cycle is determined by defined termination criterion. The outcome of this computational procedure is a set of non-dominated solutions stated as the best solutions found so far, Figure 4-3.

The mentioned optimization problem in Section 4.4 is formulated as a MOP problem subjected to a set of constraints, in which decision variables are defined as the installed capacity of the components. Moreover, the allocation coefficients of the technologies to meet heating, cooling, electricity, and transportation load are also defined as decision variables. The allocation coefficient is defined as the portions of energy load that must be provided by the corresponding component. These coefficients are defined to aid the model in selecting the best dispatch strategy if two or more components are chosen to provide energy load simultaneously. Three objective functions are considered: total NPC, RER, and CO_2 emission. The constraints represent the energy balances between components and other technical constraints, which introduce the physical concept of the problem. The following section presents the mathematical formulation for the objective functions and constrains.

4.5.1. Objective Functions

-Economic criteria: Total net present cost of the employed system over its life time is considered as one of the objective functions. The life time of the system is marked as 25 years that is equal to the longest lifespan of elements. Decision variables of the model are summarized in the following vectors:

$$\vec{P} = [P_{PV}, P_{WT}, P_{SC}, P_{HP}, P_{HST}, P_{Bio}, P_{PVR}]$$

$$\vec{\varepsilon} = [\varepsilon_{HE,HP}, \varepsilon_{HE,bb}, \varepsilon_{CO,HP}, \varepsilon_{CO,AR}, \varepsilon_{Tr,PEV}, \varepsilon_{Tr,gas}]$$

where, P_{PV} is the size of PV panels (kW) installed on the building roof, P_{WT} is the size of the wind turbine (kW), P_{SC} is the size of the solar collectors (kW), P_{HST} is the size of the heat storage tanks (m^3), P_{HP} is the size of the heat pump (kW), P_{Bio} defines the biomass boiler rated capacity, and P_{PVR} introduces the PV panels rated power, which should be installed in the rural area. $\varepsilon_{HE,HP}$ and $\varepsilon_{HE,bb}$ stand for heating and hot water allocation coefficient of the heat pump and biomass boiler. $\varepsilon_{CO,HP}$ and $\varepsilon_{CO,AR}$ are the cooling allocation coefficient of the heat pump and air refrigerators, respectively. $\varepsilon_{Tr,PEV}$ and $\varepsilon_{Tr,gas}$ are the allocation coefficient of the PEV and gasoline-cars.

Total NPC consists of investment costs, operation and maintenance costs, replacement costs of the technologies, fuel costs, rental cost of the land, biomass collection, storage and transportation costs over the project life time, Equation (4-1).

$$NPC = \sum_{j}[C_{I,j} + C_{O\&M,j} \times \frac{1}{CRF(i,T)} + C_{rep,j} \times K_j] \times P_j + [C_{elec,b} \times E_{bought} + C_{NG} \times NG_y - C_{elec,s} \times E_{Sold} + C_{Gas} \times Gasoline + Biomass_y \times (C_{b,Col} + C_{b,St} + C_{b,Tr})] \times \frac{1}{CRF(i,T)} \quad (4\text{-}1)$$

where, $C_{I,j}$ states the capital cost of the element j (C$/unit), $C_{O\&M,j}$ is the operation and maintenance cost of the component j (C$/unit), $C_{rep,j}$ is replacement cost of the component j (C$/unit). $C_{elec,b}$ is the electricity price bought from the grid (C$/kWh) , C_{NG} is the natural gas price (C$/m^3), $C_{elec,s}$ is the electricity price sold to the grid (C$/kWh), and C_{Gas} is the gasoline price (C$/litre). $El_{b,y}$, NG_y, $El_{s,y}$, and Gas_y are standing for annual electricity bought from the grid, NG consumption, electricity sold to the grid, and gasoline consumption, respectively. Moreover, biomass collection, storage and transportation costs are defined by $C_{b,Col}$, $C_{b,St}$, and $C_{b,Tr}$, respectively. *CRF* is the capital recovery factor and *K* is single payment present worth [20]. i is interest rate and *T* states the project life time.

-Renewable energy ratio (RER): The renewable energy ratio is defined as the amount of used renewable energy divided by the total used primary energy, Equation (4-2).

$$RER = \frac{Renewable\ energy}{Primary\ energy} \quad (4\text{-}2)$$

where, primary energy consumption is equal to total energy reached to the load including renewable and non-renewable sources. *Renewable energy* dedicates the energy load which is met by renewable sources.

-Environmental criteria: In this study, the pollution emission is considered as the environmental criteria. It is assumed that only CO_2 is the pollution emission since it is the major

emission. The produced CO_2 is resulted from gasoline consumption of the cars, NG burning by the backup natural gas boiler, and emission resulted by the electricity bought from the grid, Equation (4-3).

$$CO_2 = Gasoline \times EF_{Gas} + NG_y \times EF_{NG} + E_{bought} \times EF_E \quad (4\text{-}3)$$

where, EF_{Gas} is the emission factor of gasoline, $EF_{NG}$is emission factor of natural gas, and EF_E is is CO_2 emission produced by consumption of 1kWh electricity. In this study, the value for the emission factors is set as what is depicted in

Table 4-5.

4.5.2. Constraints

The feasible region of the problem is bounded by a number of constraints dictated on the decision variables. It means the constraints limit the decision variables bound, which may be resulted from physical, technological, legal, or economical restrictions. The constraints in the present study are defined by technical characteristics of the components and by matching supply and demand sections. The first equality specifies the amount of hot water demand that should be provided by NG boiler, biomass boiler and heat pump.

$$HW'_{Load}(t) = P_{HST} - HST(t) + L_{HW}(t) - HW_{SC-tank}(t) \quad (4\text{-}4)$$

$$\varepsilon_{HE,HP} + \varepsilon_{HE,bb} \leq 1 \quad (4\text{-}5)$$

$$HW_{HP-tank}(t) = max\{\varepsilon_{HE,HP} \times HW'_{Load}(t), 0\} \quad (4\text{-}6)$$

$$HW_{Bio-tank}(t) = max\{\varepsilon_{HE,bb} \times HW'_{Load}(t), 0\} \quad (4\text{-}7)$$

$$HW_{NG-tank}(t) = max\{L_{HW}(t) - [HW_{SC-tank}(t) + HW_{HP-tank}(t) + HW_{Bio-tank}(t) + HST(t)], 0\} \quad (4\text{-}8)$$

The allocation coefficient for providing hot water and heating by the ground source heat pump and biomass boiler are indicated by $\varepsilon_{HE,HP}$ and $\varepsilon_{HE,bb}$, respectively. That is, the heat pump is in charge of providing $\varepsilon_{HE,HP}$ percent of heating and hot water load while the biomass boiler is responsible for $\varepsilon_{HE,bb}$ percent. These allow model to select different schemes when a heat pump and a biomass boiler are used simultaneously. Constraint (4-6) and (4-7) introduce the amount of hot water that must be derived from the heat pump and biomass boiler. Constraint (4-8) represents the required total hot water supplied by the NG boiler. It is equal to the rest of hot water load that is not met by renewable sources and storage tank.

The heating load that must be supplied by heat pump and NG boiler within time period *t* is defined by Equation (4-9) and Equation (4-10). Constraint (4-11) determines the heating load that is yielded by the NG boiler.

$$HE_{HP}(t) = \varepsilon_{HE,HP} \times L_{HE}(t) \quad (4\text{-}9)$$

$$HE_{Bio}(t) = \varepsilon_{HE,bb} \times L_{HE}(t) \quad (4\text{-}10)$$

$$HE_{NG}(t) = L_{HE}(t) - [HE_{HP}(t) + HE_{Bio}(t)] \quad (4\text{-}11)$$

Unmet hot water and heating load are represented by Equation (4-12) and Equation (4-13). They are equal to the difference between the capacity of NG boiler and its heating and hot water load. These equations allow us to easily derive LLP for the employed system.

$$Un_{HE}(t) = max\{HE_{NG}(t) - P_{NG_{HE}}, 0\} \quad (4\text{-}12)$$

$$Un_{HW}(t) = max\{HW_{NG-tank}(t) - P_{NG\_HW}, 0\} \quad (4\text{-}13)$$

Hot water energy balance takes into account the output of the heat storage tanks, unmet hot water and load, Equation (4-14). The heating energy balance equation at the collection node, which is indicated in Figure 4-1, is guaranteed by Equation (4-15). The hot water level in the tank at the end of period t+1 is equal to the inventory level at previous time period plus the amount of hot water generated by the solar collectors, heat pump, biomass boiler and NG boiler during time period t minus the quantity of hot water consumed by the building during the same period, Equation (4-16).

$$HW_{T-load}(t) + Un_{HW}(t) = L_{HW}(t) \quad (4\text{-}14)$$

$$HE(t) = HE_{HP}(t) + HE_{Bio}(t) + HE_{NG}(t) \quad (4\text{-}15)$$

$$HST(t+1) = HST(t) + HW_{SC-tank}(t) + HW_{HP-tank}(t) + HW_{Bio-tank}(t) + HW_{NG-tank}(t) - HW_{T-load}(t) \quad (4\text{-}16)$$

The next constraint limits the annual biomass consumption to available biomass, Equation (4-17). As we have assumed a constant efficiency for NG boiler, then from Equation (4-18), we can easily extract the annual NG consumption by the system. For any time period t, total heating and hot water supplied by the biomass boiler must be less than its rated capacity, Equation (4-19).

$$\frac{\sum_{t=0}^{8760}(HE_{Bio}(t)+HW_{Bio-tank}(t))}{\eta_{bb}\times HHV_b} \leq Biomass_{Max} \quad (4\text{-}17)$$

$$NG_y = \frac{\sum_{t=0}^{8760}(HW_{NG-tank}(t)+HE_{NG}(t))}{\eta_{NGb}\times HHV_{NG}} \quad (4\text{-}18)$$

$$HE_{Bio}(t) + HW_{Bio-tank}(t) \leq P_{bio} \quad (4\text{-}19)$$

Equations (4-20)-(4-27) are applied to identify cooling flows which are shown in Figure 4-1. The allocation coefficients $\varepsilon_{CO,HP}$ and $\varepsilon_{CO,AR}$ indicate the portion of cooling load that must be met by the heat pump and air refrigerators. Hence, Equation (4-21) and Equation (4-22) are applied to calculate cooling need that should be provided by HP and AR, respectively. Equation (4-23) is used for calculating unmet cooling energy. The energy balance for cooling energy flows is given in Equation (4-24). The cooling load is equal to cooling energy provided by heat pump, AR, and unmet cooling energy.

$$\varepsilon_{CO,HP} + \varepsilon_{CO,AR} = 1 \tag{4-20}$$

$$CO_{HP}(t) = \varepsilon_{CO,HP} \times L_{Cooling}(t) \tag{4-21}$$

$$CO_{AR}(t) = \varepsilon_{CO,AR} \times L_{Cooling}(t) \tag{4-22}$$

$$Un_{Cooling}(t) = max\{CO_{AR}(t) - P_{AR}, 0\} \tag{4-23}$$

$$L_{Cooling}(t) = CO_{HP}(t) + CO_{AR}(t) + Un_{Cooling}(t) \tag{4-24}$$

Total energy supplied by the HP should not exceed its rated capacity, Equation (4-25). The electricity required for AR in time period *t* is the same as cooling energy that it requires divided by its *COP*, Equation (4-26). Likewise, the electricity consumption by the HP is calculated by using Equation (4-27).

$$HE_{HP}(t) + HW_{HP-tank}(t) + CO_{HP}(t) \leq HP(t) \tag{4-25}$$

$$E_{AR}(t) = CO_{AR}(t)/COP_{AR} \tag{4-26}$$

$$E_{HP}(t) = \frac{HE_{HP}(t) + HW_{HP-tank}(t)}{COP_{HP-HE}} + \frac{CO_{HP}(t)}{COP_{HP-CO}} \tag{4-27}$$

We have allocated the total required energy for transportation between PEV and gasoline car using allocation coefficient of $\varepsilon_{Tr,PEV}$ and $\varepsilon_{Tr,gas}$ for PEV and gasoline car, Equations (4-28) to

(4-30). Annual total gasoline consumption by the building residents can be deliberated as Equation (4-31).

$$E_{EV}(t) = \frac{\varepsilon_{Tr,PEV} \times L_T(t)}{\eta_{EV}} \quad (4\text{-}28)$$

$$GAS(t) = \frac{\varepsilon_{Tr,gas} \times L_T(t)}{\eta_{Car}} \quad (4\text{-}29)$$

$$\varepsilon_{Tr,PEV} + \varepsilon_{Tr,gas} = 1 \quad (4\text{-}30)$$

$$Gasoline_y = \frac{\sum_{t=0}^{8760} GAS(t)}{HHV_{Gas}} \quad (4\text{-}31)$$

Constraints (4-32) to (4-39) are related to electricity flows in Figure 4-1. The net electricity produced by PV panels is calculated by using Equation (4-32). Where, η_{Re} and η_{In} represent the rectifier and inverter efficiency. Correspondingly, the net generated electricity by wind turbine is considered as the output electricity of the inverter, Equation (4-33). From Equation (4-34) to (4-36), the amount of excess energy that must be sold to the grid or electricity deficit that would be bought from the network is identified. The sign of E_{EX} clarifies that the electricity is deficit or excess, Equation (4-35) and (4-36).

$$E_{PV}(t) = [E_{PV-Re}(t) + E_{PVR-Re}(t)] \times \eta_{Re} \times \eta_{In} \quad (4\text{-}32)$$

$$E_{WT}(t) = E_{WT-Re}(t) \times \eta_{Re} \times \eta_{In} \quad (4\text{-}33)$$

$$E_{EX}(t) = E_{EV}(t) + E_{Load}(t) + E_{AR}(t) + E_{HP}(t) - (E_{PV}(t) + E_{WT}(t)) \quad (4\text{-}34)$$

$$If \quad E_{EX} \geq 0 \rightarrow E_{Sold}(t) = 0 \quad (4\text{-}35)$$

$$If \quad E_{EX} < 0 \rightarrow E_{bought}(t) = 0 \quad (4\text{-}36)$$

In Figure 4-1, there are two collection points for electricity flows. The energy balance in these points is taken into account in Equation (4-37) and (4-38). Unmet electricity is defined by the difference between maximum hourly power allowed to be bought from the grid and the amount of electricity that must be bought in the time period *t*, Equation (4-39).

$$E_{PV}(t) + E_{WT}(t) = E_{RW}(t) + E_{Sold}(t) \quad (4\text{-}37)$$

$$E_{RW}(t) + E_{bought}(t) = E_{EV}(t) + E_{Load}(t) + E_{AR}(t) + E_{HP}(t) \quad (4\text{-}38)$$

$$Un_E(t) = max\{E_{bought}(t) - P_{Grid}, 0\} \quad (4\text{-}39)$$

Loss of load probability is defined as total unmet energy divided by total energy load, Equation (4-40). There is a desired level for LLP which is entered to the model by users, Equation (4-41). This illustrates the maximum LLP level that designed system can deal with. There is a limitation on the available area for installing PV panels and solar collectors on the building roof, which is represented by Equation (4-42). Finally, the minimum and maximum level of capacity of components is set by Equation (4-43).

$$LLP = \frac{Un_E(t) + Un_{Cooling}(t) + Un_{HW}(t) + Un_{HE}(t)}{L} \quad (4\text{-}40)$$

$$LLP \leq LLP_{max} \quad (4\text{-}41)$$

$$A_{PV} + A_{SC} \leq A_{Max} \quad (4\text{-}42)$$

$$P_{j,min} \leq P_j \leq P_{j,max} \quad (4\text{-}43)$$

4.5.3. Modeling Energy Supply Systems

The simulation module is based on hourly time interval analysis of energy demand, wind speed, temperature and total solar irradiation. In fact, the simulation module will be applied to calculate

the hourly energy generated by using the hourly wind velocity, total radiation on the horizontal surface, and temperature. The simulation module consists of 12 subcomponents, which calculates the energy generated by different renewable and non-renewable energy technologies for every hour, see Figure 4-4. In the last subcomponent, supplied energy is compared to demand in order to calculate operation metrics such as RER or LLP. The following section presents the mathematical models of renewable energy components which are used in the simulation module.

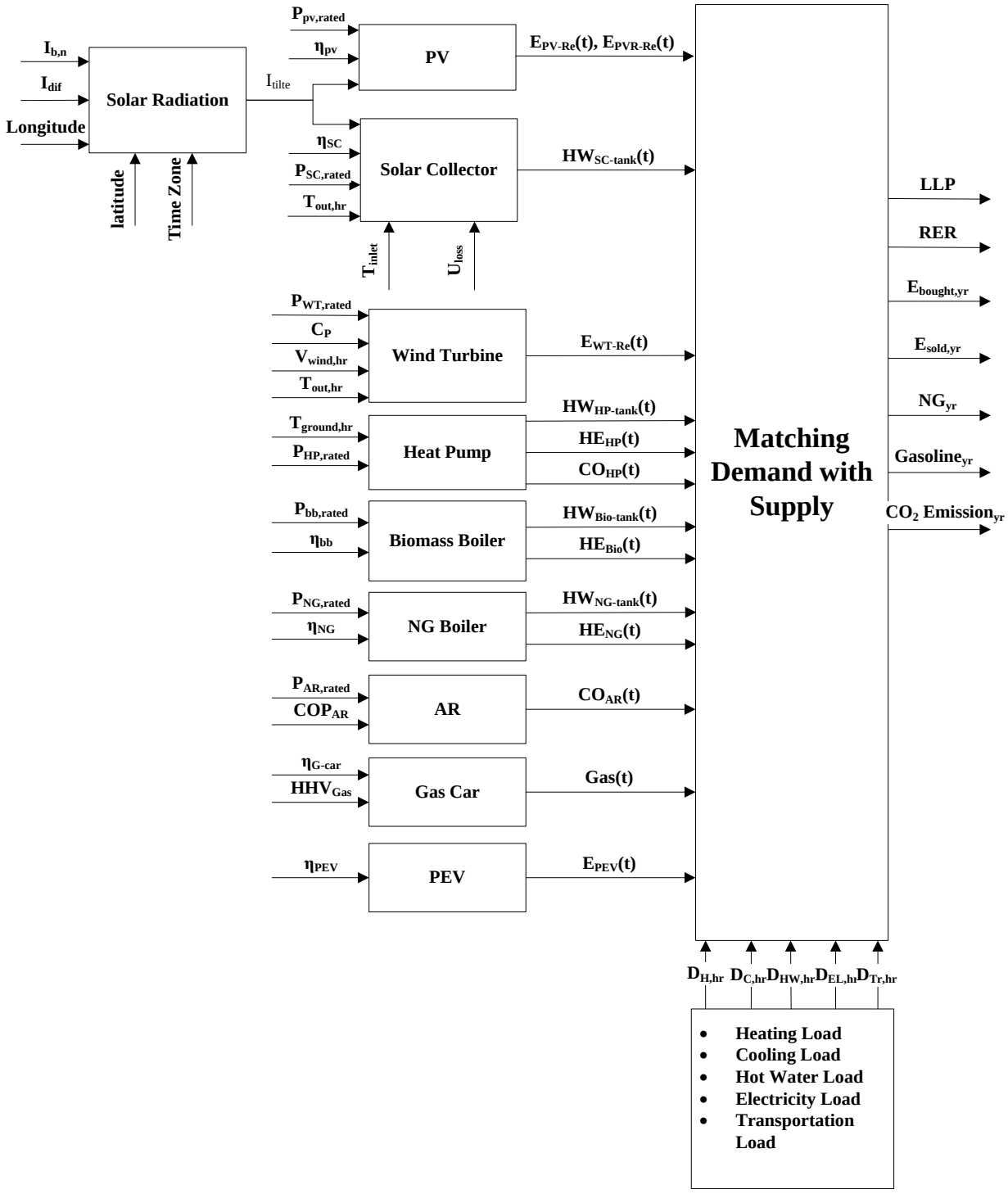

Figure 4-4: The simulation module diagram

4.5.3.1. Solar Radiation

Solar radiation on a tilted surface having a tilt angle of ε from the horizontal and an azimuth angle of ξ is the sum of the components consisting of beam ($I_{b,tilt}$), sky diffuse ($I_{d,tilt}$) and ground reflected solar radiation ($I_{r,tilt}$) [21]:

$$I_T = I_{b,tilt} + I_{d,tilt} + I_{r,tilt} \tag{4-44}$$

$$I_T = I_{tilt} = I_{b,n}[\cos(\theta) + C\cos^2\left(\frac{\varepsilon}{2}\right) + \rho(cos\chi + C)\sin^2\left(\frac{\varepsilon}{2}\right)] \tag{4-45}$$

where, $I_{b,n}$ is direct normal irradiance on a surface perpendicular to the sun's rays, θ is the angle between the tilted surface and the solar rays which is calculated by Equation (4-46), *C* is diffuse portion constant for calculation of diffuse radiation and it depends on the month [21], ρ is the reflection index which is 0.2 for grass and 0.8 for snow covered ground [21], χ is the zenith angle.

$$\cos(\theta) = [\cos\varepsilon\cos\chi + \sin\varepsilon\sin\chi\cos(\xi - \zeta)] \tag{4-46}$$

ξ and ζ are stand for the sun azimuth and plate azimuth angle, respectively. In this study the plat azimuth angle is assumed 180 degree from north. Equation (4-47), Equation (4-48), and Table 4-2 are used to calculate the sun zenith and azimuth angle [21]:

$$cos\,\chi = sin\,\delta\,sin\,\lambda + cos\,\delta\,cos\,\lambda\,cos\,\alpha \tag{4-47}$$

$$tan\,\xi = \frac{sin\,\alpha}{sin\,\lambda\,cos\,\alpha - cos\,\lambda\,tan\,\delta} \tag{4-48}$$

Table 4-2: Determination of the sign of solar azimuth

Sign of α	sign tan(ξ)	ξ
+	+	180+Arctan(tan ξ)
+	-	360+Arctan(tan ξ)
-	+	Arctan(tan ξ)
-	-	180+Arctan(tan ξ)

where, δ is the solar declination angle and it is calculated by Equation (4-49), λ is latitude per degree and α is solar angle which is determined by using Equation (4-50) [21].

$$\delta = 23.44 \sin[360(\frac{d-80}{365.25})] \quad (4\text{-}49)$$

d is the number of day when January 1st is equal to one.

$$\alpha = \frac{360}{24}(t-12) \quad (4\text{-}50)$$

where, t is solar time and it is identified by Equation (4-51) [21].

$$t = LST + EOT - 4L_{local} + 60t_{zone} \quad (4\text{-}51)$$

LST = local standard time or real time; *EOT* = equation of time to account for irregularity of the earth speed around the sun (minutes); L_{local} = local longitude (degrees East> 0 and West < 0) and t_{zone} is the time zone difference compared to GMT (East > 0 and West < 0) [21].

$$B = 360(d - 81)/364 \quad (4\text{-}52)$$

$$EOT \text{ (minutes)} = -(9.87 \sin 2B - 7.53 \cos B - 1.5 \sin B) \quad (4\text{-}53)$$

4.5.3.2. PV Panel

Hourly generated electricity by a PV panel ($E_{pv,Re}$) is computed respecting to hourly tilt radiation (I_{tilt}) on an array surface with tilt angle of 45^0 [1].

$$E_{pv,Re} = A_{PV} \times \eta_{pv} \times I_{tilt,hr} \quad (4\text{-}54)$$

There is an assumption stating the efficiency of the PV panel (η_{pv}) is remained fixed and equal to 15% throughout a whole year [1]. The PV panels and solar collectors tilt angle and azimuth angle are assumed constant over a year and set to 45^0 and 180^0, respectively.

4.5.3.3. Solar Collector

Hourly produced hot water by a solar thermal collector (STC) is calculated using a simple calculation that is indicated by Equation (4-55) [1]:

$$HW_{SC} = A_{SC} \times (\eta_{SC} \times I_{tilt,hr} - U_{loss} \times (T_{SC,in} - T_{ambeint,hr}) \quad (4\text{-}55)$$

where, U_{loss} is heat loss coefficient of the solar thermal collector (W/m^{2}K), $T_{SC,in}$ is the temperature of input flow to SC (*K*), and $T_{ambeint,hr}$ is hourly ambient temperature (*K*). It is worth mentioning that in Equation (4-55), there is this possibility that the production rates of hot water can be a negative value when there is low solar irradiation. A boundary constraint is performed to prevent the negative value of production rate where setting the infeasible value of HW_{SC} to zero [1]:

$$If\ [A_{SC} \times (\eta_{SC} \times I_{tilt,hr} - U_{loss} \times (T_{SC,in} - T_{ambeint,hr})] < 0$$
$$HW_{SC} = 0 \quad (4\text{-}56)$$

The efficiency of the solar collector (η_{SC}) is considered as a constant parameter and equal to 40% over a whole year [1]. In this study, the heat loss coefficient of the solar thermal collector is assumed constant and set at 4.5 (W/m^{2}K) [22].

4.5.3.4. Wind Turbine

Wind turbines convert the kinetic energy of wind to electrical energy. There are numerous ways for simulating a wind turbine to identify its output power. The simplest models are defined by using four characteristic parameters, V_c (cut-in speed), V_r (rated wind speed), V_f (cut-off wind speed) and P_r (rated output power). Following model, Equation (4-57), is used to calculate the power generated by a wind turbine in each hour [23].

$$E_{WT-Re} = \begin{cases} 0 & v < V_c \\ \frac{1}{2} C_p \, \rho A_r v^3 & V_c < v < V_r \\ P_r & V_r < v < V_f \\ 0 & v > V_f \end{cases} \quad (4\text{-}57)$$

where, C_p is the wind turbine power coefficient, ρ is air density (kg/m^2), A_r is rotor swept area (m^2), and v is wind speed (m/s). The air density is modeled by a function based on air temperature and wind turbine height Equation (4-58) [24].

$$\rho = \frac{353.049}{T} e^{(-0.034Z/T)} \quad (4\text{-}58)$$

Another aspect to have in mind is the height of the wind turbine hub. Wind speed (v) at a height of Z_{rot} meters from velocity measured at Z height, v_{mea}, can be estimated according to Equation (4-59). The roughness ground height (Z_0) depends on the topography and site climatic conditions [24]. To calculate wind data for another location with similar wind but different roughness height, we use Equation (4-60). In this equation we use 60 m as the height which is not affected by roughness [24].

$$V(Z_{Rot}) = V(Z_{mea}) \frac{\ln(Z_{Rot}/Z_0)}{\ln(Z_{mea}/Z_0)} \quad (4\text{-}59)$$

$$V(Z_2) = V(Z_1) \frac{\ln(60/Z_{01}) \ln(Z_2/Z_{02})}{\ln(60/Z_{02}) \ln(Z_1/Z_{01})} \quad (4\text{-}60)$$

Where, Z_{01} is the roughness height at reference location; Z_{02} is the roughness height at new location [23].

4.5.3.5. Heat Pump

In this study, a ground source heat pump is also in charge of providing heating, cooling and hot water for the building. The maximal capacity of the compressor of the heat pump and its nominal coefficient of performance (COP_{max}) are used to estimate the maximum capacity of the heat pump, Equation (4-61) [1]:

$$P_{HP} = W_{com,max} \times COP_{max} \tag{4-61}$$

Hourly heating or cooling rate of the heat pump is computed based on its electricity demand its hourly coefficient of performance (COP) [1]:

$$HP(t) = W_{com}(t) \times COP(t) \tag{4-62}$$

where, *COP* is calculated based on interpolation method reported in [25]. It is modeled as a function based on entering water temperature, Equation (4-63) [25]. In this study, COP_{max} is assumed to be 4.5 for cooling and 5.5 for heating purpose [26].

$$COP(t) = COP_{max}(k_0 + k_1 T_{ewt} + k_2 T_{ewt}^2) \tag{4-63}$$

Table 4-3: Quadratic polynomial correlation coefficients used in Equation (4-63) [25]

Coefficients	Heating	Cooling
k_0	1.53	1
k_1	-2.29609×10^{-2}	1.5597×10^{-2}
k_2	6.8744×10^{-5}	-1.5931×10^{-4}

where, T_{ewt} is the entering fluid temperature which is modeled as a function of ambient temperature, Equation (4-64). For a given temperature (T_a) the temperature of water entering into the heat pump (T_{ew}) is easily calculated as [25]:

$$T_{ew}(t) = T_{ew,min} + \left(\frac{T_{ew,max} - T_{ew,min}}{T_{d,cool} - T_{d,heat}}\right)(T_a(t) - T_{d,heat}) \tag{4-64}$$

where, $T_{d,cool}$ is summer design temperature, and $T_{d,heat}$ is heating design temperature. In vertical heat pump system, the maximum and minimum entering fluid temperature $T_{ew,max}$ and $T_{ew,min}$ are given by [25]:

$$T_{ew,max} = Min(T_g + 20^0F, 110^0F) \quad (4\text{-}65)$$

$$T_{ew,min} = T_g - 15^0F \quad (4\text{-}66)$$

where, T_g stands for ground temperature which is approximated by the mean annual surface soil temperature [25]. In this study, T_g is approximated by mean annual surface soil temperature which is 4.7 ^{0}C.

4.5.3.6. Biomass Boiler

When the biomass boiler is in operation, the output heat rate of the boiler is given by [27]:

$$Q_{bb}(t) = m_b(t)\eta_{bb}HHV_b \quad (4\text{-}67)$$

where, m_b is biomass flow rate (kg/hr), η_{bb} is the biomass boiler efficiency, and HHV_b is higher heating value of biomass (kj/kg).

4.6. Dynamic Multi Objective Particle Swarm Optimization Algorithm

Firstly, Kennedy and Eberhart in 1995 proposed the particle swarm optimization algorithm whose idea is taken from social behavior of birds flocking [28]. It can be categorized as a meta-heuristic optimization technique, which is very straightforward to implement and able to solve both discrete and nonlinear problems quickly [4]. In the PSO procedure, candidate solutions are named particles or swarms that are indicated by their position and velocity. The set of swarms fly over the feasible search space to find the optimal solution. During the search process, a particle

readjusts its position based on not only its own experience but also the experience of all swarm and look for a position that delivers better objective function. In other words, over iterations, each particle adapts its flying direction and its velocity to pursue its best experience and the best global particle. The particle experience is defined as the best solution found so far for the individual particle while the best global particle or social leader is expressed as the best solution attained among all particles [28]. The success of the PSO algorithm in single objective optimization problems is a weighty reason to implement PSO in multi-objective problems, which is called Multi-Objective Particle Swarm Optimizers (MOPSO) [4]. The main idea of MOPSO is that the output of PSO is a set of solutions which are named non-dominated solutions or Pareto front (PF). In this study, dynamic multi-objective particle swarm optimization (DMOPSO) algorithm, which was developed in the previous work of the authors [18], has been applied to simultaneously minimize total NPC of the system, fuel emission and maximize RER. The engaging advantage of this method is generating a PF with higher quality than what is resulted by well-known MOP approaches. The main idea of the proposed algorithm is that multi-leaders and dynamic cell-based density calculation strategy is utilized to update the solutions. Two methods usually are performed to select leaders in guiding swarm flights: randomly selecting one of the best solutions or using multiple leaders [18]. In the cell-based density calculation strategy, the objective space is divided to hypercube and solutions are distributed over the resulted grid [29]. It allows using the density information to achieve diversity of the swarm [18]. For detail explanation of the algorithm, readers are referred to the previous work [18].

4.7. Performance Metric

In order to evaluate the quality of the generated Pareto fronts by multi-objective algorithms, some performance metrics are proposed in the related studies to assess the quality of generated PFs. In this paper, the following three metrics are used: Spacing, Maximum spread, and Coverage. The main reason for selecting these metrics is that each one of them represents a certain aspect of PFs. Additionally; it is simple to calculate them since none of them requires having the true PF for the evaluation.

Spacing (S): It was proposed by Schott [4] and numerically measures the diversity of the obtained PF. It is evaluated by measuring relative distance between neighboring solutions on a PF, Equation (4-68) [18].

$$S = \sqrt{\frac{1}{n-1} \times \sum_{i=1}^{n} (d_i - \bar{d})^2} \tag{4-68}$$

where, n represents the number of solutions in PF, d_i is distance between a solution and the solution i, and $\bar{d}$ is the average value of all d_i. S =0 means all solutions are spaced uniformly over PF. Therefore, it is more desirable to generate a PF with less S value [18].

Maximum Spread (MS): It was proposed by Zitzler et al. [4] which defines the maximum expansion covered by the approximated set [18]. It is calculated by using the following mathematical equation [18]:

$$MS = \sqrt{\sum_{i=1}^{n} max(\|x_i^t - y_i^t\|)} \tag{4-69}$$

The main idea of this metric is that for each non-dominated solution (x_i^t) the maximum Euclidean distance between the solution and other non-dominated solutions (y_i^t) should be identified.

Coverage (C): It was recommended by Zitzler et al. [4] that is used to compare two PFs ($X'$and $X^{"}$) to determine which one is closer to the true PF, Equation (4-70) [18].

$$C\left(X', X^{"}\right) = \frac{\left|\{a^{"} \in X^{"} | \exists a' \in X' : a' \succcurlyeq a^{"}\}\right|}{|X^{"}|} \tag{4-70}$$

C = 1 means all solutions in $X^{"}$ are dominated or equal to the solutions in X' while the *C = 0* explains an opposite situation [4]. It is worth mentioning that both $C\left(X', X^{"}\right)$ and $C\left(X^{"}, X'\right)$ should be evaluated since there is the possibility of intersection between two PFs.

4.8. Results

The proposed method is applied to an apartment building located in Winnipeg, Canada. The total floor area of the building is 2940 m^2, and its foot print is equal to 980 m^2. The building has 12 two-bedroom units and 31 one-bedroom units. There are 96 people living in the building. Currently, the energy need of the building is provided by natural gas, electricity, and gasoline. The heating load is met by a natural gas boiler, and the cooling load is fulfilled by air refrigerators. The electricity demand is met by bought electricity from the grid which is produced by hydroelectricity. The gasoline guarantees the required energy for transportation of building's residents. Figure 4-5 shows the average monthly energy use of the building per type of energy carrier. Table 4-6 shows the energy consumption of the investigated building with regard to end-use sections. The electricity and natural gas consumption is estimated based on the monthly energy bill of the building. The gasoline consumption is approximated according to average fuel

efficiency of light vehicle and average distance driven of light vehicles in Canada [30]. In this figure, all energy carriers are converted to MWh. It is clear that the largest part of energy consumption in the building is related to gasoline and NG used to provide space heating, hot water, and required energy for transportation.

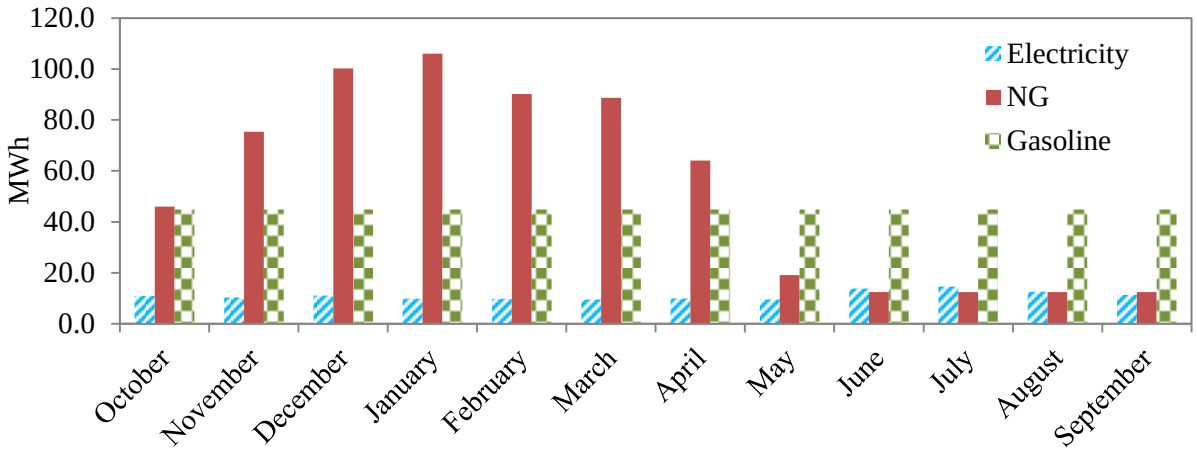

Figure 4-5: Monthly energy consumption of the building per type of energy carrier

Table 4-4: Energy use of the building by the end-use sections

End-Use	MWh/year
Space Heating	489.7157
Water Heating	149.7721
Electricity	137.14
Space Cooling	14.8
Transportation(Gasoline)	538.521

The GHG production which is the result of the energy consumption of the building is summarized summarized in

Table 4-5. The employed emission factors are taken from [31] and [32]. It has been assumed that the emission of biomass is negligible. GHG production during the manufacturing of the equipment and the shipping is not considered in this analysis.

Table 4-5: GHG production resulted by the building energy consumption [29, 30]

	Emission factor	CO_2 emission (ton/year)
Grid-electricity	0.03 ton/MWh	4
NG	56 kg/GJ	145
Gasoline	2.29 kg/lit	128.1

Monthly average direct normal, diffuse horizontal irradiance, wind speed at 10 m height, and temperature over one year for the location are plotted in Figure 4-5 to Figure 4-8. These data sets are obtained by the averaging of the measurement data over years 1990-1999 [33]. As a deterministic approach is applied in the optimization problem, the averages of hourly wind speed, solar radiation and temperature over 10 years have been entered to the simulation module. The cooling and heating requirement of the building are approximated by the means of the degree-hours concept. The method assumes that the energy needs for the building (heating and cooling) are proportional to the difference between the outside temperature and a base temperature [34]. In order to approximate the electricity demand, electricity bill data is used to estimate the daily power profile for the building.

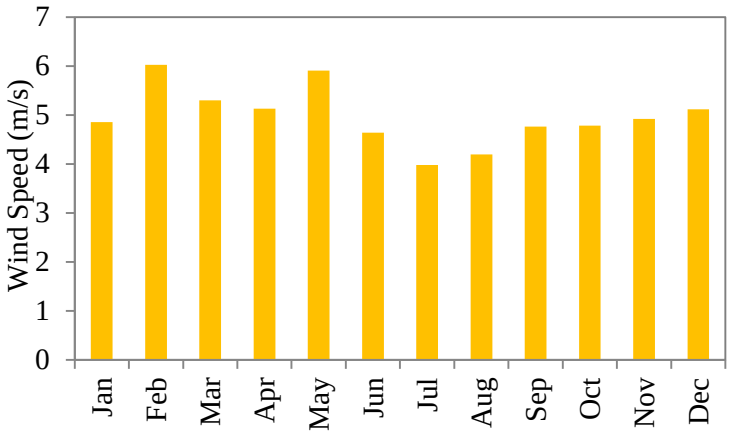

Figure 4-6: Monthly average wind speed for Winnipeg over one year

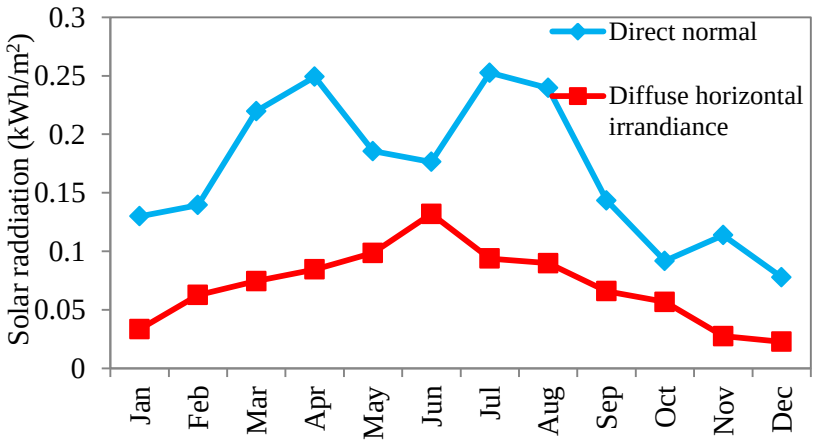

Figure 4-7: Monthly average irradiation for Winnipeg over one year

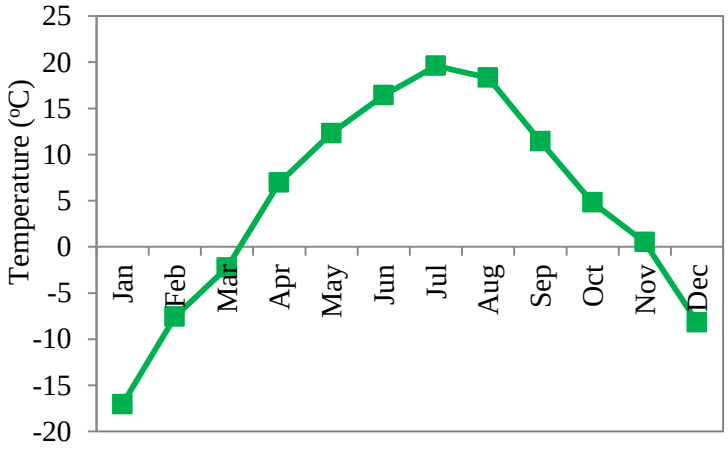

Figure 4-8: Monthly average temperature for Winnipeg over one year

The initial costs, operation and maintenance costs, and the characteristics of the components vary according to their size and used models. The economical parameters and the characteristics of components which are employed in the study are exhibited in Table 4-6. The replacement costs are assumed to be equal to the capital costs. The system life time is considered 25 years the same as PV panel life time that has the longest life time [18].

Table 4-6: Economical characteristics of the energy supply technologies [1], [35], [36], [37], [38]

Technology	Type	Investment Cost[C$]	O&M cost(C$/year)	Efficiency
PV	Poly-crystalline	$5162\times P_{PV}+2858$	1% total investment	15%
Solar collector	Glazed flat-plate	$812\times P_{SC}+2419$	1% total investment	40%
Wind turbine	Horizontal axis	$3300\times P_{WT}$	1% total investment	45%
Heat pump	Ground source	$1356\times P_{HP}+17368$	1% total investment	5
Heat storage tank	Water based	$512\times P_{HST}+1015$	2% total investment	--
Biomass boiler	Water based	$4288\times(P_{bb})^{0.727}$	2% total investment	80%

The employed economic parameters including biomass price, transportation, collection, storage costs, electricity price, NG price, gasoline and water price as well as other parameters are listed in Table 4-7.

Table 4-7: Economical parameters employed in the model

Parameters	Value
Interest rate	7%
Project life time	25yr
Biomass price(Switch grass)	135 [C$/ton]
Biomass transportation cost	1.9 [C$/ton.km]
Biomass collection cost	19 [C$/ton]
Biomass storage cost	35 [C$/ton]
Land rental cost	25000 [C$/km^2.yr]
Electricity price	0.07 [C$/kWh]
NG price	0.11 [C$/m^3]
Gasoline price	1.2 [C$/lit]
Water price	1.12 [C$/m^3]

In this study, the cost for changing all cars to PEV is not included. It is assumed that PEV price is same as the current cars price. The electrical car efficiency is assumed 88% [39] while the efficiency of gasoline car is assumed 25% [40]. The fuel efficiency of PEV and average distance driven of light vehicles in Canada are employed to estimate the daily required electric for charging PEV [30].

The resulted 3D Pareto front for the employed energy system of the building is plotted in Figure 4-9. It shows 42 non-dominated solutions with certain values of NPC, CO_2 emission, and RER. Evidently, no single optimal solution can be made out since there are three objective functions. In Figure 4-10 to Figure 4-12, the 2D graphs of obtained solutions laying over PF is

depicted. These plots can help decision makers to select an appropriate solution based on their priorities. Four solutions are selected over the PF and the component sizes of these selected solutions are shown in Table 4-8. These results show that CO_2 emission is reduced moderately (57%) by increasing RER to 66.9% where the NPC is also increased moderately (51%). When RER is set at 100%, in order to reduce CO_2 emission by 2.4 ton/year, NPC at least must be increased to C$ 705180. In this way, the produced CO_2 emission by the building energy system can be reduced from 277.1 ton/year in the current system to less than 3 ton/year.

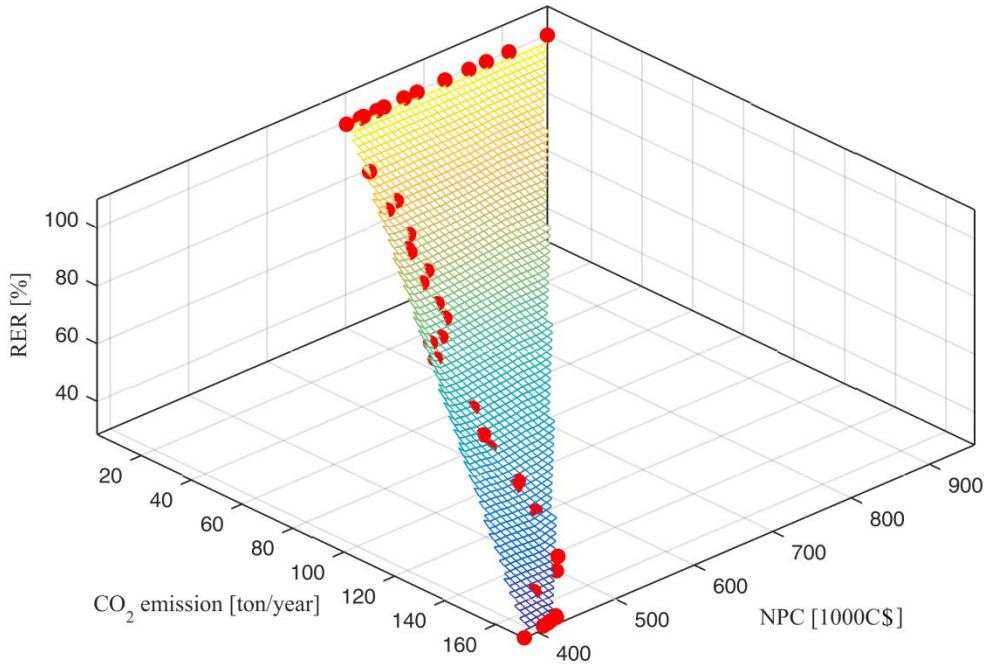

Figure 4-9: The Pareto front of the three-objective sizing problem resulted by DMOPSO

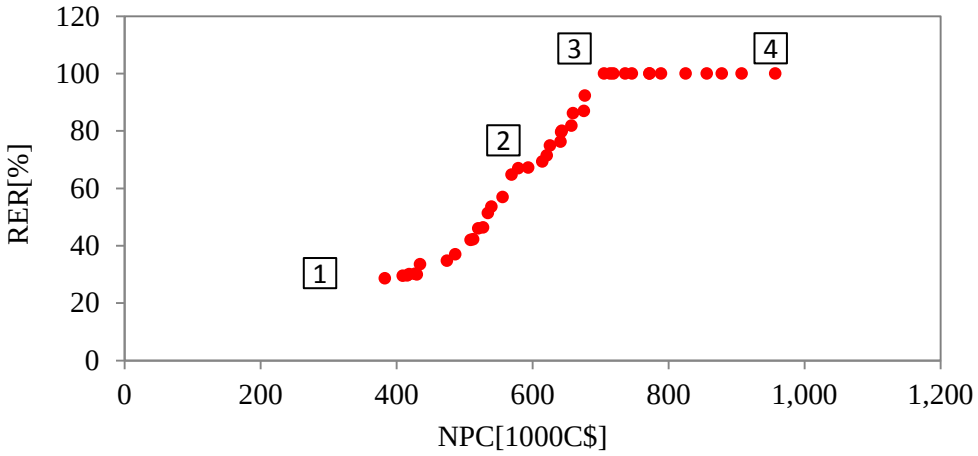

Figure 4-10: The 2D Pareto front of the three-objective sizing problem (RER vs. NPC)

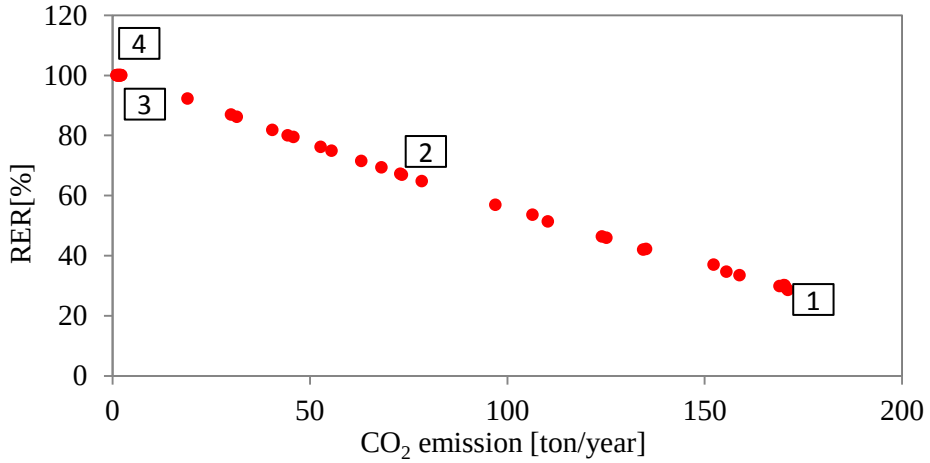

Figure 4-11: The 2D Pareto front of the three-objective sizing problem (RER vs. CO_2 emission)

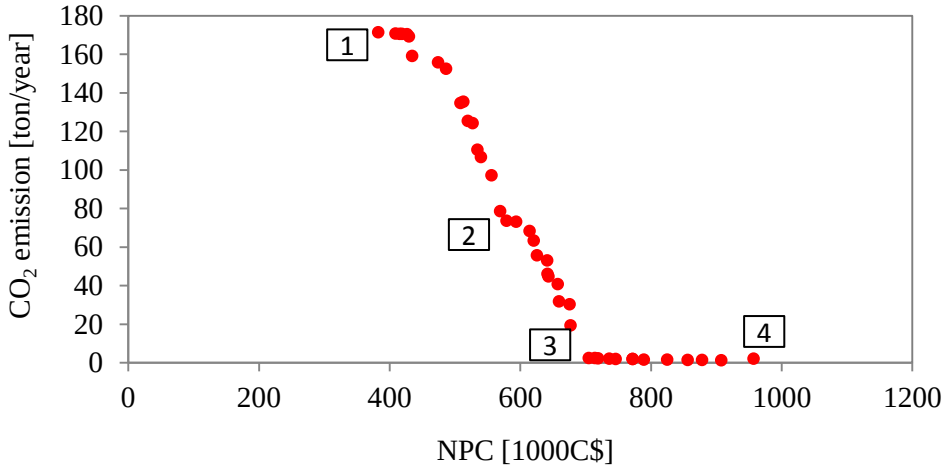

Figure 4-12: The 2D Pareto front of the three-objective sizing problem (CO_2 emission vs. NPC)

By increasing RER from 28.5% (solution 1) to 66.9% (solution 2), CO_2 emission is cut to 73.4 ton/year. Over this trend, NPC is approximately increased by 51.2% compared to solution 1. This result shows approximately a linear relation between NPC and RER when RER is increased from 66.9% to 100%. As depicted in Figure 4-10 to Figure 4-12, there are 11 solutions with RER of 100% that their difference is related to the amount of CO_2 emission, LLP, and total NPC. As Table 4-8 is also shown, using PEV and wind turbine is two first choices for increasing RER, and the next option would be using a biomass boiler. In the solution 3, RER is obtained as 100% by installing a 73 kW wind turbine, 200kW biomass boiler, and using PEV. In the solution 4, RER is achieved as 100% the same as the solution 3 while its LLP (3.4%) is lower than the solution 3 and CO_2 emission is reduced to 1 ton/year.

Table 4-8: Component size of the selected solutions laying over the PF

Generators/Objectives	Solution 1	Solution 2	Solution 3	Solution 4
PV panel [kW]	0	0	0	23
Wind turbine [kW]	68	71	73	200
Solar collector [kW]	0	0	0	0
Heat pump [kW]	0	0	0	0
Heat storage tank [m^3]	4.3	4.3	4.3	4.3
Biomass boiler [kW]	0	91	200	200
PV panel in rural area [kW]	0	0	0	0
$\varepsilon_{HE,HP}$	0	0	0	0
$\varepsilon_{HE,bb}$	0	0.4	1	1
$\varepsilon_{CO,HP}$	0	0	0	0
$\varepsilon_{CO,AR}$	1	1	1	1
$\varepsilon_{Tr,PEV}$	1	1	1	1
$\varepsilon_{Tr,gas}$	0	0	0	0
LLP [%]	5.0	4.9	4.9	3.4
NPC [C$]	383284	579654	705180	957433
RER [%]	28.5	66.9	100	100
CO_2 emission [ton/year]	171.2	73.4	2.4	1

The empirical studies are also implemented to analyze the performance of the proposed DMOPSO. It is compared to two of most well-known multi-objective optimization algorithms which are multi-objective genetic algorithm (MOGA)[41] and multi-objective particle swarm

optimization (MOPSO) [42]. All three algorithms are implemented in C++ programming environment, and then for statistical analysis purpose, each algorithm is run for 10 times. The results of coded algorithms are compared with each other based on some popular performance metrics explained in Section 4.7. The experimental results are presented in Figure 4-13, Figure 4-14, and Table 4-9 to clarify the performance of the employed algorithm. It is worth mentioning that normalized objective functions values are used to calculate the performance metrics.

The spacing metrics of obtained Pareto fronts of three algorithms are shown in Figure 4-13. From the box plot of spacing metric, it can be observed that DMOPSO, MOGA, and MOPSO are able to provide competitive results in terms of this metric.

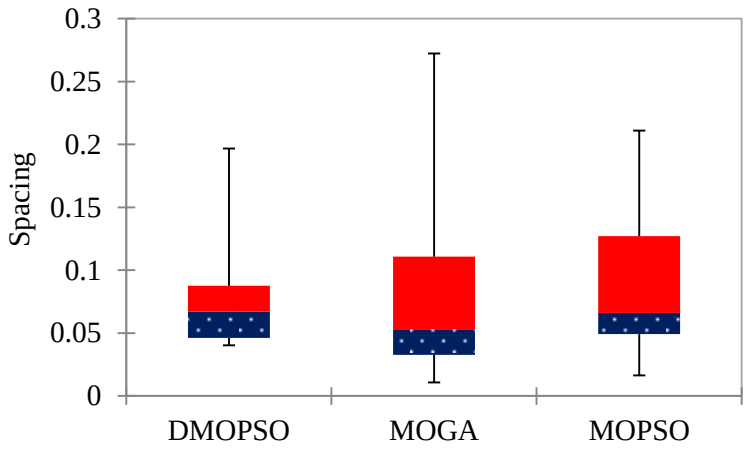

Figure 4-13: The results of spacing metric for three employed algorithms

The result of maximum spread metric for the employed algorithms is illustrated in Figure 4-14. It can be noticed that DMOPSO outperforms other two algorithms. This measure indicates that the generated Pareto front by DMOPSO algorithm covers a larger area compared to other algorithms.

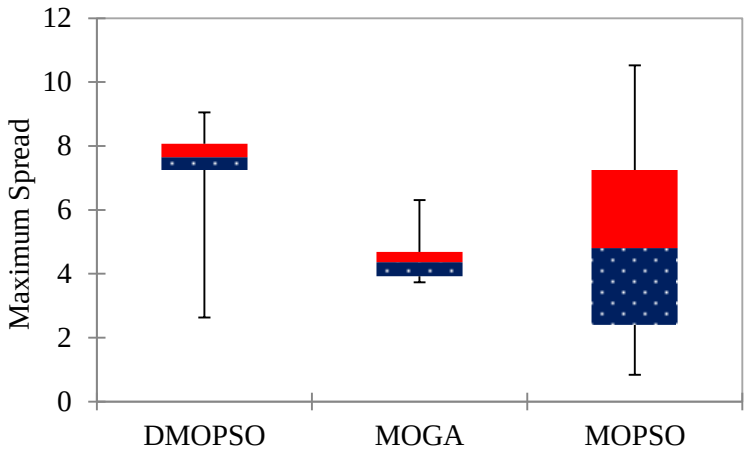

Figure 4-14: The results of maximum spread metric for three employed algorithms

As mentioned earlier, the true Pareto front of the problem is not known. Consequently, the coverage metric is used to identify which produced PF is closer to the true PF. The comparison results of the coverage metric for three employed algorithms are presented in Table 4-9. It indicates that most solutions laying over PF generated by MOGA are dominated by the solutions found by DMOPSO. For instance, 51% of solutions over PF resulted by MOGA are dominated by the produced PF of DMOPSO algorithm while 2.1% of solutions of DMOPSO Pareto front are dominated by solutions of MOGA. In addition, 14% of MOPSO solutions are worse than solutions found by DMOPSO. In summary, the MOPSO has no problem in converging to true Pareto front while it is difficult to cover a large area compared to DMOPSO. The obtained PF resulted by DMOPSO indicates the ability of this algorithm in dealing with the complex multi-objective optimization problem. It can be concluded that the generated PF by DMOPSO is more uniform and covers a larger area than two other employed algorithms.

Table 4-9: The results of coverage metric for three employed algorithms

SC(DMOPSO, MOGA)	51.2%
SC(MOGA, DMOPSO)	2.1%
SC(DMOPSO, MOPSO)	22%
SC(MOPSO, DMOPSO)	14%
SC(MOPSO, MOGA)	26.9%
SC(MOGA, MOPSO)	1.9%

4.8.1. General Discussion

In this study, a time step of one hour is considered for the analysis, which includes variations of demand and resources. The time step of one hour is considered sufficient since it is assumed that the renewable energy resources do not change significantly over one single hour. In order to evaluate the performance of employed components in solution 3, the daily simulation results through a year can be observed in Figure 4-15 to Figure 4-18. Figure 4-15 shows the daily distribution of produced electricity by the wind turbine per kWh. From this graph, it is clear that there is appropriate potential of wind energy in the location which results in the capacity factor of 31.5% for the wind turbine. It should be noted that in Figure 4-15 to Figure 4-18 day 1 refers to the first day of the year which is January first.

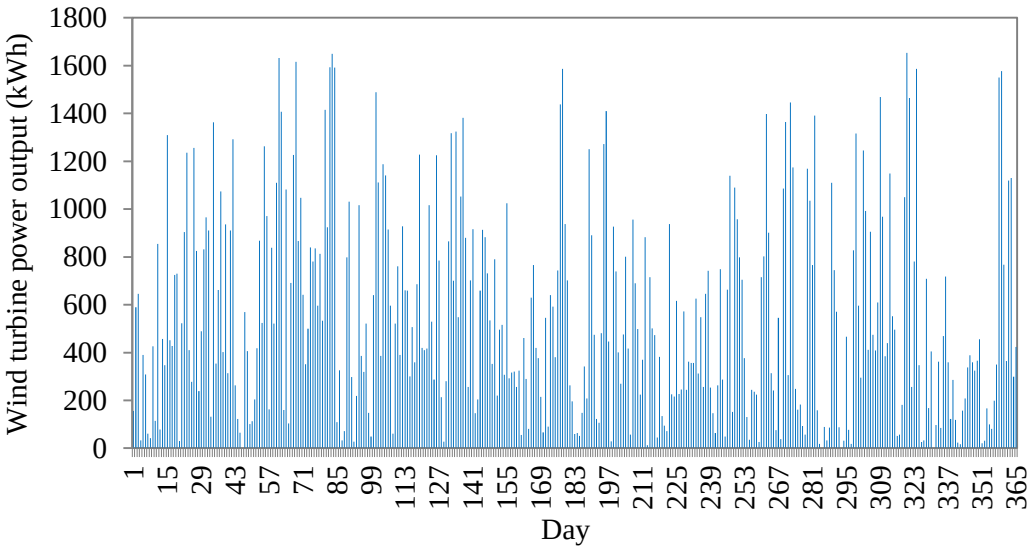

Figure 4-15: Daily produced electricity by wind turbine over one year (solution 3)

As seen from Figure 4-15, required electricity is first met by available wind energy at each time step. In case of electricity shortfall, the leftover electricity load is met by electricity that bought from the grid, Figure 4-16. Whenever renewable energy generated in electrical form is more than the electrical needs, the excess renewable energy is sold to the grid with price mentioned in Table 4-7. Figure 4-17 indicates the daily sold electricity to the grid, which is generated by the hybrid renewable energy system over one year.

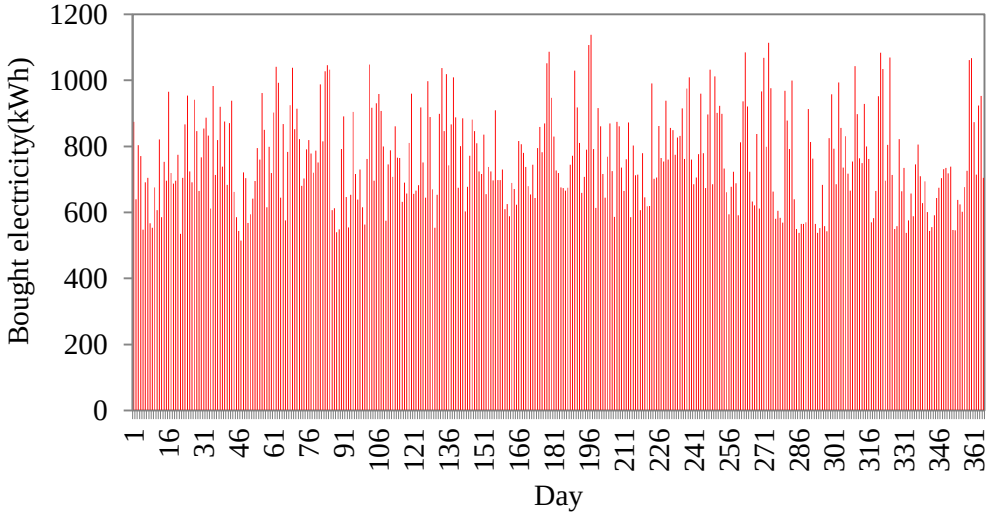

Figure 4-16: Daily electricity bought from the grid over one year (solution 3)

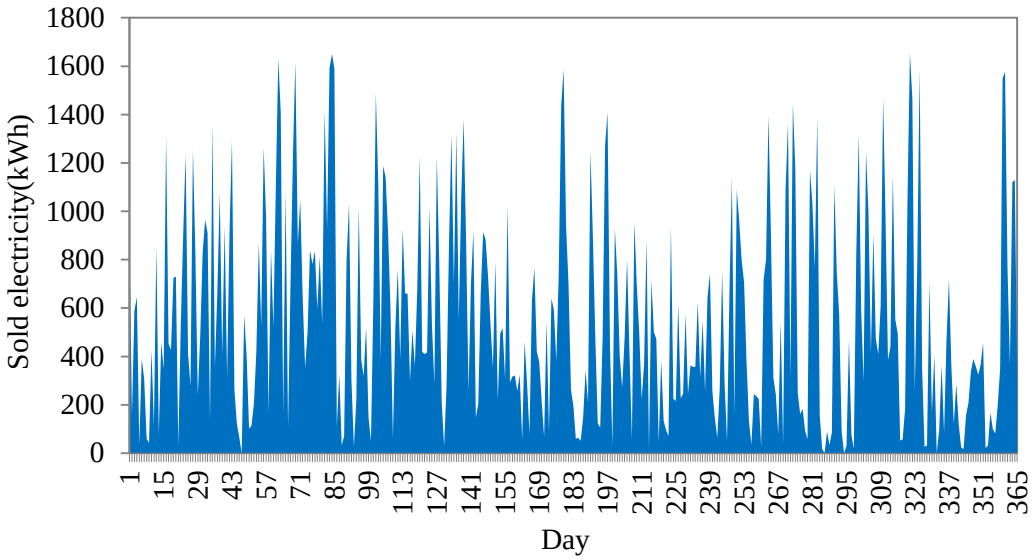

Figure 4-17: Daily electricity sold to the grid over one year (solution 3)

Figure 4-18 represents daily biomass boiler production. The biomass boiler described in the configuration proposed by the solution 3 is utilized for heating and hot water purpose. The results justify using the biomass boiler during the year.

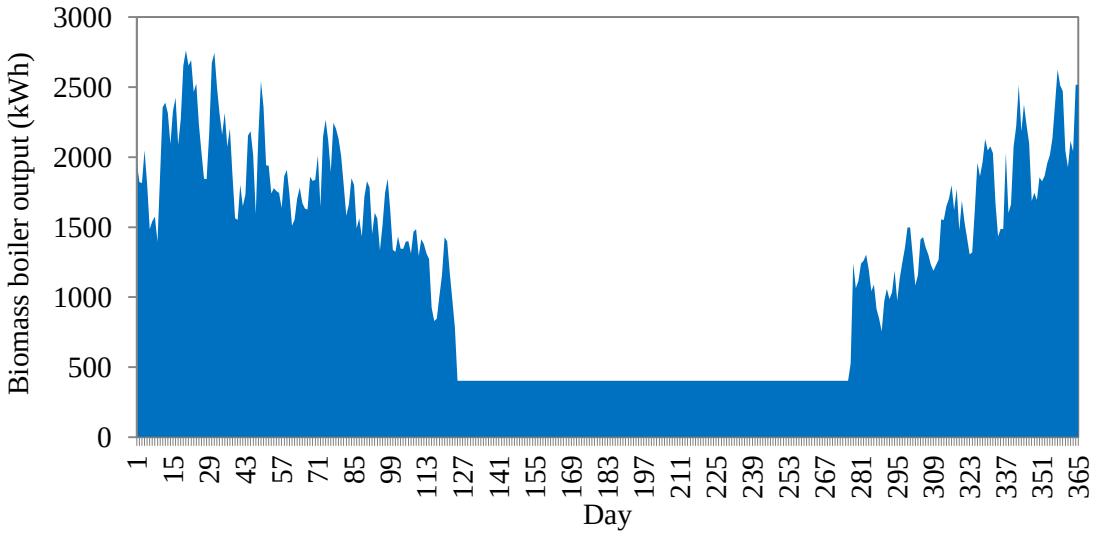

Figure 4-18: Daily biomass boiler output over one year (solution 3)

As it is seen, the boiler output is approximately constant during the summer since the daily hot water load is assumed constant through the year. It is easy to see the variation of the boiler output over the rest of year as the heating load is varied.

Table 4-10 shows the technical data related to the operation of the optimal system proposed in solution 3. Annual capacity factor for wind turbine and the biomass boiler are estimated as 31.5% and 25.4%, respectively. Annually, 201.2 MWh of produced electricity by the wind turbine is sold to the grid which can be an income for the building. It worth mentioning that all produced electricity by the wind turbines is sold to the grid and the same amount in building place is purchased from the grid.

Table 4-10: Technical details for the configuration described by the solution 3

Wind turbine capacity factor [%]	31.5
Biomass boiler capacity factor [%]	25.4
Annual bought electricity from the grid [MWh]	279.7
Annual sold electricity to the grid [MWh]	201.2

4.8.2. Sensitivity Analysis

In this study, a sensitivity analysis is performed to investigate how variations of economic parameters such as capital costs of PV panels, heat pump, wind turbine, and solar collectors can affect the values of the optimal solutions provided by the model. For this purpose, each parameter is changed by ±50%, which are stated as upper limit and a lower limit for the parameters. It is worth mentioning that for the purpose of sensitivity analysis, only solutions with RER of 100% is considered to study how the investigated parameters affect their optimal cost. In our optimization problem, the optimal solutions for the origin problem (solutions with RER of 100%) results in average NPC of C$958462, and CO_2 emission of 1.6 ton/year. The 13 parameters that we are interested to study the sensitivity of the result respect to their changes are indicated in Table 4-11. In this experiment, the number of replication is set at 5 that means the model is run 5 times for each scenario, then the average value of 5 replications is taken into account as the corresponding value. The standard deviation of 5 replications for the origin

problem is calculated as 4.3%. Figure 4-19 presents the sensitivity analysis results for the investigated input parameters.

Table 4-11: Studied parameters of the sensitivity analysis

Parameters	Abbreviation	Parameters	Abbreviation
Biomass Transportation Cost	BioT	Sold Electricity Price	SoEP
Biomass Collection Cost	BioC	PV Panel Capital Cost	PVC
Biomass Storage Cost	BioSt	Wind Turbine Capital Cost	WTC
Land Rental Cost	LaC	Solar Collector Capital Cost	SCC
Gasoline Price	GaP	Heat Pump Capital Cost	HPC
NG Price	NGP	Interest Rate	IR
Grid Electricity Price	GEP		

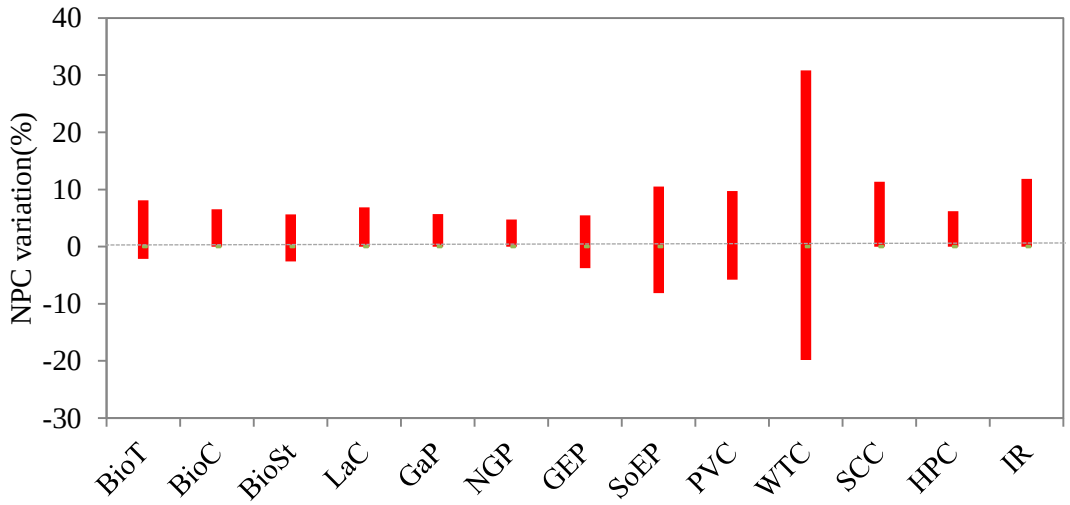

Figure 4-19: Sensitivity analysis results for the optimal design of solutions with RER of 100%

If the variation of NPC resulted by changing a parameters is less than the standard deviation, it can be concluded that the parameter does not have significant effect on NPC. Between the studied parameters, gasoline price, NG price, and heat pump capital cost do not have significant effect on total NPC of the system. The reason for this fact may be that the optimal configurations do not include solar collectors, heat pump, NG boiler, and gasoline cars. As it is obvious from the result, the wind turbine capital cost variation leads to +30% or -20% changes in total NPC of the system which means it has the highest effect on total NPC between studied parameters.

4.9. Conclusion

In this paper, a methodology has been proposed to optimize the sizing of a HRES for buildings using a simulation-based optimization approach. The model minimizes total net present cost and CO_2 emission, while simultaneously maximizes renewable energy ratio. This method allows decision makers to perform a trade-off between these three objectives by generating a Pareto front. The actual solar irradiation, temperature, and wind speed data are used in the simulation module. The performance of the proposed approach is evaluated using three well-known performance metrics and by comparing its results against two reported multi-objective algorithms in the literature. The developed methodology is applied to an apartment building in Canada to use renewable energy resources in order to displace the total fossil fuel utilized by the building utilities. The considered HRES includes a heat pump, a biomass boiler, wind turbines, solar collectors, PV panels, heat storage tanks, and PEV. In this case study, a Pareto front consisting of 42 non-dominated solutions is generated. By considering the trade-off between the three objective measures, the decision makers can select the best configuration from the generated Pareto set. The case study results show that under the chosen conditions and employed parameters, a configuration including wind turbines and PEV can increase RER and reduces CO_2 emission. In addition, a configuration with a 73 kW wind turbine, a 200 kW biomass boiler, and using PEV instead of gasoline cars can increase the RER to 100%, which has total NPC of C$705180 and results in 2.4 ton/year CO_2 emission. The sensitivity analysis helps to find that wind turbine capital cost has the most effect on total NPC of the optimal solutions.

Finally, the proposed methodology provides an important tool and systematic approach for feasible study and multi-objective optimization of an HRES. Future developments of the present work will consider stochastic issues both in demand and resource predictions. Since the

availability of renewable energy sources alters during a year, the decision making process and finding the optimal configuration should involve the stochastic modeling of uncertain parameters.

4.10. References

[1] Milan C, Bojesen C, Nielsen MP. A cost optimization model for 100% renewable residential energy supply systems. Energy 2012; 48(1): 118–127.

[2] Marszal AJ, Heiselberg P, Bourrelle JS, Musall E, Voss K, Sartori I, Napolitano A. Zero Energy Building –A review of definitions and calculation methodologies. Energy and Building 2011; 43(4): 971–979.

[3] Khalili-Damghani K, Abtahi AR, Tavana M. A new multi-objective particle swarm optimization method for solving reliability redundancy allocation problems. Reliability Engineering & System Safety 2013; 111: 58–75.

[4] Bastos-Filho CJA, Miranda P. Multi-objective particle swarm optimization using speciation. IEEE Symposium on Swarm Intelligence (SIS), 2011; 1–6.

[5] Dagdougui H, Minciardi R, Ouammi A, Robba M, Sacile R. Modeling and optimization of a hybrid system for the energy supply of a ‘‘Green’’ building. Energy Conversion and Management 2012; 64: 351–363.

[6] Lee KH, Lee DW, Baek NC, Kwon HM, Lee CJ. Preliminary determination of optimal size for renewable energy resources in buildings using RETScreen. Energy 2012; 47(1): 83-96.

[7] Prasad S, Reddy VK, Saibabu CH. Integration of renewable energy sources in Zero energy buildings with economical and environmental aspects by using HOMER. International journal of advanced engineering sciences and technologies 2011; 9(2): 212–217.

[8] Rezaie B, Esmailzadeh E, Dincer I. Renewable energy options for buildings: Case studies. Energy and Buildings 2011; 43(1): 56–65.

[9] Jiang Z, Rahimi-Eichi H. Design, modeling and simulation of a green building energy system. IEEE Power & Energy Society General Meeting 2009; 1-7.

[10] Fabrizio E, Corrado V, Filippi M. A model to design and optimize multi-energy systems in buildings at the design concept stage. Renewable Energy 2010; 35(3): 644–655.

[11] Fabrizio E, Filippi M, Virgone J. An hourly modelling framework for the assessment of energy sources exploitation and energy converters selection and sizing in buildings. Energy and Buildings 2009; 41(10):1037–1050.

[12] Ooka R, Komamura K. Optimal design method for building energy systems using genetic algorithms. Building and Environment 2009; 44(7):1538–1544.

[13] Thompson S, Duggirala B. The feasibility of renewable energies at an off-grid community in Canada. Renewable and Sustainable Energy Reviews 2009; 13(9): 2740–2745.

[14] Hassoun A, Dincer I. Development of power system designs for a net zero energy house. Energy and Building 2014; 73:120–129.

[15] Fux SF, Benz MJ, Guzzella L. Economic and environmental aspects of the component sizing for a stand-alone building energy system: A case study. Renewable Energy 2013; 55: 438–447.

[16] Rosiek S, Batlles FJ. Renewable energy solutions for building cooling, heating and power system installed in an institutional building: Case study in southern Spain. Renewable and Sustainable Energy Reviews 2013; 26:147–168.

[17] Chua KJ, Yang WM, Wong TZ, Ho CA. Integrating renewable energy technologies to support building trigeneration–A multi-criteria analysis. Renewable Energy 2012; 41:358–367.

[18] Sharafi M, Elmekkawy TY. A dynamic MOPSO algorithm for multiobjective optimal design of hybrid renewable energy systems. International Journal of Energy Research 2014; 38(15): 1949-1963.

[19] Manitoba Hydro. Technical requirements for connecting distributed recourses to the Manitoba Hydro system. Manitoba Hydro Electric Board; 2010.

[20] Sharafi M, Elmekkawy TY. Multi-objective optimal design of hybrid renewable energy systems using PSO-simulation based approach. Renewable Energy 2014; 68: 67–79.

[21] Masters GM. Renewable and efficient electric power systems. Hoboken, New Jersey: John Wiley & Sons, Inc.; 2004.

[22] NRC. RETScreen software online user manual: Solar water heating project model. Natural Resources Canada; 2005.

[23] Mesquita FGG. Design optimization of stand-alone hybrid energy systems. M.Sc. thesis, Univesity of Porto; 2010.

[24] Mathew S. Wind energy fundamentals, resource analysis and economics. Netherlands, Springer; 2006.

[25] NRC. Clean energy project analysis, RETScreen engineering & cases textbook: Ground-source heat pump project analysis chapter. Natural Resources Canada; 2005.

[26] Croteau R, Gosselin L. Correlations for cost of ground-source heat pumps and for the effect of temperature on their performance. International Journal of Energy Research 2015; 38: 433-438.

[27] D'Ovidio A, Pagano M. Probabilistic multi-criteria analyses for optimal biomass power plant design. Electric Power Systems Research 2009; 79(4) 645–652.

[28] Ahmed H, Glasgow J. Swarm intelligence: concepts, models and applications. Technical Report. School of Computing. Queen's University, Canada; 2012.

[29] Konak A, Coit DW, Smith AE. Multi-objective optimization using genetic algorithms: A tutorial. Reliability Engineering and System Safety 2006; 91(9) 992–1007.

[30] Statistics Canada. Human activity and the environment : annual statistics. Ottawa; 2009. Available from: http://www.statcan.gc.ca/pub/16-201-x/16-201-x2009000-eng.htm.

[31] The Climate Registry. Climate registry default emission factors. April 2014. Available from: http://www.theclimateregistry.org/downloads/2014/04/2014-Climate-Registry-Default-Emissions-Factors.pdf.

[32] Manitoba Hydro. Economic, load, and environmental impacts of fuel switching in Manitoba. Technical Report; August 2012. Available from: http://www.pub.gov.mb.ca/centra_2013_14_gra/pdf/appendix_15_4.pdf.

[33] Environment canada-atmospheric environment service and the national research council of Canada. Canadian weather energy and engineering data sets (CWEEDS Files). Available from: http://climate.weather.gc.ca/prods_servs/engineering_e.html.

[34] Bu O. Analysis of variable-base heating and cooling degree-days for Turkey. Applied Energy 2001;69:269–83.

[35] OFA-Ontario Federation of Agriculture. Assessment of business case for purpose-grown biomass in ontario. Technical Report; 2012. Available from:

http://www.ofa.on.ca/uploads/userfiles/files/assessment%20of%20business%20case%20for%20purpose-grown%20biomass%20in%20ontario%20march%202012.pdf.

[36] Delisle V, Kummert M. A novel approach to compare building-integrated photovoltaics/thermal air collectors to side-by-side PV modules and solar thermal collectors. Solar Energy 2014;100: 50–65.

[37] Luukkonen P, Bateman P, Hiscock J, Poissant Y, Howard D. National survey report of PV power applications in Canada 2012. IEA, Technical Report; 2013. Available from: http://cansia.ca/sites/default/files/201409_cansia_2013_pvps_country_report.pdf.

[38] Carbon Trust. Biomass boiler system sizing tool-user manual version 6.8. Technical Report; 2013. Available from: http://www.carbontrust.com/media/332513/biomass-software-tool-user-manual-v68.pdf.

[39] Katrašnik T. Energy conversion phenomena in plug-in hybrid-electric vehicles. Energy Conversion and Management 2011; 52(7): 2637–2650.

[40] Irimescu A. Fuel conversion efficiency of a port injection engine fueled with gasoline–isobutanol blends. Energy 2011; 36(5): 3030–3035.

[41] Rjlurata T, Gakuen-cho OP. MOGA: Multi-Objective Genetic Algorithms. IEEE International Conference on Evolutionary Computation 1995; 289–294.

[42] Coello CC, Lamont GB, Van-Veldhuizen DA. Evolutionary algorithms for solving Multi-objective problems. 2nd ed. New York: Springer; 2007.

Chapter 5

Stochastic Optimization of Hybrid Renewable Energy Systems Using Sampling Average Method

5.1. Abstract

The stochastic attribute of renewable energy sources and the variability of load is a preeminent barrier to design hybrid renewable energy systems. In this paper, a new methodology is advanced to incorporate the uncertainties associated with RE resources and load in sizing an HRES in the application of near zero energy buildings. Dynamic multi-objective particle swarm optimization algorithm, simulation module, and sampling average technique are used to approximate a Pareto front (PF) for the HRES design through a multi-objective optimization framework. The main aim of the design is to simultaneously minimize total net present cost, maximize renewable energy ratio, and minimize fuel emission while satisfying a desirable level of loss of load probability. The existing randomness in wind speed, solar irradiation, ambient temperature, and energy load is considered using synthetically data generation and sampling average method. The performance of the model has been examined in a building located in Canada as the case study, in which RER of the building is increased by using renewable energy technologies. The generated PF by the stochastic approach is compared to those of a deterministic model using well-known

performance metrics. Finally, a sensitivity analysis is carried out where the economic characteristics of the model are varied.

5.2. Introduction

Looking for a sustainable environment restricts the fossil fuels consumption and consequently encourages the usage of renewable energy sources [1]. In fact, RE sources are becoming popular as their negative environmental impact is not significant in contrast to the fossil fuels [2-5]. Renewable energy is titled as clean energy sources by which greenhouse gas emission can be reduced and secondary wastes are generated at minimum level. In the future, the renewable energy application is expected to increase since RE resources are local and environmental friendly. Furthermore, they can aid in cutting down the running of traditional fuels [1]. The application of hybrid renewable energy systems for remote area has attracted many attentions due to the rise in the price of fossil fuels and the resultant advances in renewable energy technologies. Generally, an HRES includes two or more renewable energy sources integrated together to improve both power reliability and system efficiency.

The main challenge of the design of HRESs is the variability and availability of RE resources [6]. The performance of HRESs is fluctuating drastically over years since the renewable resources can be distinct in terms of average values and distribution over years. Taking into account the randomness associated with RE resources and load is critical since it has significant effect on the reliability and the overall performance of HRESs. The reason for this fact is that system operation and produced power are dependent on the stochastic nature of RE sources. It is not easy to make the reliability analysis of an HRES without considering its probabilistic nature due to inherent uncertainties in renewable resources. In other words, employing reliability as an

objective in the optimization of an HRES design cannot be executed deterministically [7]. In recent past, the advancement of probabilistic design methods has become more popular among the researchers due to the diagnosing of the drawback of deterministic methods in the design of HRESs [7]. The design of such energy suppliers involves the approximation of the capacities of the generators and storage devices to fulfil a given demand. Stochastic approaches of sizing HRESs cover the issue of the RE variability in the system design [8].

A few researchers have carried out stochastic analysis of HRESs respecting to their performance and their design optimization. Table 5-1 summarizes the recent studies that applied stochastic analysis in HRESs design. Dufo-López et al. [9] studied the impact of the uncertainty of wind data on the optimal design of wind-batteries stand-alone systems by using hybrid optimization of genetic algorithm (HOGA). They considered two types of input data including measured hourly data and synthetically generated hourly wind speed data over a year. They implied that the main advantage of their approach is to consider a certain number of consecutive days of "*calmness*" for generating the wind speed data. Handschin et al. [10] proposed a "*scenario-wise*" approach to develop an engineering tool to optimize a coordinated operation of distributed generation (DG) units incorporating the uncertainties associated with electric load, power prices, and infeed from renewable resources. Arun et al. [8] utilized chance constrained programming based on the design space approach for the optimum sizing of an off-grid PV-battery system under the uncertainty of solar insolation. In their study, the set of all possible design configurations was illustrated by drawing a sizing curve in which a desirable confidence level is used to integrate the possible combinations of the PV sizes with the equivalent minimum battery capacities. Ekren et al. in [1] and [11] optimized the size of a hybrid energy system including PV/wind and battery storage employing two simulation-based optimization methods. The probabilistic distribution

functions for solar radiation, wind speed and electricity consumption were fitted employing ARENA simulation software. Lastly, they applied response surface methodology (RSM) and the OptQuest tool in ARENA to optimize the total cost of the system. They extended their work in [12] to perform a Simulated Annealing (SA) algorithm for the optimal design of the HRES. They concluded that the SA algorithm gives better result than RSM approach. In [13], for the optimal design of a renewable power generation system, the uncertainties of weather data and the operating efficiency of the studied subsystems were addressed by using probability distribution function. The stochastic annealing optimization algorithm was used to minimize the economic objective. Khan et al. [14] represented the stochastic nature of wind speed and solar radiation level by using a sensitivity analysis approach. They performed a simulation study of a hybrid energy system for application in Canada. A renewable energy simulation software (HOMER) was used as a sizing tool to discuss the cost and the performance of renewable and non-renewable energy sources. Kuznia et al. [15] presented a stochastic mixed integer programming model to identify the optimal combination and the size of a hybrid system consisting randomness in wind speed and electricity load. They created a Benders' decomposition algorithm to obtain the optimal solution. Maheri [7] developed a multi-objective optimization method for design under uncertainties of a wind-PV-diesel configuration. The probabilistic analysis was used to quantify the system reliability since there are uncertainties in renewable resources and electricity demand. To tackle the uncertainties, only the uniform distribution function was fitted to all random parameters. Roy et al. [16] developed a chance constrained programming technique to design an off-grid wind-battery system incorporating uncertainty in wind speed. In their study, Monte-Carlo simulation approach validated the system reliability where the hourly wind speed was modeled as Weibull random variable, and the cost of energy was selected as design criteria

to evaluate the proposed system configuration. Subramanyan et al. [17] used MINSOOP, NLP optimizer, and sampling techniques to pass the Pareto set for the design of a solid oxide-proton exchange membrane fuel cell (SOFC-PEM) by means of a multi-objective optimization framework. The existing randomness in fuel cell current density was modeled to convert the approach to stochastic multi-objective optimization one. Wang [18] presented multi-criteria meta-heuristic method to design an HRES including a wind turbine and PV panels according to cost, reliability, and emission criteria. Adequacy evaluation was performed to consider system uncertainties based on the primarily defined scenarios.

In summary, few articles used stochastic analysis for the design of HRESs. However, persisted researchs and development are still required to improve these systems sizing process. Most of the previous studies have only considered economic objectives at their design stage (see Table 5-1) while it is very important to size an HRES based on pollutant emission, reliability, and renewable energy ratio as well. In addition, they neglected simultaneously providing energy for heating, cooling, and appliances. Furthermore, mostly in the previous studies, the random parameters are generated using a simple distribution function.

In this paper, a new stochastic multi-objective approach is developed to incorporate the existing uncertainties in RE resource and energy load when sizing a energy supply system. The proposed methodology is trying to simultaneously examine the economic, reliability and environmental issues for different renewable energy ratio. This study is the extension of the previous work of the authors [19] with difference in involving the stochastic evaluation instead of using a deterministic design approach. The contribution of the present work is that a comprehensive energy supply system is studied incorporating uncertainties in RE resources and energy load. Moreover, similar to the previous work [19], the transport load is considered rather than

electricity, heating, and cooling load. Additionally, simple methods for synthetic generation of daily load profile and weather data has been applied to handle the existing uncertainties in the model.

Mostly, in the probabilistic analysis of HRES design, an objective function cannot be evaluated exactly but rather approximation methods are required. In this study, the sampling average approximation is integrated with dynamic multi-objective particle swarm optimization algorithm to help in handling the complex optimization problem. The generated solutions by the implemented approach are evaluated by comparing them with the solutions obtained by deterministic analysis. Then, a sensitivity analysis is carried out to identify the economic parameters that have significant impact on the design objectives. Based on the best authors' knowledge, it is the first time a MOP approach incorporating a comprehensive stochastic analysis is implemented for optimal design of a renewable energy supply system in the application of low energy buildings. In other words, it is the first time, the randomness in wind speed, solar radiation, ambient temperature, electricity load, heating and cooling load, hot water demand, and transportation load are simultaneously considered in the sizing of HRESs.

Section 5.4 explains the problem description. Section 5.5 begins with the definition of considered objective functions in the proposed design methodology, and then elaborates on the sampling average approach and the synthetic generation of random parameters. Section 5.6 describes a summary of the employed DMOPSO algorithm. Section 5.7 details the design scenarios and the results of the case study that is delivered by using the proposed design methodology.

Table 5-1: The summary of recent published studies for stochastic optimization of HRESs

Authors	System components: Wind turbine	PV panel	Solar Collector	Biomass	Heat Pump	PEV	Storage	Diesel& other	MOP	Objective functions	Stochastic parameters	Optimization approach
Ekren et al. [1]	●	●					●		NO	NPC	Wind speed, Solar radiation, Electricity load	RSM/ Simulation based Opt Quest in ARENA
Maheri [7]	●	●						●	YES	LCE/ Reliability	Wind speed, Solar radiation, Electricity load PV array efficiency	GA
Arun et al. [8]		●					●		NO	Energy cost	Solar insolation	Design space/ Chance constrained programming
Dufo-López et al. [9]	●						●		NO	NPC	Wind speed	HOGA
Handschin et al. [10]	●	●						●	NO	Operation Cost	Power prices, Power load, In feed from RE	Scenario-wise MILP
Garyfallos et al. [13]	●	●					●	●	NO	NPV	Wind speed, Solar radiation, Efficiencies of EL and FC	SA
Khan et al. [14]	●	●					●	●	NO	NPC	Wind speed, Solar radiation, Diesel price, FC cost	Sensitivity analysis HOMER
Kuznia et al. [15]	●						●	●	NO	NPC	Wind speed/ Electricity load	SMIP
Roy et al. [16]	●						●		NO	COE	Wind speed	Chance constraint programming/ Graphical method
Subramanyan et al. [17]								●	Yes	CO_2 emissions Capital cost Current density Overall efficiency	Fuel cell current density	MINSOOP/NLP/Sampling method
Wang [18]	●	●					●	●	Yes	NPC Reliability Emission	Wind speed, Solar radiation, Electricity load	Generating scenarios/ MOPSO

5.3. Nomenclature

$A(day)$	Daily amplitude of temperatures [^{0}C]	E_{WT-Re}	Wind turbine power output [kWh]
$a_{d,h}$	Random number between 0 and 1	EF_E	Emission factor for grid electricity [kg-CO_2/kWh]
$A_{mean,d}$	Mean daily amplitude of temperature [^{0}C]	EF_{Gas}	Emission factor for gasoline [kg CO_2/lit]
$A_{max,d}$	Maximum daily amplitude of temperature [^{0}C]	EF_{NG}	Emission factor for NG [kg-CO_2/m^3]
A_m	Monthly amplitude of wind speed [m/s]	$El_{b,y}$	Annual electricity bought from the grid [kWh/year]
$C_{b,Col}$	Biomass collection cost [C$/ton]	$f_{correction\_m}$	Correction factor
$C_{b,St}$	Biomass storage cost [C$/ton]	GAS	Hourly gasoline consumption [kWh]
$C_{b,Tr}$	Biomass transportation cost [C$/ton.km]	*Gasoline*	Annual gasoline consumption [lit/year]
$c_{d,h}$	Correlated values for wind speed	$h_{max,m}$	The hour of maximum daily wind speed [hr]
$C_{elec,s}$	Sold electricity price [C$/kWh]	HE_{Bio}	Heating load provided by the biomass boiler [kWh]
$C_{elec,b}$	Bought electricity price [C$/kWh]	HE_{HP}	Heating load provided by the heat pump [kWh]
C_{Gas}	Gasoline price [C$/litre]	HE_{NG}	Heating energy generated by NG boiler [kWh]
$C_{I,j}$	Capital cost of the component j [C$/unit]	$HP(t)$	Hourly heat pump output [kWh]
C_{NG}	Natural gas price [C$/m^3]	$HST(t)$	Level of hot water in storage tank in time step *t* [kWh]
$C_{O\&M,j}$	Operation& maintenance cost of the component *j* [C$/unit]	$HW_{Bio-tank}$	Hot water load provided by the biomass boiler [kWh]
$C_{rep,j}$	Replacement cost per unit for the component j [C$/unit]	$HW_{HP-tank}$	Hot water load provided by the heat pump [kWh]
COE	Cost of energy	$HW_{NG-tank}$	Hot water generated by NG boiler [kWh]
CRF	Capital recovery factor	$HW_{SC-tank}$	Hot water generated by solar collectors [kWh]
DM	Diversification metric	HW_{T-load}	Total hot water sent to load [kWh]
d_m	The number of days in a month	$H_o(day)$	Extraterrestrial solar radiation in a given day [kWh/m^2]
E_{EX}	Excess electricity [kWh]	$H_o(mont)$	Monthly averaged daily extraterrestrial solar radiation [kWh/m^2]
$El_{s,y}$	Annual sold electricity to the grid [kWh/year]	i	Interest rate [%]
E_{bought}	Bought electricity from the grid [kWh]	I_h	Hourly solar radiation [kWh/m^2]
E_{AR}	Electricity consumption by air refrigerator [kWh]	$I_{max,m}$	Monthly average of maximum solar radiation for a day [kWh/m^2]
E_{EV}	Electricity consumption by PEV [kWh]	$I_{max}(day)$	The maximum solar radiation for a day [kWh/m^2]

E_{HP}	Electricity consumption by heat pump [kWh]	$I_{max}(month)$	Maximum solar radiation in a month [kWh/m^2]
E_{Sold}	Sold electricity to the grid [kWh]	K	Single payment present worth
$\mathrm{E_{PV}}$	Net power generated by PV panels [kWh]	NPC	Net present cost
$\mathrm{E_{PV-Re}}$	PV panels power output [kWh]	NPV	Net present value
$\mathrm{E_{PVR-Re}}$	Rural PV panels power output [kWh]	LLP_{max}	Loss of load probability upper limit [%]
$\mathrm{E_{WT}}$	Net power generated by wind turbine [kWh]	LLP	Loss of load probability [%]
$Load$	Total energy load over a year [kWh]	PT	Temperature periodic term [^{0}C]
P_{Bio}	Biomass boiler capacity [kW]	RER	Renewable energy ratio [%]
P_{HP}	Heat pump capacity [kW]	SC	Set coverage metric
P_{HST}	Heat storage tank capacity [m^3]	SD	Standard deviation
P_{SC}	Solar collector capacity [kW]	SM	Spacing metric
P_{PVR}	Rural PV panel capacity [kW]	ST	Solar term of temperature [^{0}C]
P_{PV}	PV panel capacity [kW]	$T(t)$	Hourly ambient temperature [^{0}C]
P_{WT}	Wind turbine capacity [kW]	T_{base}	Base term of temperature [^{0}C]
T_{base}(day)	Daily base temperature [^{0}C]	$T_{mean}(day)$	Mean daily temperature [^{0}C]
$T_{min,m}$	Monthly averaged minimum ambient temperature [^{0}C]	$\varepsilon_{Tr,gas}$	Transportation allocation coefficient of gasoline cars
$T_{max,m}$	Monthly averaged maximum ambient temperature [^{0}C]	$\varepsilon_{Tr,PEV}$	Transportation allocation coefficient of PEV
$T_{mean,m}$	Monthly averaged mean ambient temperature [^{0}C]	$\varepsilon_{CO,AR}$	Cooling allocation coefficient of the air refrigerators
Unmet load	Unmet energy load over a year [kWh]	$\varepsilon_{CO,HP}$	Cooling allocation coefficient of the heat pump
$w_{d,h}$	Hourly wind speed [m/s]	$\varepsilon_{HE,bb}$	Heating and hot water allocation coefficient of the biomass boiler
$w_{av,m}$	Average monthly wind speed [m/s]	$\varepsilon_{HE,HP}$	Heating and hot water allocation coefficient of the heat pump
$w_{n,m}$	Average monthly night wind speed [m/s]	θ_h	The scale factor of Weibull distribution
$Weibull_{d,h}$	Random number following a Weibull distribution	$\mu_{d,h}$	Average hourly solar radiation [kWh/m^2]
ε_h	Random number	χ	Random variable with normal distribution function

5.4. Problem Description

A hypothetical grid-connected hybrid renewable energy system including renewable and non-renewable energy conversion technology is chosen as our case study. This HRES is used to increase the renewable energy ratio of a building located in Canada. As shown in Figure 5-1, this energy system may employ wind turbines, PV panels, solar thermal collectors, heat pumps, biomass boilers and heat storage tanks [19]. The employed renewable energy technologies are supposed to provide energy for electricity, heating, and cooling load. The employed backup systems such as grid and natural gas (NG) boiler help to supply the energy demand when the considered RE sources are not able to satisfy the required energy. In a city like Winnipeg, it is not legal to install a wind turbine in the city area. For this reason, it is assumed that wind turbines would be installed in the rural area of the city and its electricity can be easily sold to the grid. The rural area is supposed to be located in area that the electrical grid is established. Thus, there is no limitation to connect the employed wind turbine and PV panels to the grid and selling their produced electricity to the grid. In this study, as it is assumed that the employed system meets the technical requirements [20], it is possible to export electricity to the grid. In Figure 5-1, two alternative locations for PV panel installation are designed; it can be installed either on the top of the building roof or in the rural area. There are two options to meet required transportation of the building: using plug-in electric vehicle or gasoline cars. It is assumed that the energy required for PEV is met by electricity, if there is not enough electricity, the gasoline will be used to guarantee the load. Heat pumps or air refrigerators will cover the cooling load through summers.

It is intended to find the optimal configuration and optimal size of the employed technologies such that simultaneously minimize the total net present cost of the system for entire life time of

the system, minimize annual CO_2 emission, and maximize RER while satisfying a certain level of reliability.

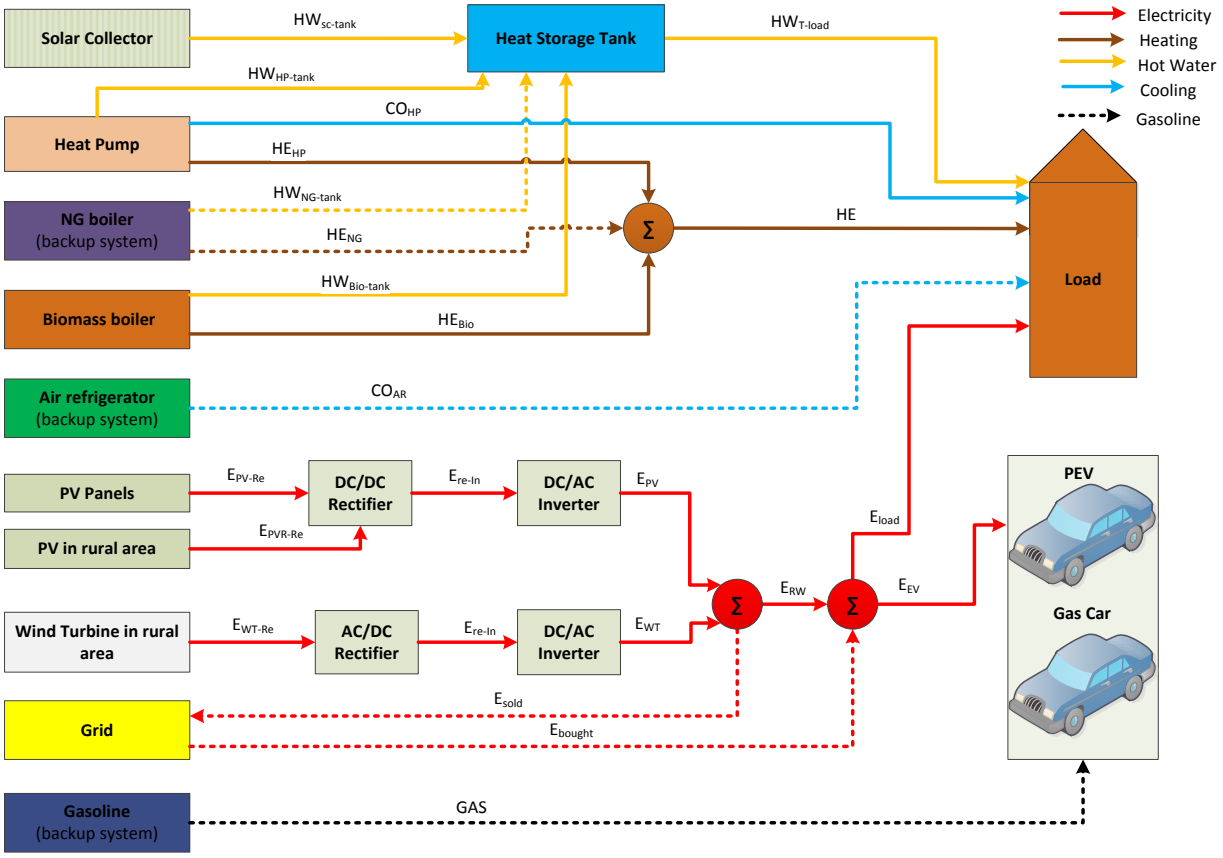

Figure 5-1: Energy flow of the proposed hybrid renewable energy system [19]

Moreover, there is uncertainty in weather data (wind speed, solar radiation, and ambient temperature) and energy load. These uncertainties have significant effect on the design space. The main aim of this study is to establish a methodology to deal with uncertainties existing in the design process of this type of energy supply systems. In other words, the developed approach returns best combination of employed technologies and their corresponding optimal size while considering randomness existing within input data. For this purpose, the design problem is formulated as a stochastic multi-objective optimization problem including three objective functions. In this regards, RE resources data, heating, cooling, and electricity load profile on an

hourly basis are generated by using the most common models (see Section 5.5.2). To specify employed technologies, their actual cost data is considered as well as their mathematical models and the technical limitations are stated. Based on these data, the three objective functions are optimized with respect to the energy balance equations as well as other technical constraints. In order to solve the complex optimization problem, a practical engineering method has been performed, which is based on hybridizing simulation with an optimization algorithm. Moreover, the sampling average approach for sizing and optimization of hybrid energy systems is employed to handle the challenges related to existing uncertainties.

5.5. Proposed Approach

This study intends to provide an engineering tool based on a simulation-based optimization approach for the proposed design problem. For this purpose, a stochastic multi-objective optimization model is developed for the mentioned design problem. The capacity of the components and the allocation coefficients of the technology to meet heating, cooling, electricity, and transportation load are defined as decision variables. The below vectors contain the summary of decision variables of the model:

$$\vec{P} = [P_{PV}, P_{WT}, P_{SC}, P_{HP}, P_{HST}, P_{Bio}, P_{PVR}]$$

$$\vec{\varepsilon} = [\varepsilon_{HE,HP}, \varepsilon_{HE,bb}, \varepsilon_{CO,HP}, \varepsilon_{CO,AR}, \varepsilon_{Tr,PEV}, \varepsilon_{Tr,gas}]$$

Three objective functions are to minimize total NPC, maximize RER, and minimize CO_2 emission. These objectives are subjected to a desirable level of reliability and other technical constraints which introduce the physical concept of the problem. The subsequent section introduces the mathematical formulation of three objective functions. Readers are referred to the

previous work for more details of the optimization problem formulation and the constraints mathematical formulation [19].

In this study, investment cost of components, their operation and maintenance cost, as well as their replacement cost are marked as total NPC. Additionally, it composes of fuel cost, rental cost of the land, biomass collection, storage and transportation cost over the project life time, Equation (5-1) [19].

$$NPC = \sum_{j} [C_{I,j} + C_{O\&M,j} \frac{1}{CRF(i,T)} + C_{rep,j} K_j] P_j + \{C_{elec,b} E_{bought} + C_{NG} NG_y - C_{elec,s} E_{Sold} + C_{Gas}(Gasoline) + Biomass_y (C_{b,Col} + C_{b,St} + C_{b,Tr})\} \frac{1}{CRF(i,T)} \quad (5\text{-}1)$$

One aim of this study is to inspect the possible approaches to increase the renewable resource utilization. A simple way to quantify this is to calculate the renewable energy ratio. It demonstrates the corresponding shares of renewable and non-renewable sources of energy consumption. There is a simple definition for RER which can be used for the future energy planning of communities. The formula below, Equation (5-2), is applied for calculating RER. It is defined as the ratio of total used renewable energy and total used primary energy [19].

$$RER = \frac{Renewable\ energy}{Primary\ energy} \quad (5\text{-}2)$$

The environmental criterion that is being considered in the optimization problem is to minimize pollution emission. In order to quantify the amount of produced pollutants, CO_2 is assumed as the only pollution emission since it is the main cause of emission. The CO_2 is emitted by gasoline

cars, natural gas boiler, and it is resulted from the electricity bought from the grid, Equation (5-3) [19].

$$CO_2 = (Gasoline)EF_{Gas} + NG_y EF_{NG} + E_{bought} EF_E \quad (5\text{-}3)$$

The maximum level for loss of load probability is applied in a constraint that the designed system should satisfy its desired level, Equation (5-4). Loss of load probability is defined as the total unmet energy divided by total energy load, Equation (5-5) [19].

$$LLP < LLP_{max} \quad (5\text{-}4)$$

$$LLP = \frac{Unmet\ load}{Load} \quad (5\text{-}5)$$

5.5.1. Sampling Average Method

In this study, sampling average method (SAM) is applied to tackle the existing randomness and consequently to approximate the objective functions. In order to acquire a model that is able to tackle the randomness, the most popular way is to optimize the expected value of an arbitrary function of the parameters, which is defined over an appropriate probability space. Suppose a multi-objective stochastic optimization problem as following [21]:

$$Minimize\ \{F_1(x), F_2(x), \dots\} \qquad \text{Subject to } x \epsilon S \quad (5\text{-}6)$$

In which, $F_v(x)$ is estimated by $\mathbb{E}\big(f_v(x,\omega)\big)$, Where, $v = (1, 2, \dots)$, S defines the bound of decision space, and ω reflects the randomness effect. Let $\omega_1, \dots, \omega_N$ as N random scenarios that are all independent, the sample average estimation of $F_v(x)$ can be calculated by [21]:

$$\frac{1}{N}\sum_{v=1}^{N} f_\vartheta(x, \omega_v) \approx \mathbb{E}(f_\vartheta(x, \omega)) \quad (5\text{-}7)$$

The basic idea of SAM is to replace the expected value function with its corresponding approximation, Equation (5-7), and then find a solution for the derived deterministic model. By a similar way, the expected value of functions in a multi-objective optimization problem can be replaced by their sample average approximations to compute an estimation of their solution. Thusly, the following deterministic multi-objective problem is resulted, Equation (5-8) [21].

$$Min\left(\frac{1}{N}\sum_{v=1}^{N} f_1(x,\omega_v),\ \ \frac{1}{N}\sum_{v=1}^{N} f_2(x,\omega_v),\ \ \ldots\right) \tag{5-8}$$

Typically, it is a complex task to exactly compute the expected value in the problem represented by Equation (5-6) that is why the approximation method is needed. In fact, Equation (5-8) is an approximation for the original problem of Equation (5-6). Hence, a solution algorithm produces a set of arbitrary and independent samples to estimate the expected value of the objective functions. Then, the complex stochastic problem is converted to a deterministic problem which can be solved by either exact algorithm, or alternatively by a (multi-objective) meta-heuristic to determine a PF for the given problem [21]. In this study, DMOPSO is used as the solution method [21].

5.5.2. Synthetic Generation of the Random Parameters

5.5.2.1. Wind Speed

In this study, the methodology that is proposed by Dufo-López et al. [22] is used to reproduce hourly wind speed data. The idea of the model is simple as described in Equation (5-9) in which the hourly wind speed data ($w_{d,h}$) is calculated [22].

$$w_{d,h} = e_{d,h}.f_{correction-m} \tag{5-9}$$

where, $e_{d,h}$ is obtained by subtracting a fraction of the average monthly value ($w_{av,m}$) from the value of $c_{d,h}$, Equation (5-10). When a negative value is resulted by Equation (5-10), it must be set as zero. $f_{correction\_m}$ is named correction factor and it is calculated by Equation (5-11). Its role is to check that monthly average of measured data is the same as the estimated wind speed data.

$$e_{d,h} = c_{d,h} - f_{substract}.w_{av,m} \quad (5\text{-}10)$$

$$f_{correction-m} = w_{av,m}.24.d_m / \sum_{month} e_{d,h} \quad (5\text{-}11)$$

where, $w_{m,h}$denotes the average of wind speed for an hour (h: $0 \leq h \leq 23$) in the month m, which is computed by Equation (5-12); d_m is the number of days in the month m; $c_{d,h}$ stands for the hourly correlated values of each day, Equation (5-13) and Equation (5-14) [22].

$$w_{m,h} = w_{n,m} + Max[0, (A_m - F_m.\left(t - h_{max,m}\right)^2] \quad (5\text{-}12)$$

where, F_m is a factor providing information about the relation between the time of day and wind speed; A_m is the monthly amplitude; $h_{max,m}$ is the hour that maximum speed in a day is occurred; and $w_{n,m}$ is the average monthly night speed [22].

If (d = 0& h=0): $c_{d,h} = Weibull_{d,h}$ (5-13)

Else: $c_{d,h} = fc.c_{d,h-1} + (1 - fc).Weibull_{d,h}$ (5-14)

where, $Weibull_{d,h}$ is a random number which is generated by a Weibull distribution function with b form factor and the scale factor of θ_h, Equation (5-15) and Equation (5-16) [22].

$$Weibull_{d,h} = [-\theta_h^b.ln(1 - a_{d,h})]^{1/b} \quad (5\text{-}15)$$

where, $a_{d,h}$ indicates a random number in range of (0 -1).

$$\theta_h = w_{m,h} / \Gamma(1 + \frac{1}{b}) \quad (5\text{-}16)$$

where, $\Gamma(1+1/b)$ is the Gamma function. In order to control that, the monthly average of measured data is the same as desired values, the cumulative distribution function of both generated series and the Weibull distribution function are compared [22]. In this study, f_c is assumed 0.9 and $f_{subtract}$ is set at 0.8 [22].

5.5.2.2. Solar Radiation

With the collected data, a mathematical model is developed to generate random hourly solar radiation, Equation (5-17). The solar radiation is divided into two parts deterministic part and random part.

$$I_h = \mu_h + \varepsilon_h \quad (5\text{-}17)$$

where, I_h is the solar radiation of the model; $\mu_{d,h}$ is the average of solar radiation for hour h, ε_h is a random number that is approximated by a normal distribution function. The distribution function is resulted by fitting the function on hourly standard deviation of solar radiation.

5.5.2.3. Ambient Temperature

According to Krenzinger et al. [23], the ambient hourly temperature can be estimated by adding one random part (δ) to a periodic term (PT), a solar term (ST) and a base term T_{base}; Equation (5-18) shows their model [23]:

$$T(t) = T_{base}(t) + PT(t) + ST(t) + \frac{\delta}{2} \quad (5\text{-}18)$$

The following section describes the mathematical model for three mentioned terms. In order to define the base term of temperature, a linear interpolation is used as it is shown in Equation (5-19). There is an experimental term for the purpose of adjusting the mean of final result [23].

$$T_{base}(t) = T_{mean}(day) + (t+1)\left\langle \frac{T_{mean}(day+1) - T_{mean}(day)}{24} \right\rangle - [1 + 0.155A(day)] \quad (5\text{-}19)$$

where, $T_{mean}(day)$ is the mean daily temperature which is identified by Equation (5-20) [23].

$$T_{mean}(day) = T_{base}(day) + SD \quad (5\text{-}20)$$

$$SD = 4.2 - 0.15(T_{min,m}) \quad (5\text{-}21)$$

The daily base temperature $T_{base}(day)$ is defined by Equation (5-22); $A(day)$ is named daily amplitude of temperatures as seen in Equation (5-23).

$$T_{base}(day) = \frac{1}{3}(T_{mean,m})\left[2 + \left\langle \frac{H_0(day)}{H_0(month)} \right\rangle\right] \quad (5\text{-}22)$$

where, $H_o(day)$ is the extraterrestrial solar radiation in a given day and $H_o(month)$ is the monthly averaged daily extraterrestrial solar radiation. $T_{min,m}$, $T_{max,m}$ and $T_{mean,m}$, respectively give the monthly averaged minimum, maximum and mean ambient temperature [23].

$$A(day) = \left(I_{max}(day) - I_{max,m}\right)\left[\frac{A_{max,d} - A_{mean,d}}{I_{max}(month) - I_{max,m}}\right] + A_{mean,d} + \delta \quad (5\text{-}23)$$

$I_{max}(day)$ is the value of maximum solar radiation for each day; $I_{max,m}$ is the monthly average of maximum solar radiation for each day; $I_{max}(month)$ is the maximum value of solar radiation in whole the month; $A_{mean,d}$ and $A_{max,d}$ are mean and maximum daily amplitude, respectively, those are calculated by Equation (5-24) and Equation (5-25)[23].

$$A_{mean,d} = T_{max,m} - T_{min,m} \tag{5-24}$$

$$A_{max,d} = 25 - 0.42(T_{min,m}) + \frac{\delta}{2} \tag{5-25}$$

where, δ is a random variable uniformly distributed between –1 and +1. The Equation (5-26) and Equation (5-27) are used to examine the periodic term according to the time of a day. The first equation is related to time before sunrise and the next one is assigned for time after t_{sr} [23].

$$If \quad t < t_{sr} \quad then \qquad PT(t) = \frac{A(day)}{4}\langle\frac{1}{2} + COS(\frac{(20+t)}{20-t_{sr}}\frac{\pi}{2})\rangle \tag{5-26}$$

$$Else \qquad PT(t) = \frac{A(day)}{8}\langle COS(\frac{(16-t)}{15-t_{sr}}\frac{\pi}{2}) + COS(\frac{(14-t)}{13-t_{sr}}\frac{\pi}{2})\rangle \tag{5-27}$$

The solar term is then determined through a simple equation in which the maximum temperature $T_{max}(day)$, a recurrent term (Δ) , and the time of the maximum solar radiation are the main terms, Equation (5-28) [23].

$$ST(t) = \langle\frac{T_{max}(day) - [T_{base}(t) + PT(15)]}{I_{max}(day)} + \Delta\rangle\, I(t-1) \tag{5-28}$$

The maximum temperature in the day is evaluated through adding a half of daily amplitude to the mean daily temperature, as seen in Equation (5-29) [23].

$$T_{max}(day) = T_{mean}(day) + \frac{A_{max}(day)}{2} \tag{5-29}$$

After generating hourly temperature for a day, a comparison between the resulted mean temperature and input data will be performed based on Equation (5-30) to updated the Δ, and then iteration is repeated for daily generation[23].

$$If\left(T_{mean}(day) - \sum\frac{T(t)}{24}\right) > 0.5 \quad then\ \Delta = \Delta + \frac{T_{mean}(day) - \sum\frac{T(t)}{24}}{I_{max}(day)} \tag{5-30}$$

5.5.2.4. Load

In the feasibility study of renewable energy systems, it is required to develop a simple method to identify an energy load profile. A cluster analysis approach that is proposed in [24] has been applied for the purpose of generating electric and hot water load profile. For a representative building, the daily information of appliances such as their utilization, energy consumption, ownership, and occupied duration is used to produce daily load profile [24].

As the load profile is directly related to the occupation pattern of the buildings, it can be a promising task to identify the building clusters [24]. In this study, five most common scenarios of building occupancy pattern are considered since there is a lack of information [24]. In Table 5-2, these five scenarios are represented [24].

Table 5-2: Occupancy scenarios for a typical house containing 3 persons [24]

Scenarios	Occupied period
1	0-9:00 & 13:00-23
2	0-9:00 & 18:00-23
3	0-9:00 & 16:00-23
4	0-24
5	0-13:00 & 18:00-23

To evaluate the daily energy and hot water load profile, firstly, an average daily consumption of each appliance is determined based on monthly energy bill and the annul Canadian appliance energy consumption [25]. Figure 5-2 represents the schematic of load profile generation process. For a specific scenario, a random load profile for appliances is generated according to a random number generator technique. By adding the random load profile of all appliances, the load profile of a specified scenario is produced which named "*Specific Profile*" since it is resulted from a certain occupation scenario [24]. The daily load profile of a specific scenario can change over

different days. The random generation is repeated 20 times to return an approximately smooth load curve for a given day [24]. A specific load profile cannot reflect the general load profile for the building since it represents only one certain scenario of occupancy pattern. Hence, five specific profiles resulted by five scenarios are aggregated to produce a typical load profile for the electricity, hot water, and required energy for transportation of the building.

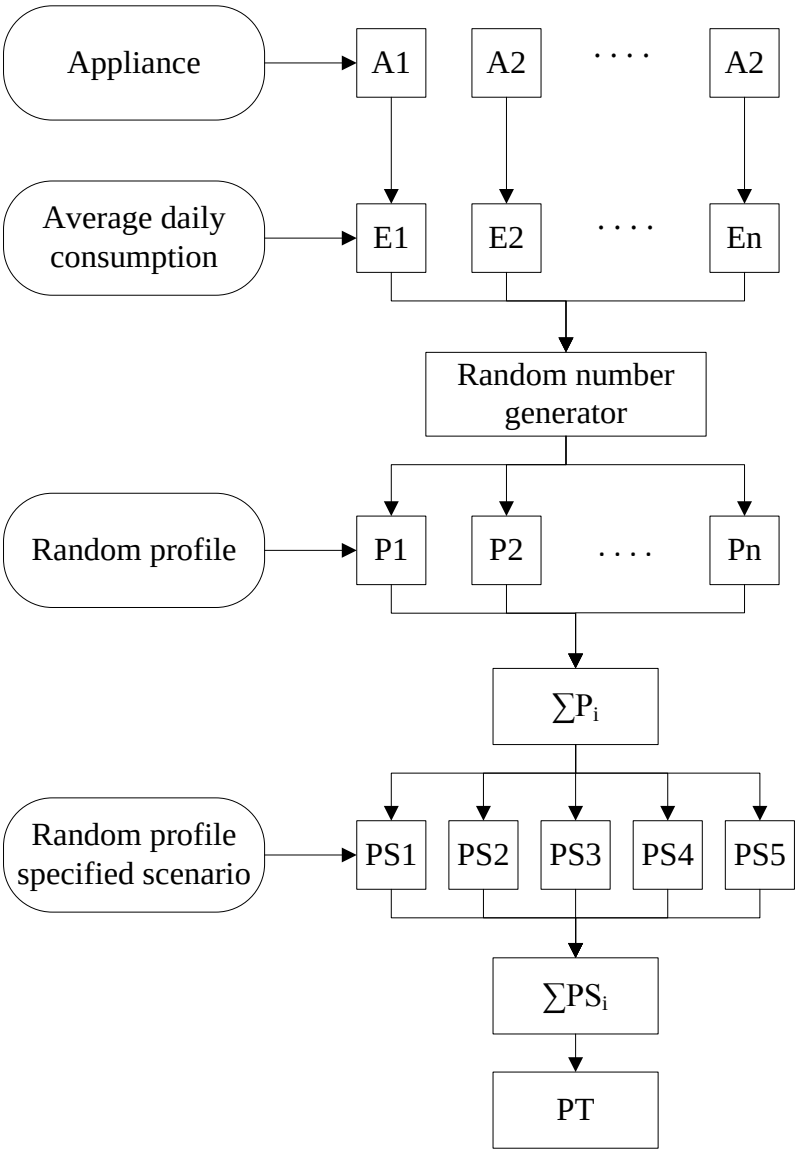

Figure 5-2: Framework of generating the electricity or hot water load profile

In Figure 5-2, A_i is appliances name; E_i is the average daily energy consumption of the appliances; *P1, P2, ..., Pn* describe random profiles those are generated for the appliances; PS_i is related to the specific profile corresponding to a particulate occupancy scenario; *PT* is a typical load profile [24] . It is worth mentioning that the heating and cooling load is approximated by degree hour [19] while other types of energy demand are estimated by using the mentioned methodology.

5.6. Solution Approach

In order to solve the mentioned stochastic multi-objective optimization problem, a simulation-based optimization approach is used to generate a Pareto front. This approach is trying to apply simultaneously the advantage of simulation and optimization methods. In complicated systems, it is difficult to handle the model uncertainties and non-linearity with a stand-alone optimization method since it requires the precise mathematical model of the system. In these cases, the simulation can be considered as a powerful assessment engine to precisely contain all details of the system and involve existing uncertainties [26]. However, simulation suffers from the fact that it is inherently unable to return the optimal solution of the problem. Thus, the integration of these two methods can be an efficient solution approach when the optimization problem is complex due to either existing uncertainties or non-linear terms.

In this study, the simulation module accommodates the mathematical models for the components of the employed system (see Figure 5-1). The main role of the simulation module is to check the feasibility of each candidate solution proposed by the optimization algorithm. The utilized optimization algorithm is developed based on the Particle Swarm Optimization (PSO) approach. Recently, PSO is implemented for multi-objective optimization problems since it was performed successfully in single objective problems [27]. This type of algorithms is named Multi-Objective

Particle Swarm Optimization [27]. In MOPSO a set of solutions named non-dominated solutions or Pareto front is derived instead of a single solution resulted by PSO. In this study, MOPSO is extended to dynamic multi-objective particle swarm optimization algorithm which was developed in the previous work of the authors [27]. By using DMOPSO a promising improvement in the quality of garneted PF is obtained compared with well-known MOP approaches. The difference between the employed algorithm and MOPSO is that multi-leaders and dynamic cell-based density calculation strategy is utilized in the performed algorithm to update the solutions [27]. For detail explanation of the algorithm, readers are referred to the previous work [27].

5.7. Results & Discussion

In order to evaluate the proposed methodology, a case study is selected which is located in Winnipeg, Canada. The case study is an apartment that contains 12 two-bedroom units and 31 one-bedroom units, and its total floor area and foot print is approximated by 2940 m^2 and 980 m^2, respectively. The current energy consumption of the building includes natural gas, grid-electricity, and gasoline. In other words, a natural gas boiler is in charge of supplying heating load and hot water demand while the cooling load is met by air refrigerators. The building residences use gasoline to provide energy of their cars. In addition, the required electricity for appliance is satisfied by hydroelectricity which is bought from the grid. The primary RER of the building is estimated as 10% and the total GHG production is calculated as 277.1 (ton/year) [19]. The average monthly energy use of the building is represented in Figure 5-3 per type of energy carriers.

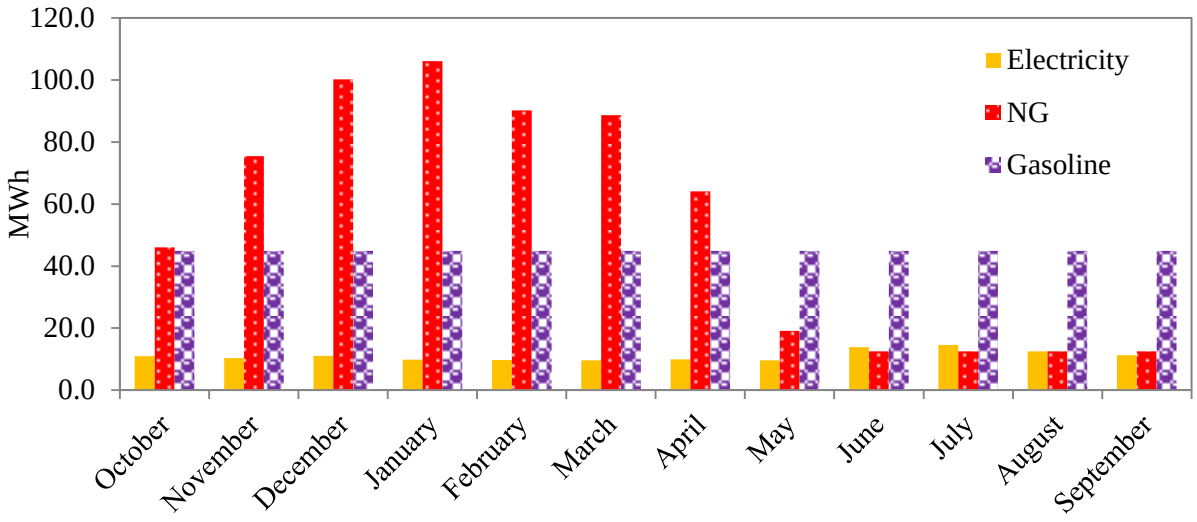

Figure 5-3: Monthly energy consumption of the building per type of energy carriers [14]

The daily average hourly wind speed at 10 m height, direct normal irradiance, and ambient temperature over one year for the location are plotted in Figure 5-4 to Figure 5-6. These figures include stochastic data which is generated by the mentioned models in Section 5.5.2 while the deterministic one is obtained by averaging the measurement data over 15 years (1990-2004) [28]. In Figure 5-4 to Figure 5-10, the data represented and labeled as stochastic are the result of stochastic model over one sample year. It is worth mentioning that in these graphs, the day 0 represents the first day of January.

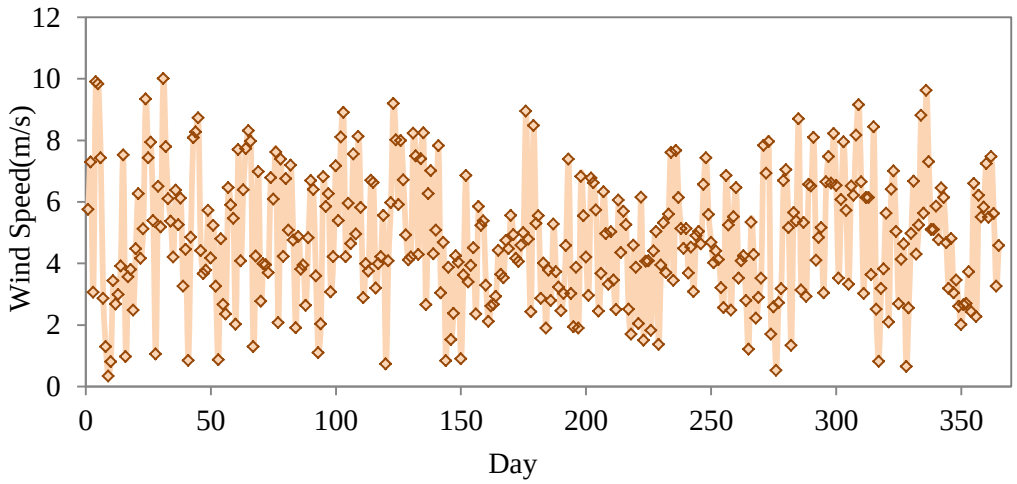

Figure 5-4: Daily average of hourly wind speed for Winnipeg

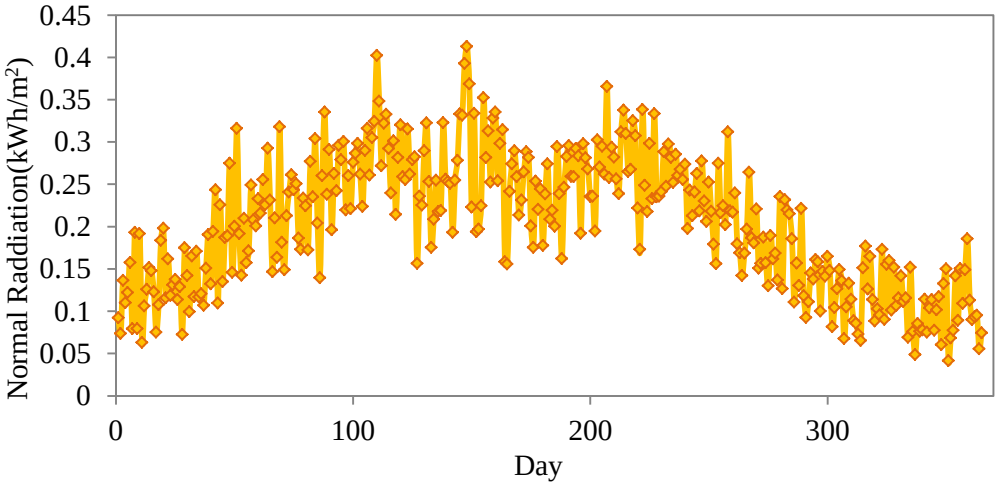

Figure 5-5: Daily average of hourly normal irradiation for Winnipeg

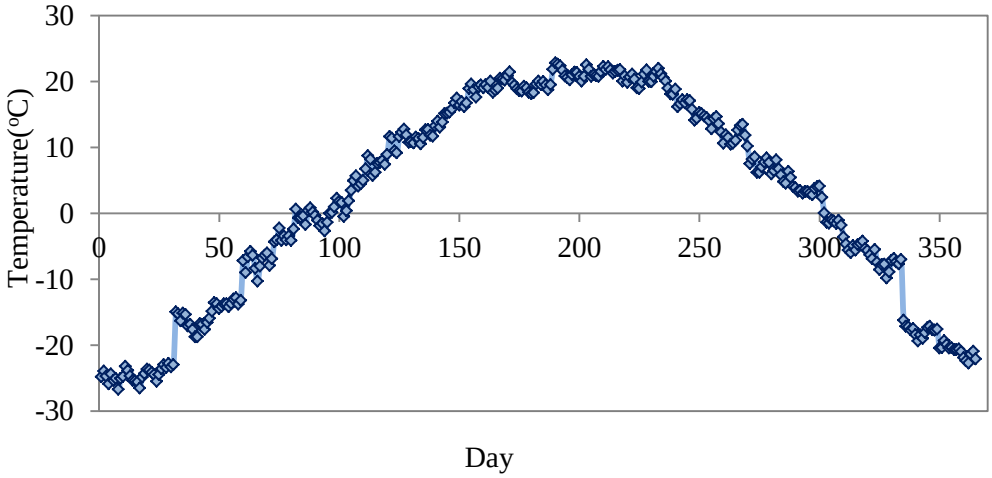

Figure 5-6: Daily average of hourly ambient temperature for Winnipeg

Similarly, Figure 5-7 to Figure 5-10 depict the required energy for different purposes (heating, cooling, HWD, electricity, and transportation) used in the stochastic model. In order to estimate the cooling and heating load, the concept of the degree-day is utilized in which it is assumed that the energy requirement for heating and cooling are directly depend upon the difference between base and outside temperature. In the deterministic model, the hourly input data over one year is entered to the model and stay constant over simulation run while the data in stochastic model is varying over years through the simulation run.

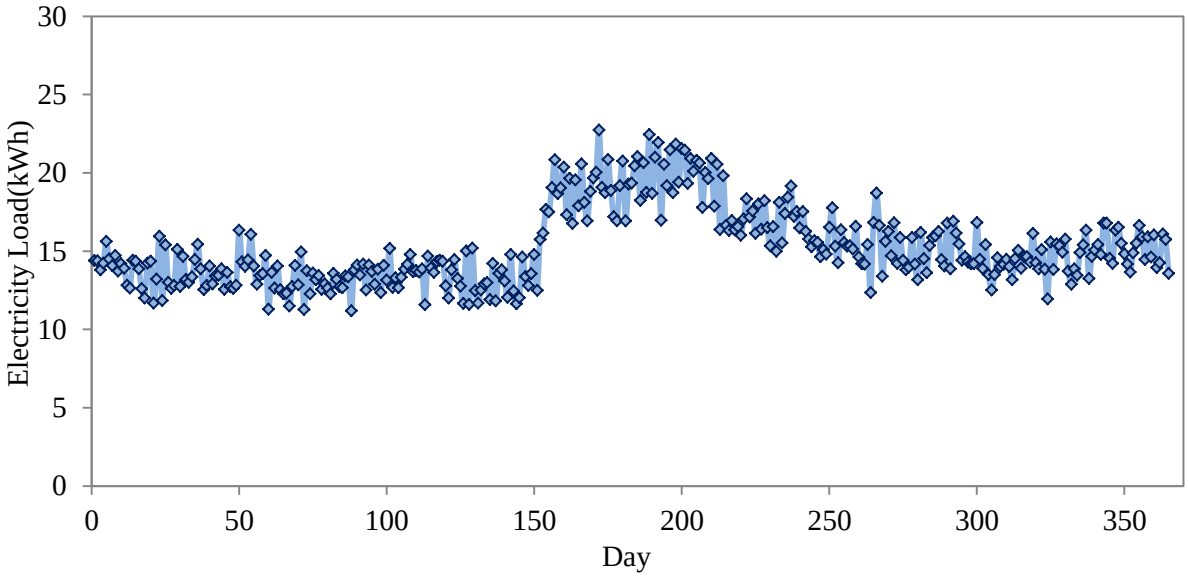

Figure 5-7: Daily average of electricity load of the building

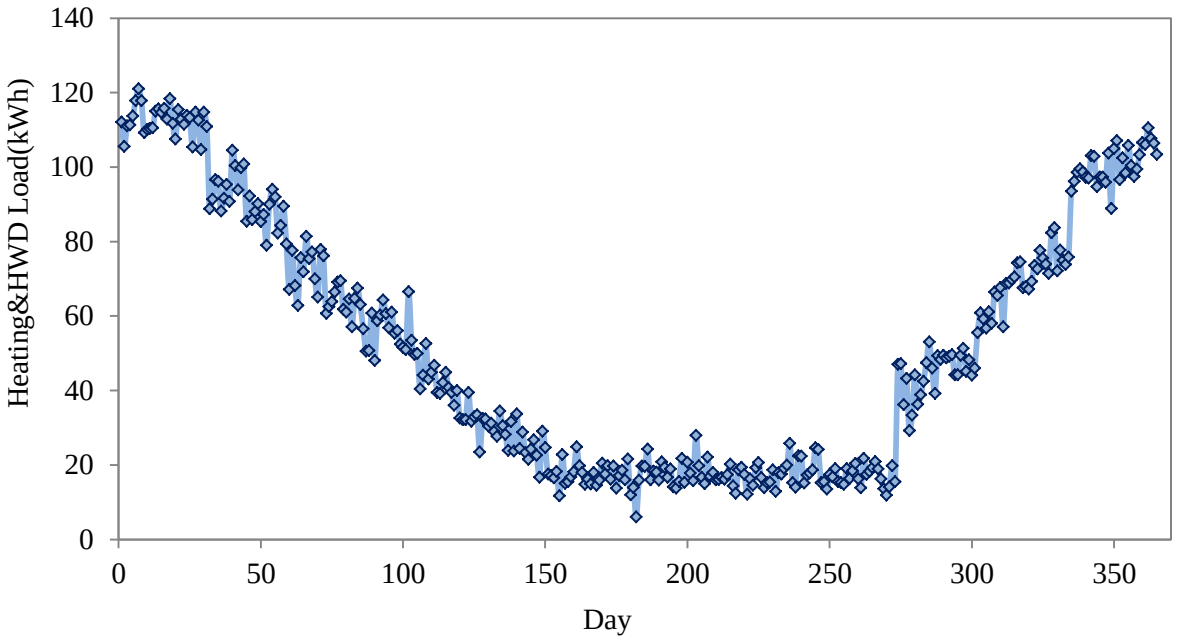

Figure 5-8: Daily average of hourly heating load of the building for space heating and hot water purpose

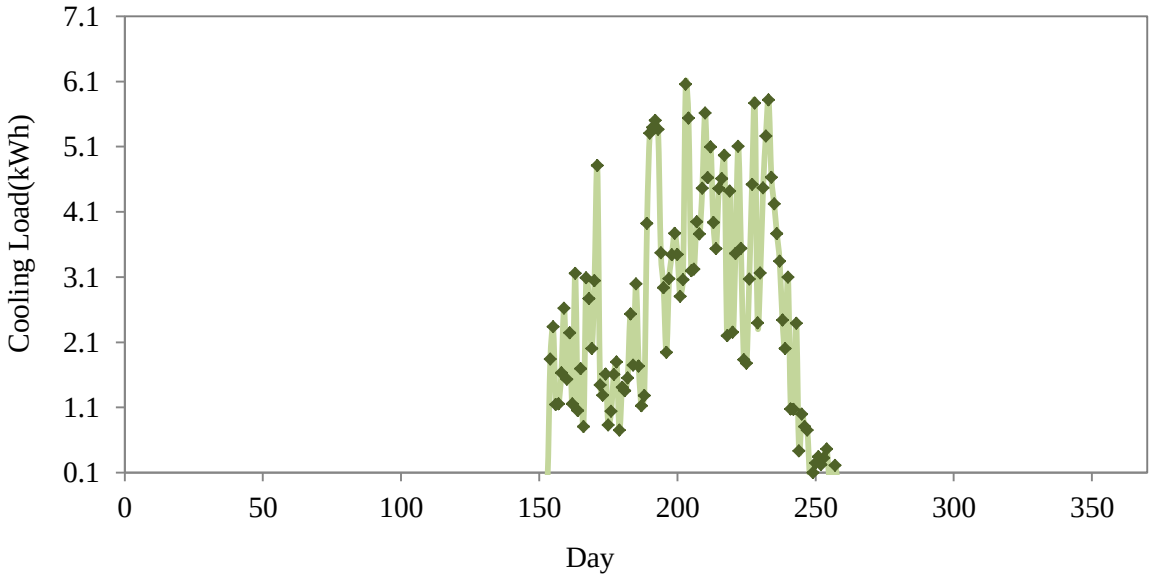

Figure 5-9: Daily average of hourly cooling load of the building

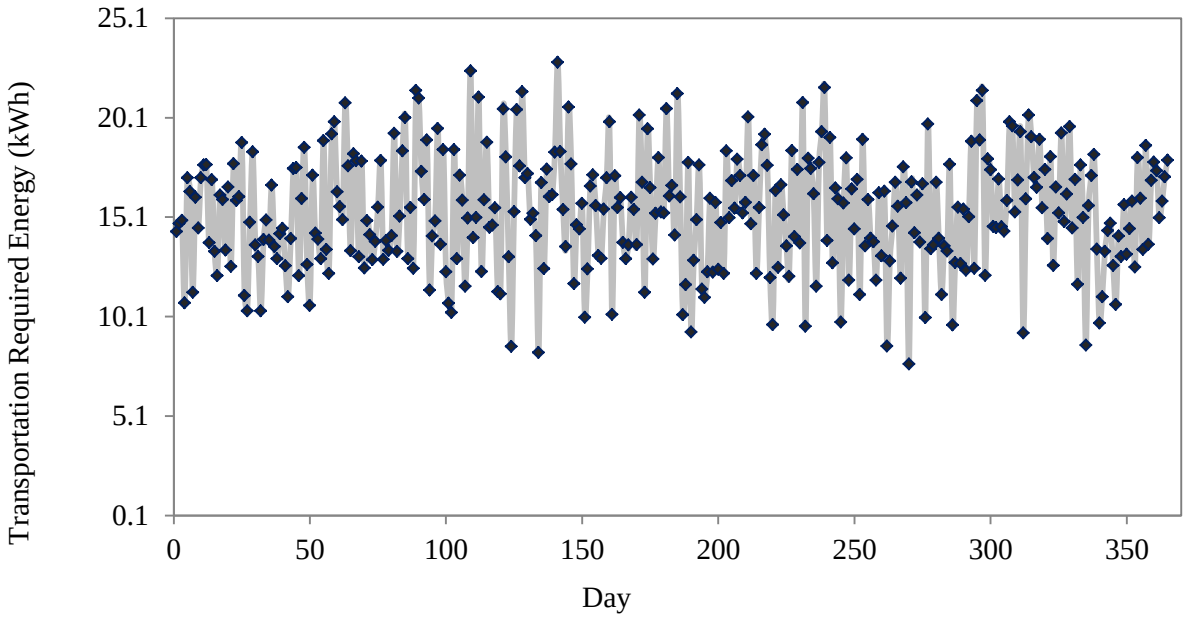

Figure 5-10: Daily average of hourly required energy for the transportation of the building

In this study, the economic parameters and characteristics of components such as the initial cost, operation and maintenance cost are considered the same as what has been exhibited in the previous work [19]. The employed HRES is implemented on hourly basis in the simulation which is coded by using C++ programming environment and executed in a 2.40 GHz Core 2 processor with 4GB of RAM.

The Pareto fronts evolved using the proposed DMOPSO for the stochastic and deterministic design approaches are shown in Figure 5-11 to Figure 5-13, which show an illustration of the trade-off solutions. These figures show the comparison between stochastic and deterministic PFs. Besides, the descriptive non-dominated solutions evolved in the stochastic and deterministic cases are listed in Table 5-3. These solutions are tagged with numbers in Figure 5-11 to Figure 5-13. In Figure 5-11, RER is outlined on the vertical axis and the curves show different value of NPC needed to obtain a design with corresponding RER value. Similarly in Figure 5-12, the curves illustrate the total net present cost required to gain the corresponding value of CO_2

emission. It is evident that the total NPC has shifted to higher level in the stochastic case when it is compared to the deterministic design surface. In addition, Figure 5-13 describes the trade-off solutions between RER and CO_2 emission. When the uncertainties are incorporated, this analysis helps us to reach up to 90% increasing in RER and with up to 99.3% less CO_2 emission than the base case. The high RER and low emission region involve high total net present cost. There are some low NPC points but these involve low RER and high emission. As seen over stochastic curves in Figure 5-11 to Figure 5-13, that is relatively a costly option to increase RER from 29.9% to 63% since that requires 31% more NPC than the design configuration represented by the solution 1. Furthermore, by moving from solution 1 toward solution 2, the CO_2 emission is reduced moderately which is less than 52% or 84.2 (ton/year). Between solution 2 and 3, the NPC would change moderately (less than 20%) while the value of RER is increased by 37%. Note that the most likely region of RER for the stochastic surface is between 29%-80% while for the deterministic PF solutions are distributed uniformly in range of 27%-100%. This can be associated with the non-linearity of the model as well as it justifies considering uncertainty analysis. In the stochastic case, it is clear from the depicted PFs that the RER can reach to 100% through different solutions. That is, there are some options for RER of 100%, in which the NPC and CO_2 emission is varied. Over these solutions CO_2 emission is reduced slightly from 3.2 ton/year to 2.6 ton/year while total NPC is increased more than 18%. Hence, between solutions with the same RER of 100%, it is more reasonable that a solution with less NPC (solution 3) would be selected since there is no remarkable difference between their CO_2 emissions.

In this type of portrayal, decision makers can conveniently distinguish the minimum NPC, CO_2 emission, or maximum possible RER that can be achieved by this graph. That is, based on decision maker's desire a convenient solution can be selected from a set of non-dominated

solutions. By retracting one step, the value of decision variables can be found where we need to install those capacities to obtain these kinds of performances.

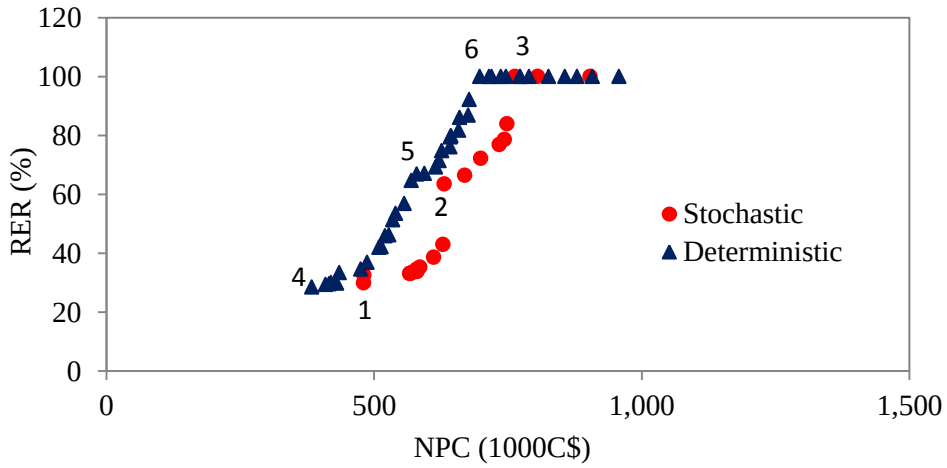

Figure 5-11: The 2D Pareto front of the deterministic and stochastic design approaches; RER vs. NPC

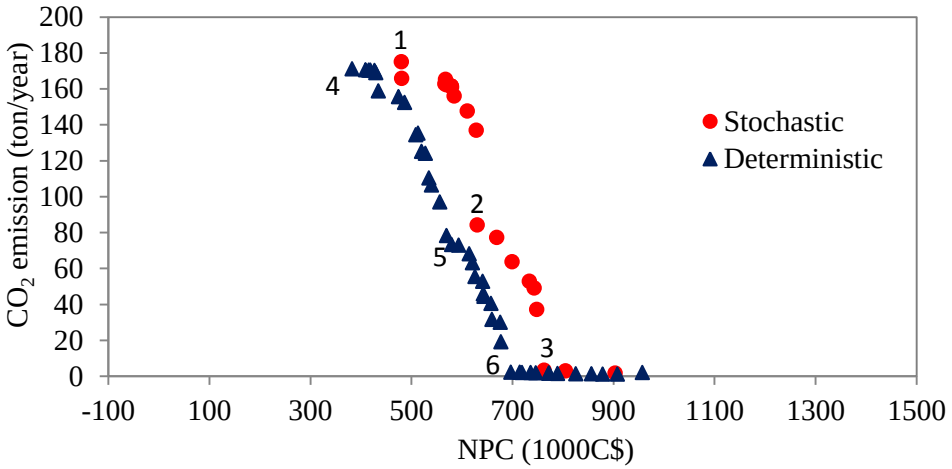

Figure 5-12: The 2D Pareto front of the deterministic and stochastic design approaches; CO_2 emission vs. NPC

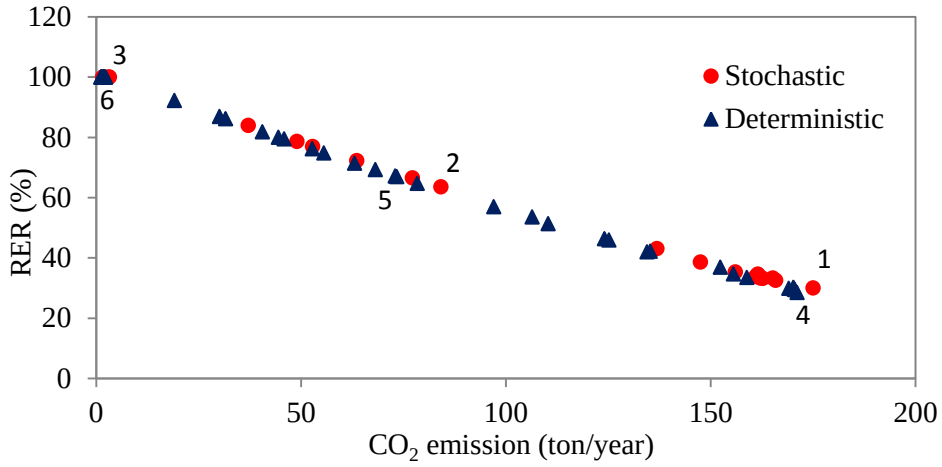

Figure 5-13: The 2D Pareto front of the deterministic and stochastic design approaches; RER vs. CO_2 emission

The Pareto front attained as the result of deterministic optimization scheme is also presented in Figure 5-11 to Figure 5-13. As shown, there is no significant difference in PFs shape while there is moderate difference in level between the deterministic and stochastic PF surfaces. The maximum, minimum, average of performance criteria for non-dominated solutions laying over the stochastic and deterministic PF surfaces are summarized in Table 5-4.

Table 5-3: Example solutions laying over the generated PF in the stochastic and deterministic cases

Generators/Objectives	Stochastic			Deterministic		
	Solution 1	Solution 2	Solution 3	Solution 4	Solution 5	Solution 6
PV [kW]	0	0	0	0	0	0
Wind turbine [kW]	94	105	116	68	71	73
Solar collector [kW]	25	0	0	0	0	0
Heat pump [kW]	0	0	0	0	0	0
Heat storage tank [m^3]	4.3	4.3	4.3	4.3	4.3	4.3
Biomass boiler [kW]	0	95	200	0	91	200
PV-rural area [kW]	0	0	0	0	0	0
$\varepsilon_{HE,HP}$	0	0	0	0	0	0
$\varepsilon_{HE,bb}$	0	0.3	1	0	0.4	1
$\varepsilon_{CO,HP}$	0	0	0	0	0	0
$\varepsilon_{CO,AR}$	1	1	1	1	1	1
$\varepsilon_{Tr,PEV}$	0.94	1	1	1	1	1
$\varepsilon_{Tr,gas}$	0.06	0	0	0	0	0
LLP [%]	4.8	4.8	4.8	5	4.9	4.9
NPC [C$]	480265	630741	763062	383284	579654	705180
RER [%]	30	63	100	28.5	67	100
CO_2 emission [ton/yr]	175.1	84.2	3.2	171.2	73.4	2.4

There is a slightly difference (less than 9%) between the average total NPC of two cases. Additionally, the range for RER and CO_2 emission that stochastic PF is able to enclose is competitive to the deterministic case. The total NPC in stochastic design shows a higher shift as the deterministic design is based on the average values of historical data while stochastic design evaluates more realistic situation. In this regards, the decision variables are distinctive for two cases as shown in Table 5-3. For instance, in the maximum RER case, the installed capacity of the biomass boiler in the deterministic approach is less than the stochastic one. In the minimum RER designs, the stochastic solution (see solution 1 in Table 5-3) use wind turbine, SC, and PEV while deterministic one only employs wind turbine and PEV. Correspondingly, this reduces total NPC more in deterministic case than stochastic case which changes the non-dominated solutions surface.

Table 5-4: The bound of different objectives obtained by the stochastic and deterministic optimization approaches

	Minimum		Average		Maximum	
	Stochastic	Deterministic	Stochastic	Deterministic	Stochastic	Deterministic
RER (%)	29.9	28.5	56.2	63	100	100
Emission(ton/yr)	1.6	1.1	106.5	87.3	175	171.2
NPC(1000C$)	480.2	383.3	646.3	595	903.4	957

Furthermore, the quality analysis of generated Pareto fronts in the stochastic and deterministic cases is performed using the well-known performance metrics. For this purpose, three metrics are employed which are named spacing metric, diversification metric, and set coverage metric [27]. The spacing metric is used to measure the distribution of individuals over PF while diversification metric determines the maximum extension that can be covered by non-dominated solutions [27]. The set coverage metric is applied to compare two given PFs and identify the closet PF to the optimal PF [27]. The readers are referred to the previous work of this study [27] for more details about the PF performance metrics definition and their mathematical calculation. Table 5-5 shows the comparison between the deterministic and stochastic PFs by using three performance metrics, obtained PF size, and running time of the algorithms.

Table 5-5: The performance metric values of the stochastic and deterministic approaches

Performance metric	Stochastic	Deterministic
Spacing	0.14	0.09
Diversification	4.24	4.96
PF size	20	42
CPU time (Second/iteration)	308	28
SC (Stochastic, Deterministic)	0%	
SC (Deterministic, Stochastic)	55%	

It seems that inclusion of uncertainties has decreased the range of objective function almost for RER and CO_2 emission, thereby providing less flexibility to designer. This fact can be clearly inferred from the diversification metric result since this metric has slightly better outcome in the deterministic case. The spacing metric of the stochastic case is greater than the deterministic

case. It means the solutions over the deterministic PF are distributed more uniform. The set coverage metric clearly shows the dominance of the deterministic PF over the stochastic one. It represents that 55% of solutions placed over the stochastic PF are dominated by the solutions resulted by the deterministic PF. Here, the set coverage metric is used to show that some of solutions of the PF generated by the stochastic model are shifted to higher NPC, less RER, and higher CO_2 emission. It is not relatively reasonable to compare these two obtained PFs based on the set coverage metric as the input data is notable different in the stochastic and deterministic cases. The PF size of the deterministic case is almost two times of the stochastic PF size. The CPU time needed to solve the stochastic problem is increased significantly (more than 11 times) compared with the deterministic case. It can be concluded that the performance of DMOPSO in the deterministic optimization problem is prominent than the stochastic case. It means when the system randomness is incorporated, the efficiency and effectiveness of DMOPSO in the developed multi-objective optimization problem is reduced. Nevertheless, stochastic analysis result is preferred over the deterministic one since it examines a significant range of possible future outcomes and consequently its results are more realistic. In other words, the stochastic optimization helps decision makers to choose a solution that is evaluated in a condition closer to the real life situation than what is predefined in the deterministic design.

Finally, sensitivity analysis is implemented to assess the impact of changing the values of parameters on the derived PF. In order to carry out the analysis, 13 parameters are considered, and then upper and lower limits for the parameters are examined to study their effect on the resulted PF. The studied parameters are summarized in Table 5-6.

Table 5-6: Studied parameters in the sensitivity analysis

Parameters	Abbreviation	Parameters	Abbreviation
Biomass Transportation Cost	BioT	Sold Electricity Price	SoEP
Biomass Collection Cost	BioC	Wind Turbine Capital Cost	WTC
Biomass Storage Cost	BioSt	Solar Collector Capital Cost	SCC
Land Rental Cost	LaC	Heat Pump Capital Cost	HPC
Gasoline Price	GaP	PV Panel Capital Cost	PVC
NG Price	NGP	Interest Rate	IR
Grid Electricity Price	GEP		

The parameters are set in their upper and lower limits to illustrate the change in the average of NPC of the solutions with RER of 100%, Figure 5-14. The average of total NPC and CO_2 emission of the solutions with RER of 100%, which are laying over the original stochastic PF (see Figure 5-11 to Figure 5-13) are estimated as C$824039 and 2.61 (ton/year), respectively. Figure 5-14 shows the changes in total NPC where the studied constants are fixed at their upper or lower limits. For example, the interest rate is reduced by 50%, then the changes in the average of total NPC of solutions with the highest RER are monitored which are 12.9% higher than the value of the base case.

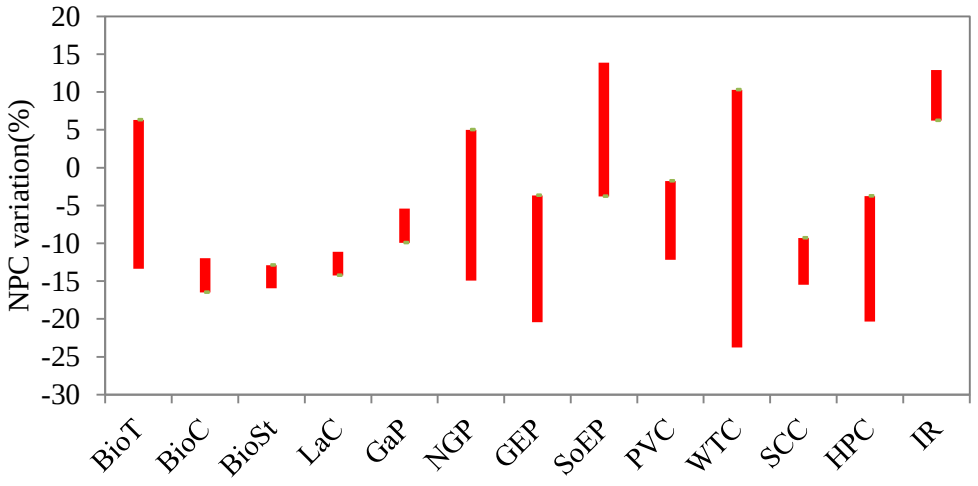

Figure 5-14: Sensitivity analysis result; NPC variation versus the parameters variation

In order to perform the sensitivity analysis, DMOPSO is run 5 times to identify the standard deviation of the average of objectives. It observes that the standard deviation of the average of NPC is set at 16.2%. In the inferring of the sensitivity analysis result, if the difference between the averages of NPC of a scenario and its original values would be less than its standard deviation that can be neglected. As it is obvious from the result, wind turbine capital cost and electricity price have more effect on total NPC than others. It is clear from Figure 5-14 that changing the solar collector and PV panels capital cost resulted in a small variation of NPC as there is small contribution for them in the obtained non-dominated solutions.

5.8. Conclusion

In this study, simulation-based optimization approach is proposed to solve optimal sizing of HRES taking into considerations the uncertainties existing in RE resources and energy demand. A dynamic multi-objective particle swarm optimization algorithm, simulation module, and sampling average technique are used to derive out a set of non-dominated solutions for an HRES applied to buildings where multiple energy sources are used.

The proposed method applies synthetic data generation to provide data series for wind speed, solar irradiance, ambient temperature, and energy load. The sampling average technique integrated with the simulation module is in charge of handing the complexity resulted by incorporating uncertainties. In the developed multi-objective optimization problem, three design criteria are considered including total net present cost of the system, renewable energy ratio, and CO_2 emission where a desirable level of loss of load probability should be satisfied. A set of renewable energy technologies is assessed in order to increase RER of a residential apartment located in Canada. The employed renewable energy technologies contain PV panels, wind

turbines, heat pumps, biomass boilers, and PEV cars. In order to evaluate the performance of the proposed approach, the obtained Pareto front is compared with the deterministic PF through well-known performance metrics. The result shows that RER can be increased by 100% in both cases while a higher NPC is observed in the stochastic case. In addition, the employed performance metric outcomes show that the quality of the generated PF in the deterministic case is better than the stochastic one. However, stochastic analysis result is more desirable since it examines a significant range of possible future outcomes and consequently its results are more informative and realistic. The sensitivity analysis is performed to identify the economic parameters that have more significant effect on the design criteria. Its finding describes that the wind turbine capital cost and electricity price have the most impact on total NPC.

For future research directions of the present work, hybridization methods based on local search techniques can be used to increase the efficiency and effectiveness of DMOPSO algorithm in the application of the stochastic multi-objective optimization problem. DMOPSO can be modified to find a PF in a more reasonable time since the incorporation of uncertainties increases the complexity of the problem.

5.9. References

[1] Ekren O, Ekren BY. Size optimization of a solar-wind hybrid energy system using two simulation based optimization techniques. Dr. Rupp Carriveau (Ed.). Fundamental and Advanced Topics in Wind Power, INTECH Open Access Publisher, Rijeka, Croatia, 2011.

[2] Thompson S, Duggirala B. The feasibility of renewable energies at an off-grid community in Canada. Renewable and Sustainable Energy Reviews 2009; 13(9): 2740–2745.

[3] Rosiek S, Batlles FJ. Renewable energy solutions for building cooling, heating and power system installed in an institutional building: Case study in southern Spain. Renewable and Sustainable Energy Reviews 2013; 26:147–168.

[4] Akella AK, Sharma MP, Saini RP. Optimum utilization of renewable energy sources in a remote area. Renewable and Sustainable Energy Reviews 2007; 11(5):894–908.

[5] Banos R, Manzano F, Montoya FG. Optimization methods applied to renewable and sustainable energy: A review. Renewable and Sustainable Energy Reviews 2011; 15(4):1753–1766.

[6] Abedi S, Alimardani A, Gharehpetian GB, Riahy GH, Hosseinian SH. A comprehensive method for optimal power management and design of hybrid RES-based autonomous energy systems. Renewable and Sustainable Energy Reviews 2012; 16(3):1577–1587.

[7] Maheri A. Multi-objective design optimization of standalone hybrid wind-PV-diesel systems under uncertainties. Renewable Energy 2014; 66: 650–661.

[8] Arun P, Banerjee R, Bandyopadhyay S. Optimum sizing of photovoltaic battery systems incorporating uncertainty through design space approach. Solar Energy 2009; 83:1013–1025.

[9] Dufo-lópez R, Bernal-agustín JL, Lujano J, Domínguez-navarro JA. Utilization of synthetically generated hourly wind speed data in the optimization of wind-batteries stand-

alone systems. In Proceeding of International Conference on Renewable Energies and Power Quality, Las Palmas de Gran Canaria, Spain, 2011.

[10] Handschin E, Neise F, Neumann H, Schultz R. Optimal operation of dispersed generation under uncertainty using mathematical programming. International Journal of Electrical Power & Energy Systems 2006; 28: 618–626.

[11] Ekren O, Ekren BY. Size optimization of a PV/wind hybrid energy conversion system with battery storage using response surface methodology. Applied Energy 2008; 85:1086–1101.

[12] Ekren O, Ekren BY. Size optimization of a PV/wind hybrid energy conversion system with battery storage using simulated annealing. Applied Energy 2010; 87:592–598.

[13] Giannakoudis G, Papadopoulos AI, Seferlis P, Voutetakis S. Optimum design and operation under uncertainty of power systems using renewable energy sources and hydrogen storage. International Journal of Hydrogen Energy 2010; 35: 872–891.

[14] Khan MJ, Iqbal MT. Pre-feasibility study of stand-alone hybrid energy systems for applications in Newfoundland. Renewable Energy 2005; 30:835–854.

[15] Kuznia L, Zeng B, Centeno G, Miao Z. Stochastic optimization for power system configuration with renewable energy in remote areas. Annals of Operations Research 2012; 210(1): 411–432.

[16] Roy A, Kedare SB, Bandyopadhyay S. Optimum sizing of wind-battery systems incorporating resource uncertainty. Applied Energy 2010; 87: 2712–2727.

[17] Subramanyan K, Diwekar UM, Goyal A. Multi-objective optimization for hybrid fuel cells power system under uncertainty. Journal of Power Sources 2004; 132: 99–112.

[18] Wang L. Integration of renewable energy sources: Reliability-constrained power system planning and operations using computational intelligence. Texas A&M University, 2008.

[19] Sharafi M, ElMekkawy TY, Bibeau EL. Optimal design of hybrid renewable energy systems in buildings with low to high renewable energy ratio. Renewable Energy 2015; 83: 1026–1042.

[20] Manitoba Hydro. Technical requirements for connecting distributed recourses to the Manitoba Hydro system, DRG 2003, Rev2, MBHydro Electric Board; 2010.

[21] Gutjahr WJ, Reiter P. Bi-objective project portfolio selection and staff assignment under uncertainty. Optimization 2010; 59: 417–445.

[22] Dufo-lópez R, Bernal-agustín JL. New Methodology for the Generation of Hourly Wind Speed Data Applied to the Optimization of Stand-Alone Systems. Energy Procedia; 2012, 14: 1973–1978.

[23] Krenzinger A, Leite RS, Farenzena DS. Synthesizing sequences of hourly ambient temperature data. Proceedings of 17th International Congress of Mechanical Engineering, Sao Paulo, Brazil, 2003.

[24] Yao R, Steemers K. A method of formulating energy load profile for domestic buildings in the UK. Energy and Buildings 2005; 37: 663–671.

[25] NRC. Energy Use Data Handbook Tables (Canada). Natural Resources Canada; 2014. Available from: http://oee.rncan.gc.ca/publications/statistics/handbook11/index.cfm.

[26] Sharafi M, ELMekkawy TY. Multi-objective optimal design of hybrid renewable energy systems using PSO-simulation based approach. Renewable Energy 2014; 68:67–79.

[27] Sharafi M, Elmekkawy TY. A dynamic MOPSO algorithm for multi-objective optimal design of hybrid renewable energy systems. International Journal of Energy Research 2014; 38(15): 1949-1963.

[28] Environment canada-atmospheric environment service and the national research council of Canada. Canadian weather energy and engineering data sets (CWEEDS Files) 2012. Available from: http://climate.weather.gc.ca/prods_servs/engineering_e.html.

Chapter 6

Conclusions & Future Research

In this chapter, the summary of the developed models and their findings are presented. Besides, the contributions of the thesis are highlighted and some future research directions are suggested.

6.1. Research Summary

In the last decades, many attempts have been reported on the optimal sizing of an HRES by applying optimization or simulation approaches. The single objective framework is the chief methodology that was executed by the previous studies. They mostly considered an economic criterion as the evaluation metric of their design. Nevertheless, it can be very prominent to address more objectives such as emission effect and reliability analysis in the design process of these energy supply systems. Particularly, literature review shows that there are not many reported studies that simultaneously provide environmental, reliability, and economic analysis for an HRES design. Currently, the applied multi-objective approach is predominantly based on Pareto-based techniques in which well-known MOP algorithms are used without modifications. Besides, most of the researchers did not observe the quality of generated Pareto fronts whereas it

is a substantial point to quantitatively evaluate the approximated set that is resulted by a multi-objective optimization algorithm. In addition, most of the reported optimization methods in the literature are applied to design a building energy supply system with RER of 100%. They did not find the best comprising points between system RER, emission, reliability, and cost. Besides, it seems that stochastic analysis of HRES is not adequately considered in the design procedure. Finally, usually available tools provide required energy for only one sector especially for appliance or heating application. It can be inferred that there is a lack in the literature to consider simultaneously all demand sectors such as appliance, heating, cooling, hot water, and transportation. Therefore, it can be concluded that persisted research and development are still needed in terms of the optimal design of HRESs.

This thesis has considered a number of existing gaps in the literature and proposed novel approaches to fill the gaps. Generally, the main idea of this thesis is to propose an optimal sizing tool to reasonably take the advantages of RE resources. The application of developed optimization tool can be in a successful feasibility study of HRESs to aid decision makers in the performance analysis of this kind of energy supply systems. In this case, for a given location, the hourly meteorological data, fluctuating energy demand, and the local economic characteristic of RE components are initialized into the model in order to identify the best compromising size and the type of components.

The employed tool adopts simulation-based optimization approaches to obtain the most affirmative combination of the examined RE ingredients. The main benefit of employing simulation is to accurately accommodate all details and uncertainties of the systems. In the meantime, optimization algorithms are used to deliver the optimal design of the systems.

In this thesis, several conflicting objectives including total net present cost, loss of load probability, total fuel emission, and renewable energy ratio are defined as evaluations metric rather than the components mathematical models. It means this study aims to highlight the multi-objective optimization of sizing an HRES incorporating quality of produced PF and addressing existing uncertainties in RE resources and energy load. Different multi-objective optimization methods based on meta-heuristic algorithms are performed into an off-grid and grid-connected case studies. In more specific manner, the summary of the accomplished research and its contributions are summarized as follows:

- In Chapter 2, an innovative optimization methodology based on ε-constraint method is proposed in order to design hybrid renewable energy systems. The application of the advanced model can be stated as the feasibility study of an HRES. The presented approach uses a simulation-based particle swarm optimization method to concurrently search for the minimum of loss of load probability, CO_2 emission, and total net present cost of the system. The proposed approach is remarkably straightforward to implement and consequently it is computational efficient. The developed model is assessed through undertaking a case study including a wind turbine, PV panels, a diesel generator, a fuel cell, an electrolyzer, batteries, and a hydrogen tank. To evaluate the application of the developed model, the obtained results are compared to the previous methods reported in the related literature. It has been shown a lower shift in the total NPC while fuel emission and LLP are remained at same levels. At the end, a sensitivity analysis is carried out to explore the change in the obtained results by altering the input economic parameters and desired level for CO_2 and LLP. The sensitivity analysis outcomes indicates that varying

the desirable limit of CO_2 emission changes the total NPC of the system more than other variables.

- The proposed model in Chapter 2 is extended to present a dynamic multi-objective PSO method aimed in sizing hybrid renewable energy systems. In a simple way, it is expected that the developed optimization tool defines the type and size of the examined RE equipment. Similar to the presented model in Chapter 2, three main criteria of design are considered which are named loss of load probability, CO_2 emission, and total NPC of the system. The proposed approach takes the advantage of obtaining a PF with higher quality over other proven methods in the related literature. The developed method is evaluated using a case study containing a wind turbine, PV panels, a diesel generator, a fuel cell, an electrolyzer, batteries, and a hydrogen tank. For the employed case study, the results imply that the wind generator is preferred over PV panels, and there is small contribution of hydrogen storage. It means, in most solutions, the electrolyzer/hydrogen tank/fuel cell is not selected as the storage device. Three prominent metrics are utilized to measure the quality of the resulted PF. Then, the obtained results by DMOPSO are evaluated through comparison with other reported MOP algorithms. The accomplished results indicate improvement in the average spacing metric than resulted PF by the previous works. The value of diversification index is less than the value of MOPSO and greater than others. The set coverage metric proves that solutions laying over DMOPSO Pareto front dominate most of solutions of MOPSO. It can be concluded that DMOPSO results in better solutions where it can comparatively generate a larger range and more uniform PF than other reported algorithms. Lastly, sensitivity analysis has been carried out to predict the outcome of the model, if the input parameters differ from what is previously

forecasted. Its result reveals that total NPC is nearly decreased 18.8% by decreasing the PV panel capital cost while change of -50% in the wind turbine capital cost leads to 3.7% variation of total NPC. Besides, there is not observation over sensitivity analysis proving the significant impact of altering investigated parameters on LLP and CO_2 emission.

- The developed DMOPSO algorithm has been applied for sizing the energy supply system of a building located in Canada. Similarly, the model minimizes total NPC and CO_2 emission, while simultaneously maximizes renewable energy ratio. The main contribution of the work is to use renewable energy ratio rather than CO_2 emissions and total NPC as optimization objectives in support of a more sustainable approach for designing building energy systems. The model' aim is to increase the RER of the inspected building through the substitution of fossil fuels with renewable energy resources. In order to evaluate the performance of candidate solutions through the optimization model, the long-term measured hourly meteorological data including hourly solar irradiation, temperature, and wind speed are entered into the simulation module. The performance of the simulation-based optimization approach is judged against two popular multi-objective algorithms using three performance metrics. An HRES containing heat pumps, biomass boilers, wind turbines, solar collectors, PV panels, and heat storage tanks is examined to provide heating, cooling, hot water and power demand of the building. In addition, the application of plug-in electric vehicles is examined instead of common gasoline cars to reduce the gasoline consumption. For the case study, a PF consisting of 42 non-dominated solutions is resulted by which the decision makers can do a trade-off between three objectives and choose the most desired configuration. The reported results present that under defined circumstances and employed parameters,

a configuration consists of a 73 kW wind turbine, a 200 kW biomass boiler, and utilizing PEV can increases RER to 100%. This alternative expands total NPC to C$705180 and reduces CO_2 emission to 2.4 ton/year. The performance analysis of the components shows a capacity factor of 31.5% and 25.4% for wind turbine and the boiler, respectively. Finally, a sensitivity analysis exhibits this fact that capital cost of wind turbine has the most remarkable effect on total NPC compared to other studied parameters.

- In the interest of handling existing randomness in RE resources and energy demand, a simulation-based optimization approach has been demonstrated in Chapter 5. The integration of the evaluated DMOPSO, simulation module, and sampling average technique helps to uncomplicatedly attain the PF for sizing a building energy supply system where multiple energy sources are testified. The synthetic data generation models are applied to yield data series of wind speed, solar irradiance, ambient temperature, and energy load. The total net present cost of the system, renewable energy ratio, and CO_2 emission are supposed as evaluation criteria where loss of load probability is used as a chief constraint with a predefined desirable level. The proposed methodology is evaluated in a case study that is employed in Chapter 4 as well. The complexity raised from incorporating uncertainties is adequately managed within the process of attaching sampling average techniques to the simulation module. Three performance metrics are used to evaluate the quality of the obtained PF against to the deterministic PF. Although, the result establishes that RER can be increased to 100% in both cases, total NPC of solutions over the stochastic PF is slightly shifted to higher level. Whereas the result proves better quality for the deterministic PF, the stochastic analysis is preferred as it assesses a larger range of possible future outcomes and consequently its results are more

realistic. Finally, to identify the impact of economic input parameters on the design criteria, a sensitivity analysis has been executed. Its result evidences that total NPC is varied more significantly when wind turbine capital cost and electricity price are changed.

6.2. Recommendations for Future Research

There are still many open-ended questions related to optimal design of HRESs, which requires further research. Several possible research directions from this study are discussed below:

- It can be interesting as future research to extend the developed optimization models by including more factual constraints of different energy resources. For instance, an improvement in the accuracy of the developed mathematical models can be resulted if the constraints related to synthetizing wind turbine into electricity network are considered. In other words, it can be more accurate and practical to take into account the security constraint since the connection of renewable technologies into electric grids may create a set of problems associated with the security of the system. It is worth mentioning that security is a system attribute representing the ability of the system to tolerate sudden disruptions such as unexpected loss of system elements.

- When the system size is increased and uncertainties are incorporated, the time that simulation-based DMOPSO algorithm requires to solve the problem is expanded exponentially. Therefore, it may conclude that the efficiency of the algorithm is less when the complexity of the problem becomes high. As a future work, a hybrid optimization algorithms based on meta-heuristic techniques can be used to return an acceptable and faster solution. This technique can be constructed by merging the developed DMOPSO

algorithm with local search methods. The main idea is that after few generations, the evolved solutions by DMOPSO are entered to the local search as starting points. Additionally, parallel processing techniques can also be coupled with DMOPSO in order to help in finding more accurate results within reasonable time.

- Further research can be continued to study the feasibility of using other renewable energy resources such as hydro-power. Moreover, it is presumed that the affair of HRESs design is not purely related to technical and economic issues. There are other aspects that can be taken into account, which may contain social factors such as the acceptance of the RE technologies by communities; Therefore, the proposed approach can be modified to embody more objectives and constraints such as social criteria, power quality, stability, security, reliability/failure analysis. For instance, the developed model can involve the probability of failure of employed components in simulation to conduct a failure analysis for HRESs.

- In this study, the developed models do not deal with the optimization of auxiliary equipment such as inverter, convertor, or charge regulator while in optimal design of HRESs, auxiliaries may have enormous importance. It can be a great idea to expand the employed approach to include the capacity optimization of auxiliaries as well.

- Dispatch strategy for providing energy at various time steps can have a noticeable impact on the efficiency or operation cost. In this study, only one dispatch strategy is predefined by the user while the model can be extended to examine different operating scenarios and consequently mark the optimal one with respect to the optimization goals.

- Future research may include using more realistic and practical data since some data of the sample test case that are used to evaluate the proposed algorithms are hypothetical. This is one reason why the model may not come up with realistic results. Thus, it would be more realistic if the developed methodology is examined based on more practical data. More accurate predicted data for hourly load can be considered since employed load data is still relatively imprecise. One of the main reasons is related to the lack of historical data for energy load. In addition, the load forecasting and fuel cost data need to incorporate their variation over years as the simulation has been run for long time (20-25 years).

Appendix

A.1. Tuning Algorithm Parameters

In the appendix section, first, the parameters tuning of the Particle Swarm Optimization algorithm is studied using design of experiment (DOE) techniques. In other words, the properties of PSO algorithm has been analyzed from the viewpoint of an optimization practitioner, in the context of a real world optimization problem, namely the optimal design of a hybrid renewable energy system what is developed in Chapter 2.

Fine–tuning of PSO parameters is an important task. The role of the inertia weight, the relationship between the cognitive and the social parameters and the determination of the swarm size are important to ensure convergence of the PSO algorithm. In our PSO algorithm, there are mainly 4 parameters to be determined: the population size (P), the inertia weight (ω), the cognitive coefficient (C_1), and the social coefficient (C_2). The method used for the parameter setting of PSO is a 3^4 full factorial design. In the experiment, the value of each parameter has been assigned three levels: low level, medium level, and high level. The low level is denoted as −1 whereas the medium and high levels are denoted as 0 and 1, respectively. It is preferred to adopt three levels design of each parameter to save computational efforts, and also test more combination than two levels design. If each parameter has four levels, then $4^4 = 256$ parameter

combinations have to be considered, while the case of three levels only needs 81 combinations. Table A-1 presents the interval for each parameter which are proposed by the related literature. In addition, Table A-2 demonstrates the best value of PSO parameters that is suggested in the literature regarding their studied problems. Here, according proposed intervals (Table A-1) and suggested value by the literatures (Table A-2); the studied interval of parameters is considered as listed in Table A-3.

Table A-1: Proposed interval for general PSO algorithm Swagatam et al. [1]

P	[20 60]
ω	[0.5 1]
C_1	[0 4]
C_2	[0 4]

Table A-2: Proposed optimal value for PSO parameters

	Bartez et al. [2]	AlRashidi et al. [3]	Swagatam et al. [1]
P	50	25	60
ω	0.25	0.7	0.7
C_1	0.25	1.2	2.04
C_2	0.25	2.5	2.04

Table A-3: Studied interval for the PSO algorithm

	Low Level (-1)	Medium Level (0)	High Level (+1)
P	20	40	60
ω	0.25	0.6	1
C_1	0.25	1.2	2
C_2	0.25	1.75	3

Furthermore, the PSO algorithm is run 20 times. That is, the number of replication is set as 20. Two responses are used which are named as total net present cost (NPC) and the running time of the algorithm that is named CPU time. It means the goal is to investigate the main effect of four mentioned factors on the employed responses.

A.1.1. Experimental Result

As mentioned above, two experiments have been run since two responses are considered. In the first experiment the response is total NPC, and in the other experiment the response is the CPU time. In this study, analysis of variance (ANOVA) is employed to analyze the data of performed experiments. By using MINITAB, ANOVA results for two experiments are given in Table A-4 and Table A-5. It is found from that parameters P, ω, C_1, C_2 and the following interactions $\omega*C_2$, C_1*C_2, and $\omega*C_1*C_2$ have significant effects on total NPC which is obtained by the algorithm as their P-values are less than considered α (5%).

Table A-4: Analysis of variance (ANOVA) result for NPC

Source	Degree of freedom	Sequential Sums of Squares	Adjusted Sums of Squares	Adjusted Mean Square Value	F-Value	P-Value
P	2	1.67104E+11	1.67104E+11	83552246132	56.63	0.0
ω	2	4.32638E+11	4.32638E+11	2.16319E+11	146.61	0.0
C_1	2	84697954643	84697954643	42348977321	28.7	0.0
C_2	2	1.47008E+11	1.47008E+11	73503837989	49.82	0.0
$P*\omega$	4	3465554734	3465554734	866388684	0.59	0.672
$P*C_1$	4	4391557199	4391557199	1097889300	0.74	0.562
$P*C_2$	4	12352564092	12352564092	3088141023	2.09	0.079
$\omega*C_1$	4	4059556847	4059556847	1014889212	0.69	0.6
$\omega*C_2$	4	20354659810	20354659810	5088664952	3.45	0.008
C_1*C_2	4	15834803282	15834803282	3958700820	2.68	0.03
$P*\omega*C_1$	8	11475964467	11475964467	1434495558	0.97	0.456
$P*\omega*C_2$	8	12685290928	12685290928	1585661366	1.07	0.378
$P*C_1*C_2$	8	7196698298	7196698298	899587287	0.61	0.770
$\omega*C_1*C_2$	8	41000957064	41000957064	5125119633	3.47	0.001
$P*\omega*C_1*C_2$	16	378087694446	37808769446	2363048090	1.60	0.061
Error	1539	2.27078E+12	2.27078E+12	1475490458		
Total	1619	3.27285E+12				

Moreover, the ANOVA result for CPU time is depicted in Table A-5. It is found that parameters P, ω, C_1, C_2 and their interactions $\omega*C_1$, and $P*\omega*C_2$ have significant effects on the running time of the algorithm because their P-values are less than 5%. It can be found that the effect of the P is so much higher than others since the F-value for P is 7409. Therefore, it can be predicted that the main effect of P will be more significant than ω, C_1, and C_2.

Table A-5: Analysis of variance (ANOVA) result for CPU time

Source	Degree of freedom	Sequential Sums of Squares	Adjusted Sums of Squares	Adjusted Mean Square Value	F-Value	P-Value
P	2	8763344	8763344	4381672	7409.41	0.0
ω	2	32345	32345	16172	27.35	0.0
C_1	2	11586	11586	5793	9.80	0.0
C_2	2	13459	13459	6730	11.38	0.0
P*ω	4	1492	1492	373	0.63	0.641
P*C_1	4	294	294	74	0.12	0.974
P*C_2	4	5602	5602	1401	2.37	0.051
ω*C_1	4	11817	1817	2954	5.00	0.001
ω*C_2	4	4952	4952	1238	2.09	0.079
C_1*C_2	4	3241	3241	810	1.37	0.242
P*ω*C_1	8	7725	7725	966	1.63	0.111
P*ω*C_2	8	13948	13948	1743	2.95	0.003
P*C_1*C_2	8	2699	2699	337	0.57	0.803
ω*C_1*C_2	8	3257	3257	407	0.69	0.702
P*ω*C_1*C_2	16	7101	7101	444	0.75	0.743
Error	1539	910112	910112	591		
Total	1619	9792974				

The residual plots for cost and CPU time are shown in Figure A-1 and Figure A-2. The models will be adequate if the residuals plot have a normal distribution.

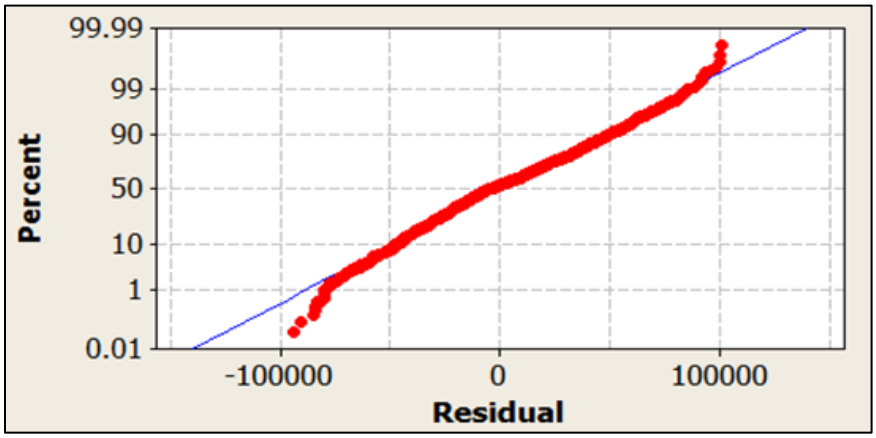

Figure A-1: Normal probability plot of the residuals for NPC

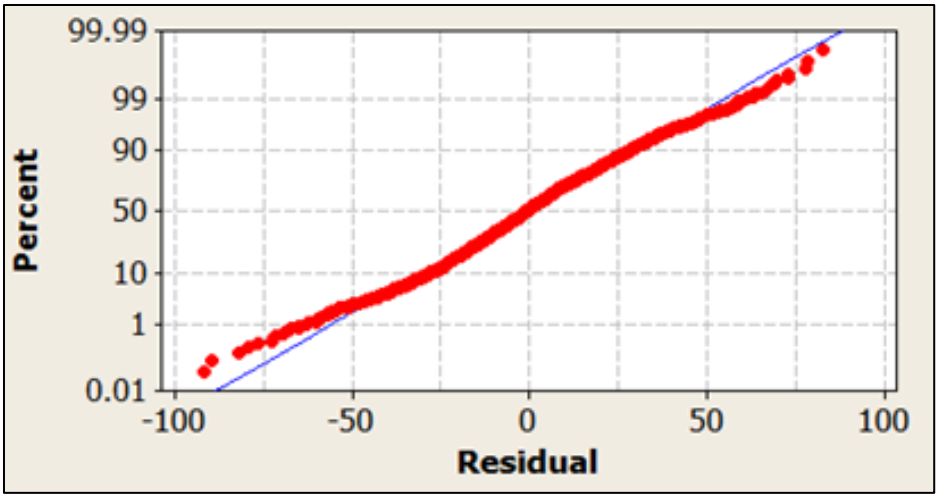

Figure A-2: Normal probability plot of the residuals for CPU time

According to residual plots for NPC and CPU time, by examining the normality plot, the general impression is that the error distribution is approximately normal. Therefore, the model is adequate and there is no evidence that the assumptions are violated.

To further determine the appropriate value of each parameter, the main effect of parameters and their interactions with significant effects are depicted in Figure A-3 and Figure A-4. The plots represent total NPC and CPU time value when parameters take the employed low level, medium, or high level.

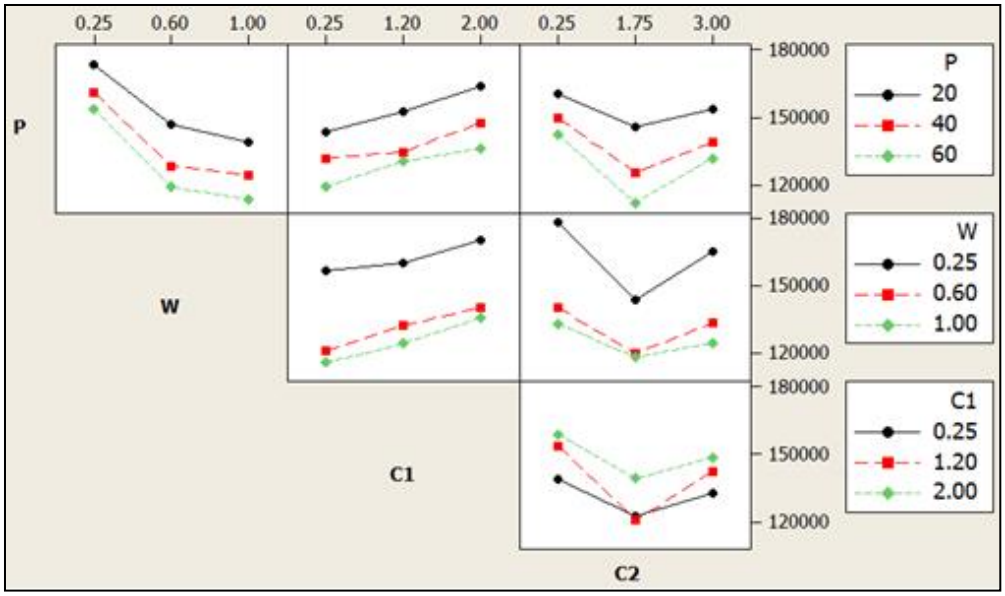

Figure A-3: The interaction plot for total NPC

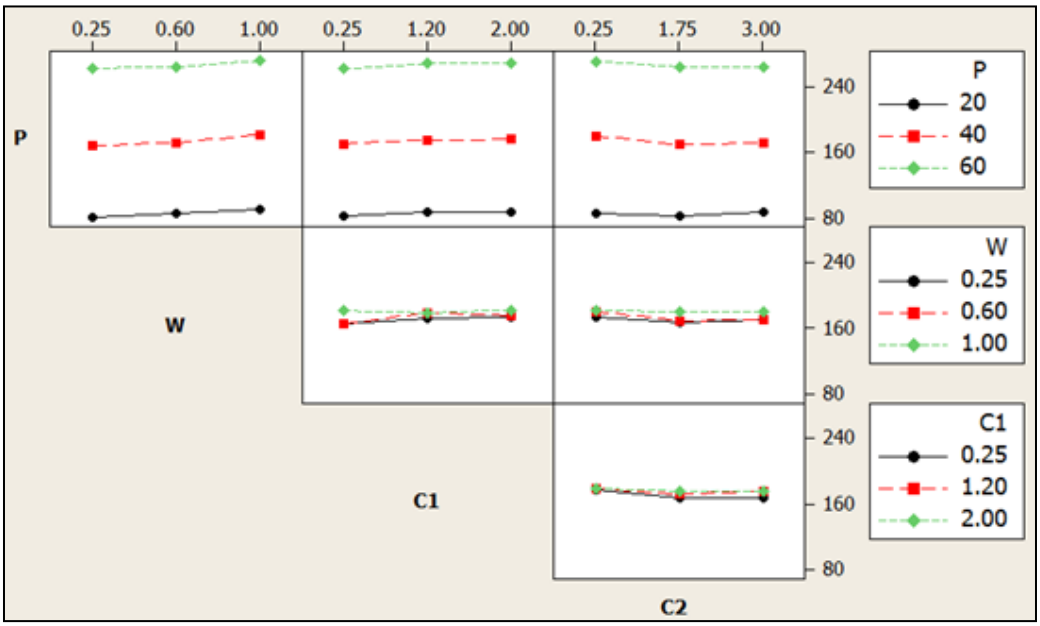

Figure A-4: The interaction plot for CPU time

From the Figure A-3, it can be found that the high level of parameters P and ω are preferred for obtaining better NPC even if the interactions are taken into account. Lower NPC is attained at medium level of C_2, regardless of P, ω, and C_1. When C_2 takes the medium level, C_1 can take medium level or low level according to the interactions of C_1*C_2. The main effect plot which is

shown in Figure A-5 indicates the low level of C_1 helps to obtain slightly better NPC. It is worth mentioning, the best value of parameters are identified based on NPC interaction plot since the main response is considered as NPC.

According to interaction plot for CPU time (Figure A-4), lowest CPU time is attained at low level of P, C_1, and ω. In addition, lowest time is attained at medium level of C_2; hence, the lowest CPU time is result by using P=20, ω =0.25, C_1=0.25, C_2=1.75. In Figure A-4, it seems that only P has significant effect on the CPU time, but the other parameter also has effect as depicted in the ANOVA result table of this experiment, Table A-5. In Figure A-4, the effect of ω, C_1, and C_2 are not clear since the effect of P is so much greater than the others, and the scale of the figure is adjusted to show that. In summary, the lowest NPC is resulted by setting the parameters as presented in Table A-6.

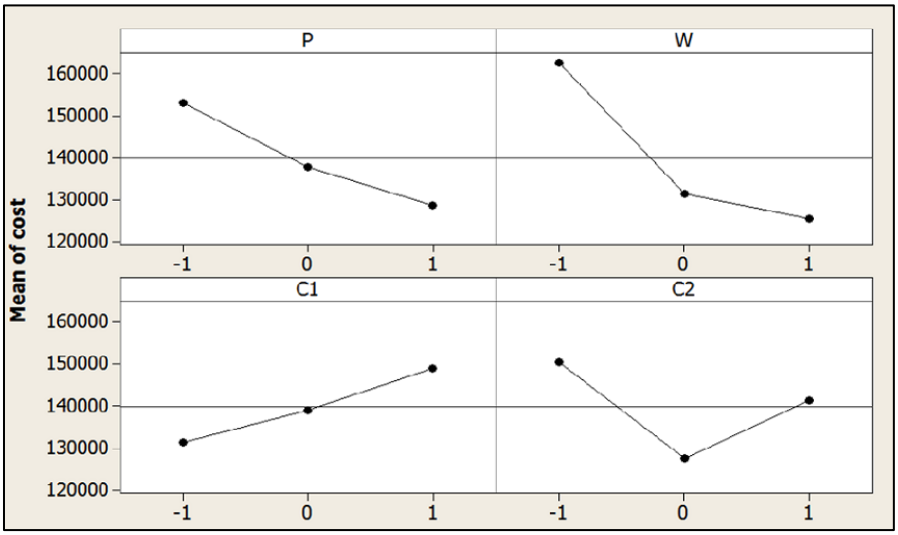

Figure A-5: Main effect plot for total NPC

Table A-6: Best values for the parameters to obtain the least NPC

Parameter	value
P	60
ω	1
C_1	0.25
C_2	1.75

By comparing the identified values for the parameters with those are proposed in the literatures, it is found that the value for *P* is the same as one proposed by Swagatam et al. in [1]. The proposed value for ω is 1 while in [1] and [3] is suggested as 0.7. The value for C_1 is the same as one proposed by Bartez et al. [2]. Finally, the proposed values for C_2 is different from those are proposed in the literatures [1-3]. Hence, in the next step, a combination is selected by using the literatures results and nearest value to the obtained results. That is, $\omega = 0.7$ and C_2=2.04 the same as the literature result and *P*=60 and C_1=0.25. It means the *P* and C_1 are fixed at 60 and 0.25, respectively, then the effect of ω and C_2 is studied in a 2^2 factorial design. There are two factors with two levels. The result of this experiment is shown in Table A-7 and Figure A-6.

Table A-7: ANOVA result for NPC versus ω and C_2

Source	Degree of freedom	Sequential Sums of Squares	Adjusted Sums of Squares	Adjusted Mean Square Value	F-Value	P-Value
ω	1	20182846	20182846	20182846	0.64	0.469
C_2	1	5029492	5029492	5029492	0.16	0.710
ω*C_2	1	5131655	5131655	5131655	0.16	0.708
Error	4	126552682	126552682	31638171		
Total	7	156896674				

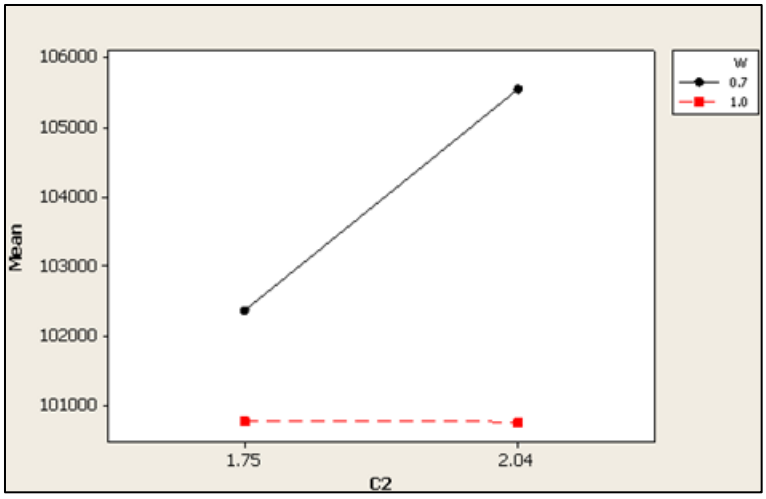

Figure A-6: The interaction plot for NPC versus ω and C_2

The interaction plot indicates that the low level of C_2 is better than its high level; also minimum NPC is attained at high level of ω. Therefore, for this problem the parameters should be set at P = 60, ω = 1, C_1 = 0.25, and C_2 =1.75.

The parameters are set at the best combination which is recognized from the experiment, and then the algorithm is run 20 times. The average of minimum cost obtained by this combination is compared with the average NPC of other combinations. Its result shows approximately 31% improvement for achieved averaged NPC.

A.2. Supporting Calculations

In this section, the calculation and assumption that are applied in Chapters 4 and 5 are demonstrated.

A.2.1. Formula for Estimating Heating and Cooling Load

In this study, the degree-days method estimates the energy requirement for cooling and heating purpose [4]. Instead of using day as the time step, the degree-days concept is applied in hourly basis. The idea of the method is that the required energy for heating/cooling of a building is

related to the difference between a base and the outdoor temperature. The base temperature is defined as the temperature that the heating/cooling is required when the outdoor temperature is higher or lower than that [4]. According to degree-day concept, the hourly energy consumption for heating/cooling purpose, Q_{hr} (Wh) can be approximated as [4];

$$Q_{hr} = \frac{K_{tot}}{\eta} D_{hr} \quad \text{(A-1)}$$

where, K_{tot} is the total heat transfer coefficient which is related to the envelope of buildings (W/^{o}C), η is the efficiency of the heating/cooling components and D_{hr} states the value of degree-hour for heating or cooling. The heating degree-hour for heating goal (HD_{hr}) can be calculated by using Equation (A-2) [4].

$$HD_{hr} = (T_b - T_m)^+ \quad \text{(A-2)}$$

where, T_m is the hourly outside temperature and T_b represents the base temperature. Similar to the calculation of HD_h, cooling degree-hour (CD_{hr}) is calculated as following [4]:

$$CDD = (T_m - T_b)^+ \quad \text{(A-3)}$$

In the previous studies, it is common to assume the base temperature as 18^{o}C and 22^{o}C in heating and cooling degree-hour calculations, respectively [4].

$$K_{tot} = UA \quad \text{(A-4)}$$

where, U is the overall heat transfer coefficient of the building envelope (W/m^2 ^{o}C), A is the net area of walls, door, roof, ceiling, floor, and windows (m^2).

A.2.2. Formula for Estimating Monthly Gasoline Consumption

$$Gasoline_m = N_{car} \frac{\eta_{fuel} \times D_m}{100} \quad \text{(A-5)}$$

where, N_{car} is number of car in the building, η_{fuel} is fuel efficiency (litres per 100 kilometres) of light vehicles, D_m is average distance driven of light vehicles in Canada. In this study, the η_{fuel}= 10.6 and $D_m = 1333.3(km)$, and N_{car} is 33 [5].

A.2.3. Assumption and Parameters Values Used in Chapters 4 and 5

Table A-8: Key parameters values used in the calculation of the case study described in Chapters 4 and 5

Number of car in the building	33
Air conditioner EER	8
Gasoline density (kg/m^3)	737
Gasoline HHV(MJ/kg)	47
Natural gas HHV (MJ/kg)	52
Total floor area (m^2)	2940
NG-Boiler efficiency	60%

Table A-9: Thermal Characteristic of the building described in Chapters 4 and 5

Roof (W/m^{2}K)	0.38
Wall(W/m^{2}K)	0.77
floor(W/m^{2}K)	0.54
Windows(W/m^{2}K)	2.18

Table A-10: Total heat transfer coefficient of the building (UA) described in Chapters 4 and 5

Roof(W/K)	372.4
Floor(W/K)	529.2
Wall(W/K)	813.12
Windows and door(W/K)	497.04
Total(W/K)	2211.76

A.3. References

[1] Swagatam D, Ajith A, Amit K. Particle swarm optimization and differential evolution algorithms: Technical Analysis, Applications and Hybridization Perspectives. Studies in Computational Intelligence (SCI) 2008; 116:1–38

[2] Bartez B, De-Vegt M, Parsopoulous K E. Designing particle swarm optimization with regression trees. Technical Report, Reihe CI 173/04, University of Dortmund; 2004.

[3] AlRashidi M R, AlHajri MF. Optimal planning of multiple distributed generation sources in distribution networks: A new approach. Energy Conversion and Management 2011; 52: 3301–3308.

[4] Orhan B, Hüsamettin B, Tuncay Y. Analysis of variable-base heating and cooling degree-days for Turkey. Applied Energy 2001; 69: 269–283.

[5] Statistics Canada. Human activity and the environment : annual statistics. Ottawa; 2009. Available from: http://www.statcan.gc.ca/pub/16-201-x/16-201-x2009000-eng.htm.

[6] ASHRAE handbook: heating, ventilating, and air-conditioning systems and equipment. Inch-pound edition, American Society of Heating, Refrigerating and Air-Conditioning Engineers; 2012.